Developing CMV as a Vaccine Vector

Thesis submitted in candidature for the degree of Doctor of Philosophy (PhD)

Evelina Statkute

September 2017

Division of Infection and Immunity
Cardiff University

Declaration

This work has not been submitted in substance for any other degree or award at this or any other university or place of learning, nor is being submitted concurrently in candidature for any degree or other award.

Signed ……(candidate) Date 25/9/2017

STATEMENT 1

This thesis is being submitted in partial fulfilment of the requirements for the degree of PhD

Signed ……(candidate) Date 25/9/2017

STATEMENT 2

This thesis is the result of my own independent work/investigation, except where otherwise stated, and the thesis has not been edited by a third party beyond what is permitted by Cardiff University's Policy on the Use of Third Party Editors by Research Degree Students. Other sources are acknowledged by explicit references. The views expressed are my own.

Signed ……(candidate) Date 25/9/2017

STATEMENT 3

I hereby give consent for my thesis, if accepted, to be available online in the University's Open Access repository and for inter-library loan, and for the title and summary to be made available to outside organisations.

Signed ……(candidate) Date 25/9/2017

STATEMENT 4: PREVIOUSLY APPROVED BAR ON ACCESS

I hereby give consent for my thesis, if accepted, to be available online in the University's Open Access repository and for inter-library loans **after expiry of a bar on access previously approved by the Academic Standards & Quality Committee.**

Signed ……(candidate) Date 25/9/2017

Acknowledgements

This adventure would not have been possible if it wasn't for the encouragement and support of everyone around me.

I am grateful to Life Sciences Research Network Wales and the Medical Research Council for funding this project. I am also thankful to Dr Zsolt Ruzsics for providing me bacteria stabs of M50 and SCP BACs.

I owe the greatest debt of gratitude to my supervisor Dr Richard Stanton who has motivated, inspired and had confidence in me throughout my time in Cardiff. His immense knowledge, humour, enthusiasm, guidance, optimism and patience (of a saint) made him the best supervisor I could have asked for.

I would also like to thank my advisors Professor Gavin Wilkinson, Dr Ian Humphreys and Professor Awen Gallimore for their expertise, invaluable insights and for challenging my thinking.

I am especially thankful to Mat Clement, Silvia Gimeno and Morgan Marsden for their assistance with the animal work and teaching me more about mouse CMV biology.

I would also like to give a special thanks to everyone in the lab for being like a second family to me here in Wales and making the atmosphere at work fun and lively even during rainy days.

I am forever thankful to my parents Dalia and Egidijus and my brother Martynas for their endless love, support and believing in me at times when I didn't believe in myself.

Lastly, I would like to thank James for being my rock and making me a gazillion cups of tea that made writing up more enjoyable.

"A smooth sea never made a skilled sailor."
-Franklin D. Roosevelt

Summary

There is an increasing need to develop anti-cancer vaccines that elicit strong and durable immune responses and are able to break immune tolerance to cancer antigens. Cytomegaloviruses (CMV) induce one of the strongest immune responses of any viral vector – as much as 20% of all $CD8^+$ T cells can be specific for a single epitope, thus making them an exciting candidate for vaccine development. The majority of work, however, has been based on replication-competent viruses. In humans, the use of replication-competent human CMV (HCMV) vectors would not be permitted due to safety concerns, however replication-deficient vectors may not induce immune responses of the same magnitude as wildtype HCMV. In an attempt to make CMV vectors safer, I utilised a tetracycline repressor (tetR)-based system and generated a total of 55 mouse and human CMV vectors in which viral replication was dependent on inducible expression of multiple different viral genes. Having analysed the ability of the vectors to replicate *in vitro* and *in vivo*, I generated three vectors which replicated well in the presence of doxycycline, but in its absence replicated poorly *in vitro*, and did not appear to replicate *in vivo*. Importantly, in a direct comparison, the level of control was more stringent than viruses previously characterized in the literature.

Adenoviruses are one of most widely used vectors in cancer immunotherapy, induce strong T-cell responses, and could be used in a prime-boost regiment with CMV vectors. However, we found that in a prophylactic regimen, a recombinant human adenovirus (Ad) encoding human 5T4 tumour-associated antigen alone did not protect against 5T4-expressing tumour challenge. We tested the immunogenicity of 5T4 in two mouse strains and established three 5T4-expressing cancer models in which vectors can be tested. In future work, we hope to use our inducible CMV/Ad vaccine regimen in these models.

Table of Contents

List of Figures

List of Tables

List of abbreviations

°C	Degrees Celsius
Δ	Deletion
µL	Microliter
µm	Micrometre
µM	Micromolar
A	
aa	Amino acid
Ab	Antibody
Ad	Adenovirus vector
ADC	Antibody-Drug Conjugate
Ag	Antigen
AIDS	Acquired Immunodeficiency Syndrome
ALL	Acute Lymphoblastic Leukaemia
Amp	Ampicillin
ANOVA	Analysis of variance
APC	Antigen presenting cells
APC	Adenomatous Polyposis Coli
ATCC	American Tissue Culture Collection
B	
BAC	Bacterial artificial chromosome
BAGE	B melanoma antigen
bp	Base pairs
BDCRB	2-Bromo-5,6-dichloro-1-beta-D-ribofuranosyl benzimidazole
BMDC	Bone Marrow-derived Dendritic Cells
C	
CAR	Chimeric Antigen Receptor
CAR	Coxsackievirus and adenovirus receptor
CCMV	Chimpanzee CMV
CEA	Carcinoembryonic antigen
CLIP	Class II-associated invariant chain peptide
CMV	Cytomegalovirus
CNS	Central nervous system
CPE	Cytopathic Effect
CTL	Cytotoxic T lymphocyte
CTRL	Control
Cy7	Cyanine 7

D

DC	Dendritic Cells
dd	Destabilising domain
DE	Delayed early
DMEM	Dulbecco's Modified Eagle's Medium
DMSO	Dimethyl Sulfoxide
dNTP	Deoxynucleotide
DOX	Doxycycline
dpi	Days post-infection
DSG	Desmoglein
DTT	Dithiothreitol

E

EBV	Epstein-Barr virus
EDTA	Ethylenediaminetetraacetic Acid
eGFP	Enhanced Green Fluorescent Protein
EGFR	Epidermal Growth Factor Receptor
ELISpot	Enzyme-Linked ImmunoSpot
EM	Electron microscope
EMT	Epithelial Mesenchymal Transition
Eqn	Equation
ER	Endoplasmic Reticulum
ERGIC	ER-Golgi intermediate compartment

F

FACS	Fluorescence-activated cell sorting
FBS	Foetal Bovine Serum
FDA	Food Drug Agency
FI	Fluorescence index
FITC	Fluorescein isothiocyanate
FKBP	FK506 binding protein
FLP	Flippase
FMO	Fluorescence Minus One
FRT	Flippase Recognition Target
FSC	Forward scatter
FSC-A	Forward scatter area
FSC-H	Forward scatter height

G

GAGE	G antigen

gB	Glycoprotein B
GB	Golgi body
GFP	Green fluorescent protein
gH	Glycoprotein H
gM	Glycoprotein M
GM	Growth media
GMCMV	Green Monkey CMV
GM-CSF	Granulocyte macrophage colony-stimulating factor
gp	Glycoprotein
GPCMV	Guinea Pig CMV
H	
HAART	Highly active antiretroviral therapy
HBSS	Hanks' Balanced Salt solution
HCMV	Human CMV
HIV-1	Human Immunodeficiency Virus
HCT	Hematopoietic Cell Transplant
HFFF	Human Foetal Foreskin Fibroblasts
h-TERT	Human Telomerase Reverse Transcriptase
HLA	Human Leukocyte Antigen
HNSCC	Head and Neck Squamous Cell Carcinoma
hpi	Hours post-infection
HRP	Horseradish Peroxidase
HSPG	Heparan sulphate proteoglycan
HSV	Herpes Simplex Virus
I	
ICS	Intracellular Cytokine Staining
IE	Immediate early
IFN-y	Interferon γ
IHC	Immunohistochemistry
IL	Interleukin
IPTG	Isopropyl β-D-1-thiogalactopyranoside
IRF3	Interferon Regulatory Transcription Factor 3
IRL	Internal Repeat Long
IRS	Internal Repeat Short
i.v.	Intravenously
K	
Kan	Kanamycin

kb	Kilobases
KLRG1	Killer cell lectin-like receptor subfamily G member 1
KO	Knock out
kV	Kilovolt
L	
L	Late
LB	Luria broth
LGR5	Leucine-rich repeat-containing G-protein coupled receptor 5
LI	Large intestine
LLC1	Lewis lung carcinoma 1
lncRNA	Long non-coding RNA
LTR	Long Terminal Repeat
M	
MIIC	MHC class II compartment
MAFFT	Multiple Alignment using Fast Fourier Transform
MAGE	Melanoma antigen
MART-1	Melanoma-associated antigen recognized by T cells 1
MCMV	Mouse CMV
MEM	Minimum Essential Medium
MEF	Mouse embryonic fibroblasts
miRNA	MicroRNA
MHC	Major Histocompatibility Complex
MIE	Major Immediate Early
MIEP	Major Immediate Early Promoter
MLP	Major late promoter
MOI	Multiplicity of infection
MSHV	*Miniopterus schreibersii herpesvirus*
MT	Microtubules
MUC	Mucin
MVA	Modified Vaccinia Ankara virus
N	
n/a	Not applicable/ not available
nd	Not determined
NEC	Nuclear egress complex
NF-κB	Nuclear factor kappa-light-chain-enhancer of activated B cells
ng	Nanogram
NKT cells	Natural killer T cells

NTG	N-methyl-N'-nitro-N-nitrosoguanidine
nM	Nanomolar
NY-ESO	New York oesophageal squamous cell carcinoma
O	
ORF	Open Reading Frame
P	
PAMP	Pathogen-associated molecular pattern
PB	Pacific Blue
PBL	Peripheral Blood Leukocytes
PBS	Phosphate Buffered Saline
PCR	Polymerase chain reaction
PE	Phycoerythrin
PerCP	Peridinin-Chlorophyll
PFA	Paraformaldehyde
PFU	Plaque forming Units
PHA	Phytohemagglutinin
pi	Post-infection
PKR	Protein Kinase R
PML	Promyelocytic leukaemia
PPi	Pyrophosphate
PSA	Prostate-specific antigen
Q	
qPCR	Quantitative PCR
R	
RAE-1γ	Receptor activating ligand
RBC	Red Blood Cell
RCC	Renal cell carcinoma
RCMV	Rat CMV
RCMVE	Rat CMV England
RhCMV	Rhesus CMV
rpm	Revolutions per minute
RSV	Rous Sarcoma Virus
RT	Room temperature
rtTA	Reverse tetracycline transactivator
S	
SA	Sialic acid
SA-APC	Streptavidin -Allophycocyanin

s.c.	Subcutaneously
SCP	Small capsid protein
SD	Standard Deviation
SDS	Sodium dodecyl sulphate
SFU	Spot forming units
SI	Small intestine
SIV	Simian immunodeficiency virus
SMCMV	Squirrel monkey CMV
SNPs	Single-nucleotide polymorphism
SR	Scavenger receptor
SSC	Side scatter
SSX	Synovial Sarcoma X-chromosome
SV40	Simian virus 40
T	
TAP	Transporter associated with Antigen Processing
TCR	T cell receptor
TetO	Tetracycline operator
TetR	Tetracycline repressor
Th cells	T helper cells
TIL	Tumour infiltrating lymphocytes
TK	Thymidine kinase
TLR	Toll-like receptor
TMP	Trimethoprim
TNF-α	Tumour Necrosis Factor α
TRE	Tetracycline response element
TRL	Terminal Repeat Long
T_{RM} cells	Tissue Resident Memory T cells
T_{EM} cells	Effector Memory T cells
T_{CM} cells	Central Memory T cells
TRP	Tyrosinase-related protein
TRS	Terminal Repeat Short
tTA	Tetracycline transactivator
TuHV	Tupaiid herpesvirus
U	
U_L	Unique long
U_S	Unique short

V

VA	Viral-associated
v/v	Volume/volume
VCAM	Vascular cell adhesion molecule
vICA	Viral inhibitor of caspase-8 apoptosis
vMIA	Viral mitochondria-localized inhibitor of apoptosis

W

w/v	Weight/volume
WT	Wild type
WT1	Wilms' tumour 1

X

X-GAL	5-Bromo-4-Chloro-3-Indolyl β-D-Galactopyranoside

Chapter 1 Introduction

Cancer Immunology came to prominence as breakthrough of the year in 2013 (Bartlett et al. 2013). Since then, at least 54 agents for treating cancer have been Food Drug Agency (FDA)-approved (CenterWatch 2017). Development of anti-cancer vaccines, however, has been a challenging task with slow progress. For the generation of effective vaccines, it is necessary to optimise the induction of therapeutic immune responses. Viruses have many properties that make them attractive vaccine vectors. Adenoviruses (Ad) have provided one of the most efficient means to generate a therapeutic T cell response and are widely used in vaccine initiatives, making up 25% of total vector usage in cancer gene therapy trials (Fooks et al. 1995; Jacobs et al. 1994). However, other viruses have properties that may make them even more effective. Pioneering work using cytomegaloviruses (CMV) has demonstrated the potential of these viruses in the vaccine development field, due to their unique capacity to generate strong Effector Memory T cell (T_{EM}) responses (Hansen, Sacha, et al. 2013; Hansen et al. 2009; Hansen et al. 2011). However, to date, most human CMV (HCMV) vaccines have been based on replication competent virus. We sought to improve HCMV vaccine vector safety while retaining immunogenicity, with a view to exploiting the ability of both HCMV and Adenovirus vectors to induce T-cell responses in cancer immunotherapy.

1.1. T cell subsets

The induction of a T-cell response is a key aim of many cancer vaccine strategies. T lymphocytes are part of the adaptive immune system and can be classified into T helper (Th) cells ($CD4^+$ T cells), cytotoxic T cells ($CD8^+$ T cells), natural killer T (NKT) cells, regulatory T cells (T_{Regs}; $CD4^+$ T cell subset) and γδ T cells. T cells, by definition, express a T cell receptor (TCR) that is responsible for binding peptide antigen (Ag) presented on the cell surface by major histocompatibility complex (MHC). $CD8^+$ T cells recognize peptides presented by MHC class I molecules, whereas $CD4^+$ T cells, including $T_{Regs,}$ recognize peptides presented by MHC class II molecules, NKT cells bind lipid-based antigens presented by CD1d (a non-classical MHC molecule) and γδ T cells recognize CD1a and CD1d molecules (Luoma et al. 2014). TCRs are comprised of a heterodimer of α and β chains joined by a disulphide bond, except on γδ T cells, where the TCR is comprised of a distinct range of γ and δ chains that define their specificity. Activation of T cells results in durable antigen-specific immune responses.

1.2. CD4$^+$ and CD8$^+$ T cell development

T lineage cells arise from lymphoid progenitors that are produced in the bone marrow and migrate to the thymus to proliferate, differentiate and mature. T cell precursors, thymocytes, start off as double-negative cells since they do not express CD4 or CD8 markers (Germain 2002). Expression of recombination-activating gene results in rearrangement of β TCR chains (Variable (V); Diversity (D) and Joining (J) gene segments). Successful rearrangement is followed by expression of both CD4 and CD8 co-receptors. These immature thymocytes, also termed double positive, rearrange α TCR chains (V and J gene segments) to form TCRs. The process of V(D)J rearrangement of TCR chains generates a broad repertoire of TCRs with affinity for a wide variety of peptides. αβ T cells then undergo positive selection where they interact with cortical epithelial cells expressing either MHC class I or class II complexes presenting endogenous peptides (Germain 2002). Only CD4/CD8 lineage-committed αβ T cells that receive the survival signal migrate to thymic medulla and undergo negative selection that eliminates self-reactive T cells (Germain 2002). During thymic development, T cells undergo a process termed 'central tolerance' that selects out high avidity T cells that would otherwise react to self-proteins.

1.3. *αβ* T cell receptor-CD3 complex

TCRs are heterodimeric transmembrane proteins comprised of disulphide-linked α and β chains (Kuhns et al. 2006). Each chain is divided into variable (V) and constant domains (C) (Kuhns et al. 2006). The variable domains of α and β chains are involved in antigen recognition and structurally resemble the Fab fragment of an antibody (Kuhns et al. 2006). The TCR does not contain signalling motifs required for T cell activation, differentiation and proliferation upon antigen encounter (Birnbaum et al. 2014). The CD3 molecule (comprised of invariant chains called γ, δ, ε and ζ), however, contains intracellular signalling motifs and binds to the variable antigen recognition region of the TCR, forming the TCR-CD3 complex. Only the γ, δ, ε chains are extracellular and form heterodimers CD3γε and CD3δε which bind to the variable αβ heterodimer domains whereas ζζ homodimers form an intracellular region of the complex (Kuhns et al. 2006).

1.4. Major histocompatibility complexes I and II

Major histocompatibility complex (MHC) I and II are molecules expressed on the cell surface that play a role in antigen presentation to T cells. MHC class I molecules are expressed on all nucleated cells as well as platelets whereas MHC class II molecules are expressed on antigen-presenting cells (APCs) (e.g. dendritic cells (DCs), macrophages, B cells) and in

response to interferon gamma (IFN-γ) can also be expressed on fibroblasts, endothelial cells and epithelial cells (Mulder et al. 2011; Geppert & Lipsky 1985).

The MHC locus in humans is called human leukocyte antigen (HLA) whereas in mice it is known as the H-2 locus. In humans, MHC class I molecules are called HLA-A, HLA-B, HLA-C, HLA-E, HLA-F, HLA-G and HLA-H whereas in mice they are H-2D, H-2K and H-2L. Class II molecules in humans are called HLA-DP, HLA-DQ and HLA-DR. In mice, MHC class II molecules are called H-2A(I-A) and H-2E(I-E).

MHC class I molecules consist of heterodimers of alpha (or heavy) chain and β_2-microglobulin (Hewitt 2003). The alpha chain is comprised of three extracellular domains: α_1 and α_2 that form the antigen binding domain and α_3 which interacts with β_2-microglobulin, as well as transmembrane and cytoplasmic domains (Hewitt 2003). MHC class II molecules are made up of an α and a β chain. Each chain has two extracellular domains called α_1, α_2 and β_1, β_2 (Jones et al. 2006). The α_1 β_1 domains form the antigen-binding region (Dasgupta et al. 2014).

1.5. Antigen processing and presentation

T cell receptors can only recognize peptides bound to the MHC molecules. The peptides presented are derived from whole proteins and first need to be processed into shorter epitopes. MHC class I molecules usually bind peptides 8-10 amino acids in length (Hewitt 2003) whereas for MHC class II molecules the peptides recognized are longer (13-25 aa) (ten Broeke et al. 2013). MHC class I-restricted epitopes tend to be acquired from endogenous proteins (viral or self) in the cytosol that get broken down in the proteasome or by giant tripeptidyl aminopeptidase II complex and are then transported into the lumen of the ER by the transporter associated with antigen processing (TAP) protein (Raghavan et al. 2008). In the endoplasmic reticulum (ER), the peptides are assembled onto MHC class I molecules. The MHC class I α chains in the ER are bound to an ER chaperone protein calnexin that stabilizes them. Binding to β2-microglobulin leads to release of the complex from calnexin and binding to a peptide loading complex consisting of tapasin, MHC class I, ERp57, calreticulin and TAP transporters (Raghavan et al. 2008). The peptide may be further modified/cleaved by ER-associated aminopeptidases and is then loaded onto the MHC class I molecule (Raghavan et al. 2008). Peptide containing MHC class I complex is then released and transported to the plasma membrane.

MHC class II molecules tend to recognize exogenous peptides acquired from the endocytic pathway. The α and β chains of the MHC class II molecule associate with an invariant chain in the ER that stabilizes the molecule and transports the complex via the trans-Golgi network to the late endosomal MHC class II compartment (MIIC) (Rocha & Neefjes 2008). There, the invariant chain is cleaved by cathepsin S and L to produce a small peptide fragment called class II-associated invariant chain peptide (CLIP) (Rocha & Neefjes 2008). An accessory protein called DM (DO in B cells) replaces CLIP residing in the peptide binding groove with the antigenic peptide (Rocha & Neefjes 2008). The MHC class II-peptide complexes are then transported to the cell membrane.

1.6. T cell activation

T cells interact transiently and non-specifically with many different APCs by binding to adhesion molecules such as ICAM-1. When T cells recognise their respective peptides bound to the MHC class I or II complex, a conformational change in adhesion molecule LFA-1 on T cells is induced via TCR signalling which also aids tighter binding to ICAM-1 or ICAM-3 expressed on APCs, thus resulting in the formation of an immunological synapse (Brownlie & Zamoyska 2013). A three signal T cell activation model has been proposed for the process of antigen presentation, resulting in differentiation of naïve T cells into either antigen-specific T helper cells or cytotoxic T lymphocytes (CTL). The first signal, also known as Ag-specific activation, is the interaction of TCR and antigen bound to the MHC molecule. The second signal (co-stimulation) leads to interaction of co-stimulatory molecules CD80/86 expressed on the APC and receptors (CD28) on the surface of T cells (Goral 2011). Co-stimulation is required to maintain T cell activation. The absence of co-stimulatory signal may lead to limited T cell proliferation, T cell anergy or apoptosis (Harding et al. 1992). Lastly, signal 3 leads to upregulation of cytokines such as interleukin (IL)-12 and their receptors on the surface of T cells (Goral 2011). Release of cytokines results in clonal expansion of T cells. The magnitude of the T cell response may be affected by factors such as the antigen, its concentration and the TCR binding affinity (Keck et al. 2014). Repeated T cell exposure to antigens maintains large populations of T cells. The majority (~90-95%) of antigen-specific T cells, however, are eliminated when antigen exposure is low (Harty & Badovinac 2008). The remaining 5-10% of antigen-specific T cells become long-lived central memory or effector memory T cells that can respond more rapidly and effectively upon subsequent antigen encounter.

1.7. T cell roles in controlling tumours

The recent success of checkpoint inhibitors has highlighted the important role that T cells play in controlling malignancies. Several characteristics make T cells an appealing cancer therapy: 1) they can differentiate between normal and malignant cells; 2) immune responses are broad and robust (10,000-fold clonal expansion once activated); 3) they can migrate to the tumour and 4) the generation of a memory T cells can provide long term therapeutic benefit (Perica et al. 2015).

$CD4^+$ helper T cells play a critical role in promoting adaptive immune responses by priming and activating $CD8^+$ T cells, generating $CD8^+$ memory T cells (Shedlock & Shen 2003) or recruiting NK cells and macrophages to tumour sites (Durrant et al. 2000). In addition to this, $CD4^+$ T cells also prime and induce maturation of APCs and B cells. Studies have demonstrated a role for infiltrating antigen-specific cytotoxic $CD4^+$ T cells in arresting tumour progression (Tran et al. 2014; Matsuzaki et al. 2015; Shklovskaya et al. 2016; Greenberg et al. 1985). Tumours expressing MHC class II peptides can be killed by direct cytotoxic action of $CD4^+$ T cells mediated in part by perforin and granzyme release (Quezada et al. 2010; Haabeth et al. 2014). Although haematopoietic tumours and melanomas can express MHC class II (Mendez et al. 2009), the vast majority of somatic cells and solid tumours do not (although expression can be induced by IFN-γ) (Ting et al. 2002; Chamuleau et al. 2006). Consequently, the majority of direct anti-tumour immune responses are thought to be executed by $CD8^+$ T cells. $CD8^+$ T cells directly lyse cells expressing target peptides. The ratio of CD8 T cells/T_{Regs} have been associated with benefit on overall survival of cancer patients (Gooden et al. 2011). Tumour infiltrating memory $CD8^+$ T cells have shown clinical effect in Merkel cell carcinoma (Paulson et al. 2011) and colorectal cancer patients (Galon et al. 2006).

Although T_{Regs} play an important role in suppressing autoimmunity (they are important in maintaining self-tolerance in autoimmune diseases as well as allergy), in cancer, these cells augment tumour growth progression. T_{Regs} release cytokines that suppress other immune cells (T cells, B cells, NK cells, DCs and macrophages) (Sakaguchi et al. 2009). Poor prognosis has been associated with large frequencies of T_{Reg} tumour infiltrating lymphocytes (TIL) in tumour tissues. Depletion of T_{Regs} in a mouse cancer model, has been shown to result in increased infiltration of $CD8^+$ T cells into the tumour site and establishment of anti-tumour immunity upon second tumour challenge (Shimizu et al. 1999; Li et al. 2010). Analysis of tumour-antigen (5T4) specific $CD4^+$ T cell responses in colorectal cancer patients showed correlation between more advanced stages of cancer and weak T cell responses

induced. The loss of T cell responses was caused by induction of antigen-specific T_{Regs}. Depletion of T_{Regs} using cyclophosphamide, however, enhanced 5T4-specific $CD4^+$ T cell responses in patients (Scurr et al. 2013).

1.8. Adoptive T cell therapy

The majority of tumour antigens are self-antigens and consequently poor immunogens due to the central tolerance mechanism established in the thymus (section 1.2). T cells capable of targeting tumour antigens therefore tend to be low frequency, low avidity and may even be anergic (Crespo et al. 2013; Staveley-O'Carroll et al. 1998). In addition to this, cancer patients undergo multiple rounds of chemotherapy treatment that suppresses their anti-tumour immune responses. Adoptive T cell therapy is one form of cancer immunotherapy that has gained interest in the community. Adoptive T cell therapy is an alternative to cancer vaccines and has been successful in treating cancer, when harnessed correctly. Using this approach, cytotoxic T cells specific for the cancer are isolated from a patient, modified to recognize and destroy cancer cells, expanded *ex vivo* and re-infused back into the patient to increase T cell frequency, specificity, avidity and enhance effector function (Perica et al. 2015). Tumour-specific T cells can be generated by stimulating them with a tumour-specific antigen presented by autologous APCs (i.e. DCs). For effective treatment it is important to obtain large numbers of cells; it has been suggested that at least 1-10% of $CD8^+$ T cells need to be antigen-specific (2-20× 10^9 T cells/inoculum in humans) (Yee 2005). Additional things to consider are longevity of T cells, their capacity to migrate to tumour sites and the strength of anti-tumour response.

In order to generate effective T cell cancer therapy, it is important to break tolerance which may, however, result in autoimmunity and put the individual at risk. The most success in clinical trials has been achieved by stimulating T cells with tumour antigens that tend to be neonatal, expressed in compartments (e.g. testes) or exogenous (viral antigens). Adoptive T cell therapy has shown promise in leukaemia and Epstein–Barr virus (EBV)-associated post-transplant lymphoproliferative disease (Heslop et al. 1996). The use of T cells expressing α and β chains specific for melanoma-associated antigen recognized by T cells 1 (MART-1) have resulted in tumour regression in melanoma (Morgan et al. 2006). Anti-CD19 chimeric antigen receptor (CAR) T cell therapy in acute lymphoblastic leukaemia (ALL) patients led to complete remission in 90% patients (Maude et al. 2014). The use of $CD8^+$ T cells from a matched donor, stimulated against Wilms tumour antigen 1 showed transient anti-leukemic responses in some patients (Chapuis et al. 2013). Other types of cancer in which adoptive therapy has been applied include ovarian cancer, renal cell

carcinoma, B cell ALL and neuroblastoma (Davila et al. 2014; Childs et al. 2000; Lamers et al. 2006; Park et al. 2007). Adoptive cell therapy has been adapted to DCs to generate a drug (sipuleucel-T (Provenge)) approved by the United States Federal Drug Administration to treat prostate cancer.

Although adoptive T cell therapy can clearly be beneficial, its routine use in cancer treatment is constrained by the fact it is both expensive, cell production costs >£25,000 per patient (Sharpe & Mount 2015), technically complex and labour intensive. Cells may need to be cultured for 4-16 weeks (Yee 2005) whilst the patient remains hospitalized. Another disadvantage to using adoptive T cell therapy includes thermal instability - cells require cryopreservation, storage and transport (Yee 2005). Finally, on-target off-tumour toxicity poses a possible threat to patients (Tey 2014; Johnson et al. 2009) whereby engineered TCR chains and the endogenous TCR chains may re-arrange to create a TCR with distinct specificities.

1.9. Development of cancer vaccines

1.9.1. Criteria to consider when designing vaccines

While adoptive T-cell therapy is designed to deliver a transient therapeutic immune response, vaccination with a cancer antigen has the potential to stimulate a sustained T-cell response *in vivo* either prophylactically or therapeutically. Ideally, a vaccine vector should first and foremost be effective - a single dose of the vaccine should confer life-long immunity to the cancer preferably within 2 weeks after administration (Beverley 2002). The vaccine should activate B cells, APCs, Th cells and CTLs that would produce pro-inflammatory cytokines as well as generate memory T and B cells. Secondly, the vaccine should be safe in the entire population including immunocompromised individuals, and transmission of the pathogen should be inhibited (Beverley 2002). For virus vectors, this means that there should be limited replication and expression of viral proteins. Mortality rates of >1 in 10^6 would not be considered safe in most countries. In addition to this, there should be no pleiotropic effects induced by these vaccines. Ideally, the vaccine should also be affordable. In addition to this, the route of administration is important. The preferential route of vaccine administration is oral, nasal or transcutaneous. Less favoured route of administration are injections since delivery requires trained personnel. High thermal stability (does not require cold chain) is another requirement that would greatly reduce the cost. Other requirements

include allogeneity of the vaccine so that individuals with polymorphic MHC alleles could receive the same vaccine.

1.9.2. Virus-based cancer vaccines

Currently available vaccines used to treat cancer include tumour cell vaccines, antigen vaccines (proteins or peptides), DC vaccines (the most successful thus far, e.g. Sipuleucel-T, Provenge, licensed for use in prostate cancer patients) and vector-based vaccines (viruses, bacteria, yeast). The innate immunogenicity of viral and bacterial vectors is likely to stimulate pathogen-associated molecular pattern (PAMP) recognition and thus, robust immune responses. Viral vectors provide an effective mechanism for high level, sustained *in vivo* expression of cancer antigens in an autologous setting, permit delivery of multiple antigens and co-delivery of immunostimulatory molecules that promote appropriate responses (e.g. IL-2) and allow for direct delivery to the site of the tumour. Consequently, this helps to promote targeting of the immune response to the active tumour. Virus-based vectors infect cells that present peptides bound to MHC class I and II complexes on the cell surface. The peptide is presented more efficiently to the immune system and can induce a more robust immune response.

According to the Wiley gene therapy clinical trial database (Figure 1), only 29% of vaccines targeting cancer currently being tested in clinical trials are non-viral. The most widely used vector is adenovirus, followed by retroviruses (18%) and members of the *Poxviridae* family of viruses (vaccinia viruses, fowlpox viruses, canarypox viruses and Modified Vaccinia Ankara virus (MVA)) that comprise 14% of total vectors being developed. The remaining 32% of vectors include herpes simplex viruses (HSV), lentiviruses, measles viruses, Newcastle disease viruses, polioviruses, Semliki forest viruses, Simian viruses and Vesicular stomatitis viruses.

One of the most successful cancer vaccines is a replication-deficient adenovirus encoding WT p53 protein under the control of Rous Sarcoma Virus (RSV) promoter called Gendicine. This vaccine has been approved by the Chinese State Food and Drug Administration in 2003 for treating head and neck squamous cell carcinoma (HNSCC) patients. Phase II/III clinical trials in neck squamous cell carcinoma patients showed that when Gendicine was used with radiotherapy, 64% of the patients exhibited complete regression whilst 29% had partial regression (Peng 2005). Gendicine has also enhanced hepatocellular carcinoma patient survival and 33% of lung cancer patients had partial regression and the use of the vaccine alleviated disease symptoms (Peng 2005).

A canarypox virus-based vaccine (ALVAC-CEA-B7.1)(see Table 1) encoding carcinoembryonic antigen (CEA) and B7.1 co-stimulatory molecule found on APC that has a T cell activating receptor has shown induction of CEA-specific T cells and stabilisation of disease in three patients (Hörig et al. 2000). PSA-TRICOM under the name of PROSTVAC is a vaccine regimen that consists of sequential vaccinia virus priming and fowlpox virus boost vaccinations. This vector expresses prostate-specific antigen (PSA) and proteins expressed on APCs (LFA-3, ICAM-1, and B7.1) and infects a broad range of cells including professional APCs such as DCs. Evaluation of six clinical trials showed that PROSTVAC induced a ≥ 2-fold increase in PSA-specific T cell counts in 57% of patients (Gulley et al. 2014). In addition to this, lower frequency of T_{Regs} and higher $CD4^+$ T cell counts were linked to longer overall survival (Gulley et al. 2014). An MVA virus encoding a tumour-associated 5T4 antigen (TroVax) developed by Oxford BioMedica (Kim et al. 2010) has been tested in colorectal, renal cell carcinoma and prostate cancer patients. TroVax induced low frequencies of 5T4-specific T cells as well as 5T4-specific antibodies that were associated with progression-free survival (Harrop et al. 2010; Harrop et al. 2013). In a phase III clinical trial conducted in renal patients, TroVax did not meet its primary endpoint of prolonging the overall survival, however, a group of patients were identified that showed signs of improvement (Amato et al. 2010).

1.9.2.1. Oncolytic vaccines

A different approach to replication-defective anti-cancer vaccines (described in section 1.9.2) is the use of oncolytic vectors which have been designed to selectively replicate in tumour cells. As part of their replication cycle, oncolytic vectors lyse tumour cells, thus promoting the anti-tumour effect. In 2005, H101 was the first oncolytic vaccine approved by the Chinese State Food and Drug Administration for treating nasopharyngeal cancer. When tested in a Phase III clinical trial, H101 induced responses in 78.8% of head and neck or oesophagus squamous cell cancer patients receiving chemotherapy treatment as well as the vaccine compared to 39.6% in patients treated with chemotherapy alone (Xia et al. 2004). A herpesvirus-based oncolytic vector that has been FDA approved for treating advanced melanoma called T-VEC, expresses granulocyte macrophage colony-stimulating factor (GM-CSF). Advanced melanoma patients receiving T-VEC in a phase III trial showed better responses and an improvement in overall survival (23.3 months compared to 18.9 months) (Andtbacka et al. 2015).

A major challenge in developing an effective cancer immunotherapy is to induce a sufficiently strong and durable immune response, capable of overcoming tolerance, poor

immunogenicity and an immunosuppressive tumour microenvironment. Although the aforementioned vectors have shown efficacy in clinical trials, especially oncolytic vectors, their use would not be suitable in immunocompromised patients due to safety concerns. There is a clear need to develop and enhance more effective vaccine delivery system capable of generating more potent and effective tumour-specific immune responses.

Figure 1: Vector usage in current cancer gene therapy trials. (Generated using data from (Wiley 2017))

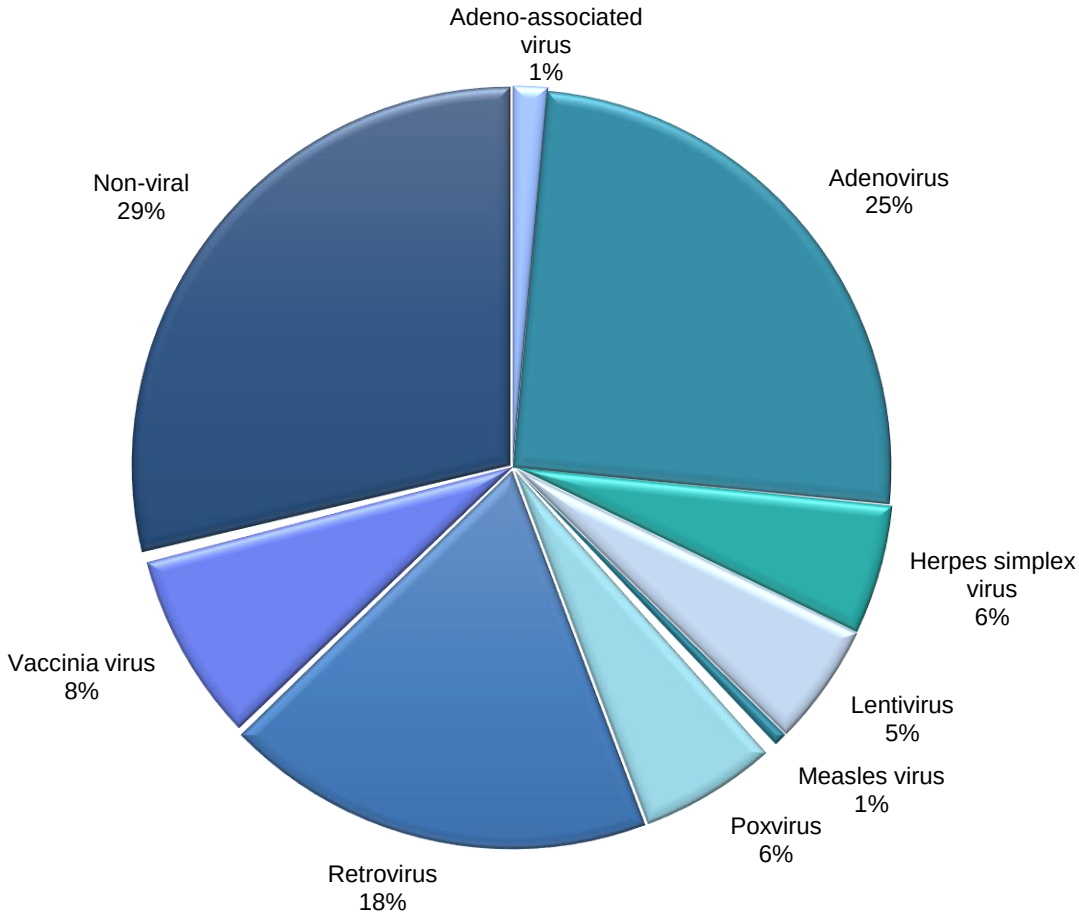

Table 1: Recent clinical trials using viral vectors as vaccine carriers (adapted from: (Cawood et al. 2012))

Vaccine name	Virus	Tumour-associated antigen/Modifications	Immunostimulatory gene	Outcome	References
ALVAC-CEA-B7.1	Canary pox	CEA	B7.1	16% patients with CEA-specific T cell responses showed disease stabilisation	(Hörig et al. 2000)
TRICOM-PSA (PROSTVAC)	Vaccinia/Fowlpox	PSA	TRICOM: (LFA-3, ICAM-1, and B7.1)	Compiled data showed that 57% of patients tested had a 2-fold increase in the frequency of PSA-specific T cells following vaccination	(Gulley et al. 2014)
OXB-301 (TroVax)	MVA	5T4		Well tolerated vaccine. Higher 5T4-specific antibody levels linked to improved patient survival. No difference in the overall survival was seen in phase III clinical trial conducted in renal cell carcinoma patients.	(Amato et al. 2010; Harrop et al. 2010; Harrop et al. 2007)
Gendicine	Ad	E1 replaced with Rous Sarcoma Virus (RSV) promoter and WT p53		Approved by State Food and Drug Administration of China in 2003 for treating head and neck squamous cell carcinoma. In clinical trials: 64% of late-stage head and neck squamous cell carcinoma (HNSCC) tumours experienced complete regression and 32% experienced partial regression.	(Pearson et al. 2004)
Oncolytic vectors					
JX-594	Vaccinia	ΔThymidine kinase	GM-CSF	Tested in phase I and I/II trials in liver cancer, melanoma and colorectal cancer patients: partial responses, stable disease and lymphocyte infiltration	(Park et al. 2008; Hwang et al. 2011; Breitbach et al. 2011)
OncoVex-GMCSF/ Talimogene laherparepvec (T-VEC)	HSV	ΔICP34.5 and ΔICP47	GM-CSF	Approved by the FDA in 2015 for treatment of melanoma. In phase I, I/II and III melanoma, breast, head and neck, gastrointestinal cancer: induction of local and systemic tumour specific T cell responses, decreased regulatory T cells; prolonged progression-free survival, tumour-specific responses and complete remission	(Hu et al. 2006; Harrington et al. 2010; Senzer et al. 2009; Kaufman et al. 2010; Bilsland et al. 2016)
Oncorine (H101)	Ad	Δ E1B-55kDa		In 2005, the State FDA of China approved the use of Oncorine for treating nasopharyngeal cancer	(Ma et al. 2009)

Ad – adenovirus; CEA - carcinoembryonic antigen; FDA- Food and Drug Administration; GM-CSF - granulocyte-macrophage colony-stimulating factor; HSV – Herpes Simplex virus; ICAM - intercellular adhesion molecule; LFA - Lymphocyte function-associated antigen; MVA- Modified Vaccinia Ankara virus; PSA – prostate specific antigen; WT – wild type.

1.9.3. Cancer antigens

A key requirement for a cancer vaccine, is that it must raise an immune response against a protein present on the tumour. Cancer antigens were first discovered in 1960s and since then have been widely used in attempts to eradicate cancer (Black et al. 1963). Currently, tumour antigens (see Table 2) are classified into: 1) differentiation antigens (e.g. tyrosinase; Tyrosinase-Related Protein, TRP1/gp75; TRP2; glycoprotein 100, gp100 and Melanoma antigen, Melan-A) (Vigneron 2015) expressed on tumours as well as normal differentiated cells; 2) overexpressed proteins (e.g. HER2; Wilms' Tumour 1, WT1; Epidermal Growth Factor Receptor, EGFR; telomerase and survivin)(Vigneron 2015; Bright et al. 2014) that provide a growth advantage to the cell; 3) mutant proteins (e.g. ras*, β*-raf, CDK4, p53, BCR-ABL) (Vigneron 2015) that promote cell cycle deregulation, a replicative advantage or tissue invasiveness; 4) antigens altered post-translationally (e.g. mucin 1, MUC1) (Ghosh et al. 2013); 5) oncoviral antigens (E6 and E7 from HPV; T antigen of Simian virus 40 (SV40) and antigens from EBV) (Tashiro & Brenner 2017); 6) idiotypic antigens (Ig, TCR) (Zarour et al. 2003); 7) proteins normally restricted to testes (e.g. New York oesophageal Squamous cell carcinoma 1, NY-ESO-1; melanoma antigen, MAGE; B melanoma antigen, BAGE; G antigen, GAGE and Synovial Sarcoma X-chromosome breakpoint 1, SSX-1) (Zendman et al. 2003) and 8) oncofoetal proteins (e.g. CEA and 5T4) whose expression is normally restricted to testes, ovaries or trophoblasts yet absent on somatic cells (Woods et al. 2002; Shuster et al. 1977).

The vast majority of proteins expressed on cancerous cells are also expressed on normal tissues. Tumour-specific antigens are expressed only on neoplastic cells whereas tumour-associated antigens are antigens also found on normal tissues that display more abundant expression on tumours. Tumour-associated antigens do not bind T cells as well as tumour-specific antigens since these are foreign and more immunogenic (Stone et al. 2015).

Table 2: Tumour antigens and their distribution (adapted from (Wurz et al. 2016))

Antigen	Cancer types
B melanoma antigen (BAGE)	Glioblastoma; ovarian
Carcinoembryonic antigen (CEA)	Colorectal cancer
Epidermal growth factor (EGF)	Non-small cell lung cancer
Epidermal growth factor receptor (EGFR)	Non-small cell lung cancer
G antigen (GAGE)	Cervical
Glycoprotein 100 (gp100)	Melanoma
Human papillomavirus 16 (HPV-16)	Cervical; squamous cell carcinoma of the head and neck
Melanoma antigen 3 (MAGE-A3)	Melanoma; non-small cell lung cancer
Melanoma antigen C2 (MAGE-C2)	Gastric; melanoma; multiple myeloma
Melanoma antigen D4 (MAGE-D4)	Colorectal cancer
Melanoma antigen (Melan-A)	Melanoma
Mucin 1 (MUC1)	Non-small cell lung cancer; breast; prostate
New York oesophageal squamous cell carcinoma 1 (NY-ESO-1)	Ovarian; melanoma
Synovial sarcoma X-chromosome breakpoint 1 (SSX1)	Prostate; multiple myeloma
Survivin	Melanoma; glioma; solid tumours
Telomerase	Pancreatic
Wilms' Tumor-1 (WT1)	Ovarian; uterine; acute myelogenous leukaemia
5T4	Renal cell carcinoma; colorectal cancer; prostate

1.9.3.1. 5T4

5T4 protein is a heavily N-glycosylated, transmembrane protein that is 72 kD in size (Hole & Stern 1990). It is made up of an extracellular domain comprising of leucine-rich repeats that play a role in protein-protein interactions, a transmembrane domain and a short cytoplasmic tail (Shaw et al. 2002). Human 5T4 protein shares 81% sequence identity with mouse 5T4. The two proteins differ primarily around the regions containing glycosylation sites (Shaw et al. 2002).

5T4 is classed as an oncofoetal tumour-associated antigen since it is highly expressed (see Table 3) on primary and metastatic solid tumours (cervical, colorectal, gastric, ovarian, prostate, lung and renal cancers) as well as human trophoblasts (Southall et al. 1990; Stern et al. 2014). It has been shown that 5T4 downregulates E-cadherin (Carsberg et al. 1996), enhances matrix metalloproteinase activity (F. V Castro et al. 2012), inhibits Wnt/β-catenin signalling, activates non-canonical Wnt pathways (Kagermeier-Schenk et al. 2011), disrupts actin microtubules (Carsberg et al. 1996) and is involved in facilitating CXCL12/CXCR4 chemotaxis (Southgate et al. 2010). The aforementioned roles are linked to epithelial mesenchymal transition (EMT), which is important for metastatic spread/invasion of cancer cells. Overexpression of 5T4 in mouse fibroblasts, epithelial cells and canine epithelial cells leads to altered cell morphology with reduced adherence and increased cellular motility (Carsberg et al. 1995; Carsberg et al. 1996). In addition to this, higher 5T4 expression has been associated with worse clinical outcomes in colorectal, gastric, ovarian and head and neck squamous cell carcinoma patients (Wrigley et al. 1995; Starzynska et al. 1992; Starzynska et al. 1998; Kerk et al. 2016).

The limited tissue distribution of 5T4 in healthy adults, its association with metastasis and expression on cancer stem cells all make this molecule an exceptionally attractive therapeutic target. Stern and Harrop used the criteria devised by the National Cancer Institute to calculate the rank of 5T4 antigen among other priority cancer vaccine target antigens. Interestingly, 5T4 ranked 9th out of 75 tumour-associated antigens, higher than NY-ESO-1, CEA, gp100, PSA and p53 (Stern & Harrop 2017). To date, four different approaches have been adopted to target 5T4: 1) an antibody–superantigen fusion protein, 2) an antibody-drug conjugate (ADC) 3) CAR T cell therapy and 4) TroVax cancer vaccine (Stern & Harrop 2017). An antibody-superantigen fusion protein developed under the name of ANYARA (naptumomab estafenatox) has been evaluated in numerous clinical trials (Eisen et al. 2014). The use of naptumomab estafenatox together with interferon α has improved survival rates of advanced renal cell carcinoma (RCC) patients (Elkord et al. 2015; Hawkins et al. 2016). An ADC targeting 5T4 is

currently undergoing preclinical trials but thus far has shown improvement in survival of mouse models of ALL, an effect further enhanced when ADC was used in conjunction with dexamethasone (McGinn et al. 2017). The use of anti-5T4 antibody-drug conjugate (MEDI0641) in a HNSCC model resulted in durable tumour-regression and depletion of cancer stem cells (Kerk et al. 2016). CAR T cell therapy program developed by Oxford BioMedica (OXB-302) is currently undergoing analyses of the most recent clinical trial. Previous work tends to suggest, however, that 5T4 epitope-specific CTL cells are efficient at killing 5T4 expressing cancer cells as well as impede tumour growth completely when prophylactically inoculated into cancer models (Tykodi et al. 2012; Al-Taei et al. 2012). Lastly, TroVax has undergone ten phase I and II clinical trials in different cancer settings and although the primary endpoints of the clinical trials were not met, this vaccine was well tolerated and induced humoral and cellular responses that delayed tumour progression (Hawkins et al. 2009; Amato et al. 2009).

Table 3: 5T4 expression in cancer evaluated using immunohistochemistry of cryostat sections (adapted from (Stern & Harrop 2017))

Cancer	% Positive 5T4 expression
Bladder	100
Breast	96
Cervical	100 97
Colorectal	100 54
Gastric	56 40 52
Non-small cell lung cancer	100 >95
Mesothelioma	100
Ovarian	71 100 79
Pancreatic	100 >95
Prostate	100 84
Renal	95

The table shows a summary of multiple studies (references not shown) identifying 5T4 expression in different types of cancer. Immunohistochemistry was used to confirm 5T4 positive tumours using the monoclonal antibody 5T4 was originally identified with.

1.10. Adenoviruses

1.10.1. Classification

Adenoviruses are safe, effective and widely used vaccine vectors, capable of inducing specific T-cell responses. The *Adenoviridae* family of viruses consists of three genera that infect mammals, birds and fish and are called *Mastadenoviruses*, *Aviadenoviruses* and *Ichtadenoviruses*, respectively. In addition to this, two genera *Atadenoviruses* and *Siadenoviruses* are found in vertebrate species (International Committee on Taxonomy of Viruses (ICTV) 2016). Each genus is further subdivided into a total of 62 species of viruses. Human adenoviruses are part of *Mastadenovirus* genus. Currently, there are seven human mastadenoviruses that are called A-G that were classified based on serology, hemagglutination and oncogenic properties. Genome analysis of the hexon capsid protein led to diversification of human mastadenoviruses into 57 serotypes with the most common ones being human serotypes 2 and 5 (subgroup C).

1.10.2. Disease and tropism

Adenoviruses were first isolated from adenoid tissue-derived cell culture. Since then, work using these viruses has revealed that they infect a wide variety of dividing and non-dividing cells. Interestingly, virus tropism may be species-dependent (see Table 4). Human adenovirus species A-C and E infect primarily the respiratory tract, species B- E are associated with eye infections, species A, C, D, F and G infect intestinal tract whereas species B and C affect urinary tract and tonsils/adenoids, respectively (Arnberg 2012). Other species-specific tissues include pharynx, pancreas, spleen, liver, myocardium and central nervous system (CNS) (Wold & Ison 2013).

Approximately 2-5% of respiratory infections in humans are caused by adenoviruses. In accordance with serotype-specific tropism, adenovirus serotypes 3, 5 and 7 have been associated with lower respiratory tract infections; serotypes 4 and 7 are responsible for acute respiratory diseases; serotypes 8, 19 and 37 are known for causing epidemic keratoconjunctivitis whereas serotypes 40 and 41 are associated with gastroenteritis. In immunosuppressed and immuno-naïve individuals, adenoviruses have also been linked to incidents of fatal pneumonia, hepatitis and encephalitis (Ison 2006).

Table 4: Human Adenovirus Receptor usage and Tropism adapted from (Arnberg 2012)

Species	Serotypes	Receptors	Tropism
A	12, 18, 31	hCAR	Cryptic (enteric, respiratory)
B1	3, 7, 16, 21, 50	CD46, DSG-2, CD80, CD86	Respiratory, ocular
B2	11, 14, 34, 35	CD46, DSG-2, CD80, CD86	Renal, ocular, respiratory
C	1, 2, 5, 6	hCAR, HSPG, VCAM-1, SR, MHC-I-α2	Respiratory, ocular, lymphoid, hepatic
D	8-10, 13, 15, 17, 19, 20, 22-30, 32, 33, 36-39, 42-49, 51, 53, 54	SA, CD46, hCAR	Ocular, enteric
E	4	hCAR	Ocular, respiratory
F	40, 41	hCAR	Enteric
G	52	nd	Enteric

hCAR, human Coxsackievirus and adenovirus receptor; DSG-2, desmoglein-2; HSPG, heparan sulfate proteoglycan; VCAM-1, vascular cell adhesion molecule 1; SR, scavenger receptor; MHC-I, major histocompatibility complex class I; SA, sialic acid; nd, not determined.

1.10.3. Immunogenicity

Adenoviruses are highly immunogenic viruses. The first trigger of innate immunity is adenovirus fiber protein binding to Coxsackievirus and adenovirus receptor (CAR) which activates ERK1/2, JNK, MAPK and Nuclear factor kappa-light-chain-enhancer of activated B cells (NF-κB) and upregulates chemokines (IL-8, GRO-alpha, GRO-gamma and RANTES and interferon-inducible protein 10) (Tamanini et al. 2006). The presence of extracellular virions activates the complement system which leads to blocking of viral attachment and entry. Pre-existing neutralizing antibodies are found in the majority of the population and prevent virus uptake (Nwanegbo et al. 2004; Zhang et al. 2013; Piedra et al. 1998). During natural adenovirus infection, neutralizing antibodies to the fiber and penton are induced whilst vaccination using adenovirus vectors/multiple infections result in accumulation of neutralizing antibodies to the hexon (Bradley et al. 2012; Yu et al. 2013). The binding of neutralizing antibodies block Ad receptor binding and entry and lead to macrophage uptake (Schagen et al. 2004). Interestingly, virion binding to factor X (an enzyme of the coagulation pathway) serves as a protection mechanism against inactivation by complement and neutralization by IgM antibodies (Doronin et al. 2012; Z. Xu et al. 2013). Adenovirus PAMPs trigger toll-like receptors, TLRs (e.g. TLR2 and TLR9) in a cell type-specific manner which activate type I IFN (Appledorn et al. 2008). Secretion of IFN acts a chemoattractant for lymphocytes, monocytes and DCs. Adenoviruses infect APCs (i.e. DCs) and stimulate their maturation which results in improved activation of the adaptive immune response (Morelli et al. 2000). T-cell responses are induced by the structural proteins (i.e. capsid). Adenovirus-specific $CD4^+$ and $CD8^+$ T cells recognize hexon and have been found in PBMCs of seropositive patients. $CD8^+$ T cells exist in larger frequencies than $CD4^+$ T lymphocytes (Wold & Ison 2013). The $CD8^+$ T cells exhibit an effector memory phenotype (Bassett et al. 2011).

A lot of work in the adenovirus field has been carried out in mice and involves the use of recombinant vectors. It has been shown that within minutes of systemic adenovirus administration, innate immune responses to the vector are induced and increase until about 24 h post infection (pi). NK cell activation is dependent on accessory cells (i.e. macrophages and DCs) and occurs hours after the administration of Ad vectors (Peng et al. 2001; Ruzek et al. 2002; Zhu et al. 2010). Transcription of genes is not required for induction of innate immune responses (Schnell et al. 2001; Muruve et al. 1999). The dose of the virus used, on the other hand, plays an important role in the induction of innate immune responses but not to adaptive immune responses (Liu & Muruve 2003). The route of vector administration together with the level of pre-existing neutralizing antibody levels plays a more important role in the induction of humoral immune

responses (neutralizing antibodies) than dosage (Harvey et al. 1999). Recombinant adenovirus vectors are cleared within 2-3 weeks due to $CD4^+$ and $CD8^+$ T cell responses to the vector and the expression cassette (Yang et al. 1994; Yang et al. 1996; Zhu et al. 2007).

1.10.4. Genomic organization

Adenoviruses are double stranded DNA viruses that are approximately 26-46 kb in length. Conserved genes are encoded in the centre of the genome whilst genes specific to the particular species are located at the termini. The ends of the genome (Figure 2) contain identical inverted terminal repeats (36-200 base pairs, bp) necessary for viral DNA replication. Adenoviruses contain genes encoding over 40 proteins. Early proteins (E1A, E1B, E2A, E2B, E3 and E4) are expressed before the onset of viral DNA replication whereas late proteins (L1-L5 and UXP) are expressed afterwards (Tollefson et al. 2007). The E1A gene products activate gene transcription and alter the cell cycle so that it enters the S phase. The E1B proteins prolong cell survival by inhibiting apoptosis. The E2 region encodes proteins that play a role in DNA synthesis whereas E3 and E4 proteins are essential for immunomodulation of the host cell environment, transcription, splicing and translation. Some late gene products (L1-L5 and UXP) are viral capsid proteins whereas others may play a role in DNA replication, virion assembly and DNA packaging (Tollefson et al. 2007). In addition to early and late proteins, adenoviruses encode four intermediate gene products (IX, IVa2, VA RNAs I and II) that are vital for DNA packaging, and modulating host cell responses.

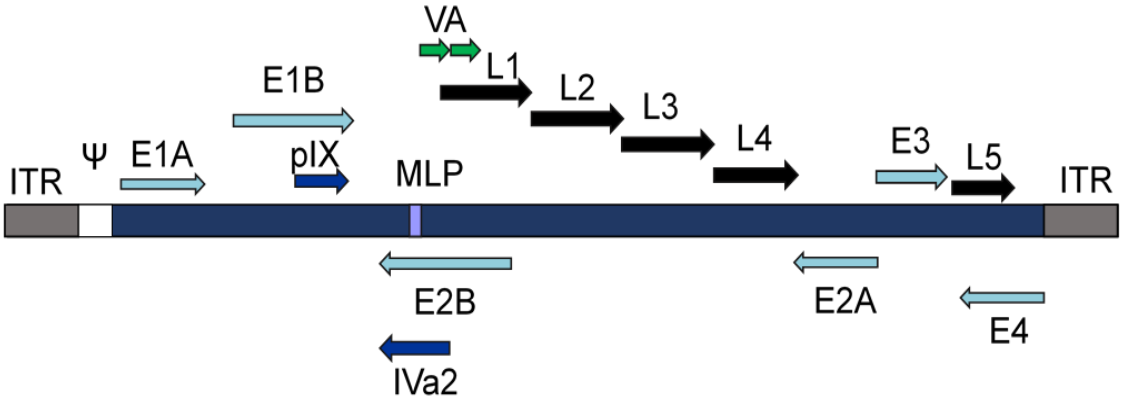

Figure 2: Genome organization of Ad5. The genome is ~36 kb in size divided into early (light blue), intermediate (dark blue) and late transcription units (black). Inverted terminal repeats (ITRs) on either end of the genome play a role in DNA synthesis whereas the packaging signal (Ψ) is involved in packaging viral DNA into the virion. Major late promoter (MLP) is required for late gene transcription. Viral-associated (VA) RNAs (green) play a role in virus replication, interferon signalling and RNA interference pathway.

1.10.5. Generation of adenovirus vectors

Adenoviruses have been well characterized and thus, modifications to the genome making these viruses safe and less immunogenic have also been established. Three different types of replication-deficient adenovirus vectors have been constructed. In first-generation vectors, E1 and (in some vectors) the E3 region are removed and may be replaced with an expression cassette (Danthinne & Imperiale 2000). Since proteins produced from the E1 region are required for trans-activating expression of other viral genes, these vectors are replication-deficient and need to be grown in complementing cell lines that express the E1 proteins (e.g. HEK293, 911 and PER.C6) (Danthinne & Imperiale 2000). The E3 gene products are non-essential for virus growth *in vitro* and therefore do not need to be trans-complemented (Danthinne & Imperiale 2000). First-generation vectors can accommodate ~5-8 kb of foreign DNA, due to DNA packaging constraints (Danthinne & Imperiale 2000; Vetrini & Ng 2010). Second-generation vectors are also E2/E4-deleted to allow insertion of 10-14kb DNA (Danthinne & Imperiale 2000). The E4 region is essential for virus replication; these vectors must be grown in cells that also trans-complement the E4 region. In addition to this, a third generation of vectors have also been developed. These vectors, termed 'gutted vectors' have all of the viral genes deleted and only encode the cis-acting sequences which increases the coding capacity of these vectors to 37 kb (Danthinne & Imperiale 2000). Growing these vectors up requires a helper virus encoding adenovirus genes, and a number of techniques must be used to reduce contamination of virus stocks with the helper virus (Parks et al. 1996).

1.10.6. Currently available anti-cancer vectors

To date, there have been over 500 clinical trials using adenoviruses in gene therapy settings (Wiley 2017). Several characteristics account for the widespread use of these vectors. Adenoviruses induce strong cellular and humoral immune responses. Due to the small genome size, adenoviruses have been well characterized and can be easily manipulated. In addition to this, adenoviruses can be stably grown to high titre stocks with strong transgene expression. These viruses infect both dividing and non-dividing cells of different types without integrating into the host genome. The use of first-third generation adenovirus vectors ensures safety of these vectors whilst also allowing accommodation of large foreign DNA inserts. First-generation vectors with the E1 deleted region are one of the most commonly used type of adenovirus vectors. Some of these vectors encode costimulatory molecules like CD40 ligand, IL-2, IL-7, IL-12, GM-CSF, IFN-α, β and γ whereas others express tumour-associated antigens (gp100, pp65, a-fetoprotein, MUC-1 and PSA). A number of studies have used adenovirus vectors that encode pro-apoptotic genes (*p53*, tumour necrosis factor (TNF)-α and TNF-related apoptosis-inducing ligand, TRAIL) as well as cell cycle inhibitors (pRB, p21 and p16),

anti-angiogenic agents (endostatin), epidermal growth factor receptors and sodium iodine symporter.

Numerous vectors have been tested in clinical trials but the most widely studied are Advexin and Gendicine that encode the pro-apoptotic protein p53 in the E1 region (Gabrilovich 2006). P53 is a tumour suppressor mutated in about 50% of cancer patients which results in cell cycle disruption and neoplasia. Targeting this protein would thus allow selective cell killing. Advexin has shown promise in non-small cell lung cancer, squamous cell carcinoma of the head and neck, hepatocellular carcinoma, glioma, breast, ovary, prostate, bladder and colorectal cancers (Nemunaitis & Nemunaitis 2011; Senzer & Nemunaitis 2009; Roth 2006; Wold & Ison 2013). The use of Gendicine as treatment for head and neck squamous cell carcinoma was approved in 2003 by the State Food and Drug Administration of China (Peng 2005). Since then, it has been estimated that over 7000 patients have been treated with Gendicine (Ma et al. 2009). Another vector called sitimagene caradenovec, encoding herpes virus thymidine kinase (TK) (serves as a suicide gene as it converts prodrugs to active drugs) has been used in phase I/II and III clinical trials and has improved survival rates in patients with operable high-grade glioma (van Putten et al. 2010). Treatment with a nucleoside analogue ganciclovir results in phosphorylation of ganciclovir. Ganciclovir triphosphate is incorporated into DNA and kills TK expressing cells. Similar vectors have also been used for treating hepatocellular carcinoma and prostate cancer models (Sangro et al. 2010; Cheon et al. 2000). Replication-deficient adenovirus vector (CTL-102) encoding bacterial enzyme nitroreductase has been studied together with a pro-drug (CB1954) in phase I/II clinical trials and showed low cytotoxicity and induction of antibodies in prostate cancer patients (Palmer et al. 2004). More recently, preclinical studies looking at adenovirus vector encoding guanylate cyclase 2C (a receptor serving as a biomarker, expressed primarily on intestinal epithelium that shows dysregulated signalling in colorectal cancer due to loss of hormone ligands, guanylin and uroguanylin), fused to a $CD4^+$ T cell epitope have shown the safety of this vector and strong anti-tumour responses (Snook et al. 2016). In addition to this, adenovirus vector expressing human papillomavirus type 16 and 18 antigens have shown great promise in cancer models in mice (Khan et al. 2017). The large number of trials that use these viruses underlines their safety and immunogenicity.

1.11. Cytomegaloviruses

1.11.1. Classification and significance

Cytomegaloviruses (CMV) have recently come to prominence as potentially powerful vaccine vectors. CMV are members of the *Herpervirales* order, the *Herpesviridae* family, *Betaherpesvirinae* subfamily, the genus *Cytomegalovirus*. The *Cytomegalovirus* genus consists of 8 species of viruses. Other genera that belong to herpesviridae family (see Figure 3) are muromegaloviruses (mouse and rat viruses) and roseoloviruses (human herpesvirus types 6A, 6B and 7) whereas three species that have not yet been assigned to a genus are *Caviid betaherpesvirus* (guinea pig) 2, *Suid betaherpesvirus* (porcine) 2, *Tupaiid betaherpesvirus* 1 (tree shrew) (International Committee on Taxonomy of Viruses (ICTV) 2016).

The viruses within the *Betaherpesvirinae* subfamily exhibit higher level of evolutionary and genetic heterogeneity than other viruses within the *herpesviridae* family. These viruses are highly species-specific, infect differentiated hematopoietic and epithelial cells from homologous species, display similar cytopathology under the electron microscope (EM) and exhibit longer replication cycles during *in vitro* infection (Görzer et al. 2010; Cunningham et al. 2010; Bobek et al. 2010; Renzette et al. 2011).

1.11.2. Prevalence

Human CMV (HCMV) is a ubiquitous pathogen found in 45-100% of humans worldwide, depending on the age and socioeconomic status of the population sampled (Cannon et al. 2010). Generally, in developing countries most people will contract the virus in the first few years of life whereas in developed countries, where the seroprevalence is lower, the virus tends to be gradually acquired through life and thus associated with a higher rate of primary infection during pregnancy (Cannon et al. 2010; Gratacap-Cavallier et al. 1998; Griffiths et al. 1985; Staras et al. 2006). Interestingly, HCMV infection rates tend to be higher in females than males as a study in Germany had demonstrated 49% seroprevalence compared to 42.5% in males (Hecker et al. 2004; Staras et al. 2006). Additional risk factors that associate with higher incidence of HCMV infection include premature birth, lower household income, household crowding, ethnicity and age (Cannon 2009; Bate et al. 2010; Pembrey et al. 2013). Although the total seroprevalence rate in US is 59%, it varies greatly between different states (Cannon 2009). For example, there are 40% of HCMV seropositive individuals in Albany, New York compared to 79% in Houston (Ho 1990).

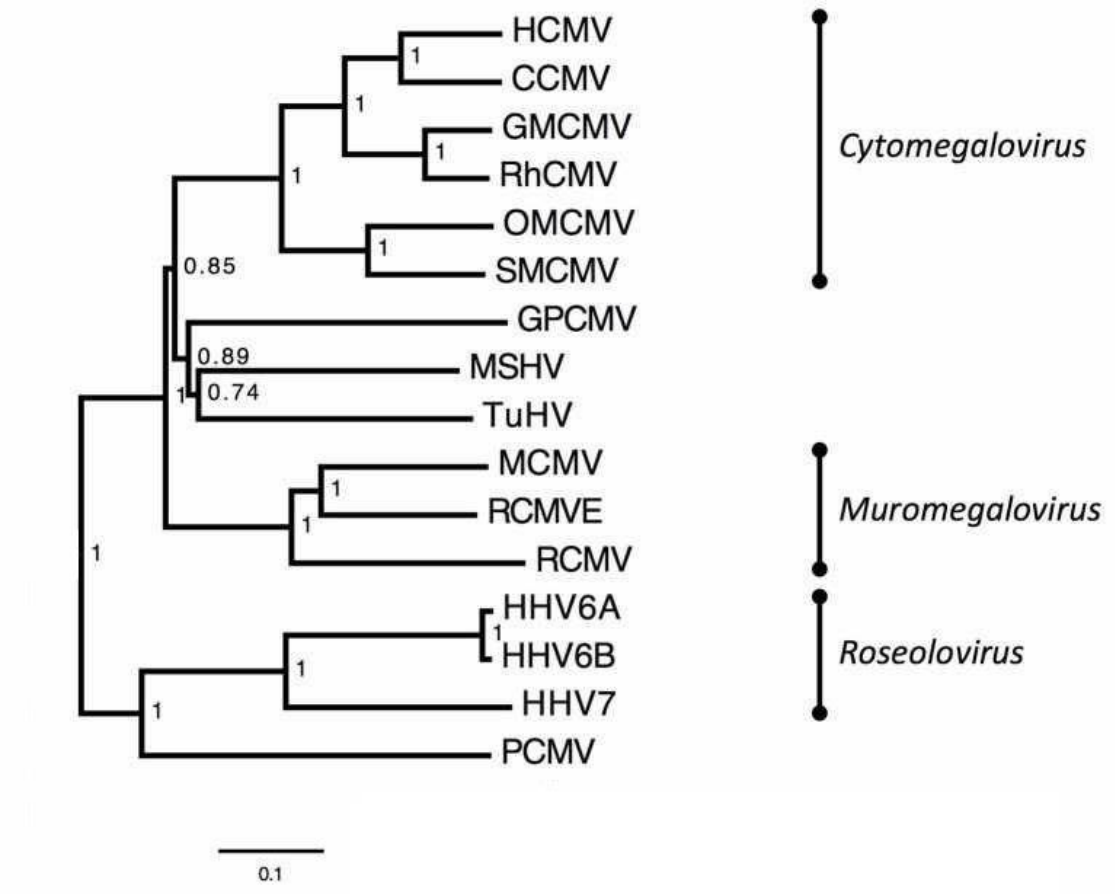

Figure 3: Evolutionary comparison of viruses in the *Betaherpesviridae* family (adapted from (Wilkie et al. 2015)). The phylogenetic neighbour-joining tree was generated using amino acid sequences of essential genes (U38, U39, U40, U41, U57, U60, U77, and U81) from viruses of the *Betaherpesviridae family.* The scale bar represents nucleotide differences/nucleotide. HCMV, human cytomegalovirus; CCMV, chimpanzee cytomegalovirus; GMCMV, green monkey cytomegalovirus; RhCMV, rhesus cytomegalovirus; OMCMV, owl monkey cytomegalovirus; SMCMV, squirrel monkey cytomegalovirus; GPCMV, guinea pig cytomegalovirus; MSHV, Miniopterus schreibersii herpesvirus; TuHV, tupaiid herpesvirus 1; MCMV, murine cytomegalovirus; RCMVE, rat cytomegalovirus England; RCMV, rat cytomegalovirus; HHV6A, human herpesvirus 6A; HHV6B, human herpesvirus 6B; HHV7, human herpesvirus 7; and PCMV, porcine cytomegalovirus.

1.11.3. Tropism

CMV is a species-specific virus that displays very wide tissue tropism, enabling it to infect the majority of organs in the host. Despite species-specificity, the HCMV Towne strain can replicate in chimpanzee fibroblasts *in vitro* (Sinzger & Jahn 1996) whereas, mouse CMV (MCMV) is capable of infecting rats (Smith et al. 1986). In many cases when CMV crosses species, virus can enter cells, express immediate early genes but fails to promote efficient virus DNA synthesis and proceed to late stages of infection.

HCMV can readily be detected in bodily fluids (saliva, semen, urine) with epithelial cells thought to be an important primary site of infection and, ultimately, virus shedding (Sinzger & Jahn 1996). Virus dissemination through the host is mediated primarily in the bloodstream by cells of the immune system, most notably monocytes, macrophages and DCs. Permissive endothelial cells include capillaries and venules lining the brain, in the lung, gastrointestinal tract, cardiac endothelial cells, and microvessels in placenta (Sinzger & Jahn 1996). CMV has also been shown to infect fibroblasts and specialized parenchymal cells such as smooth muscle cells in gastrointestinal tract, neuronal cells and hepatocytes (Sinzger & Jahn 1996; Revello & Gerna 2010; van Den Pol et al. 1999). Following initial infection, the virus establishes latency for the lifetime of the host. CMV is known to persist in bone marrow-derived hematopoietic cells (e.g. $CD34^+$ progenitors and $CD14^+$ monocytes) and endothelial cells (arterial walls). Studies have shown that infection of monocytes with HCMV is limited to expression of latency transcripts with the full transcriptional cascade and progeny virus being produced only when the cells differentiate into macrophages or DCs (Ioudinkova et al. 2006; Mendelson et al. 1996).

The immune system plays a critical role in controlling CMV infections through life. In an immune-naïve individual, the virus spreads to all organs except for pancreas, kidney, spleen, adrenal, small bowel, placenta, liver, brain, bone marrow, and heart (Bissinger et al. 2002). In immunocompromised patients, the disseminated virus can be associated with severe multi-organ disease. Infection can be detected in mucosal layers of the stomach, duodenum, ileum and rectum (Sinzger & Jahn 1996).

1.11.4. Transmission

HCMV is transmitted person-to-person via bodily secretions such as urine, saliva, breast milk and genital secretions or fomites contaminated with secretions (Cannon 2009; Staras et al. 2008). There is no evidence suggesting that the virus could be spread by aerosols, therefore, good personal hygiene (e.g. handwashing) is one of the most effective ways of reducing viral transmission (Stowell et al. 2012). In seropositive adults, the virus is shed in 7-20% population, and those with greater numbers of sexual partners

or STDs are more susceptible to HCMV infection (Sohn et al. 1991; Chandler et al. 1985; Coonrod et al. 1998; Hyde et al. 2010; Pereira & Maidji 2008).

Although of great clinical significance, the rate of HCMV transplacental transmission is remarkably low with only about 0.5-4% of newborns become infected with HCMV in developed countries and 2-4% in developing countries (Kaye et al. 2008; Mussi-Pinhata et al. 2009; Schopfer et al. 1978; Stagno et al. 1982). HCMV-seronegative pregnant women that become infected with HCMV pose a greater risk of passing the virus to their foetus than seropositive mothers do (Mocarski et al. 2013). In seropositive women, congenital infection with HCMV is observed following re-infection or reactivation of latent virus (Mocarski et al. 2013). Approximately 33% of mothers experiencing a primary infection transmit the virus to their foetus as compared to 1% of HCMV-seropositive mothers (Kenneson & Cannon 2007; Cannon et al. 2011). Seropositive mothers secrete neutralizing antibodies in their breast milk that impede virus transmission to about 69% of nursed infants (Ehlinger et al. 2011). Approximately 95% of HCMV-seropositive mothers shed virus in their milk from day 9 to 3 months postpartum (Vochem et al. 1998; Asanuma et al. 1996; Hotsubo et al. 1994; Jim et al. 2004; Ahlfors & Ivarsson 1985). Newborns infected with HCMV shed virus for many months to years in their saliva and urine and this serves as a route for viral transmission, most notably to siblings (Cannon et al. 2011). About 10% of women shed HCMV in their vaginal excretions around the time of delivery (Stagno et al. 1982). In about 50% of cases where a newborn comes into contact with the virus during delivery it becomes infected (Reynolds et al. 1973). Infection of newborns at the time of delivery or breastfeeding does not cause clinical disease unless the newborn is premature or of low birth weight.

1.11.5. Disease

HCMV infection in healthy individuals is usually sub-clinical and 90% of primary infections in pregnant women is asymptomatic (Stagno et al. 1986; Griffiths & Baboonian 1984). Immunocompetent individuals will occasionally develop infectious mononucleosis that manifest as prolonged fever, fatigue, headache, skin rash, splenomegaly, hepatomegaly, myalgia or enlarged lymph nodes (Correa et al. 2011). HCMV can also be a cause of enteritis, transverse myelitis, thrombosis, haemolytic anaemia, encephalitis, myocarditis as well as various eye condition problems in otherwise healthy adults (Abgueguen et al. 2010; Markomichelakis et al. 2002; Veldhuis et al. 2004; Fux et al. 2003; Sato et al. 2004). HCMV infection in these patients is usually controlled by the immune system, although, there have been rare cases in which death has been reported (Studahl et al. 1994; Arribas et al. 1996). Whilst adults are twice as

likely to be febrile, children are more prone to develop hepatomegaly and splenomegaly (Pannuti et al. 1985).

Although the majority of newborns will remain asymptomatic, 12.7% may display signs of petechiae, jaundice with associated hyperbilirubinemia, hepatosplenomegaly, thrombocytopenia, chorioretinitis, seizures, microcephaly and others (Dollard et al. 2007). Premature babies and those of low birth weight are highly susceptible to HCMV disease, often manifesting as hepatomegaly or pneumonitis (Stagno et al. 1981; Kumar et al. 1984). Preterm neonates that acquire HCMV through vertical transmission develop neutropenia, lymphocytosis, thrombocytopenia, hepatosplenomegaly and respiratory problems (Yeager et al. 1983). Congenital HCMV infection acquired postpartum from the mother can result in sepsis-like syndrome apnea, bradycardia, grey pallor and bowel distention (Vochem et al. 1998; Hamprecht et al. 2008; Hamprecht et al. 2001). One of the most common symptoms in HCMV-infected newborns is sensorineural damage characterized by hearing loss (25%), eyesight problems (11%) and learning difficulties affecting 12-25% of neonates (Boppana et al. 1992; Istas et al. 1995; Dollard et al. 2007). The level of viremia is linked to the severity of congenital disease (Boppana et al. 2005; Bradford et al. 2005; Lanari et al. 2006) and high virus loads detected in placenta have been linked to stillbirth (Iwasenko et al. 2011).

In immunosuppressed and immunocompromised individuals such as Acquired Immunodeficiency Syndrome (AIDS) patients or solid organ transplant recipients, latent virus reactivates. Severe HCMV disease symptoms are usually observed in immunocompromised patients and have been associated with HCMV viremia (Drew 2007). The onset of HCMV disease is usually observed 4-8 weeks after solid organ transplant (Fishman 2011). In liver transplant patients, where the donor is HCMV-seropositive and the recipient is seronegative (D^+R^-), the rate of HCMV infection within the first year after transplant is 17.6% (Freeman et al. 2004). Pneumonitis, gastrointestinal disease, hepatitis, retinitis, pancreatitis, myocarditis, encephalitis and peripheral neuropathy are all symptoms that have been linked to end-organ-disease in transplant patients. Pneumonitis and gastrointestinal disease are the two most common symptoms in hematopoietic cell transplant (HCT) patients. HCT recipients (D^+R^-) usually develop complications and have the lowest survival rates (Nichols et al. 2002). Heart transplant patients can develop cardiac allograft vasculopathy which greatly affects graft survival (Potena & Valantine 2007). Studies looking at hospital care costs required for HCMV-associated symptoms in organ transplant showed that these patients require longer hospital stay and have a higher cost of care (Falagas et al. 1997; Legendre et al. 2000; Mauskopf et al. 2000). Hospital readmission of renal and heart transplant patients

raised hospital costs by $22,598 and $42,111, respectively (Henderson et al. 2001). HCMV has been associated with atherosclerosis (Derhovanessian et al. 2011) and cancer (Cobbs 2011; Melnick et al. 2012; Soroceanu et al. 2011) but lack of direct scientific proof makes this topic controversial. Apart from increased susceptibility to bacterial and fungal infections in immunocompromised, HCMV has also been shown to weaken immune responses to vaccines (Pawelec et al. 2009).

1.11.6. Treatment

Currently available CMV antiviral drugs (ganciclovir, valganciclovir, foscarnet and cidofovir) target the viral DNA polymerase and HCMV DNA synthesis (Fishman 2007; Snydman et al. 2011). Ganciclovir and its prodrug valganciclovir are nucleoside analogue drugs that are phosphorylated to ganciclovir triphosphate but when incorporated into DNA strand, they terminate DNA synthesis (Littler et al. 1992). Patients are treated with ganciclovir/valganciclovir for two weeks or until symptoms subside and virus is no longer detected in the blood. Foscarnet, on the other hand, targets pyrophosphate (PPi) binding sites on viral DNA polymerase and prevents cleavage and release of a PPi moiety which inhibits DNA synthesis (Zahn et al. 2011). In cases where HCMV mutates and becomes resistant to ganciclovir/valganciclovir, foscarnet or cidofovir are used instead (Razonable 2011). Occasionally, acyclovir and valaciclovir (500 mg/m^2 intravenously (i.v.) 3 times daily for 1 month, followed by 800 mg 4 times daily for 6 months) are prescribed for HCMV treatment, however, their mode of action is non-specific to HCMV since it does not encode a thymidine kinase necessary to phosphorylate acyclovir to make it biologically active against the viral DNA polymerase (Meyers et al. 1988; Prentice et al. 1994).

The use of the aforementioned drugs with the exception of acyclovir is strictly regulated since all of them are associated with toxicity. Ganciclovir is recommended for patients who are Human Immunodeficiency Virus (HIV)-positive or who are HCMV-seropositive and whose CD4$^+$ T cell counts are lower than 50 cells/µl (www.cdc.gov). Antiviral therapy is recommended to all HCMV-seronegative patients undergoing kidney, liver, pancreas, heart and lung transplants as well as individuals receiving immunosuppressive treatment to prevent organ rejection (Kidney Disease: Improving Global Outcomes (KDIGO) Transplant Work Group 2009; Kotton et al. 2010). In the organ pre-transplant setting, prophylaxis with i.v. ganciclovir and oral valganciclovir is the standard procedure whereas post-transplant, their use is deferred in case they induce graft failure. To limit virus transmission in blood transfusions, HCMV-seronegative blood is preferred but when it is unavailable, seropositive blood products are filtered to remove latently infected leukocytes. CMV seropositive immunoglobulin is available for the treatment in

ganciclovir-resistant infections. Passive immunization using T cells from HCMV-seropositive donors have shown good results in HCT recipients but this method is not routinely used due to costs and time-effectiveness (Walter et al. 1995; Cobbold et al. 2005; Einsele & Hamprecht 2003; Peggs et al. 2011; Peggs et al. 2009). Prophylactic immunization of renal transplant patients with live-attenuated Towne strain induced antibody and cellular immune responses that protected against challenge with low dose of Toledo (Plotkin et al. 1989; Jacobson et al. 2006). Interestingly, the use of highly active antiretroviral therapy (HAART) in HIV-infected individuals has an indirect effect in reduction of HCMV viremia, severity of the disease and opportunistic infections (Snydman et al. 1993; Steininger et al. 2006).

The recommendation for treating congenital HCMV disease symptoms is by i.v. ganciclovir administered (6 mg/kg of body weight) every 12 hours for 6 weeks (Mofenson et al. 2009). In an attempt to prevent and treat congenital disease, neutralizing HCMV-specific IgG are either given to pregnant women with primary CMV or infected newborn (Mussi-Pinhata et al. 2009; Nigro et al. 2012; Nigro et al. 2005). Several promising antiviral drugs exist that have not yet been FDA-approved and are not yet available on the market. One of these drugs (maribavir) targets UL97, however, more testing to determine the dosage and safety of the drug needs to be carried out. A distinct mode of mechanism is used by Letermovir (AIC246) which is highly specific for HCMV and targets ppUL56 terminase subunit that blocks late stages of viral replication (Goldner et al. 2011). Antiviral therapy, although effective at controlling lytic CMV replication, cannot eliminate latent virus pools.

The National Vaccine Program Office in the United States have placed HCMV as a priority in vaccine development (Arvin et al. 2004). Up until now the attempts to generate a CMV vaccine include a subunit vaccine made of glycoprotein B (gB) in an oil-in-water MF59 adjuvant that has been tested in a phase II clinical trial and decreased HCMV infection in pregnant women by 50% in another trial (Pass et al. 2009; Griffiths et al. 2011). A bivalent DNA vaccine (VCL-CB01/TransVax/ASP0113) comprised of DNA plasmids encoding gB and pp65 are undergoing clinical trials at the moment but thus far have shown tolerance, induction of T cell responses and reduction of CMV viremia (Schleiss 2009; Wloch et al. 2008; Kharfan-Dabaja et al. 2012). Other attempts to generate an effective CMV vaccine include a recombinant canarypox vector encoding pp65 (Berencsi et al. 2001); a chimeric virus made up of Towne and Toledo strains (Heineman et al. 2006); alphavirus replicon vaccine expressing CMV gB or pp65/IE1 (Bernstein et al. 2009); defective virus particles (dense bodies) containing immunogenic peptide (IE1) (Becke et al. 2010); a chimeric replication-deficient adenovirus vaccine

encoding HCMV epitopes (Zhong et al. 2008) and vectors expressing activating NK cell receptor ligands (Slavuljica et al. 2010). Before a CMV vaccine gets FDA approved, however, many factors need to be considered: 1) serostatus; 2) age; and 3) risk group of the individuals to be vaccinated.

1.11.7. Viral strains

For HCMV work to progress, it is important to work with CMV strains that closely resemble clinical CMV isolates. Complete genomes sequenced from patient samples and passaged strains have shown that CMV exhibits a high level of genome heterogeneity; it is more diverse than any other betaherpesvirus (Cunningham et al. 2010; Görzer et al. 2010; Görzer et al. 2008; Renzette et al. 2011; Sijmons et al. 2015; Mocarski Jr. 2007; Davison 2007). Sijmons *et al* analysed 100 clinical HCMV isolates and showed that 77% of clinical HCMV isolates contain open reading frame (ORF)-disrupting mutations and only a minority of clinical viral isolates (23%) are genetically intact (Sijmons et al. 2015). It has been suggested that superinfection with multiple HCMV strains may serve to trans-complement deleterious mutations (Cicin-Sain et al. 2005).

Thus far, a lot of work in the CMV field has been carried out using the AD169, Toledo and TB40 HCMV strains. The limitations to using AD169 (Chee et al. 1990) and Towne (Dunn et al. 2003; E. Murphy et al. 2003) are that these lab-adapted strains have been extensively propagated *in vitro* and contain a lot of mutations, deletions and have genome rearrangements (Ahlqvist & Mocarski 2011; Cunningham et al. 2010; Dargan et al. 2010; Cui et al. 2012).

To address the issue of genome stability, low-passage HCMV isolates have been cloned into a bacterial artificial chromosome (BAC) (FIX, TB40/E, PH) but the original virus stock has not been sequenced prior to BAC cloning, therefore the viruses may have acquired mutations that may affect virus biology. In addition to this, most BACs contain prokaryotic sequences in place of US2, US3, US6 and US11 genes that are involved in viral tropism and NK cell recognition (Murrell et al. 2013; Magri et al. 2011). The Merlin HCMV strain has been designated as the first World Health Organization reference sequence for HCMV. Stanton and others cloned a low-passage (p5) strain Merlin genome into a BAC (Stanton et al. 2010). Any acquired mutations were repaired by comparing the sequence to the sequence of the original clinical sample. This clone contains the WT CMV genome complement, and virus derived from the BAC differs from the original clinical virus just by the addition of a loxP site in between US28 and US29 (Stanton et al. 2010).

1.11.8. Genomic organization

HCMV is the largest human virus ever characterized. Its genome comprises of linear double-stranded DNA, approximately 236 kbp in size containing 3'-single base overhangs at each termini (Davison 2007). The DNA can be subdivided into unique long U_L (193,019 bp) and unique short U_S (35,481 bp) regions with inverted and terminal repeats on either side containing cis-acting signals (pac1 and pac2) necessary for genome cleavage, isomerisation and encapsidation (Wang & McVoy 2011). Closely related CMV strains tend to have terminal repeats of a similar size (e.g. HCMV and guinea pig CMV terminal repeats are 1000 bp whereas MCMV terminal repeats are only 50 bp long). HCMV and chimpanzee CMV genomes are the only ones to encode inverted *a* sequence repeats, thus their genomes are also known as class E genomes. As a result of sequence inversion, class E genomes form 4 equimolar isomers (Davison 2007). Other CMV genomes (RhCMV and MCMV) are class A genomes since their unique sequences are flanked by direct sequence repeats (Hansen et al. 2003; Rivailler et al. 2006; Davison 2007). The structure for HCMV is best depicted using the following configuration: 5' *ab*-U_L-*b'a'c'*-U_S-*ca* 3'. In the Merlin strain of HCMV, the *a/a'* repeat is 578 bp long, the *b/b'* (Terminal Repeat Long, TRL and Internal Repeat Long, IRL) is 1324 bp and *c/c'* (Terminal Repeat Short, TRS and Internal Repeat Short, IRS) is 2537 bp in length. Several HCMV strains that have been heavily passaged contain a duplicated *a'* sequence.

A substantial proportion of the HCMV genome is comprised of 15 gene families that tend to be located at the extremities of the U_L region or in U_S. The herpesvirus core genes: (Figure 4) have homologues in other herpesviruses that are responsible for virus replication and encode virion structural proteins. Comparison with the genomes of simian cytomegalovirus suggest that genes close to the distal regions of the U_L region have been acquired relatively recently. The numbering system of genes UL148-UL133 (U_L/*b'* sequence) is inverse because the element was first characterised in strain Toledo; unfortunately the U_L/*b'* sequence is inverted in strain Toledo (Cha et al. 1996). The current genome nomenclature is as follows: RL1-13, UL1-150, IRS1, US1-US34, TRS1. Genomic analysis of HCMV DNA led to identification of 167 protein-coding genes, 4 genes coding for large non-coding RNAs (lnRNA), 2 oriLyt RNAs and 23 microRNAs (miRNAs) (Grey et al. 2005; Dunn et al. 2005; Pfeffer et al. 2005; Stark et al. 2012; Cunningham et al. 2010). Similarly to genes coding for miRNA and long non-coding RNA (lncRNA), genes encoding proteins of different kinetic classes (immediate early, early and late) do not form distinct clusters and are interspersed throughout the genome. The location of origin of DNA synthesis (oriLyt) is conserved in herpesviruses and is found between genes UL57 and UL69.

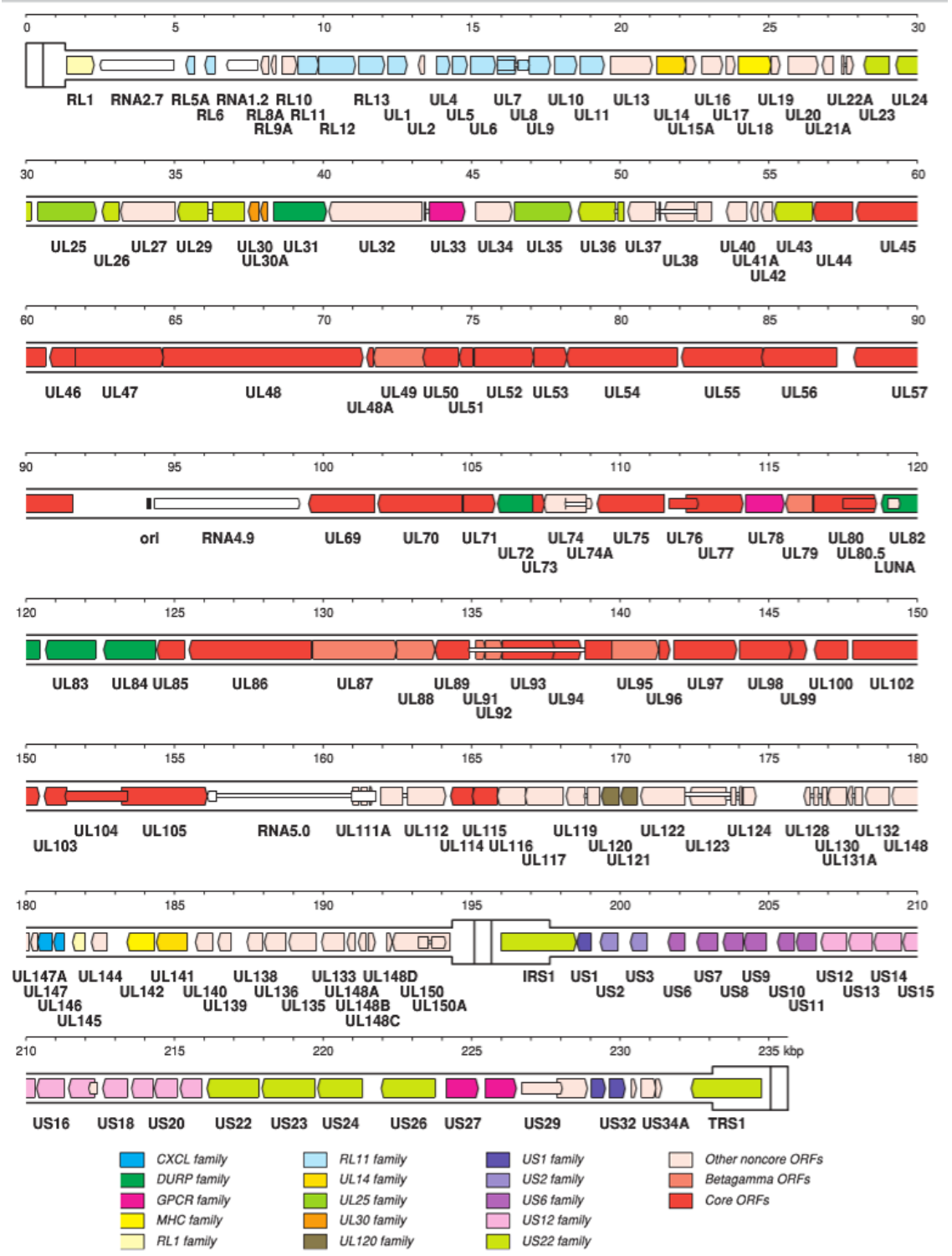

Figure 4: Genomic structure of WT HCMV (strain Merlin)(Mocarski et al. 2013). Inverted repeats (terminal repeat long/internal repeat long (TRL/IRL) and terminal repeat short/internal repeat short (TRS/IRS)) are represented as broader lines. Protein-coding regions are colour-coded (see legend) whereas introns are indicated by white bars. Essential (core) genes are displayed in red. CXCL - chemokine (C-X-C motif) ligand; DURP- deoxyuridine triphosphatase-related protein; GPCR - (G protein-coupled receptor; MHC – major histocompatibility complex; RL – repeat long; UL- unique long; US – unique short; ORF- open reading frame.

1.11.9. Essential and non-essential genes

The annotation of the HCMV genome has changed over the years. Sequencing of the lab-adapted AD169 HCMV genome, followed by bioinformatic analysis, led to the identification of 208 ORFs with 14 gene duplications (Chee et al. 1990; Eain Murphy et al. 2003). Analysis of an earlier passage HCMV strain (Toledo) led to the addition of 19 additional ORFs. More recently, alignment of a clinical HCMV strain and chimpanzee CMV (CCMV) (the most evolutionary similar virus to HCMV), along with analysis of a clinical strain (Merlin) at passage 3, resulted in refinement of the number of protein-coding ORFs to 165 ORFs (Davison et al. 2003). Other groups have used *in silico* pattern-based approaches (ProCeryon and Bio-Dictionary) as well as deep sequencing of viral RNA transcripts to predict the number of protein-coding genes (Gatherer et al. 2011; E. Murphy et al. 2003; Rigoutsos et al. 2003; Novotny et al. 2001), while analysis of temporal mRNA expression by ribosome profiling has led to identification of 751 translated ORFs, some of which have been confirmed by mass spectrometry (Stern-Ginossar et al. 2012).

Functional analysis of Towne genome deletion mutants revealed that only 45 of the gene products are essential (Table 5) for virus replication in fibroblasts (Dunn et al. 2003). The core genes U44-UL105; Ul114-115) clustered in the middle of the genome (Figure 4) are largely essential, with non-essential genes located at either end of the genome. 78% of these core proteins are conserved and found in other herpesviruses (Dunn et al. 2003). More than 50% of the conserved genes encode structural capsid proteins, tegument gene products and envelope proteins (Mocarski Jr. 2007). Deletion of some ORFs impaired viral replication in endothelial and epithelial cells, but not fibroblasts, suggesting that these proteins play an important role in cell tropism, while other gene products actually appeared to inhibit replication (Dunn et al. 2003). Overall, 117 proteins were non-essential for HCMV growth in fibroblasts. These results were validated by another group that used random transposon mutagenesis targeting approximately 150 ORFs and found that AD169 HCMV genome encoded 41 essential, 88 non-essential and 27 augmenting ORFs (Yu et al. 2003). Sequence alignment of HCMV genome to other betaherpesviruses has shown that CCMV is the closest evolutionary relative (163/168 protein homologs), followed by rhesus CMV (111 homologs), guinea pig CMV (84), MCMV and rat CMV (75 homologs), however, these numbers may change as more protein coding ORFs are discovered in CMV (Mocarski et al. 2013).

Table 5: Essential and non-essential HCMV genes (adapted from (Dunn et al. 2003)).

ORFs	Conservation	Function	Growth	ORFs	Conservation	Function	Growth
UL32	β-herpes	Tegument	Essential	**UL2**	CMV	Unknown	10^{-1}–10^{-2}
UL34	CMV	Unknown (transcription)	Essential	**UL11**	CMV	Glycoprotein	10^{-2}-10^{-3}
UL37.1	β-herpes/CMV	Anti-apoptotic	Essential	**UL12**	CMV	Unknown	10^{-1}-10^{-2}
UL44	Core	DNA replication	Essential	**UL14**	CMV	Unknown	10^{-2}-10^{-3}
UL46	Core	Capsid	Essential	**UL20**	CMV	TCR homolog	10^{-2}–10^{-3}
UL48	Core	Tegument	Essential	**UL29**	β-herpes	Unknown	10^{-2}-10^{-3}
UL48.5	Core	Capsid protein	Essential	**UL31**	β-herpes	Transcription	10^{-2}-10^{-3}
UL49	Core	Unknown	Essential	**UL35**	β-herpes	Tegument/transcription	10^{-2}-10^{-3}
UL50	Core	Egress	Essential	**UL38**	β-herpes	Unknown	10^{-2}-10^{-3}
UL51	Core	DNA packaging/cleavage	Essential	**UL47**	Core	Tegument-DNA release	10^{-3}–10^{-4}
UL52	Core	DNA packaging/cleavage	Essential	**UL65**	CMV	Unknown (pp67 virion protein)	10^{-2}-10^{-3}
UL53	Core	Egress	Essential	**UL72**	Core	dUTPase	10^{-3}-10^{-4}
UL54	Core	DNA polymerase	Essential	**UL74**	β-herpes	Glycoprotein O	10^{-3}–10^{-4}
UL55	Core	Glycoprotein B	Essential	**UL88**	β-herpes	Tegument	10^{-2}-10^{-3}
UL56	Core	DNA packaging/cleavage	Essential	**UL97**	Core	Protein kinase	10^{-2}–10^{-3}
UL57	Core	ssDNA binding protein	Essential	**UL103**	Core	Unknown	10^{-2}-10^{-3}
UL60	CMV	Unknown (oriLyt?)	Essential	**UL108**	CMV	Unknown	10^{-2}-10^{-3}
UL70	Core	Helicase/primase	Essential	**UL114**	Core	Uracil DNA glycosylase	10^{-3}–10^{-4}
UL71	Core	Unknown	Essential	**UL129**	CMV	Unknown	10^{-2}-10^{-3}
UL73	Core	Glycoprotein N	Essential	**UL132**	CMV	Unknown	10^{-2}-10^{-3}
UL75	Core	Glycoprotein H	Essential	**US13**	CMV	Unknown	10^{-1}–10^{-2}
UL76	Core	Unknown	Essential	**US23**	β-herpes	Unknown	10^{-2}-10^{-3}
UL77	Core	DNA packaging/cleavage	Essential	**TRS1**	CMV	Transcription/egress	10^{-2}–10^{-3}
UL79	Core	Unknown	Essential	**Growth like wild type (68 mutants, 78 ORFs)**			
UL80	Core	Capsid assembly	Essential	**UL3**	CMV	Unknown	Dispensable
UL84	β-herpes	DNA replication	Essential	**UL4**	CMV	Glycoprotein	Dispensable
UL85	Core	Capsid	Essential	**UL5**	CMV	Unknown	Dispensable
UL86	Core	Capsid	Essential	**UL6**	CMV	Unknown	Dispensable
UL87	Core	Unknown	Essential	**UL7**	CMV	Unknown	Dispensable
UL89.1	Core	DNA packaging/cleavage	Essential	**UL8**	CMV	Unknown	Dispensable

UL90	CMV	Unknown	Essential	**UL10**	CMV	Unknown	Dispensable
UL91	β-herpes	Unknown	Essential	**UL13**	CMV	Unknown	Dispensable
UL92	β-herpes	Unknown	Essential	**UL15**	CMV	Unknown	Dispensable
UL93	Core	Unknown	Essential	**UL16**	CMV	Immunomodulation	Dispensable
UL94	Core	Unknown (tegument)	Essential	**UL17**	CMV	Unknown	Dispensable
UL95	Core	Unknown	Essential	**UL18**	CMV	MHC homolog	Dispensable
UL96	β-herpes	Unknown	Essential	**UL19**	CMV	Unknown	Dispensable
UL98	Core	Alkaline nuclease	Essential	**UL24**	β-herpes	Tegument	Dispensable
UL99	Core	Tegument	Essential	**UL25**	β-herpes	Tegument	Dispensable
UL100	Core	Glycoprotein M	Essential	**UL27**	β-herpes	Unknown	Dispensable
UL102	Core	Helicase/primase	Essential	**UL33**	β-herpes	G protein receptor	Dispensable
UL104	Core	DNA packaging/cleavage	Essential	**UL36**	β-herpes	Anti-apoptotic	Dispensable
UL105	Core	Helicase/primase	Essential	**UL37.3**	β-herpes	Unknown	Dispensable
UL115	Core	Glycoprotein L	Essential	**UL39**	CMV	Unknown	Dispensable
UL122	β-herpes	IE2 (transcription)	Essential	**UL42**	CMV	Unknown	Dispensable
Severe growth defect (12 mutants)				**UL43**	β-herpes	Tegument	Dispensable
UL21	CMV	Unknown	$<2\times10^{-4}$	**UL45**	Core	Ribonucleotide reductase	Dispensable
UL26	CMV	Tegument (transcription)	$<2\times10^{-4}$	**UL59**	CMV	Unknown	Dispensable
UL28	β-herpes	Unknown	$<2\times10^{-4}$	**UL62**	CMV	Unknown	Dispensable
UL30	CMV	Unknown	$<2\times10^{-4}$	**UL64**	CMV	Unknown	Dispensable
UL69	Core	Tegument (transcription)	$<2\times10^{-4}$	**UL67**	CMV	Unknown	Dispensable
UL82	β-herpes	Tegument (transcription)	$<2\times10^{-4}$	**UL78**	CMV	G protein receptor	Dispensable
UL112	β-herpes	Major early protein	$<2\times10^{-4}$	**UL83**	β-herpes	Tegument	Dispensable
UL113	β-herpes	Major early protein	$<2\times10^{-4}$	**UL89.2**	Core	DNA packaging/cleavage	Dispensable
UL117	β-herpes	Unknown	$<2\times10^{-4}$	**UL109**	CMV	Unknown	Dispensable
UL123	CMV	IE1	$<2\times10^{-4}$	**UL110**	CMV	Unknown	Dispensable
UL124	CMV	Latent transcript (ORF152)	$<2\times10^{-4}$	**UL111a**	CMV	IL-1O homolog	Dispensable
US26	β-herpes	Unknown	$<2\times10^{-4}$	**UL116**	CMV	Unknown	Dispensable

CMV – cytomegalovirus; IE – immediate early; IL- interleukin; MHC – major histocompatibility complex; ORF – open reading frame; ssDNA – single stranded DNA; TCR – T cell receptor; UL- unique long; US – unique short.

1.11.10. Replication cycle

Infection (Figure 5) begins with attachment of virion glycoproteins to their cellular receptors. The glycoprotein-receptor binding results either in a pH-independent entry as seen in fibroblasts, where the virus fuses with the plasma membrane at the cell membrane or endocytic viral entry (in endothelial and epithelial cells) that may be either pH-dependent or pH-independent (Compton et al. 1992; Ryckman et al. 2006; Sinzger 2008). The virus enters DCs via a pathway that resembles macropinocytosis and is pH-independent (Haspot et al. 2012). Upon envelope fusion, ppUL47 and ppUL48 mediate viral uncoating and tegument proteins are released into the cytoplasm where they interact with cellular proteins and modulate the environment to enable virus replication. The viral nucleocapsid is transported to the nuclear pores via cytoskeletal filaments by a dynein/dynactin motor protein complex. These microtubules may also play a role in virus release (Mocarski Jr. 2007). Next, the nucleocapsid interacts with nuclear pores and the viral DNA is released from the portal into the nucleus. After entering the nucleus, viral DNA localizes with promyelocytic leukaemia (PML)-bodies which are matrix-associated structures that act as an intrinsic defence mechanism against the virus. Viral pp71 protein acts to relieve transcriptional suppression by degrading a PML-body protein. ppUL84 binds to IE2 and attracts other viral proteins to PML-bodies and initiates transcription of viral genes (Spector & Tevethia 1994). The viral genome circularies and RNA pol II transcribes immediate early genes (α or IE genes). Translation of genes is carried out by host cell ribosomes. Once IE1 is expressed, it disrupts the PML-bodies in the nucleus thus enhancing viral gene expression and consequently, replication (Wilkinson et al. 1998; Kelly et al. 1995). Immediate early genes act as transactivators of expression of other CMV genes by binding to cellular transcription factors. This in turn, activates the transcription of delayed early genes (β or DE) which can be further classified into β_1 and β_2 that play a role in DNA synthesis. IE1-p72, IE2-p86, ppUL84, UL112-UL113 and ppUL44 proteins attract other replisome proteins. ppUL84 binds to the origin of replication and initiates DNA replication. Although initially lytic DNA replication is likely to proceed in the theta form it switches to the rolling circle mechanism of replication, then covalent head-to-tail concatemers are cleaved to single genome units (Challberg 1996). In fibroblasts, DNA synthesis starts at about 14-16 hours post infection (hpi) and reaches a peak at about 24 hpi (10,000 genomes/cell) (Towler et al. 2012; Pari 2008). In other cell types, such as epithelial cells and astrocytomas, the virus only replicates to 1,000 genome copies per cell. Expression of L genes (γ) (48-72 hpi) which are involved in virion formation, maturation and release relies on expression of delayed early genes. Late genes can be categorized into leaky late (γ_1) or true late (γ_2) genes. This depends on the pattern of expression – the majority of late genes are leaky since their expression is DNA replication-independent and commences even if no DE genes have been expressed.

True late genes are absolutely dependent on DNA replication for expression. Viral maturation and release takes place in this final stage of viral replication at 48-72 hpi.

Viral procapsids assemble in the nucleus adjacently to the DNA replication compartment. The scaffold inside the capsids is replaced with viral DNA that is cleaved at pac (cleavage/packaging) sites as the DNA is being encapsidated. Terminase, consisting of two proteins pUL56 and pUL89 plays a role in encapsidation. pUL56 binds to the pac sequences and allows the DNA to be packaged whereas pUL89 mediates the cleavage of viral DNA at these sites (Bogner 2002). UL51, UL52, UL56, UL77, UL80, UL89, UL93 and UL95 gene products may also play a role in encapsidation (Mocarski Jr. 2007). Newly formed nucleocapsids are translocated to the cytoplasm by a nuclear egress complex (NEC) via a two-step envelopment and de-envelopment process (Tandon & Mocarski 2012; Britt 2007). During the first stage of envelopment and de-envelopment process, the virus passes through the inner nuclear membrane and as it leaves the nucleus, it loses its envelope by merging with the outer nuclear membrane. As the capsids transit through the nuclear envelope, pUL53/NEC remains attached. pUL50 becomes incorporated into the virion as a tegument protein together with other proteins (viral proteins, cellular proteins and RNAs) that bind to the nucleocapsid in the cytoplasmic assembly compartment (Kattenhorn et al. 2004; Varnum et al. 2004; Terhune et al. 2004; Greijer et al. 2000; Mocarski Jr. 2007). Virions acquire their final envelope by budding through ER-Golgi intermediate compartment (ERGIC)/endosomal/exosomal membranes and exit the cells via an exocytic vesicle (Tandon & Mocarski 2012; Tooze et al. 1993; Britt 2007; Liu et al. 2011). These last stages of viral maturation and release are usually completed within 24 hours. The peak of virion release occurs at around day 5 post infection until the cells die.

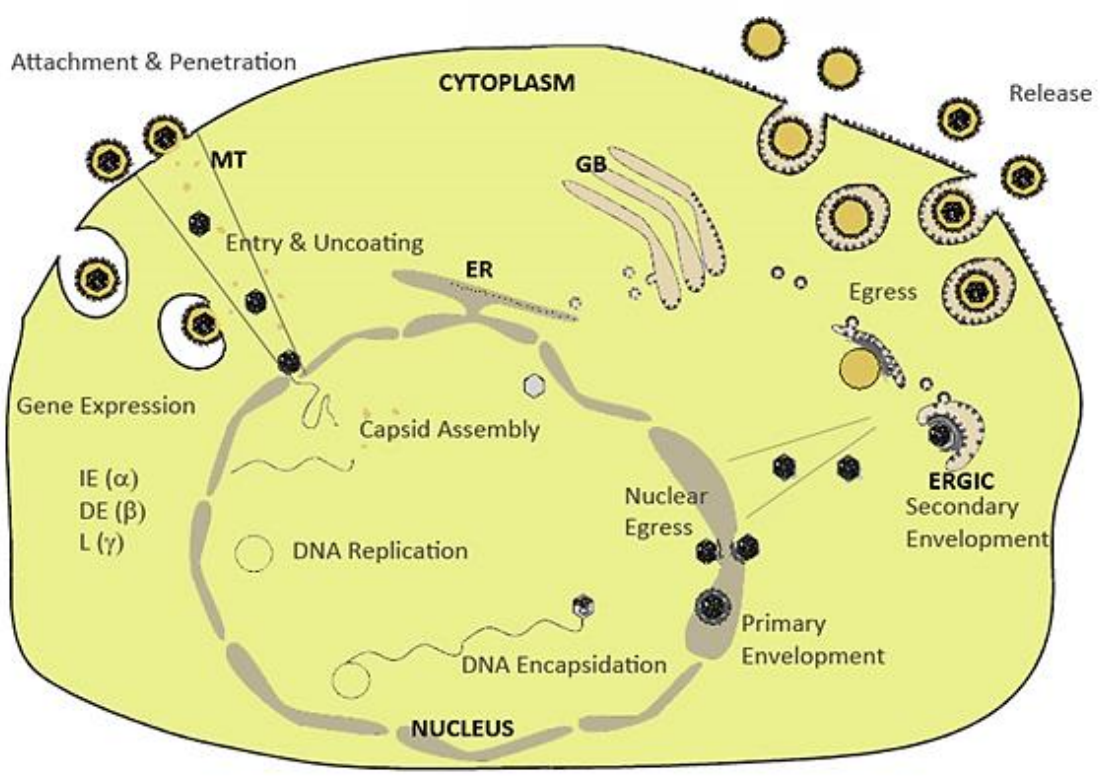

Figure 5: HCMV replication cycle (adapted from (Mocarski et al. 2013)). HCMV gains entry into cells either via fusion at the plasma membrane or endocytic pathway. Upon entry and uncoating, the nucleocapsid is transported into the nucleus. Immediate early genes are expressed and facilitate DNA synthesis. Next, viral DNA is encapsidated and as it leaves the nucleus, it is enveloped. Secondary envelopment occurs at the ER-Golgi intermediate compartment. Lastly, infectious virions are released via exocytosis. MT – microtubules; IE – immediate early; DE- delayed early; L- late; ER – endoplasmic reticulum; GB- Golgi body; ERGIC - The ER-Golgi intermediate compartment.

1.11.11. Latency and reactivation

A characteristic feature of all herpesviruses is establishment of latency - a state in which the virus persists in the host for a prolonged period of time without producing any progeny virions. In response to certain stimuli, it reactivates and goes into a lytic replication cycle to produce infectious virions. HCMV establishes latency in bone marrow-derived mononuclear myeloid progenitor cells ($CD14^+$ monocytes, and their $CD34^+$ progenitors) where DNA is present as a non-integrated episome at very low frequency (<1 in 10,000 cells) and low genome copy numbers (2-10 genomes/cell) (Slobedman & Mocarski 1999; M. B. Reeves et al. 2005; Hahn et al. 1998). There have been studies suggesting that HCMV may establish latency in non-hemopoietic cells as well. *In vitro* work has suggested that HCMV establishes latency in DCs and endothelial cells, however evidence confirming this has not been obtained *in vivo* (M B Reeves et al. 2005).

In vitro, the virus is maintained as an episome in close proximity to nuclear structures called PML-bodies which are also important for IE gene expression (Tang & Maul 2006). It has been suggested that the major immediate early promoter (MIEP) enhancer may play a role in inducing latent viral state and maintaining latency in dividing hematopoietic progenitor cells (Reeves & Sinclair 2008; Reeves 2011; Reeves & Sinclair 2010; Stinski & Isomura 2008). During latency, the MIEP is repressed by epigenetic modifications such as methylation and de-acetylation and binding of heterochromatin 1 protein leads to transcriptional silencing (Poole, Wills, et al. 2014; Kumar & Herbein 2014). Histone deacetylase inhibiting drugs result in de-repression of the inhibited MIEP state leading to viral reactivation (Reeves & Sinclair 2008; Reeves 2011; Sinclair 2010). Therefore, regulation of MIEP expression may act as a 'switch' from latency to reactivation.

Although no new virions are produced during latency, latency is not a transcriptionally quiescent state, a number of latency-associated transcripts have been discovered. CMV latency-specific transcripts localize to the HCMV major IE region (Kondo et al. 1996). Transcriptional profiling studies of $CD14^+$ cells identified the following transcripts: long noncoding RNA (RNA2.7, RNA4.9) and mRNA coding for UL144, UL44, UL50, UL84, UL87, UL95, UL138 and antisense RNA from the UL81–82 region (LUNA) (Kumar & Herbein 2014). Numerous other transcripts were identified in $CD34^+$ progenitors in addition to those found in $CD14^+$ cells: mRNA coding for US17, UL28/29, UL37/38, UL133/135 and UL114 (Kumar & Herbein 2014). Other groups have also detected UL111a (LAvIL-10) and US28 transcripts (Kondo et al. 1994; Bego et al. 2005; Goodrum et al. 2007; Avdic et al. 2011; Poole et al. 2013; Beisser et al. 2001; Kumar & Herbein 2014). UL111a (LAvIL-10), UL144 and US28 play immune evasion roles. LAvIL-10 affects the cellular IL-10 levels by downregulating hsa-miR-92a which in turn leads to

increase in GATA2 levels and expression of cIL-10 (Poole, Avdic, et al. 2014). The anti-inflammatory and immunosuppressive functions of IL-10 allows HCMV to persist.

A study looking at immune responses to latency-associated transcripts in healthy seropositive adults showed that all 4 (LUNA and UL138, US28 and LAvIL-10) latency-associated proteins that were examined were immunogenic, and that the responses were $CD4^+$ T cell mediated with IFN-y effector function that also secreted cIL-10 (Mason et al. 2013). A number of miRNAs have been detected in latently infected cells including miR-UL112.1, miR-US4.1, UL148D, miR-UL112.1, miR-US4.1 miR-US25–1, miR-US25–2 and miR-US33 that work to induce and maintain latent viral state (Kumar & Herbein 2014). Viral mir112.1 inhibits expression of UL123 mRNA (IE72) necessary for major immediate early (MIE) gene expression.

1.11.12. Immunomodulation

Even though CMV induces one of the strongest, broadest and most durable cellular and humoral responses of any virus, the virus establishes latency and persists for the lifetime of the host where it may sporadically reactivate (Cannon et al. 2010; Schoenfisch et al. 2011; Sylwester et al. 2005; Bitmansour et al. 2001; Jackson et al. 2011). In order to persist for the lifetime of the host, CMV has evolved mechanisms to counteract cellular responses that may inhibit viral replication. The fact that only about 26% of the viral genome is essential for replication implies that majority of the genome may play roles in modulation (Table 6) of the host cell environment (Dunn et al. 2003).

During its replication cycle, HCMV forms double-stranded RNA intermediates that activate proteins of the IFN pathway (protein kinase R (PKR) and 2'-5' oligoadenylate synthetase) via TLR3 (Tabeta et al. 2004). Input pp65 protein can block interferon regulatory transcription factor (IRF) 3, IRF1, and/or NF-κB, however, the mechanism is not very well characterized (Marshall & Geballe 2009).

Viral input pp71 protein de-represses immediate early gene transcription by binding to a PML-body protein Daxx (which would otherwise play a role in mediating apoptosis) and degrading it (Saffert & Kalejta 2006). Expression of immediate early genes results in accumulation of the p53 protein, however, the IE2 gene product (pp86) and pUL44 bind to p53 and block its activity (Kwon et al. 2012). Other HCMV-encoded anti-apoptotic proteins are viral mitochondria-localized inhibitor of apoptosis (vMIA, UL37) and viral inhibitor of caspase-8 apoptosis (vICA, UL36) (Poncet et al. 2004). vMIA blocks apoptosis by sequestering Bax in the mitochondria whereas vICA binds to caspase-8

and blocks activation of Fas/Fas ligand pathway (Poncet et al. 2004; Skaletskaya et al. 2001).

The DNA-dependent activator detects viral DNA in the cytosol and activates IRF3 and NF-κB/IFN-like response and RIP3-dependent cell necrotic death in HCMV and MCMV infected cells, respectively (Kaiser et al. 2008; Upton et al. 2010; Upton et al. 2012; Sung & Schleiss 2010). pIRS1 or pTRS1 target this IFN response in HCMV infected cells (Child et al. 2004; Marshall et al. 2009; Marshall & Geballe 2009) whilst in MCMV infected cells, m142 and m143 inhibit PKR activation (Budt et al. 2009; Marshall & Geballe 2009).

HCMV also encodes genes (UL21.5, US27, US28, UL33, UL78 and UL144) that mimic cellular cytokine and chemokine receptors to alter host cellular signalling (McSharry et al. 2012). It has been hypothesized that CMV has acquired genes from the host that have mutated over time (Alcami & Koszinowski 2000). HCMV encodes and secretes a cellular IL10 gene homolog (UL111A) that is likely to play a broad anti-inflammatory role. gpUS2, gpUS3,gpUS6 and gpUS11 play a role in retaining MHC I molecules loaded with HCMV peptides in the ER and degrading them which consequently allows CMV to escape recognition by cytotoxic T cells (Jackson et al. 2011). Although safe from cytotoxic T cells, HCMV infected cells become more susceptible to NK cell mediated lysis (Jackson et al. 2011). To counteract this, HCMV encodes genes that either 1) downregulate NK activating ligands (UL16); 2) mimic HLA class I (UL18); 3) up-regulate HLA-E (UL40); or 4) sequester activating ligands in the Golgi (UL142) (Prod'homme et al. 2012; Yang & Bjorkman 2008; Prod'homme et al. 2010; Ashiru et al. 2009). HCMV also encodes proteins RL11-13 and UL118-119 that bind IgG and protect against antibody-dependent cytotoxicity (Sprague et al. 2008).

Table 6: Immunomodulatory genes encoded by HCMV and their targets (adapted from (McSharry et al. 2012; Wilkinson et al. 2015))

Gene	Target/Role
miR112	miRNA against MICB
RL11-13	IgG
UL16	MICB, ULBP1, ULBP2
UL18	HLA-1 homologue, binds LIR1
UL21.5	Mimics a soluble chemokine receptor
UL33	Mimics a chemokine receptor
UL36	Inhibits apoptosis
UL37	Inhibits apoptosis
UL40	Upregulates HLA-E and gpUL18
UL78	Mimics a chemokine receptor
UL83	Binds NKp30
UL111A	IL-10 homologue
UL118-119	IgG
UL135	Inhibits synapse formation
UL141	PVR, Nectin 2 TRAIL-R
UL142	MICA
UL144	Mimics TNF receptor
US2	Promote proteasomal degradation of MHC Class I heavy chains
US3	Retains MHC class I complexes in ER
US6	Blocks TAP
US11	Promote proteasomal degradation of MHC Class I heavy chains
US18	MICA; NK cell activating ligand B7-H6 (Fielding et al. 2017)
US20	MICA; NK cell activating ligand B7-H6 (Fielding et al. 2017)
US27	Mimics a chemokine receptor
US28	Mimics a chemokine receptor

ER – endoplasmic reticulum; gp – glycoprotein; HLA- human leukocyte antigen; IgG- immunoglobulin G; IL- interleukin; LIR - leukocyte Ig-like receptor; MHC – major histocompatibility complex; MICA - MHC class I chain-related protein A; MICB - MHC class I chain-related protein B; mIR-microRNA, NK- natural killer; PVR- poliovirus receptor; TAP - transporter associated with antigen processing; TNF – tumour necrosis factor; TRAIL-R - ; tumour necrosis factor-related apoptosis-inducing ligand receptor; UL- unique long; ULBP- UL16 binding protein; US – unique short.

1.11.13. Immunogenicity of CMV

1.11.13.1. Immune responses to HCMV in humans

Prior to virus entry, extracellular virions bind to the cell surface and CMV glycoproteins gB and gH activate pattern recognition receptors TLR1 and TLR2; resulting in induction of NF-κB and inflammatory cytokine release (Boehme et al. 2006). The innate cellular immune responses to CMV involves professional APCs, phagocytes and NK cells. NK cells play an important role in initial control of virus infection (Villard 2011; Jackson et al. 2011). T-cell responses to CMV are very variable – in some individuals a dominant response to a single peptide can dominate whereas in others, a broad range of antigens are recognized; a particularly detailed screen was able to detect response covering 39 ORFs (Sylwester et al. 2005). Interestingly, the frequencies of CMV-specific $CD8^+$ T cells inflate throughout life, a process termed 'memory inflation' (Klenerman & Oxenius 2016). CMV-specific $CD8^+$ T cells in the blood may make up 5-10% of total $CD8^+$ T cells but in some individuals, can be as high as 30% (Sylwester et al. 2005). Majority of CMV-specific T cells tend to be effector-memory T cells characterized by lack of lymph node-homing receptor expression and thus, found in peripheral blood and non-lymphoid tissues. Unlike central memory T cells which differentiate, proliferate and provide effector functions only following antigen stimulation, effector memory T cells provide immediate protection and release high amounts of inflammatory cytokines.

$CD4^+$ T cells do not inflate to the same extent as $CD8^+$ T cells, however they do display the characteristic T_{EM} phenotype and release cytokines like IFN-γ and TNF-α (Sylwester et al. 2005; Gamadia et al. 2004). CMV-specific $CD4^+$ T cells make up 0.45% of $CD4^+$ T cell pool and may be as high as 24% in some CMV-seropositive patients (Pachnio et al. 2016). Interestingly, in individuals with asymptomatic CMV infection, the $CD4^+$ T cell response is detected before $CD8^+$ T cell response whereas in symptomatic patients, it is in reverse order thus demonstrating the important role of $CD4^+$ T cells (Gamadia et al. 2004). $CD4^+$ T cells have also shown to be highly useful in controlling CMV in transplant patients. The frequencies of $CD4^+$ T cells in kidney transplant patients can be used to predict the risk of virus replication for 8 weeks (Egli et al. 2008).

Clearance of acute primary CMV infection has been attributed to cell-mediated responses, however, antibodies also play an important role (Sester et al. 2005). Studies have suggested that CMV-specific antibodies may play a role in controlling virus dissemination. Antibodies may arise 2-4 weeks after primary infection and are presumably raised to all expressed CMV proteins, but substantial specific response to

pp65, pp150, pp52, gB, gH/gL and IE1 have been used to follow infections (Genini et al. 2011).

1.11.13.2. MCMV-elicited immune responses in mice

Studies in the mouse model of CMV have demonstrated the importance of $CD4^+$, $CD8^+$ T cells and NK cells in primary infection (Jonjić et al. 1990; Bukowski et al. 1984; Walton et al. 2008). Although antibodies do not appear to play a role in primary infection, they are of great importance in controlling reactivation of the virus (Jonjić et al. 1994). Both $CD8^+$ T cells and NK cells control virus replication in majority of the organs whereas $CD4^+$ T cells are crucial in controlling CMV in salivary glands (Jonjić et al. 1990).

Infectious dose plays an important role in the magnitude of the immune response induced. Mice injected with two different doses of MCMV showed that a higher dose of MCMV resulted in stronger inflationary responses where up to 20% of all $CD8^+$ T cells were pp89-specific (Karrer et al. 2003). In addition to this, the majority of these cells (75-85%) were associated with the functional effector memory phenotype. A lower virus dose during primary infection resulted in smaller memory inflation (Redeker et al. 2014). Re-infection, however, may rescue this partial memory inflation (Trgovcich et al. 2016). Trgovcich *et al* noted that single transcriptional reactivation was not sufficient to restore memory inflation in mice injected with low virus dose (Trgovcich et al. 2016). Conversely, other groups have suggested that the expansion of T cells with effector memory phenotype may in fact be due to chronic replication/reactivation of the virus and low-level expression of virus antigens is essential (Seckert et al. 2012; Beswick et al. 2013).

1.11.14. Murine cytomegalovirus – model system for human CMV

Understanding of human CMV biology requires a model system since these viruses are associated with morbidity and they do not grow in cells derived from other species. To date, the majority of work helping to elucidate HCMV pathology and immunology has been done in mice.

Both HCMV and MCMV are large (230 kb) double-stranded DNA viruses that encode approximately 170 ORFs. The overall structure of the viral genomes is relatively similar. The HCMV genome is comprised of unique long and unique short regions flanked by inverted repeats, MCMV only contains one unique region. This means that the MCMV genome does not have an isomeric structure as seen in HCMV. Comparative sequence analysis of viral DNA shows that homology of the two viruses is 42.5% (DNA) and 78 genes are conserved (Streblow et al. 2006). Over millions of years, these CMVs have

co-evolved with their respective hosts which means that these viruses have become highly adapted to their host species, encoding proteins tailored to interact with host proteins and mechanisms that may not be found in other species. MCMV genes that have sequence homologues in HCMV are designated with an 'M' followed by the gene number whereas those specific to MCMV have an 'm'. Some proteins have functional homologs that are located in different regions of the genome, for example the M144 gene product acts as a MHC class I homolog, similar to HCMV pUL18 (Rawlinson et al. 1996). MCMV IE1 and IE3 proteins are functional homologs of HCMV IE1 and IE2, respectively (Messerle et al. 1992). Even amongst functional homologues, differences exist. For example, IE1 in MCMV does not bind chromatin whereas HCMV IE1 protein does (Maul & Negorev 2008). In addition to this, HCMV IE2 plays a role in cell cycle arrest whereas MCMV IE3 does not (Maul & Negorev 2008).

Analogous receptors are believed to play a role in viral entry and the overall mechanism of entry is conserved (Streblow et al. 2006). After viral entry into permissive cells, lytic replication cycle is induced. The two viruses express proteins of different temporal classes that are expressed at immediate early, early and late stages of the infection. Expression of immediate early proteins activates early protein expression, whilst genome replication is required for late protein expression. Structural analysis of HCMV and MCMV virion composition have shown that similar cellular proteins (actin, annexin I/IV, histone 2A, translation factor EF1a, glyceraldehydes 3-phosphate dehydrogenase, cadherin and the RhoGDP dissociation factor) as well as 37 homologous virion proteins have been incorporated into infectious virions (Baldick & Shenk 1996; Kattenhorn et al. 2004)(Murrell. I; unpublished work). The viruses establish latency in similar cell types and are able to reactivate upon stimulus such as immunosuppressive drugs (Sweet 1999).

Like HCMV, susceptible animals are usually asymptomatic when infected with MCMV (Krmpotic et al. 1999). Both MCMV and HCMV acquire adaptive mutations when cultured *in vitro*. Acquisition of mutations can also be studied to understand viral resistance to antiviral drugs since both HCMV and MCMV are inhibited by nucleoside analogues that target the viral DNA polymerase protein. Immune responses induced upon infection with MCMV and HCMV are broad and diverse. CMV-specific $CD8^+$ T cells are inflationary and increase over time in mice and humans infected with MCMV and HCMV, respectively (Karrer et al. 2003; Khan et al. 2002). Interestingly, however, the frequency of $CD4^+$ T cells in latently infected patients increase over time whereas in mice the levels remain the same (Walton et al. 2008; Pourgheysari et al. 2007).

When it comes to understanding HCMV pathogenesis, MCMV is a useful tool that enables a CMV virus to be studied *in vivo*, in its natural host. Numerous disease models have been established in mice and include: interstitial pneumonitis, hepatitis, myocarditis, adrenalitis, atherosclerosis, hearing loss and hemopoietic failure retinitis (Shellam et al. 2006; Bradford et al. 2015). Since MCMV is not transmitted vertically, understanding congenital disease is less straightforward and requires direct injection of the virus into the vulva (Shellam et al. 2006). In addition to this, MCMV is not recommended for studies of congenital CNS impairment (Shellam et al. 2006).

Overall, MCMV is one of the most convenient models used in understanding HCMV biology due to relatively high virus homology, low costs and well-established animal procedures. Although the two viruses clearly differ in some respects, understanding the similarities as well as the differences between the two viruses can enable rational interpretation of experiments.

1.11.15. Cytomegaloviruses in vector design

Conventional vaccine vectors induce strong $CD8^+$ T cell responses that expand upon vaccination and then contract over time. Once the infection is cleared by the immune system, low levels of specific memory T cells are maintained in the host. Cytomegaloviruses on the other hand, induce inflationary $CD4^+$ and $CD8^+$ T cell responses of an effector-memory phenotype. These increase over time and remain fully functional (can produce IFN-γ and TNF-α when stimulated) and show no signs of exhaustion (Klenerman & Oxenius 2016). The half-life of terminally differentiated inflationary $CD8^+$ T cells is approximately 40-60 days (Snyder et al. 2008; Kim et al. 2015). High frequencies of CMV-specific T cells circulate in the blood and reside in tissues such as the liver and lung (Karrer et al. 2003; Akulian et al. 2013; Ward et al. 2004). Memory T cells make up approximately 10% of $CD4^+$ and $CD8^+$ T cell memory cells in the peripheral blood (Sylwester et al. 2005).

The growing interest in CMV as vaccine vectors is based on a series of studies undertaken over recent years in the mouse and rhesus macaque models that have sought to redirect the strong immune response generated to CMV onto a series of antigens from a variety of infectious agents and cancer cells. T cell expansions characteristic of MCMV responses have been observed to inserted transgenes in mice vaccinated with a single dose of MCMV encoding either influenza A virus or lymphocytic choriomeningitis virus epitopes (Karrer et al. 2004). The T cell responses generated were observed to elicit protective immunity. Moreover, an MCMV recombinant encoding a $CD8^+$ T cell-specific epitope for an Ebola nucleoprotein induced lasting (>8 months)

protection in prophylactically vaccinated mice who received a single vaccine dose. High levels of $CD8^+$ T cells induced protection in vaccinated animals (Tsuda et al. 2011). A follow-up study showed that this protection was durable even after 119 days (Tsuda et al. 2015). Work by Redwood *et al,* showed that MCMV encoding murine zona pellucida 3 (mouse ovary Ag) induced sterility of vaccinated mice (Redwood et al. 2005). Another group inserted *Mycobacterium tuberculosis* Ag 85A into an MCMV vector and compared the immune responses to an empty control vector. Surprisingly, both viruses induced protective NK cell responses showing that Ag specificity is not required to protect against *M. Tuberculosis* (Beverley et al. 2014). Targeting *Listeria monocytogenes* with MCMV encoding a *Listeria monocytogenes* epitope together with NKG2D receptor activating ligand (RAE-1γ) induced strong and durable $CD8^+$ T cell response protective of subsequent challenge with the pathogenic bacteria (Trsan et al. 2013). Antibody-conferred protection was described in a study where a single dose of tetanus toxin encoding MCMV induced long-term protection in mice (>13 months) (Tierney et al. 2012).

The most ground-breaking work in CMV vaccine vector development, however, was carried out by Louis J Picker's group in Oregon. Live-attenuated RhCMV vectors encoding simian immunodeficiency (SIV) antigens were used to vaccinate rhesus macaques that were later repeatedly challenged (intra-rectally) with a highly virulent SIVmac239 strain (Hansen et al. 2009). Surprisingly, half of the animals became elite controllers and were able to resist SIV infection (Hansen et al. 2011). Protected rhesus macaques displayed transient SIV viremia in sites other than the site of virus challenge (e.g. draining lymph nodes, bone marrow, spleen and liver) with occasional viral blips that waned by week 70 (Hansen et al. 2013). In addition to this, the levels of tissue-associated SIV DNA and RNA of 89% (8/9 animals) of protected rhesus macaques were at the limit of detection and in one animal the levels were 454 copies per 10^8 cells (Hansen et al. 2013). The immune responses associated with this remarkable control of SIV infection were very broad, consisting of unusual and diverse supertopes (MHC class II and HLA-E restricted) (Hansen et al. 2013). When the protective immune responses were analysed, it became apparent that the $CD8^+$ T cells were of effector memory phenotype, residing in close proximity to viral entry sites (Hansen et al. 2011). In comparison, immune responses mediated by an adenovirus vector displayed the canonical central memory phenotype, and were not protective (Hansen et al. 2011). The authors showed that a recombinant RhCMV vector can be used to superinfect a seropositive rhesus macaque; possibly due to the presence of immune evasion genes (Hansen et al. 2010). Whereas majority of virus-based vectors (e.g. adenoviruses) can only be used once due to pre-existing immunity; this characteristic feature of

cytomegaloviruses makes them highly attractive for use in CMV-based vaccine development.

Not only are CMV vectors effective against infectious agents but they can also be utilized as anti-cancer therapy. Two groups have tested recombinant MCMV vaccines in the B16 melanoma cancer model. An MCMV mouse tyrosinase-related protein (TRP2) recombinant induced long-term protection against tumour formation that was mediated solely by a TRP2-specific antibody response (G. Xu et al. 2013). The second group modified gp100 tumour-associated antigen to make it more immunogenic. Vaccination with the MCMV-gp100KGP recombinant resulted in protection against aggressive lung B16-F10 melanoma cells driven by a $CD8^+$ T cell response (Qiu et al. 2015). $CD8^+$ T-cell response has also been suggested to play a role in tumour growth delay observed in a murine prostate cancer model (PSA-expressing Transgenic Adenocarcinoma of the Mouse Prostate; TRAMP-PSA) immunized with MCMV vector encoding a PSA epitope (Klyushnenkova et al. 2012).

As the studies move toward clinical trials, vaccine vector safety becomes a priority. Health concerns in immune-naïve and immunosuppressed individuals require the use of non-replicating virus vectors. However, attenuated CMV is unable to induce immune responses comparable to WT virus (Snyder et al. 2011). It has been hypothesized that chronic low-level replication of the virus is responsible for the characteristic immune responses seen to date in vaccine vectors (O'Hara et al. 2012). Alternative strategies allowing limited virus replication are therefore needed (O'Hara et al. 2012).

1.11.16. T-REx system

Gene regulation systems are essential in the gene therapy setting. The ideal expression system should 1) be highly specific; 2) not exhibit pleiotropic effects; 3) induce high levels of the gene of interest; 4) be cost-effective and 5) be strictly regulated and inhibit leaky gene transcription. Prokaryotic conditional expression systems meet most of the requirements. Tetracycline-regulated systems, in particular, have been widely used. These systems rely on expression of tetracycline repressor (tetR) that responds to an antibiotic called tetracycline or its derivative – doxycycline (DOX). TetR homodimers bind with high specificity to tetracycline operator and induce or block gene transcription. Multiple variants of this regulation system exist: 1) Tet-On; 2) Tet-Off and 3) TREx (see Figure 6).

In the Tet-Off system, the *Escherichia coli* (*E. coli*) *tetR* is fused to HSV VP16 activation domain to generate a chimeric protein called tetracycline transactivator (tTA). This

protein recognizes the tetracycline response element (TRE) which comprises of a minimal promoter and seven tetracycline operator (tetO) sequence repeats. If the tTA binds to the tetO, it activates gene expression from the TRE. In the presence of tetracycline, tetracycline binds to the tTA and causes a conformational change. This, in turn prevents tTA from binding to the tetO sequences, and gene expression is turned off. The Tet-On system, on the other hand, relies on reverse tTA (rtTA) which was obtained through mutating tTA so that it would bind to tetO only in the absence of tetracycline. Thus, addition of DOX activates gene expression. The T-REx system responds to tetracycline in a similar way to the Tet-On system, however, the major difference is the absence of a transactivation domain in the tetR protein which makes it less toxic than Tet-On or Tet-Off systems since transactivation domains are known to interact to cellular proteins genes and affect their expression (Yao et al. 1998; Hillen & Berens 1994; Hall & Struhl 2002). In the T-Rex system, gene expression is driven from an intact promoter (as compared to the minimal promoter used in Tet-On/Tet-Off) and two tetO sequences are placed downstream of the promoter. TetR homodimers bind to the two tetO (TetO2) sequences with high specificity (binding constant =2 x 10^{11} M^{-l}) and inhibit transcription (Hillen & Berens 1994). Addition of DOX prevents tetR from binding to the tetO and relieves this repression, allowing the gene downstream of TetO2 to be expressed (Yao et al. 1998).

Several groups have used tetracycline-regulated systems to generate cell lines with transient protein expression (Nagarajan & Sinha 2008; Krishnapuram et al. 2013; Tian et al. 2009; Bai et al. 2013). One such attempt resulted in development of a cell line secreting pig growth hormone where mRNA expression could be regulated by 10-fold in response to DOX (Jiang et al. 2012). Others have used the tetR-based system to generate vectors with tetR-regulated promoters to target expression of specific genes within the vector (Debowski et al. 2015; Heinz et al. 2011). Analysis of tet-responsive green fluorescent protein (GFP) expression *in vivo* showed that the highest regulation by tet-responsive promoters could be achieved 16h after addition of anhydrotetracycline (tetracycline analogue)(Debowski et al. 2013). Multiple groups have looked at gene expression *in vivo* using tet-based regulation systems that have shown promising results and no reported toxicity (Sato et al. 2013; Debowski et al. 2013; Huang et al. 2015). In addition to this, several transgenic animal models have been generated using these systems (Tillack et al. 2015; Heindorf & Hasan 2015). Concerns over leakiness of tetracycline-regulated system led to advanced improvements such as Tet-On 3G that is 10-100 fold more sensitive to DOX (Fan et al. 2012). In addition to this, rtTA variants have been generated that are 7-fold more active and 100-fold more sensitive to DOX than the original Tet-On system (Zhou et al. 2006). Modifications with improved

background expression and 25-fold higher inducible expression have also been observed (Peacock et al. 2012).

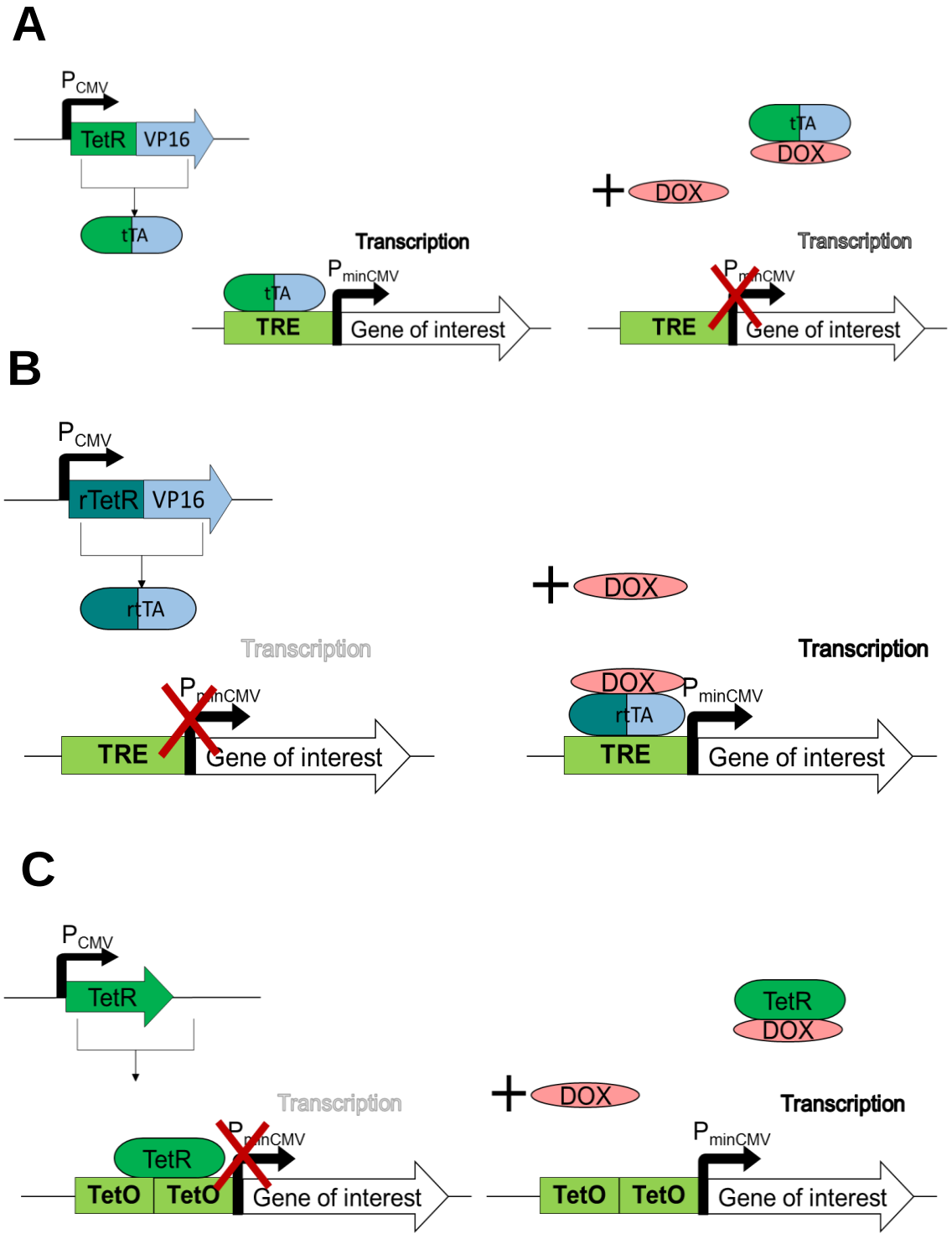

Figure 6: Tet-Off (A), Tet-On (B) and TREx (C) systems. A: in the Tet-Off system, tetracycline transactivator protein (tTA) through binding to tetracycline response element (TRE) in the absence of doxycycline (DOX) allows downstream gene transcription. Addition of DOX blocks the binding to TRE and thus, transcription. B: reverse tetracycline transactivator protein requires DOX to bind to TRE and enable gene transcription. C: tetR binds to tetracycline operators (tetO) in the absence of DOX and prevent gene transcription. DOX, however, binds to tetR and blocks the binding to tetO and transcription can commence.

1.12. Hypothesis

A HCMV virus in which replication is controlled by doxycycline would be a safe vector, that is capable of inducing an immune response comparable to wild type virus.

1.13. Aims of the current study

The aims of this project were:

Adenovirus-specific

i. To generate replication-deficient Adenovirus serotype 5 vectors encoding a human tumour-associated antigen (human 5T4).
ii. To test immunogenicity of 5T4 in two mouse strains (BALB/c and C57bl/6).
iii. To compare immunogenicity of first-generation (E1 and E3 genes deleted) and second-generation (E1, E3 and E4 genes deleted, except for E4-ORF6) adenovirus vectors *in vivo*.
iv. To establish murine cancer models expressing the 5T4 antigen.
v. To test the efficacy of Ad-h5T4 prophylaxis in cancer models.

CMV-specific

i. To construct conditionally replicating human and mouse CMV vectors by using tetR-based (TREx) system.
ii. To analyse virus replicative capacity *in vitro*.
iii. To determine whether propagation of virus vectors results in mutations that impair conditional control of virus replication.
iv. To test safety of conditional MCMV vectors *in vivo*.
v. To test immunogenicity of conditional MCMV vectors *in vivo*, as compared to adenovirus.

Chapter 2 Methods

2.1. Buffers, media and gels

1 x TD buffer pH 7.4	750 mM NaCl (Fisher Scientific), 50 mM KCl (Sigma), 10 mM $Na_2HPO_4 \cdot 12H_2O$ (AnalaR), 250 mM Tris-base; pH adjusted with HCl to 7.4. The solution was autoclaved and stored at 4°C.
1x TAE buffer	50x TAE buffer (National Diagnostics) diluted 1:50 with ddH_2O
2x media	50% (v/v) ddH_2O; 20% (v/v) 10x Minimum Essential Medium (MEM) (Life technologies); 20% (v/v) Foetal Bovine Serum (FBS) (Life Technologies), 0.45% (v/v) sodium bicarbonate (Life Technologies); 100,000 Units penicillin (Life technologies); 100mg/ml streptomycin (Life technologies); 4 mM L-glutamine (Life Technologies)
4% paraformaldehyde (PFA) solution	4% (w/v) paraformaldehyde (Acros Organics) in phosphate buffered saline (PBS) (Life Technologies)
6x loading buffer	30% glycerol (Fisher) in ddH_2O; 0.025 % (w/v) bromophenol blue (Sigma); 0.025 % xylene cyanole (Sigma)
Ampicillin (*Amp*) stock	100 mg/ml ampicillin (Melford) in ddH_2O
Blocking buffer	5% (w/v) fat-free milk (Marvel)
Chloramphenicol stock	12.5 mg/ml chloramphenicol (Melford) in 70% ethanol
Collagenase	5% FBS (v/v); 1 mg collagenase D (Roche); 5 mM CaCl2; 50 µg DNAse 1 (Sigma) in RPMI
Dialysis buffer	10 mM Tris-HCl pH 7.8, 135 mM NaCl (Fisher Scientific), 1mM $MgCl_2(H_2O)_6$, (Acros Organics) 10% glycerol (v/v) (Fisher)
Fluorescence-activated cell sorting (FACS) buffer	2% FBS; 0.05% sodium azide (Sigma) in PBS
Freezing media	90% FBS; 10% Dimethyl Sulfoxide (DMSO) Hybri-Max (Sigma)
Growth media 1 (GM1)	Dulbecco's Modified Eagle's medium (DMEM) (Sigma) with 10% v/v FBS; 250 Units penicillin; 250 µg/ml of streptomycin
Growth media 2 (GM2)	DMEM supplemented with 10% v/v FBS (Invitrogen), 250 Units of penicillin, 250 µg/ml of streptomycin, 0.26 mg/ml of L-glutamine and 97 mg/ml of sodium pyruvate.
Growth media 3 (GM3)	RPMI-1640 (Life Technologies) with 10% v/v FBS (Life Technologies), 250 Units of penicillin, 250 µg/ml of streptomycin and 0.26 mg/ml of L-glutamine
Heavy CsCl solution	3.69 M Caesium chloride (Melford) in 100 ml of TD buffer; sterilized using 22 µm filter (Merck Millipore)
Isopropyl β-D-1-thiogalactopyranoside (IPTG) stock	0.1M isopropyl β-D-1-thiogalactopyranoside (Melford), in ddH_2O
Kanamycin stock	25 mg/ml Kanamycin (Melford) in ddH_2O
LB Agar	LB broth and 15% (w/v) agar (Oxoid)
LB Agar (sucrose)	LB broth, 5% (w/v) D-sucrose (Fisher scientific), 15% (w/v) agar, 1% (w/v) tryptone (Fisher) and 0.5% (w/v) yeast extract (Oxoid)

Light CsCl solution	2.14 M Caesium chloride (Melford) in 100 ml of TD buffer; sterilized using 22 µm filter (Merck Millipore)
Luria Bertani (LB) broth	LB broth low salt powder (Melford) in ddH_2O
Lysis buffer	1× NuPAGE LDS sample buffer (Life Technologies); 10% (v/v) Dithiothreitol (DTT) (Sigma) in ddH_2O
MOPS buffer	1× NuPAGE MOPS Sodium dodecyl sulphate (SDS) Running Buffer (ThermoFisher Scientific)
Overlay medium A	2× media mixed 1:1 ratio with Avicel (IMCD UK Limited)
Overlay medium B	0.8% carboxymethyl cellulose (Sigma) in GM2
Red blood cell (RBC) lysis buffer	155 mM NH_4Cl (Sigma), 10 mM $KHCO_3$, 1 mM Ethylenediaminetetraacetic Acid (EDTA) (Alfa Aesar), pH 8
Saponin buffer	2% FBS; 0.5% (w/v) saponin (Acros Organics) and 0.05% (v/v) sodium azide in PBS;
Sorbitol cushion	20% (w/v) D-sorbitol (Sigma) in ddH_2O
Streptomycin solution	200 mg/ml of streptomycin sulphate (Melford) in ddH_2O
Transfer buffer	2× NuPAGE transfer buffer (Life Technologies); 10% (v/v) methanol in ddH_2O
Wash buffer for western blot	Phosphate buffered saline (Oxoid); 0.1% (v/v) Tween20 (Sigma) in ddH_2O
X-gal stock	40 mg/mL 5-bromo-4-chloro-3-indolyl β-D-galactopyranoside (X-gal) (Melford) in DMSO (Fisher)

Table 7: Antibodies used in this study

Immunogen	Company	Catalogue number	Species	Conjugate	Dilution	Application	Size
β-actin	Sigma	A-2066	Rabbit	-	1/2000	Western Blot	40 kDa
***E. coli* TetR (residues 1-50)**	Novus biologicals	NBP1-78424	Rabbit	-	1/1000	Western Blot	23 kDa
Mouse 5T4	R&D Systems	AF5049	Sheep	-	1/2000	Western Blot	72 kDa
Mouse IgG (H+L)	Bio-Rad	170-6516	Goat	HRP	1/2000	Western Blot	-
Rabbit IgG (H+L)	Bio-Rad	170-6515	Goat	HRP	1/2000	Western Blot	-
Sheep IgG	Sigma	A3415	Donkey	HRP	1/2000	Western Blot	-
Mouse M123/IE1	CapRi	HR-MCMV-12	Mouse	-	1/1000	Western Blot IHC/Titration	95 kDa
Mouse IgG (H+L)	Life Technologies	A-11020	Goat	Alexa Fluor 594	1/2000	IHC/Titration	-
MHC Class I H2 Kb + Db	Abcam	ab112492	Mouse	PE	1/50	Stability assay	-
Mouse IgG2a	Beckman coulter	A09141	Mouse	PE	1/50	Stability assay	-
Hexon (Adenovirus serotype 2)	Merck Millipore	AB1056	Goat	-	1/5000	IHC/Titration	-
Goat IgG	Santa Cruz Biotechnology	Sc-2056	Donkey	HRP	1/1000	IHC/Titration	-
Mouse CD3 Clone: 17A2	BioLegend	100205	Rat	PE	1/100	ICS/Tetramer staining	
Mouse CD4 Clone: RM4-5	BioLegend	100547	Rat	Brilliant Violet 605	1/100	ICS/Tetramer staining	-
Mouse CD8a Clone: 53-6.7	BioLegend	100725	Rat	PB	1/100	Tetramer staining	-
Mouse CD8a Clone: 53-6.7	BioLegend	100732	Rat	PerCP	1/100	ICS	-
Mouse/human CD27 Clone: LG.7F9	ThermoFisher Scientific	12-0271-82	Armenian hamster	PE	1/100	Tetramer staining	-
Mouse/human CD44 Clone: IM7	BioLegend	103012	Rat	APC	1/100	Tetramer staining	-
Mouse/human CD44 Clone: IM7	BioLegend	103028	Rat	APC/Cy7	1/100	ICS	-
Mouse CD69 Clone: H1.2F3	BioLegend	104537	Armenian Hamster	Brilliant Violet 711	1/100	Tetramer staining	-
Mouse CD103 Clone: 2EF	BioLegend	121416	Armenian Hamster	PerCP/Cy5.5	1/100	Tetramer staining	-
Mouse/human KLRG1 (MAFA) Clone: 2F1/KLRG1	BioLegend	138410	Syrian hamster	FITC	1/100	ICS/Tetramer staining	-
Mouse TNF-α Clone: MP6-XT22	BioLegend	506306	Rat	PE	1/100	ICS	-
Mouse IFN-γ Clone: XMG1.2	BioLegend	505810	Rat	APC	1/100	ICS	-

APC - Allophycocyanin; Cy7 – cyanine 7; FITC - Fluorescein isothiocyanate; HRP - Horseradish peroxidase; ICS- intracellular cytokine staining; IHC – immunohistochemistry; KLRG1- Killer cell lectin-like receptor subfamily G member 1; PB- Pacific Blue; PE – Phycoerythrin; PerCP- Peridinin Chlorophyll.

2.2. Cell lines

Growth media used for culturing all the cell lines listed above are described in Tables 8 and 9. Human foetal foreskin fibroblasts (HFFFs), a kind gift from Dr Graham Farrar (CAMR, Salisbury, UK), were immortalized with human telomerase reverse transcriptase (HF-hTERTs) as previously described by (McSharry et al. 2001). HFFFs expressing tetracycline repressor (HFFF-tets) (Stanton et al. 2010) served as a positive control in experiments looking at repression of virus replication. NIH 3T3-tet cell line was generated by transfection of an immortalized mouse embryo fibroblast cell line, NIH 3T3 (American Tissue Culture Collection, ATCC CRL-1658) with retrovirus expressing the tet-repressor and selected in puromycin (1 µg/ml) at 48 hours pi. A complementing cell line, expressing E1 protein called T-REx-293 (human embryonic kidney cells)(Graham & Smiley 1977) and HF-TERTs transfected with the Coxsackie-adenovirus receptor (HF-CAR) (McSharry et al. 2008) were used for adenovirus work.

To establish tumour models, three different cell lines were used: 1) 4T1 mouse mammary carcinoma cells (ATCC CRL-2539); 2) CT26 mouse colon carcinoma (ATCC CRL-2638) provided by Professor Awen Gallimore and 3) L/L2 (LLC1) were purchased from ATCC (CRL-1642). For peptide stability assays, TAP-deficient human lymphoblast T2 cell line transfected with D^b and K^b and thereof referred to as T2 D^b and T2 K^b, respectively, were a generous gift from Professor Awen Gallimore. *Apc*$^{fl/fl}$ small intestine and large intestine samples were provided by Dr Lee Parry (Cardiff University).

2.2.1. Maintenance of cell lines

In vitro cell culture was carried out under sterile conditions in a Class II biological safety cabinet (Microflow). The cells were cultured at 37˚C in Sanyo CO_2 incubators supplemented with 5% CO_2 until 80-90% confluent. Adherent cells were washed with PBS and incubated with 3 ml of 0.05% trypsin-EDTA (Life Technologies) at 37˚C until all the monolayer had detached. Trypsin-EDTA was then neutralized with media containing FBS and the cells were split and re-seeded into tissue culture flasks and passaged until necessary. Cells growing in suspension were split by pelleting at 1,500 revolutions per minute (rpm) for 3 min, then washing the cells with 10 ml of PBS and re-suspending the cell pellet in growth media and then dividing into the required volume (Table 9) and seeding back into tissue culture flasks.

2.2.2. Counting cells

Cell counts were determined by pipetting 20 µl of cells into a disposable BVS100 counting chamber (Immune Systems) and counting the number of cells in a 4×4 square

using an inverted light microscope (Nikon TMS). To calculate the total cell number in 1 ml of media, the number obtained was multiplied by 10^4.

2.2.3. Cryopreservation of cells

Cells were trypsinized and counted as described in section 2.2.1 and 2.2.2, respectively. The cells were collected by spinning at 1,500 rpm for 3 min. The cell pellet was then re-suspended in freezing media to the required volume and aliquoted out into cryovials (ThermoFisher Scientific) that were then incubated in an isopropanol-based freezing vessel (Nalgene) at -80˚C. Following a 24-hour incubation, the cryovials were transferred to a vapour phase liquid nitrogen tank

2.2.4. Resuscitation of frozen cells

Cryovials containing frozen cells were placed in a 37˚C water bath until all the cells in suspension had thawed. Next, cells were pipetted into 10 ml of pre-warmed growth medium and centrifuged at 1,500 rpm for 3 min at room temperature (RT) to remove any cryoprotectant. The cell pellet was then resuspended in 15 ml PBS and after spinning the tubes at 1,500 rpm for 3 min (RT), the cell pellet was reconstituted in compatible growth medium, seeded into a tissue culture flask and incubated at 37˚C 5% $CO_{2.}$

Table 8: Cell lines and subculturing conditions

Cell line	Growth media	Application	Subcultivation ratio/ cell density
HFFF	GM1 (see 2.1)	Growing HCMV stocks/testing virus growth	1:3-1:5
HF-hTERTs			
HFFF-tets		Testing HCMV vector replication/growth	
T-REx-293		Growing Ad stocks	1:8-1:10
HF-CAR		Expression of protein from recombinant Ad vectors	1:3-1:5
L/L2 (LLC1)		Establishment of cancer model in mice	1:4-1:6
NIH 3T3	GM2 (see 2.1)	Growing MCMV stocks and testing virus growth	1:3-1:5
NIH 3T3-tet		Testing MCMV vector replication/growth	
4T1	GM3 (see 2.1)	Establishment of cancer models in mice	1:6 to 1:8
CT26			1:4 to 1:10
T2 D^b		Stability assay	3 x 10^5 and 1 x 10^6/ml
T2 K^b			

Table 9: Volumes of medium used for culturing and infecting cells

Culture vessels	Cell number for seeding	Media volume (ml) for seeding cells	Media volume (µl) for infecting cells
T150	4×10^6	15-20	-
T75	3×10^6	10-15	-
T25	6×10^5	5	-
Plates			
6-well	2.5×10^5	2	500
12-well	1.25×10^5	1	300
24- well	6.25×10^4	0.5	200

2.3. BAC-cloned viruses

2.3.1. HCMV

BAC-cloned Merlin HCMV strain (GenBank accession number GU179001.1) referred to as 'pAL1111' was provided by Dr Richard Stanton (Cardiff University) (Stanton et al. 2010). pAL1111 contains the complete HCMV genome.

2.3.2. MCMV

K181^{Perth} (GenBank accession number: AM886412) plasmid designated as pARK25 was a kind gift from Dr Ian Humphreys and encodes a MCMV strain K181 genome (Cardiff University) (Redwood et al. 2005). The BAC plasmid was transfected into empty SW102 *E. coli* cells as detailed in section 2.4.9. M50 and SCP viruses cloned into BACmids were kindly provided by Dr Zsolt Ruzsics (Rupp et al. 2005). M50 and SCP viruses are a Smith strain of MCMV.

2.3.3. Adenovirus

Replication-deficient human adenovirus serotype 5 lacking E1 and E3 regions (first generation) as well as a virus missing the E4 gene (second-generation), were supplied by Dr Richard Stanton (Stanton et al. 2008). The E1 region of the virus was replaced with an expression cassette containing the HCMV MIE promoter and its polyadenylation sequence.

2.4. Molecular biology techniques

2.4.1. Oligonucleotide design and storage

Oligonucleotide primers (listed in Appendix A) were designed using CLC Main Workbench 7 software and Oligo Explorer 1.2. The forward and reverse primers were designed to have a similar melting temperature of 60-65°C and exhibit minimal or no primer-dimer formation, self-annealing and secondary structure. The primers were purchased from Eurofins MWG at de-salted purity. The lyophilized primers were reconstituted with ddH_2O to 100 µM concentration and were stored at -20°C.

2.4.2. Polymerase Chain Reaction (PCR)

PCR was either used 1) to amplify regions of DNA required for recombineering or 2) for screening positive BAC clones. 50 µl PCR reactions were set up on ice in thin-walled DNAse and RNAse-free tubes (ELKay) containing ddH_2O, 5 µl of HIFI buffer (Expand High fidelity; HIFI, 11732641001, Roche), 3% (v/v) DMSO (Fisher), 1 µl of template DNA, 1 µl of deoxynucleotides (dNTPs) (NEB), 1 µM forward and reverse primers (see

Appendix A) and 0.5 µl of HIFI polymerase (HIFI, 11732641001, Roche). All PCR reactions were performed using T3000 Thermocycler (Biometra). The extension time in PCR programs (Table 10 and Table 11) was modified accordingly to the length of the region to be amplified whereas annealing temperature was changed depending on the melting temperature of the primers.

Table 10: PCR protocol LONG for *amp/sacB/lacZ* cassette

Stages	Temperature (˚C)	Time	Cycle
Pre-heating	99	2 min	-
Initial denaturation	95	2 min	1
Denaturation **Annealing** **Extension**	95 55 68	30 s 30 s 4 min 30 s	33
Final extension	68	15 min	1
Hold	4	∞	-

Table 11: PCR protocol HIFI for *kan/rpsL/lacZ* cassette and other inserts

Stages	Temperature (˚C)	Time	Cycle
Pre-heating	99	2 min	-
Initial denaturation	94	2 min	1
Denaturation **Annealing** **Extension**	94 55 72	15 s 30 s 3 min	34
Final extension	72	7 min	1
Hold	4	∞	-

2.4.3. DNA gel electrophoresis

0.7% (w/v) agarose gels were prepared by dissolving 0.35g of Hi-Res Standard Agarose (AGTC Bioproducts) in 50 ml of TAE buffer (see section 2.1). The solution was supplemented with 0.5 µg/ml of ethidium bromide (Sigma), poured into pre-assembled gel casts and left at RT for 30 min to solidify. DNA samples to be analysed were diluted with 1× agarose loading buffer (see section 2.1) and loaded onto the gel alongside 10 µl of HighRanger Plus 100 bp DNA Ladder (Norgen biotek) which served as a standard weight measure. The electrophoresis was carried out in TAE buffer at 100 Volts for 1-2 hours. The DNA bands were visualized using the GeneSys gel doc system.

2.4.4. DNA isolation and extraction from agarose

DNA fragments to be excised were visualized under a UV transilluminator (Spectroline TVC-312A) with minimal UV exposure time to prevent DNA damage. The isolated bands were placed in a clean 1.5 ml Eppendorf tube (Fisher Scientific) and weighed. The DNA purification was carried out using Geneflow Q-Spin gel extraction/PCR purification kit according to the instructions provided by the manufacturer. In brief, the agarose was mixed with capture buffer and melted at 60˚C and the solution was transferred to the columns supplied by the manufacturer. The columns were centrifuged at 13,000 rpm for 30 s. The flow-through was discarded and the columns were washed with 500 µl of wash buffer. Following centrifugation at 13,000 rpm for 1 min, the collection tube was replaced and the DNA was eluted with 30 µl of ddH_2O.

2.4.5. Miniprep

BAC DNA was isolated from SW102 *E. coli* cells containing the BAC of interest using the QIAGEN Spin Miniprep Kit (27016) buffers. Single colonies were inoculated in 5 ml LB cultures (section 2.1) containing 12.5 µg/ml chloramphenicol and incubated overnight in a shaking incubator at 32˚C at 250 rpm. The following day, the cells were pelleted at 4,000 rpm (4˚C) for 5 min. The supernatant was discarded and the cells were re-suspended in 250 µl of P1 buffer supplemented with RNase A. The cells were lysed by adding 250 µl of P2 buffer and incubating at RT for 5 min. To terminate the lysis step, 250 µl of N3 buffer were added and the tubes were centrifuged at 13,000 rpm for 10 min. To precipitate the DNA, supernatants were transferred to a new 1.5ml Eppendorf tube (Fisher Scientific), mixed with 750 µl of isopropanol (Fisher) and spun at 13,000 rpm at 4˚C for 10 min. Cell pellets were then washed with 500 µl of 70% ethanol for 10 min at RT. The pellets were then dried at 37˚C to remove residual ethanol and the pellet was re-suspended in 30 µl of ddH_2O.

2.4.6. Maxi prep

To isolate transfection grade BAC DNA, SW102 *E. coli* containing the BAC of interest were grown in large scale cultures and purified using NucleoBond BAC100 kit (Macherey-Nagel) in accordance with the manufacturer's instructions for low-copy number plasmids. First, 500 ml of overnight culture was pelleted by spinning at 6,000 rpm at 4˚C for 15 min. The cell pellet was then mixed with 24 ml of S1 buffer and upon addition of 24 ml of S2 buffer, incubated for 5 min at RT. 24 ml of N3 was then added and the cell lysates were incubated on ice for 5 min then centrifuged at 6,000 rpm (4˚C) for 15 min. The cellular debris was discarded and supernatant was filtered and applied to a pre-equilibrated column. The column was washed twice with 18 ml of wash buffer and then eluted with 15 ml of N5 buffer (pre-heated to 50˚C). The BAC DNA was then precipitated by adding 11 ml of isopropanol (Fisher) to the eluted DNA and spinning at 15,000 rpm and 4°C for 30 minutes. The supernatant was discarded and the cell pellet was washed with 5ml of 70% (v/v) ethanol and centrifuged at 15,000 rpm for 15 minutes. The ethanol was removed, the pellet was allowed to air-dry and DNA was then reconstituted in 100 µl of 10 mM TAE buffer pH8.

2.4.7. Determination of DNA concentration

To quantify DNA and evaluate its' purity, ND1000 spectrophotometer (NanoDrop) was cleaned then equilibrated with 2 µl of ddH_2O. Next 2 µl of solvent was pipetted onto the lower measurement pedestal to generate a reference for the 2 µl of DNA sample that was loaded afterwards.

2.4.8. Restriction digestion

Ten µl restriction digestion reactions containing 8 µl of DNA, 20 Units of restriction nuclease (NEB) and 1 µl of compatible NEB buffer were incubated at 37˚C for 1 hour. The generated DNA fragment sizes were resolved by gel electrophoresis (see section 2.4.3).

2.4.9. Transfection of BAC DNA into SW102 *E. coli*

Empty SW102 *E. coli* cells were inoculated into 5 ml of low salt LB media and incubated overnight at 32 °C in a shaking incubator (200 rpm). Next, 500 µl of overnight culture were mixed with 25 ml of LB media (section 2.1) and were placed back in the shaking incubator until the A_{600} reached 0.6. Then, the cells were chilled on ice for 15 min on a rocking platform (200 rpm). For one transfection reaction, 1.5 ml of SW102 *E. coli* cells were pelleted by spinning at 13,000 rpm for 1 min at 0°C. The supernatant was discarded and the cells were subjected to two successive rounds of washing with 1 ml of ice cold water and spinning at 13,000 rpm for 1 min (0°C). The cells were resuspended in 30 µl

of water, mixed with 10 ng of high purity DNA and transferred to a 0.2 cm cuvette (Bio-Rad, Hertfordshire, UK) and pulsed at 2.5 kV. The transfected cells were recovered with 1 ml of LB for 1 hour at 32°C in a shaking incubator. Stable transfectants were selected on LB agar plates (section 2.1) supplemented with 12.5 µg/ml chloramphenicol and screened by minipreparing DNA, performing restriction digestion and sequencing.

2.4.10. Recombineering

E. coli strain SW102 containing the BAC of interest was grown overnight at 32°C in LB medium supplemented with 12.5 µg/ml of chloramphenicol. Next, 500 µl of overnight culture was diluted in 25 ml of LB and incubated at 32°C until A_{600}=0.6. Lambda red gene expression was induced by incubating SW102 *E. coli* cells at 42°C for 15 min. Following a 15min incubation on ice, the cells were centrifuged three times at 4,500 rpm for 5 min (0°C) with 2 washes with 25 ml of ice-cold ddH_2O in between. After the final spin, cell pellet was resuspended in 500 µl of ddH_2O. Either purified PCR product or oligonucleotide primers (Appendix A) purchased from MWG Operon (Germany) at de-salted purity were mixed with 25 µl of SW102 *E. coli* cells, transferred to a 0.2 cm cuvette and electroporated at 2.5 kV. In the first round of recombineering, *lacZ/kan^r/RpsL* cassette was amplified with oligonucleotide primers containing 70 bp homology arms flanking the genes of interest. The cells were recovered with 1 ml of LB for 1 h at 32°C and selected onto LB agar plates containing 12.5 µg/ml chloramphenicol, 80 µg/ml 5-bromo-4-chloro-3-indolyl-β-D-galactopyranoside (X-gal), 200 µM IPTG and 25 µg/ml kanamycin. In the second round, *lacZ/kan^r/RpsL* cassette was seamlessly removed using oligonucleotide primers containing the modification of choice. The cells were recovered in 5 ml of LB (section 2.1) for 3h at 32°C and plated onto LB plates with 12.5 µg/ml chloramphenicol, 80 µg/ml X-gal, 200 µM IPTG and 200 µg/ml streptomycin.

2.4.11. Sequencing BACs

Following recombineering, to verify that the BAC contained the correct modification, the modified region in the miniprepared BAC DNA was amplified with sequencing primers (Appendix A) and purified as described in section 2.4.4. Sequencing reactions were set up using Mix2Seq kit (Eurofins Genomics) according to manufacturer's guidelines. Fifteen µl of BAC DNA were mixed with 2µl of either the forward or reverse sequencing primers at 10 µM concentration and aliquoted into Mix2Seq tubes (Eurofins Genomics) that were sent away to be sequenced.

2.4.12. Generating glycerol stocks

Overnight bacterial cultures grown in appropriate antibiotic and containing the BAC of interest were mixed with 15% glycerol (v/v) (Fisher), aliquoted into a freezing cryovial and stored at -80°C.

2.4.13. Virus DNA deep-sequencing

Purified virus DNA was sequenced on the MiSeq (Illumina) as previously described (Murrell et al. 2016).

2.4.14. Western blot

Cells were lysed with 200 µl of 1x NUPAGE LDS buffer (Life Technologies) containing 10% DTT (Sigma) and boiled at 100°C for 10 min. For analysing protein expression within tissues, the tissue of interest was washed with PBS and sonicated in 100 µl of lysis buffer for 30 s at 20% maximum amplitude using Vibra-Cell VCX130 sonicator (Sonics). The proteins were then loaded onto a NUPAGE 10% Bis-Tris gel (Life Technologies) and separated by running the gel at 200 Volts for 1 hour in manufacturers running buffer. To determine the size of the protein of interest, 7 µl of Novex Sharp Pre-stained Protein Standard (ThermoFisher Scientific) was loaded alongside the samples. Once electrophoresed, the proteins within the gel were transferred onto Amersham nitrocellulose membrane (GE Healthcare) at 20 Volts in transfer buffer (section 2.1) for 1 h in a Trans-Blot SD semidry transfer cell (Bio-Rad). The membrane was blocked overnight at 4°C in blocking buffer (0.1% Tween in PBS, 5% milk) and then washed three times with wash buffer (0.1% Tween in PBS). Next, the membrane was probed with a primary antibody (Table 7) at 4°C overnight. Following three washes with wash buffer, a horse radish peroxidase conjugated secondary antibody was added and the membrane was incubated at RT for 1 h, then exposed using AutoChemi imaging system and SuperSignal reagent (ThermoFisher Scientific) following the manufacturer's instructions.

2.4.15. Quantitative PCR (qPCR)

To quantify virus copy numbers in mouse organs, DNA extracted from tissue homogenates as described in section 2.5.2.8 and cell-free supernatants as described in section 2.5.2.7 were added to a qPCR reaction consisting of 500 nM primers and 1× iQ™ SYBR® Green Supermix. The samples were prepared in triplicates and analysed using QuantStudio 12K Flex Real-Time PCR system under the following thermal-cycling conditions: 50˚C for 2 min; 95˚C for 10 min; 40 cycles at 95˚C for 15s and 60˚C for 1 min followed by 95˚C incubation for 15s; 60˚C for 1 min and 95˚C for 15 min. Virus backbone was amplified using primers IE1F (AGCCACCAACATTGACCACGCAC) and IE1R (GCCCCAACCAGGACACACAACTC) whilst amplification of murine β-actin with β-actin

F (GGGCTATGCTCTCCCTCAC) and β-actin R (GATGTCACGCACGATTTCC) served as an additional control. Serial dilutions of K181 BAC and DNA extracted from NIH 3T3 cells were used to generate a standard curve.

2.5. *In vitro* techniques

2.5.1. HCMV

2.5.1.1. Transfection into mammalian cells

HCMV BACs were transfected into HFFF-hTERTs and HFFF-tets (10^6 cells) using Amaxa Basic Nucleofector kit (Lonza) as per manufacturer's guidelines. The cells were trypsinized (see section 2.2.1) and centrifuged at 90 × g for 10 minutes at RT. The cell pellet was then mixed with 100 µl of nucleofector solution and 4 µg of BAC DNA and transferred to a cuvette (supplied by the manufacturer) which was placed into a nucleofector device and electroporated using program T-16. Growth medium was added to the cuvette and the cells were transferred to a 60 mm^2 tissue culture flask (Corning).

2.5.1.2. HCMV virus stock preparation

HCMV virus stocks were generated by co-culturing HFFF-hTERTs with cell-associated virus from transfected cells or by infecting sub-confluent cells (80%) with cell-free virus as described in section 2.5.4 using multiplicity of infection (MOI) of 0.1. To disperse viral infection throughout the monolayer, the cells were trypsinized weekly as detailed in section 2.2.1 and re-seeded back into the same flask. Once 100% of cells were infected, the supernatant was harvested every other day until all of the cells were lysed and stored at -80°C.

2.5.1.3. Virus preparation and storage

Supernatants from HCMV infected cells were thawed in a water bath at 37°C and pelleted at 1,500 rpm for 3 min at RT. Cellular debris was discarded and the supernatants were pooled and centrifuged at 14,000 rpm for 2h at 21°C. Concentrated HCMV virions in the form of a visible pellet were reconstituted in growth media, aliquoted, and stored at -80°C.

2.5.1.4. Titration by plaque assay

To determine virus stock concentration for downstream experiments, 2.5×10^5 HFFFs or HFFF-hTERTs were seeded in a 6-well plate (Corning) and incubated at 37˚C overnight. The next day, the media was aspirated and replaced with 500 µl of fresh growth media and 100 µl of serially diluted virus was added to the cells in duplicates and incubated for

2 h at 37˚C. Following this, the virus was removed and semi-solid overlay medium A (section 2.1) was added to the plates to prevent cell-free spread of virus. After incubating the plates for 2-3 weeks, the semi-solid overlay medium was removed, the wells were washed twice with PBS and plaques were counted using a light microscope. To determine the titre of HCMV stock, the following formula was applied;

Eqn 1*:*

$$Titre\ (PFU/ml) = Number\ of\ plaques\ per\ well\ \times 10\ \times dilution\ factor$$

2.5.2. MCMV

2.5.2.1. Transfection of NIH 3T3 cells

Prior to the day of transfection, 8x10^5 NIH 3T3 cells were seeded in a 60 mm^2 Corning CellBIND flasks and incubated overnight. All the transfection steps were carried out using Effectene transfection reagent (QIAGEN) following the manufacturer's instructions. In brief, 1 µg of BAC DNA was mixed with DNA condensation buffer to a final volume of 150 µl. Next, 8 µl of enhancer were added to the mixture and incubated at RT for 5 min. Effectene-DNA complex formation was then induced upon incubating the condensed DNA with 25 µl of Effectene transfection reagent for 5-10 minutes at RT. Finally, 1ml of growth medium B was mixed with the complexes and was then added to the cells.

2.5.2.2. Virus stock preparation from transfected cells

Transfected NIH 3T3s were propagated for 14 days in 25 cm^2 Corning CellBIND flasks (Corning) until 80% of the cells displayed cytopathic effect (CPE). The supernatant, containing cell-released virions was then collected every other day and stored at -80˚C until all the cells were 100% infected. The infected cell monolayer was scraped and frozen down at -80˚C. To expand virus infections, the cell-free supernatant was used to infect one 75 cm^2 then one 150 cm^2 flask and so on until twelve 150 cm^2 flasks. Alternatively, the cells were infected with virus stock at an MOI of 0.005-0.01 as described in section 2.5.2.3.

2.5.2.3. Infection with cell-free virus

A day before the infection, cells were seeded in a plate or a cell culture flask and allowed to adhere. Next, the supernatant was removed and 200 µl of virus was incubated with the cells at 37˚C for 1 hour. Afterwards, the virus was aspirated and replaced with growth media, then incubated at 37˚C.

2.5.2.4. Virus purification on sucrose gradient

Supernatants, as well as the cells were defrosted at 37˚C in a water bath and all of the subsequent steps were carried out at 4°C to minimize the loss of virus titre. Cells in the cell culture supernatants were pelleted at 2,000 rpm for 5 min. The cell-free virus was then transferred to 250 ml virus pots and centrifuged at 12,000 rpm for 100 min whilst the cell pellet containing cell-associated virus was re-suspended in 5 ml of cold DMEM (Sigma), sonicated in a sonicating water bath (Fisher Scientific, FB15053) for 7 min and centrifuged at 3,000 rpm for 5 min to remove cellular debris. The supernatant from the cell-associated virus was transferred to a fresh tube and incubated on ice. The cell-free virus pellet was re-suspended in 5 ml of DMEM (Sigma), sonicated in a sonicating water bath (Fisher Scientific, FB15053) for 7 min and centrifuged at 3,000 rpm for 5 min. The supernatants were pooled and the virus was centrifuged at 18,100 rpm for 100 min over a 20% sorbitol cushion (see section 2.1). The supernatant was removed and the pellet was re-suspended in growth media 2, sonicated in sonicating water bath (Fisher Scientific, FB15053) for 5 min and centrifuged at 3,000 rpm for 5 min. Cellular debris was discarded and the virus was stored at -80°C.

2.5.2.5. Titration by plaque assay

MCMV virus titres were determined by incubating 200 µl of serially diluted virus stock in duplicates onto 1×10^5 of NIH 3T3s in a 12-well plate for 1 h at 37˚C. The virus was removed and overlay medium B was added to the cells and incubated for 6 days at 37˚C. Following this, the medium was discarded and the cells were fixed for 4h with 10% formaldehyde (Fisher) (in PBS) and then stained with 0.1% crystal violet (Sigma Aldrich). The plaques were counted using an inverted light microscope. Plaque forming units in 1 ml were calculated using the following equation:

Eqn 2*:*

$$Titre\ (PFU/ml) = Number\ of\ plaques\ per\ well\ \times 5\ \times dilution\ factor$$

2.5.2.6. Quantification of viral particles in mouse tissues

Liver, lung, spleen and salivary glands isolated from mice were homogenized in 1ml of DMEM (Sigma) containing Falcon round-bottom polypropylene tubes using IKA T10 basic homogenizer (model number: T10 B S2) To sterilize the probe of the homogenizer between samples within the same group, the probe was submerged in 70% ethanol and rinsed three times with PBS. An additional step where the probe was washed in bleach was added to ensure no cross-contamination between different sample groups. NIH-3t3 were then inoculated with serial dilutions of organ homogenates in duplicates and plates spun at 1,000 × g for 30 min. The supernatant was aspirated, 1 ml of CMV media was

added and the plates were incubated for 6 days at 37°C. Then, the overlay media was flicked off and the cell monolayer was fixed and stained with 10% formaldehyde (Fisher) (in PBS) and 0.1% crystal violet (Sigma Aldrich). To determine the plaque forming unit/gram of tissue, the following formula was used:

Eqn 3: $$PFU/g = \frac{number\ of\ plaques \times dilution\ factor}{Tissue\ weight\ (g)}$$

2.5.2.7. Cell-free viral DNA extraction

DNA was extracted from virus stocks and cell-free supernatants using QIAamp MinElute Virus Spin Kit (QIAGEN) following the manufacturer's protocol. In brief, 200 µl of virus was mixed with 25 µl of protease and 200 µl of buffer AL supplemented with 28 µg/ml of carrier RNA and incubated at 56˚C for 15 min. Addition of 250 µl of 100% ethanol to the lysate at RT for 5 min facilitated the binding of viral RNA and DNA to the membrane of the MinElute column. The tubes were centrifuged at 8,000 rpm for 1 min and the collection tube was replaced. Next, the tubes were washed with 500 µl of AW1 buffer, followed by 500 µl of AW2 buffer and precipitated with 500 µl of 96-100% ethanol. The flow-through was discarded and the column was dried by spinning at 20,000 x g for 3 min and the DNA was eluted using 20-150 µl of buffer AVE, incubating at RT for 1 min and centrifuging at 20,000 x g for an additional minute. The extracted DNA was then stored at -20°C.

2.5.2.8. Cell-associated viral DNA extraction from mouse tissues

Viral DNA was extracted from either the lung, liver, spleen or salivary glands using DNeasy Blood & Tissue (QIAGEN) buffers and columns. First, snippets of mouse tissues were lysed by incubating the sample in 360 µl of ATL buffer and 0.8 mg of proteinase K and incubating overnight at 200 rpm at 56˚C. Next, the samples were passed through a 23 and 27-gauge needles until the solution was homogenous. Then, buffer AL and 96-100% ethanol was mixed in a 1:1 ratio and 800 µl were added to the samples which were then vortexed and transferred into a DNeasy mini spin column and centrifuged at 6,000 x g for 1 min or until all of the sample had gone through the filter of the column. The supernatant was discarded and the columns were washed once by adding 500 µl of AW1 and then 500 µl of AW2 buffer and spinning at 6,000 x g for 1 min. The flow through was removed and the DNA was eluted by aliquoting 200 µl of elution buffer, incubating for 1 min at RT and spinning at 6000 x g for 1 min. The DNA was then stored at -20°C.

2.5.2.9. Growth assay

Supernatants from 1×10^5 NIH 3T3 or NIH 3T3-tet cells infected at MOI of 0.1 in tetracycline-free growth medium containing 1 µg of DOX were collected daily until all the cells had been killed/lysed, and stored in two aliquots at -80˚C. The supernatants were then serially diluted to 10^0, 10^{-1}, 10^{-2} and 10^{-3} and titrated as described in section 2.5.2.5.

2.5.2.10. Peripheral lymphocyte extraction

Blood (see section 2.6.4.3) was transferred into a 1.5 ml (1 ml) Eppendorf containing Red Blood Cell lysis (RBC) buffer (section 2.1) and incubated at RT for 5 min. The samples were then centrifuged at 1,500 rpm for 5 min. The pellet was washed in 1 ml of PBS and spun 1,500 rpm for 5 min. The cells were then reconstituted in GM3 media.

2.5.2.11. Splenocyte isolation

To isolate splenocytes, spleens were mashed through a 70 µm strainer (Fisher Scientific, cat no 22363548) using a plunger top of a 5ml syringe. The filter was washed twice with 10 ml of PBS and once a single cell suspension was obtained, the cells were centrifuged at 1,500 rpm for 5 min at RT. The supernatant was discarded and the cells were resuspended with 3 ml of RBC lysis buffer and incubated for 5 min. The lysis was terminated by adding 3 ml of PBS after which the cells were spun for 5 min at 1,500 rpm. Cell pellet was reconstituted in 5 ml of GM3 media and the cells were counted and frozen as described in sections 2.2.2 and 2.2.3, respectively.

2.5.2.12. Intestine processing

Peyer's patches were removed from small intestine and colon isolated from mice. Faeces were removed and the intestines were flushed with PBS. The intestines were cut longitudinally. Intestinal tissue was placed in 20 ml of PBS and vortexed to remove any debris. Then, the tissue was transferred into 20 ml of Hank's Balanced Salt Solution (HBSS) (ThermoFisher Scientific) supplemented with 5 mM EDTA, 10% FBS and 25 mM HEPES (Life Technologies) and incubated in a water bath (37˚C) at 200 rpm for 20 min.

2.5.2.13. Isolation of lamina propria lymphocytes

Intestinal tissue described in section 2.5.2.12 was washed in ml GM3 medium. The tissue was placed in a 1.5 ml Eppendorf containing 600 µl of GM3 medium and cut with scissors. For collagenase treatment, the tissue was transferred into 5 ml of RPMI (supplemented with 5% FBS, 250 Units of penicillin, 250 µg/ml of streptomycin and 2.4 mg/ml of collagenase A) and incubated at 37˚C at 100 rpm for 30 min. The suspension was filtered using a 40 µM cell strainer. Cells were centrifuged and reconstituted in GM3 medium.

2.5.3. Adenovirus

2.5.3.1. Transfection of 293-TREx

One day before transfecting adenovirus BACs, $2x10^6$ 293-TREx cells were seeded in a 60 mm^2 Corning CellBIND flask and incubated at 37˚C overnight. The same transfection protocol was carried out as the one described in section 2.5.2.1.

2.5.3.2. Expanding virus stocks

To bulk up existing virus stocks, 293TREx cells of 80–90% confluency were infected with purified virus with an MOI of 0.1/flask. When virus stocks had not been previously generated, virus extracted from transfected cells was used to infect the required number of flasks.

2.5.3.3. Extraction of virus from infected cells

Infected cells starting to detach from the flask and showing CPE were harvested and centrifuged at 1,500 rpm for 3 min. The cell pellet was resuspended in 5 ml of PBS and an equal volume of tetrachloroethylene (Fisher) was added. Following a 30s shake of the tube containing cells and tetrachloroethylene (Fisher), the tube was centrifuged at 2200 rpm 20 min. The top layer containing the virus was either purified on a caesium chloride gradient as described in section 2.5.3.4 or stored at -80°C.

2.5.3.4. Purification by caesium chloride (CsCl) gradient

Adenoviruses were purified on a caesium chloride gradient as previously described (Alba et al. 2012). First, the extracted virus prep was layered on top of 1.6 ml of heavy and 3 ml of light caesium chloride solution in an ultracentrifuge tube (Beckman Coulter). The tubes were then filled to the top with PBS and centrifuged at 90,000 × g for 2h at RT. The virus layer was then extracted using a 21-gauge needle attached to a 2ml syringe and then transferred to sterilized dialysis tubing (Medicell International, London) and dialyzed as described in section 2.5.3.5.

2.5.3.5. Dialysis

Virus in dialysis tubing (described in section 2.5.3.4) was placed in 2 l of dialysis buffer and incubated on a rocker for 2 hours at 4°C. Then dialysis buffer was replaced and the virus was dialyzed overnight at 4°C with constant rocking. The following day, the virus was removed from the dialysis tubing, aliquoted and stored at -80°C.

2.5.3.6. Titration by immunofluorescence

A 12-well plate (Corning) was seeded with 5x10^5 293TREx cells in 1 ml of growth media. The following day, 100 µl of serially diluted virus was added to the wells in duplicates and the plate was incubated at 37 ˚C for 48 hours. Next, the media was removed and the wells were incubated at RT for 5-10 min to air dry. Following this, 1 ml of acetone-methanol mix (50:50) was added to the wells and the plate was chilled at -20˚C for 10 min. Following the removal of acetone-methanol mix, the cells were washed three times with 1 ml of PBS and 500 µl of PBS containing anti-hexon primary antibody (1/5000) was added, then the plate was incubated on a rocking platform at 37˚C or 1 hour. Next, the antibody was removed and the cells were washed three times with PBS then 500 µl of diluted HRP-conjugated anti-goat antibody (1/1000) was added and the plate was incubated at 37˚C for 1 hour with constant rocking. Upon washing the cells 3 times with PBS, the infected cells were stained using a peroxidase substrate kit DAB SK-4100 (Vector laboratories) following the manufacturer's instruction. Once brown precipitate had formed, the plates were viewed under a microscope and infected cells were counted in five different fields of the well. To determine the titre, the following formula was applied:

Eqn 4:

$$Virus\ titre\ (PFU/ml) = \frac{Average\ number\ of\ infected\ cells\ per\ field\ \times 150\ (fields/well\ )}{0.1\ ml\ \times dilution\ factor}$$

2.5.4. Infections with HCMV and adenoviruses

Fibroblasts were seeded either in a 6-well plate (Corning) or a cell culture flask a day prior to infection. Once the volume of virus required was calculated using Eqn5 (see below), the virus was diluted in growth media. The media was aspirated from the cells and the virus was applied onto the cells for 2 h at 37 °C on a rocking platform (5-10 rpm). Subsequently, the virus was removed and replaced with 2 ml of growth media and the cells were incubated at 37 °C.

Eqn 5:

$$Volume\ (ml) = \frac{Multiplicity\ of\ infection\ \times Number\ of\ cells}{Virus\ titer\ (PFU/ml)}$$

2.5.5. Viral spread assay

NIH 3T3s (for MCMV) and HFFF-hTERTs (for HCMV) were transfected with BAC DNA as described in sections 2.5.2.1 and 2.5.1.1, respectively, and cultured until formation of

a single plaque. Then, the cells in the flask were trypsinized as detailed in section 2.2.1 and split into two flasks. Every 2-3 days the growth media in flask 1 was replaced with regular growth media whereas the media in flask 2 was supplemented with 1 µg/ml of DOX. The rate of virus infection was compared between the two flasks by eye using an inverted microscope.

2.5.6. Plaque size measurements

To quantify cell-associated viral spread, fibroblasts were infected with CMV (see sections 2.5.2.3 and 2.5.4), covered with overlay medium and incubated for 6 and 14 days, respectively. After the indicated time of infection, the overlay medium was removed and the cells were washed twice with PBS. For HCMV plaques, the cells were covered in PBS and images of plaques were taken using Zeiss Observer Z1 microscope and Zen software at 4× magnification. For MCMV, the cells were fixed and stained with IE1 antibody as described in section 2.5.7. Images of plaques were taken using Zeiss Observer Z1 microscope and Zenworks program at 10x magnification. To determine plaque sizes, the images were loaded onto Fiji and free-hand drawing tool was used to outline the shape of the plaque and measure its area.

2.5.7. Intracellular IE1 staining

After a 14-day infection with HCMV and 6-day incubation with MCMV, the overlay medium was removed and the cells were washed twice with PBS. Upon fixing the cells with acetone-methanol mix (50:50) for 5 min at RT, the acetone-methanol mix was aspirated and the cells were washed with PBS, then incubated with primary anti-IE1 antibody (see Table 7) at 37˚C for 30 min on a rocking platform. Excess unbound antibody was removed by washing twice with PBS and the cell monolayer was incubated at 37 ˚C for 30 min on a rocking platform with AlexaFluor 594 conjugated anti-mouse antibody (1:500). Cells were then washed twice with PBS and visualized using a Leica fluorescent microscope (Leica, Germany) at 4× and 10× magnification. Pictures of IE1 stained cells were taken using Openlab 3 software and further analysed using Fiji.

2.6. Preclinical animal models

2.6.1. Animals and ethics

All experiments were conducted under UK Home Office project licenses (30/2891, 30/3428 and 30/2969). Female C57BL/6 and BALB/c mice were purchased from (Envigo or Charles River, UK) and housed in Cardiff University Animal Research Lab. The mice were quarantined for one week in the animal facility before experiments were conducted. Mice were 6-8 weeks old at the time of vaccination. Mice immunizations, tumour challenge, tumour measurements, saliva collection, tail vein blood collection and organ harvest was performed by colleagues in the lab holding a UK Home Office project license in accordance with Home Office regulations.

2.6.2. Mice immunization

Mice were injected subcutaneously (s.c.) into the chest region with 50 µl of 8×10^5 plaque forming units (PFU) of recombinant adenoviruses (RAds) on day 0 and again on day 42. Mice were weighed on the day of injection and thereafter until the weight of the mice had recovered to the starting weight. For MCMV experiments, BALB/c were intraperitoneally injected with 400 µl containing 2×10^5 PFU of virus into the left flank. Viruses were diluted in sterile PBS (Life Technologies) and incubated on ice until the time of injection.

2.6.3. Adenovirus-specific techniques

2.6.3.1. Induction of tumour growth

One week after the RAd boost injection (see section 2.6.2), tumour cells, resuspended in PBS (Life Technologies) (10^5/100 µl 4T1 and CT26 and 2×10^5/50 µl LLC1) were subcutaneously injected into the left flank of either BALB/c or C57BL/6 mice. 4T1 and CT26 were used in the BALB/c mouse strain and took 7 and 10 days for the tumours to form, respectively. LLC1 cells were implanted into C57BL/6 strain and took approximately 11 days to grow to a palpable size.

2.6.3.2. Analysis of tumour bearing mice

Tumour development was evaluated 3 times a week. Once palpable tumour nodules had formed, the greatest longitudinal diameter (length) and the greatest transverse diameter (width) of the tumour were measured with an external caliper. To determine tumour volume, Eqn6 (see below) was used. To comply with Home Office regulations, tumour growth was measured until the tumours reached 14 mm in diameter, after which time the mice were sacrificed. In instances when the tumour had become necrotic, mice were

monitored daily and any signs of discharge, redness, crater-like appearance or mouse discomfort indicated that the mice needed to be culled.

Eqn 6:

$$Tumour\ volume\ (mm^2) = width\ (mm) \times length\ (mm) \times\ smaller\ value\ (width\ or\ length) \times (3.14/6)$$

2.6.4. MCMV-specific techniques

2.6.4.1. Doxycycline delivery *in vivo*

To enable replication of conditionally-replicating MCMV *in vivo*, mice injected with MCMV were given irradiated DOX feed (TD.01306, Envigo) at a concentration of 625 mg/kg for 1 week and 2 weeks. The feed was stored at 4°C and replenished in mice cages every other day.

2.6.4.2. Collection of murine saliva samples

Mice were anesthetized with isoflurane (Piramal Healthcare). Sublingual cavity was then rinsed with 20 µl of sterile PBS. Saliva samples were stored at -20˚C until further analysis.

2.6.4.3. Tail vein blood collection

Mice were placed in a heating chamber at 37˚C for 20 minutes. The mice were then placed in a mouse restrainer. The tail of the mouse was sprayed with anaesthetic ethyl chloride B.P fine spray. A small cut in the tail was then made with a sterile scalpel blade (Swann-Morton) and the blood was collected in a heparin-coated microvette (Sarstedt).

2.7. 5T4 epitope mapping

2.7.1. Peptide pools and matrix systems

Human 5T4 peptide pools were kindly provided by Prof Awen Gallimore. These peptide pools were generated by using forty-one 20mers (Table 12), overlapping by 10 aa that covered the entire length of h5T4 protein (Appendix B). The peptide pools were designed by Dr Martin Scurr by adapting a matrix system (shown in Table 13) whereby 5-7 peptides at a concentration of 5 µg/ml per peptide would make up a single peptide pool. The peptides were ordered from GLBiocem (Shanghai, China) at a 95% purity.

2.7.2. *Ex vivo* Enzyme-Linked ImmunoSpot (ELISpot) assay

Polymer-backed 96-well filtration plates (MerckMillipore) were washed once with 70% ethanol followed by four washes with PBS. The plates were pre-coated with anti-mIFN-γ antibody (15 µg/ml) overnight at 4°C. The following day, the antibody was discarded and the wells were blocked with 100 µl of RPMI 5% at 37°C for 1 h. Next, splenocytes isolated as described in section 2.5.2.11 were plated out in duplicate wells/condition and stimulated with either whole 5T4 protein (10 µg/ml, Oxford BioMedica) (provided by Prof Awen Gallimore), 5T4 peptide pools (5 µg/ml per peptide, GL Biochem, China) or individual 5T4 peptides (5 µg/ml/peptide, Severn Biotech) for 18-24 h (37°C, 5% CO_2). As a positive control, Phytohemagglutinin (PHA) was used at a concentration of 10 µg/ml. The cells were discarded and the plates were handled as per the instructions supplied by the manufacturer. In brief, the wells were washed 5 times with 150 µl of PBS. 50 µl/well of biotinylated rat anti-mouse interferon-gamma antibody diluted to 1 µg/ml in PBS was added to the wells and the plate was incubated for 2 hours at room temperature. Next, unbound antibody was removed with 5 washes with PBS and the plate was incubated with 50 µl of Streptavidin Alkaline Phosphatase Polymer diluted to 1µg/ml per well for 1 hour at RT. Finally, the antibody was discarded, the plates were washed with PBS and 50µl/well of colour development buffer (BCIP/NBT-plus substrate, Mabtech) was added to each well and incubated at RT in the dark for 10-15 min. To terminate the reaction, the plate was rinsed with ddH_2O and was left to air-dry. The numbers of spot forming units were quantified using an automated ELISpot plate reader (CTL Immunospot, USA).

2.7.3. Peptide stability assay

Peptide stability assay was performed as previously described by (Gallimore et al. 1998). In brief, T2 K^b and T2 D^b cells were counted and $4x10^5$ cells/peptide/time point were centrifuged at 1,600 rpm for 4 min at RT. The cells were washed twice with PBS followed by a spinning step at 1,600 rpm for 4 min at RT. The cell pellet was resuspended in 100 µl of 0% RPMI containing 20 µM peptide (Table 14) for 1h at 37°C (5% CO_2). Next, the cells were washed 3 times with cold 0% RPMI, the cell pellet was resuspended in 1 ml of 0% RPMI and the plate was incubated for a further 0, 2 or 4 hours at 37°C (5% CO_2). At each time point, 250 µl of cells were transferred to a v-bottom 96-well plate (ThermoFisher Scientific) and centrifuged at 1,600 rpm for 4 min. The cells were resuspended in 50 µl of PBS containing either anti-MHC Class I H2 Kb + Db-PE (Table 7) or anti-Mouse IgG2a-PE antibody (isotype control) and incubated at 4°C for 30 min. After that, the plate was spun at 1,600 rpm for 4 min and washed once with PBS. The cell pellet was fixed with 2% (v/v) PFA (section 2.1) and the samples were analysed on Accuri C6 flow cytometer as described in section 2.11.

Table 12: h5T4 20mers

No.	Sequence	No.	Sequence	No.	Sequence
1	MPGGCSRGPAAGDGRLRLAR	**15**	LPSLRQLDLSHNPLADLSPF	**29**	LQGLPHIRVFLDNNPWVCDC
2	AGDGRLRLARLALVLLGWVS	**16**	HNPLADLSPFAFSGSNASVS	**30**	LDNNPWVCDCHMADMVTWLK
3	LALVLLGWVSSSSPTSSASS	**17**	AFSGSNASVSAPSPLVELIL	**31**	HMADMVTWLKETEVVQGKDR
4	SSSPTSSASSFSSSAPFLAS	**18**	APSPLVELILNHIVPPEDER	**32**	ETEVVQGKDRLTCAYPEKMR
5	FSSSAPFLASAVSAQPPLPD	**19**	NHIVPPEDERQNRSFEGMVV	**33**	LTCAYPEKMRNRVLLELNSA
6	AVSAQPPLPDQCPALCECSE	**20**	QNRSFEGMVVAALLAGRALQ	**34**	NRVLLELNSADLDCDPILPP
7	QCPALCECSEAARTVKCVNR	**21**	AALLAGRALQGLRRLELASN	**35**	DLDCDPILPPSLQTSYVFLG
8	AARTVKCVNRNLTEVPTDLP	**22**	GLRRLELASNHFLYLPRDVL	**36**	SLQTSYVFLGIVLALIGAIF
9	NLTEVPTDLPAYVRNLFLTG	**23**	HFLYLPRDVLAQLPSLRHLD	**37**	IVLALIGAIFLLVLYLNRKG
10	AYVRNLFLTGNQLAVLPAGA	**24**	AQLPSLRHLDLSNNSLVSLT	**38**	LLVLYLNRKGIKKWMHNIRD
11	NQLAVLPAGAFARRPPLAEL	**25**	LSNNSLVSLTYVSFRNLTHL	**39**	IKKWMHNIRDACRDHMEGYH
12	FARRPPLAELAALNLSGSRL	**26**	YVSFRNLTHLESLHLEDNAL	**40**	ACRDHMEGYHYRYEINADPR
13	AALNLSGSRLDEVRAGAFEH	**27**	ESLHLEDNALKVLHNGTLAE	**41**	YRYEINADPRLTNLSSNSDV
14	DEVRAGAFEHLPSLRQLDLS	**28**	KVLHNGTLAELQGLPHIRVF		

Table 13: Matrix system used for making up thirteen h5T4 peptide pools

	1	***2***	***3***	***4***	***5***	***6***
7	1	2	3	4	5	6
8	7	8	9	10	11	12
9	13	14	15	16	17	18
10	19	20	21	22	23	24
11	25	26	27	28	29	30
12	31	32	33	34	35	36
13	37	38	39	40	41	

Table 14: Individual 5T4 peptides used in *ex vivo* ELISpot

Mouse strain	Sequence
C57BL/6	VSFRNLTHL
	NSLVSLTYV
	SAPSPLVEL
	TSYVFLGIV
BALB/c	LSHNPLADL
	RGPAAGDGR
	GGCSRGPAA
	RSFEGMVVAALLAGR

2.8. Tetramerization

Fluorescent tetrameric pMHCI complexes were produced by mixing conjugated streptavidin and biotinylated pMHCI monomers at a 1:4 molar ratio. Briefly, 30 ug biotinylated M123/pp89 H2-L^D-restricted $_{168}$YPHFMPTNL$_{176}$ (Peptide synthetics). monomers were tetramerized over 100 mins by mixing with appropriate Streptavidin-Allophycocyanin (SA-APC) (For every 10 µg of monomer 8 µl of SA-APC was used) (Life-Technologies).

2.9. Tetramer staining

Isolated murine lymphocytes were centrifuged at 2,000 rpm for 2 min (RT) and washed once with 200 µl of PBS. Following another spin at 2,000 rpm for 2 min, the supernatant was removed and the cells were stained with 25 µl of Zombie Aqua fixable viability dye (BioLegend) (1:500 in PBS) at RT for 5 min avoiding exposure to light. 100 µl of PBS was then added and the cells were centrifuged at 2,000 rpm for 2 min (RT). The supernatant was discarded and the cells were stained with 25 µg/ml of SA-APC conjugated pp89/M123 tetramer for 15 min at 37˚C. Cells were then washed with 100 µl FACS buffer and stained with anti-CD16/32 Fc-block (Biolegend) (1:50 in FACS buffer) for 20 min at 4°C with limited exposure to light. Subsequently, the cells were washed with 100 µl FACS buffer, centrifuged at 2,000 rpm for 2 minutes, and the supernatant was removed. Cells were then stained with the following anti-mouse antibodies, anti-CD3, anti-CD4, anti-CD8, anti-CD27, anti-CD44, anti-CD69 and anti-CD103, (Table 1), all 1/100 in FACS buffer and incubated for 20 min at 4˚C. Cells were then washed with 100 µl FACS buffer and centrifuged at 2,000 rpm for 2 minutes. Supernatant was removed and the cells were reconstituted in 200 µl of FACS buffer and analysed with an Attune NxT flow cytometer (Thermo-Fisher) using FlowJo software (TreeStar inc, USA).

2.10. Intracellular cytokine staining (ICS)

Resuscitated murine splenocytes were pipetted into a V-bottomed 96-well plate containing 200 µl of RPMI (10% FBS; L-glutamine; pen/strep) and stimulated with 3 µg/ml of MHCI-restricted peptides (M123/pp89 H2-L^D-restricted $_{168}$YPHFMPTNL$_{176}$) or with 3 µg/ml MHCII-restricted peptides (IAHQRITLTARCLRL and SQQKMTSLPMSVFYS; Innovative Peptide Solutions). For MHCI-restricted peptide stimulated wells, 2 µg/ml of Brefeldin A (Sigma) was added after 1 hour of stimulation and incubated for a further 5 hours at 37˚C 5% CO_2. For MHCII-restricted peptides 2

µg/ml of Brefeldin A was added after 2 hours of peptide stimulation and incubated for a further 4 hours at 37˚C 5% CO_2. Post-stimulation, cells were centrifuged at 2,000 rpm for 2 min (RT). The supernatant was discarded, and the cells were washed with 100 µl of FACS buffer and centrifuged at 2,000 rpm for 2 min (RT). Cell pellets were stained using 25 µl of Zombie Aqua fixable viability dye (BioLegend) (1:500 in PBS) for 5 minutes avoiding any exposure to light. Cells were then washed with 100 µl FACS buffer and centrifuged at 2,000 for 2 min (RT). Cells were then washed with 100 µl FACS buffer and stained with anti-mouse anti-CD16/32 Fc-block (Biolegend) (1:50 in FACS buffer) for 20 min at 4°C with limited exposure to light. Cells were further washed using 100 µl FACS buffer and centrifuged at 2,000 rpm for 2 minutes. The supernatant was discarded and the cells were stained for the following cell surface markers, anti-mouse anti-CD3, anti-CD4, anti-CD8, anti- Killer cell lectin-like receptor subfamily G member 1 (KLRG1) and anti-CD44 (Table 1) (all 1/100) (Biolegend) and incubated for 20 min at 4˚C. Cells were then washed in 100 µl FACS buffer. Cells were then fixed with 4% PFA solution for 20 mins at 4°C. Cells were then washed with 100 µl FACS buffer and 25µl of Saponin buffer was added to the cells for 20 mins 4°C. Cells were then washed with an excess of Saponin buffer and FACS buffer. Cells were then stained with the following intracellular anti-mouse antibodies, anti-IFN-γ and anti-TNF-α for 20 mins 4°C. Cells were then washed using 100 µl of FACS buffer and spun at 2,000rpm for 2 mins. Cells were then reconstituted in 200 µl of FACS buffer and analysed using an Attune NxT flow cytometer FlowJo software.

2.11. Flow cytometry

To look at enhanced Green Fluorescent Protein (eGFP) and phycoerythrin (PE) expression in infected cells, cells were harvested as detailed in section 2.2.1 and washed twice with PBS (Life Technologies), followed by a spin at 1,500 rpm for 3 min. The cell pellet was then resuspended in 200 µl of PBS (Life Technologies) to get a single cell suspension and fixed in 2% (v/v) PFA (section 2.1) for 15 min at 4˚C. eGFP expression and (PE) fluorescence was monitored on Accuri C6 flow cytometer via the FL1 and FL2 detector, respectively, and analysed on Accuri C6 264 software. The cell gating strategy involved differentiating the cells based on forward scatter (FSC) which is proportional to the size of the cell and side scatter (SSC) which indicates cell granularity. In instances where extracellular staining was required, washed cells were stained with primary antibody at 4˚C for 30 min. After that, unbound antibody was removed by washing the cells with PBS (Life Technologies) and secondary antibody

was added at 4 ˚C for an additional 30 minutes. The cells were washed and fixed with 2% PFA (section 2.1) then analysed on the flow cytometer.

2.12. Statistical analysis

Statistical analyses were performed using GraphPad Prism 6 software (GraphPad Software, Inc., CA, USA). To compare 2 sets of data, unpaired student's t test was performed with two tailed distribution whereas for multiple datasets either unpaired one-way ANOVA or two-way ANOVA tests were performed with an additional Tukey's post-test. Survival rates were graphed using Kaplan and Meier method and analysed using the log-rank (Mantel-Cox) or Gehan-Breslow-Wilcoxon test. Data was plotted as mean ± standard deviation (SD) and statistical significance in figures and tables is indicated as follows; *$p < 0.05$; **$p < 0.01$; ***$p< 0.001$ and ****$p<0.0001$.

Chapter 3 Results

3.1. Generation and analysis of conditionally replicating CMV in vitro

Multiple viruses were generated during the course of this study. More information regarding the generation and analysis of these vectors is provided in subsequent sections. The vectors are listed in Table 15 (human CMV) and Table 16 (mouse CMV), along with some key characteristics, and are shown for reference purposes. The names of all the viruses are displayed in column 1. Names use the following nomenclature (refer to tables 15 and 16): ($M^{1}_{SV40}{}^{2}1^{3}M44^{4}$) where 1 represents the species specificity of the vector (H for human and M for mouse), 2 – promoter driving expression of tetR (SV40, RSV or MCMV IE for human CMV vectors and SV40, RSV or HCMV IE promoters for mouse CMV), 3 represents the number of tetO inserted upstream of essential CMV genes and 4 is the gene being regulated. Three tetR-based MCMV vectors (M_{RSV}2M100-tetR-P2A-M36; M_{HCMVie}2M100$_{RSV}$IE2; M_{RSV}2M100$_{HCMVie}$IE2) have two copies of *tetR* – one replacing m157 and the second in either IE2 (M122) or at the end of M36. pAL numbers represent an internal laboratory reference to be used by members of the group. Wild type (WT) viruses as well as viruses sent by collaborators (M50-1 and SCP-GFP) have distinct names.

Table 15: Human CMV vectors used and generated in this study

Name	pAL number	(1) Species	(2) tetR promoter	Location of *TetR*	(3) Number of tetO	(4) Location of tetO
WT Merlin	1111	Human	-	-	-	-
H2UL131A	1938	Human	-	-	2	UL131A
H_{SV40}	1916	Human	SV40	RL13	-	-
H_{RSV}	1917	Human	RSV	RL13	-	-
H_{MCMVie}	1924	Human	MCMV IE	RL13	-	-
H_{SV40}1UL44	2048	Human	SV40	RL13	1	UL44
H_{SV40}2UL44	2049	Human	SV40	RL13	2	UL44
H_{RSV}1UL44	2145	Human	RSV	RL13	1	UL44
H_{RSV}2UL44	2051	Human	RSV	RL13	2	UL44
H_{MCMVie}1UL44	2135	Human	MCMV IE	RL13	1	UL44
H_{MCMVie}2UL44	2136	Human	MCMV IE	RL13	2	UL44
H_{RSV}1UL54	2141	Human	RSV	RL13	1	UL54
H_{RSV}2UL54	2142	Human	RSV	RL13	2	UL54
H_{MCMVie}1UL54	2147	Human	MCMV IE	RL13	1	UL54
H_{MCMVie}2UL54	2148	Human	MCMV IE	RL13	2	UL54
H_{SV40}1UL75	2017	Human	SV40	RL13	1	UL75
H_{SV40}2UL75	2018	Human	SV40	RL13	2	UL75
H_{RSV}1UL75	2025	Human	RSV	RL13	1	UL75
H_{RSV}2UL75	2026	Human	RSV	RL13	2	UL75
H_{MCMVie}1UL75	2027	Human	MCMV IE	RL13	1	UL75
H_{MCMVie}2UL75	2028	Human	MCMV IE	RL13	2	UL75
H_{RSV}1UL85	2115	Human	RSV	RL13	1	UL85
H_{RSV}2UL85	2123	Human	RSV	RL13	2	UL85
H_{MCMVie}1UL85	2116	Human	MCMV IE	RL13	1	UL85
H_{MCMVie}2UL85	2130	Human	MCMV IE	RL13	2	UL85
H_{RSV}1UL100	2122	Human	RSV	RL13	1	UL100
H_{RSV}2UL100	2125	Human	RSV	RL13	2	UL100
H_{MCMVie}1UL100	2131	Human	MCMV IE	RL13	1	UL100
H_{MCMVie}2UL100	2129	Human	MCMV IE	RL13	2	UL100
H_{RSV}1UL123	2127	Human	RSV	RL13	1	UL123
H_{RSV}2UL123	2126	Human	RSV	RL13	2	UL123
H_{MCMVie}1UL123	2117	Human	MCMV IE	RL13	1	UL123
H_{MCMVie}2UL123	2121	Human	MCMV IE	RL13	2	UL123

(1)- species specificity of the vector; (2) – promoter driving tetR expression; (3) – number of tetO; (4) – the gene being regulated. pAL – plasmid number used for laboratory reference. MCMV IE - mouse cytomegalovirus immediate early; RSV – Rous Sarcoma virus; tetR – tetracycline repressor; WT – wild type.

Table 16: Mouse CMV vectors used and generated in this study

Name	pAL number	Strain	(1) Species	(2) tetR promoter	Location of *TetR*	(3) Number of tetO	(4) Location of tetO
WT K181	1918	K181	Mouse	-	-	-	-
M_{SV40}	1931	K181	Mouse	SV40	m157	-	-
M_{RSV}	1937	K181	Mouse	RSV	m157	-	-
M_{HCMVie}	1978	K181	Mouse	HCMV IE	m157	-	-
WT FRT	2208	Smith	Mouse	-	-	-	-
M50-1	2168	Smith	Mouse	CMV	M50	2	M50
SCP-GFP	2169	Smith	Mouse	CMV	m48.2 (SCP)	2	-
M_{SV40}1M44	2053	K181	Mouse	SV40	m157	1	M44
M_{SV40}2M44	2054	K181	Mouse	SV40	m157	2	M44
M_{RSV}1M44	2056	K181	Mouse	RSV	m157	1	M44
M_{RSV}2M44	2057	K181	Mouse	RSV	m157	2	M44
M_{HCMVie}1M44	2058	K181	Mouse	HCMV IE	m157	1	M44
M_{HCMVie}2M44	2133	K181	Mouse	HCMV IE	m157	2	M44
M_{SV40}1M75	2060	K181	Mouse	SV40	m157	1	M75
M_{SV40}2M75	2061	K181	Mouse	SV40	m157	2	M75
M_{RSV}1M75	2063	K181	Mouse	RSV	m157	1	M75
M_{RSV}2M75	2064	K181	Mouse	RSV	m157	2	M75
M_{HCMVie}1M75	2065	K181	Mouse	HCMV IE	m157	1	M75
M_{HCMVie}2M75	2066	K181	Mouse	HCMV IE	m157	2	M75
M_{RSV}1M85	2124	K181	Mouse	RSV	m157	1	M85
M_{RSV}2M85	2120	K181	Mouse	RSV	m157	2	M85
M_{HCMVie}1M85	2068	K181	Mouse	HCMV IE	m157	1	M85
M_{HCMVie}2M85	2069	K181	Mouse	HCMV IE	m157	2	M85
M_{RSV}1M100	2119	K181	Mouse	RSV	m157	1	M100
M_{RSV}2M100	2118	K181	Mouse	RSV	m157	2	M100
M_{HCMVie}1M100	2071	K181	Mouse	HCMV IE	m157	1	M100
M_{HCMVie}2M100	2072	K181	Mouse	HCMV IE	m157	2	M100
M_{RSV}1M123	2074	K181	Mouse	RSV	m157	1	M123
M_{RSV}2M123	2075	K181	Mouse	RSV	m157	2	M123
M_{HCMVie}1M123	2077	K181	Mouse	HCMV IE	m157	1	M123
M_{HCMVie}2M123	2099	K181	Mouse	HCMV IE	m157	2	M123
M_{RSV}2M100 $_{HCMVie}$IE2	2304	K181	Mouse	RSV and HCMV IE	m157 and IE2	2	M100

M_{HCMVie}2M100$_{RSV}$IE2	2307	K181	Mouse	HCMV IE and RSV	m157 and IE2	2	M100
M_{RSV}2M100-tetR-P2A-M36	2311	K181	Mouse	RSV and endogenous M36	End of M36	2	M100

(1) - species specificity of the vector; (2) – promoter driving tetR expression; (3) – number of tetO; (4) – the gene being regulated. pAL – plasmid number used for laboratory reference. HCMV IE - human cytomegalovirus immediate early; IE – immediate early; RSV – Rous Sarcoma virus; tetR – tetracycline repressor; WT – wild type.

Table 17: Growth properties of tet-regulated HCMV vectors

Name	Virus growth	Difference in HFFF-HTERTs -/+ DOX	HFFF-HTERTs vs HFFF-TET
WT Merlin	✓	X	X
H2UL131A	✓	✓	✓
H_{SV40}	✓	X	X
H_{RSV}	✓	X	X
H_{MCMVie}	✓	X	X
H_{SV40}1UL44	n/a	X	X
H_{SV40}2UL44	n/a	X	X
H_{RSV}1UL44	✓	X	X
H_{RSV}2UL44	X	X	X
H_{MCMVie}1UL44	✓	X	X
H_{MCMVie}2UL44	✓	X	X
H_{RSV}1UL54	✓	X	✓
H_{RSV}2UL54	✓	✓	X
H_{MCMVie}1UL54	✓	X	X
H_{MCMVie}2UL54	✓	X	X
H_{SV40}1UL75	✓	X	X
H_{SV40}2UL75	✓	X	X
H_{RSV}1UL75	✓	X	X
H_{RSV}2UL75	✓	X	X
H_{MCMVie}1UL75	✓	X	X
H_{MCMVie}2UL75	✓	✓	X
H_{RSV}1UL85	✓	X	X
H_{RSV}2UL85	✓	X	X
H_{MCMVie}1UL85	✓	X	X
H_{MCMVie}2UL85	✓	X	X
H_{RSV}1UL100	✓	X	X
H_{RSV}2UL100	✓	X	X
H_{MCMVie}1UL100	✓	X	X
H_{MCMVie}2UL100	✓	X	X
H_{RSV}1UL123	✓	✓	✓
H_{RSV}2UL123	✓	X	X
H_{MCMVie}1UL123	✓	X	X
H_{MCMVie}2UL123	✓	X	X

Virus growth refers to productive transfection producing infectious virus virions. Difference in HFFF-HTERTs -/+ DOX was measured by transfecting viral BAC DNA into HFFF-HTERTs supplemented with DOX. After appearance of plaques the cells were split in half and grown in -/+ DOX. Differences in plaque sizes are represented as a '✓'. 'HFFF-HTERTs – hTERTs vs HFFF-TET' comparison was performed by infecting HFFF-HTERTs – hTERTs (regular fibroblasts) and HFFF-TET (constitutively expressing tetR) monolayers under a semi-solid overlay. Plaque sizes were compared between these two cell types.
DOX – doxycycline; n/a – not applicable; HFFF-HTERTs - hTERT immortalized human foetal foreskin fibroblasts; HFFF-TET - human foetal foreskin fibroblasts transduced with tetR; WT – wild type; ✓ - productive infection/observed differences in virus growth; X – non-productive infection/no differences observed in virus growth.

Table 18: Growth properties of tet-regulated MCMV vectors

Name	Productive virus infection	Difference in NIH 3T3s -/+ DOX	NIH 3T3s vs NIH 3T3-Tets
WT K181	✓	X	X
M_{SV40}	✓	X	X
M_{RSV}	✓	X	X
M_{HCMVie}	✓	X	X
WT FRT	✓	X	X
M50-1	✓	✓	✓
SCP-GFP	✓	✓	✓
M_{SV40}1M44	X	X	X
M_{SV40}2M44	X	X	X
M_{RSV}1M44	✓	X	X
M_{RSV}2M44	✓	X	X
M_{HCMVie}1M44	✓	X	X
M_{HCMVie}2M44	✓	X	X
M_{SV40}1M75	X	X	X
M_{SV40}2M75	X	X	X
M_{RSV}1M75	✓	X	X
M_{RSV}2M75	✓	X	X
M_{HCMVie}1M75	✓	X	X
M_{HCMVie}2M75	✓	X	X
M_{RSV}1M85	✓	X	X
M_{RSV}2M85	✓	X	X
M_{HCMVie}1M85	✓	X	X
M_{HCMVie}2M85	✓	X	X
M_{RSV}1M100	✓	X	X
M_{RSV}2M100	✓	X	X
M_{HCMVie}1M100	✓	X	X
M_{HCMVie}2M100	✓	X	X
M_{RSV}1M123	✓	X	X
M_{RSV}2M123	✓	X	X
M_{HCMVie}1M123	✓	X	X
M_{HCMVie}2M123	✓	X	X
M_{RSV}2M100$_{HCMVie}$IE2	✓	✓	✓
M_{HCMVie}2M100$_{RSV}$IE2	✓	✓	✓
M_{RSV}2M100-tetR-P2A-M36	✓	✓	✓

BAC DNA transfections leading to production of infectious virions is shown in column 1. Difference in NIH 3T3s -/+ DOX was measured by transfecting viral BAC DNA into NIH 3T3s supplemented with DOX. After appearance of plaques, the cells were divided up and grown in -/+ DOX. Differences in plaque sizes are represented as a '✓'. 'NIH 3T3s vs NIH 3T3-Tets' comparison was performed by infecting NIH 3T3s (regular fibroblasts) and NIH 3T3-Tets (constitutively expressing tetR) monolayers under a semi-solid overlay. Plaque sizes were compared between these two cell types.

DOX – doxycycline; NIH 3T3s – mouse embryo fibroblasts; NIH 3T3-Tets – mouse embryo fibroblasts transduced with tetR; WT – wild type; ✓ - productive infection/observed differences in virus growth; X – non-productive infection/no differences observed in virus growth.

3.1.1. Construction of HCMV vectors using TREx system

3.1.1.1. Insertion of *tetR* in place of RL13

In order to generate safe and effective HCMV vectors, I elected to control virus replication using the TREx system. While the Tet-Off system allows repression of constitutively expressed genes upon addition of DOX, both the TREx and Tet-On systems only allow expression in the presence of DOX; thus, a vector would be rendered dependent on DOX for replication. A key difference between the two systems, however, is the fact that Tet-On is an activation system whereas TREx relies on de-repression. In addition to this, in TREx vectors, the gene of interest is expressed from an endogenous native promoter, and is therefore expressed at the natural time and amount whilst in Tet-On vectors, expression of the gene is under the control of an exogenous promoter. Since I wanted to minimise disruption to the natural CMV infection cycle, I adopted the TREx system. To engineer the vectors, two elements need to be inserted into the virus backbone – the *tetR* and tetO. In the absence of tetracycline or its analogue DOX, tetR homodimers bind to tetO inserted upstream of the target gene and inhibit transcription initiation, thereby preventing virus replication. Addition of DOX blocks the binding of tetR to the tetO, thus allowing for gene to be expressed and, as a result, the virus is able to replicate. It is crucial that *tetR* replaces a non-essential virus gene and does not interfere with expression of other virus proteins. In HCMV, mutations in RL13 are rapidly selected when clinical strains are grown *in vitro* and thus far, no beneficial function has been ascribed to the gene, making it an ideal location for inserting transgenes (Stanton et al. 2010).

The *tetR* was inserted via two rounds of recombineering (see Figure 7). First by replacing the RL13 gene with a *Amp^r/LacZ/sacB* selection cassette and selecting for ampicillin resistance and blue colouring, and then performing a second round of recombineering and replacing the cassette with the *tetR* gene. Colonies were screened for loss of the recombineering cassette (by selecting on sucrose; sacB makes colonies sensitive to sucrose). At this point, DNA was prepared from individual colonies, BACs were screened by restriction digest analysis, and sequenced to confirm that no major genome re-arrangements or mutations had occurred in the region of interest. Next, it was important to determine the level and timing of expression of tetR, to ensure it would suppress transcription of essential virus genes described in section 3.1.1.2. Since transcription of RL13 occurs late in the CMV replication cycle, it was necessary

to test alternative promoters that would drive earlier *tetR* gene expression. For this, a recombineering selection cassette was inserted upstream of *tetR* and then replaced with well characterized promoters (either SV40, RSV or MCMV IE) to generate three parental viruses: H_{SV40}, H_{RSV} or H_{MCMVie}, respectively. To confirm that no genome re-arrangement had occurred during recombineering, the viruses were digested with *Hin*dIII and their restriction digest pattern (Figure 8) was compared to that of WT Merlin. The viruses were also sequenced to ensure that no mutations had occurred during PCR amplification.

Sufficient levels of tetR are required to efficiently repress genes. To select vectors with the highest tetR expression, human fibroblasts were infected with all the vectors and cell lysates were analysed for tetR levels (Figure 9). IE1 and actin controls were used to indicate productive infection with no evidence of toxicity. Interestingly, RSV promoter driven expression could be detected as early as 8 h pi and increased over the course of infection until 72 hours. Unexpectedly, tetR expression could not be detected when driven by either the SV40 or MCMV IE promoter even at late stages of virus infection. Although SV40 and RSV are strong viral promoters, they failed to induce detectable levels of tetR expression in HF-hTERTs. These BACs have been transfected, and all produced infectious virions (Table 17) that grew to good titres, thus, insertion of the tet repressor did not affect their viability.

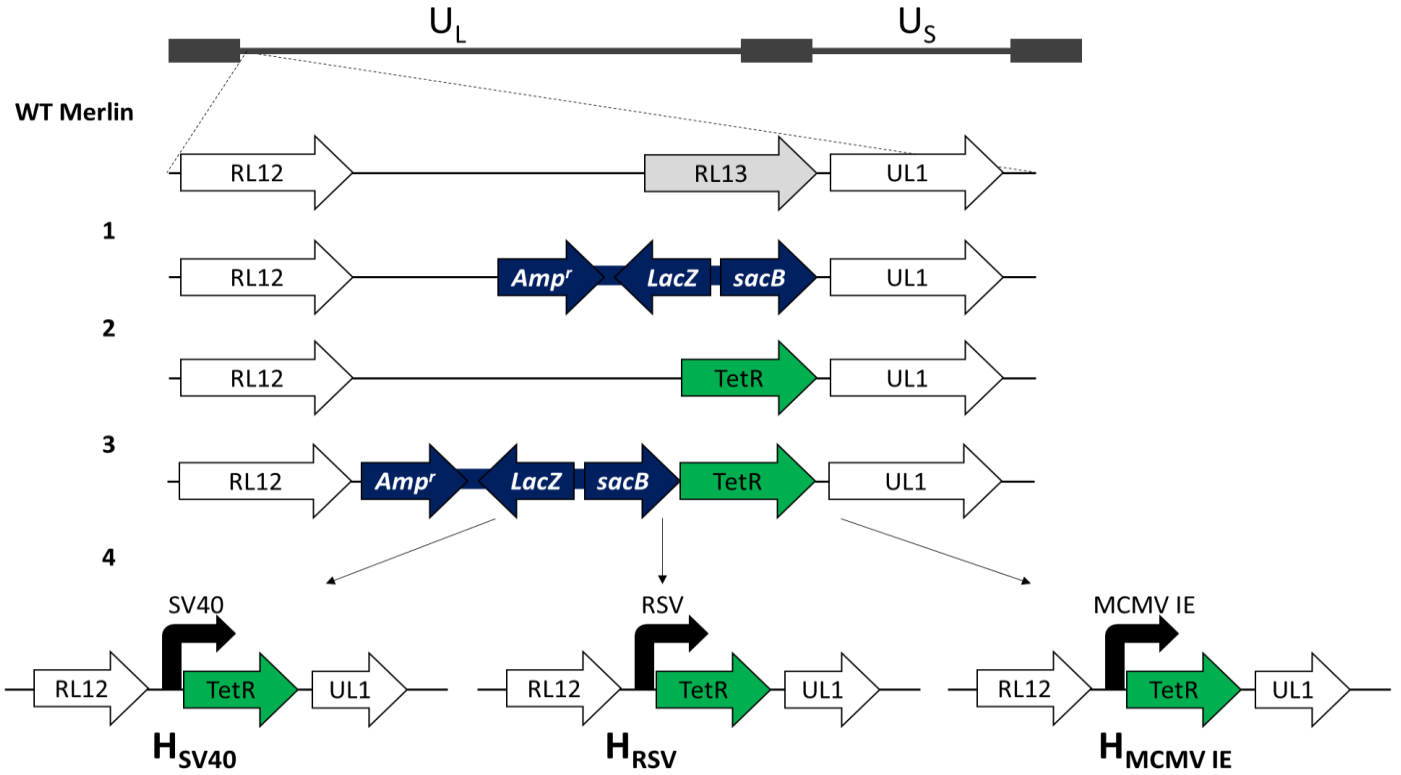

Figure 7: Cloning of tetracycline repressor expression cassette into human CMV vectors. Vectors H_{SV40}, H_{RSV} and $H_{MCMV\ IE}$ were generated via four steps of recombineering (numbers of the left). First, RL13 gene in WT Merlin strain (schematic depicted at the top) was replaced with the Amp^r/LacZ/sacB selection cassette (step 1) which was then replaced with the tetR gene (green) (step 2). In the third step of recombineering, Amp^r/LacZ/sacB selection was inserted upstream of tetR and then replaced (step 4) with either SV40, RSV or MCMV IE promoters. Arrows indicate the orientation of protein-coding regions. *Amp^r/LacZ/sacB* selection cassette is displayed in blue. Black arrows represent the promoters.

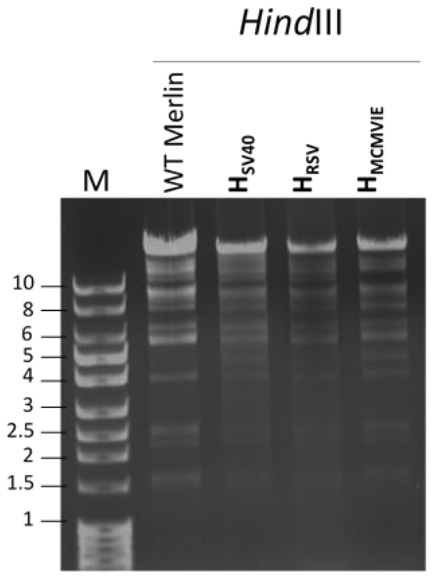

Figure 8: Restriction endonuclease (*Hind*III) fragment profiles of WT Merlin, H_{SV40}, H_{RSV} and H_{MCMVie} DNA. H_{SV40}, H_{RSV} and $H_{MCMV\ IE}$ BAC DNA was purified and digested with *Hind*III for 1 hour (37˚C). DNA fragments were compared to digested WT Merlin BAC DNA to confirm that no recombination or major mutations had arisen during BAC generation. The marker (M) lane (kb) is depicted on the left.

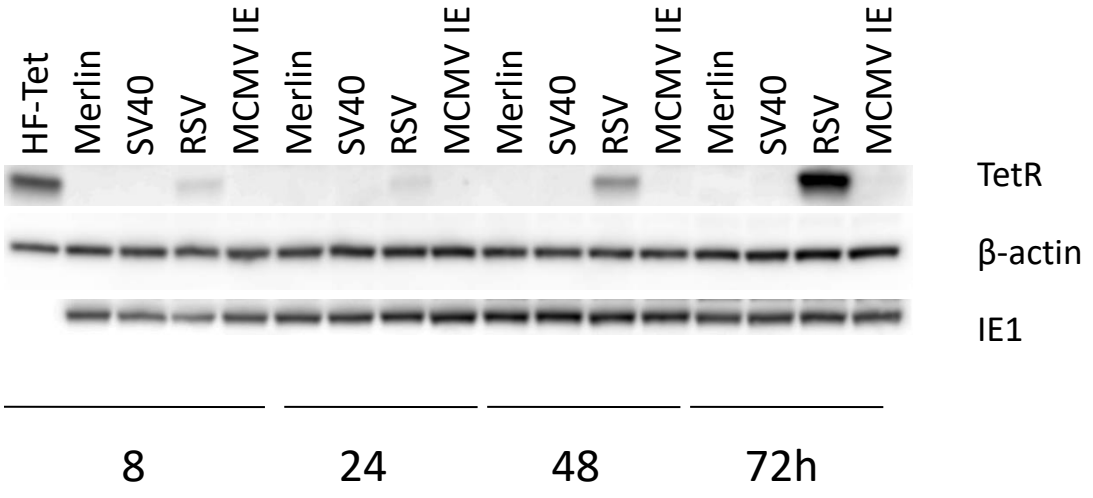

Figure 9: RSV promoter-driven expression of tetR detected in human fibroblasts as early as 8 h pi. Expression levels of tetR (inserted at the RL13 locus) regulated by SV40, RSV and MCMV IE promoters were analysed at 8, 24, 48 and 72 hpi. HFFFS were infected at an MOI of 5 with the various HCMV constructs and cell lysates were collected at indicated times. Expression of tetR in H_{SV40}, H_{RSV} and H_{MCMVie} viruses was compared to WT Merlin (negative control) and HF-Tet cell line (positive control) that constitutively express tetR and has previously been shown to efficiently repress gene expression (Stanton et al. 2010). IE1 expression represents HCMV infections whilst β-actin served as a housekeeping protein.

3.1.1.2. Insertion of tetO upstream of UL44, UL54, UL75, UL85, UL100 and UL123

The fact that tetR binds to tetO can be utilised in the context of vector development since careful positioning of tetO sequences close to transcription start sites can ablate formation of the transcription initiation complex (Yao et al. 1998). Previous work by Stanton *et al*, has shown that the location of tetracycline operator sequences affects the degree of gene regulation and thus, virus replication (Stanton et al. 2010). In their work, one or two tetO were inserted 19 and 44 bp upstream of the RL13 gene. Of these four configurations, only the presence of a single tetO 19 bp upstream enabled tight control of RL13 expression. When regulating UL131A, one or two tetO were placed 4, 16 or 33bp upstream of the gene translation start site. Strong control of transcription occurred in vectors containing 2 tetO 16 or 33 bp in front of the coding region (Stanton et al. 2010). From these experiments, it was apparent that tetO worked when placed 16-33 bp upstream of the ATG, whereas the number of tetO required was gene-dependent. I therefore inserted a selection cassette 20 bases upstream of six different HCMV genes (Figure 10). In the second round of recombineering, I replaced the cassette with a 100 bp oligonucleotide spanning the insertion site and containing one or two tetO sequences to generate a total of 28 vectors (Table 15). HCMV genes were chosen in which no other genes were directly upstream or in close proximity to the gene of interest, to facilitate insertion of tetO.

HCMV genes are conventionally divided into three distinct kinetic classes (immediate early, early and late), where immediate early genes control the expression of early genes and early genes express proteins that replicate the viral genome, which in turn is required for the expression of late structural genes. I wanted to see whether suppressing gene expression at different stages of the replication cycle would have an effect in inducing differential control of virus replication. I therefore selected an immediate early (UL123/UL122, IE1/IE2), early (UL44 DNA polymerase processivity factor and UL54, DNA polymerase catalytic subunit that both make up the DNA polymerase complex) and late (UL75, gH (required for entry); UL85, minor capsid protein and UL100, gM (required for entry)) genes as my targets. All of the genes selected were highly conserved among the *Betaherpesvirinae* family, with homologues both in human and mouse CMV. Deletion of any of these genes would render the virus inactive as there are no other gene products with complementing functions.

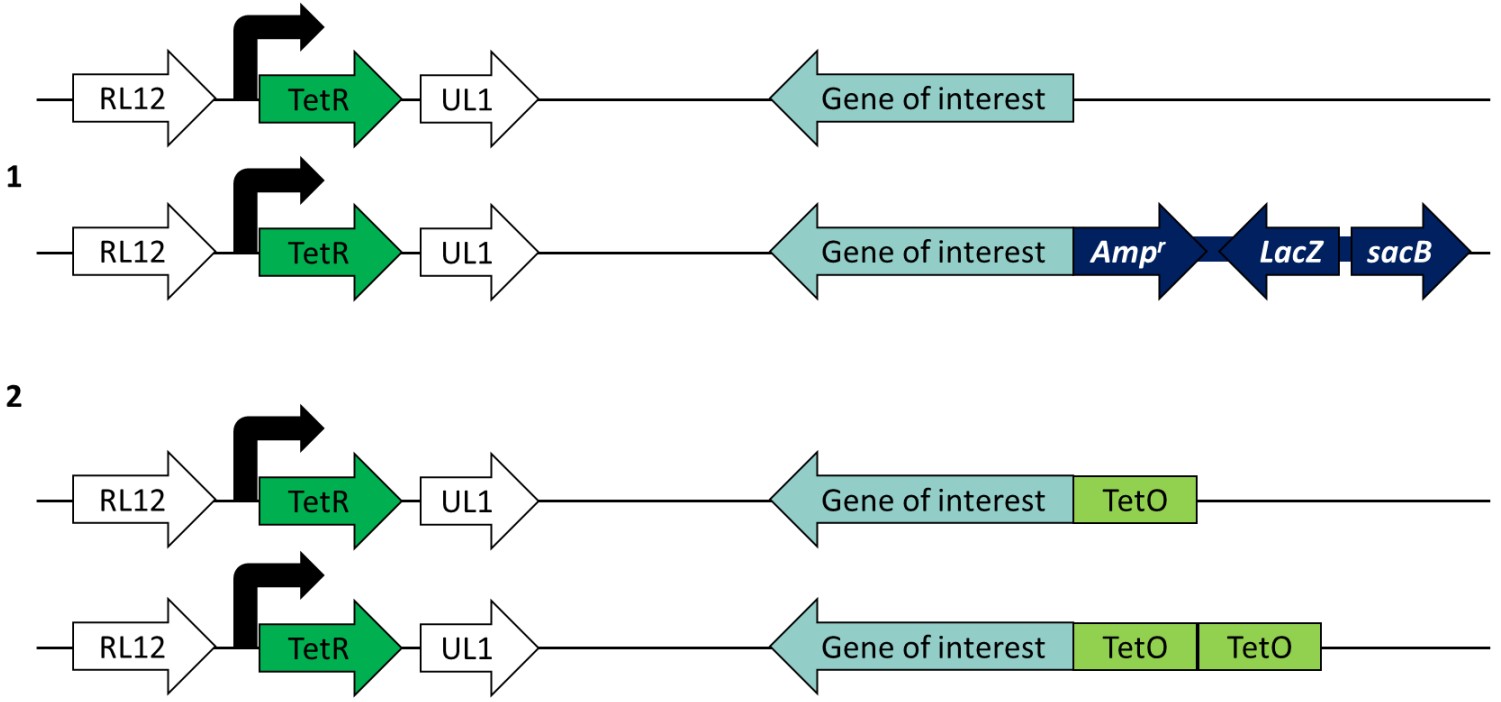

Figure 10: **Steps in cloning tetracycline operators (tetO) in HCMV vectors.** TetO were inserted into HCMV vectors via two steps of homologous recombineering. In the first step, *Amp*^{r}*/LacZ/sacB* selection cassette (displayed in dark blue) was inserted upstream of the 'gene of interest' (light blue). The 'gene of interest' represents either UL44, UL54, UL75, UL85, UL100 or UL123, a gene that may be transcriptionally controlled by tetR binding. In the second step, the selection cassette was replaced with either one or two copies of tetO (light green). Arrows indicate the orientation of protein-coding regions. Green boxes illustrate the tetracycline operator gene. A promoter is represented by a black arrow (upstream of *tetR* gene).

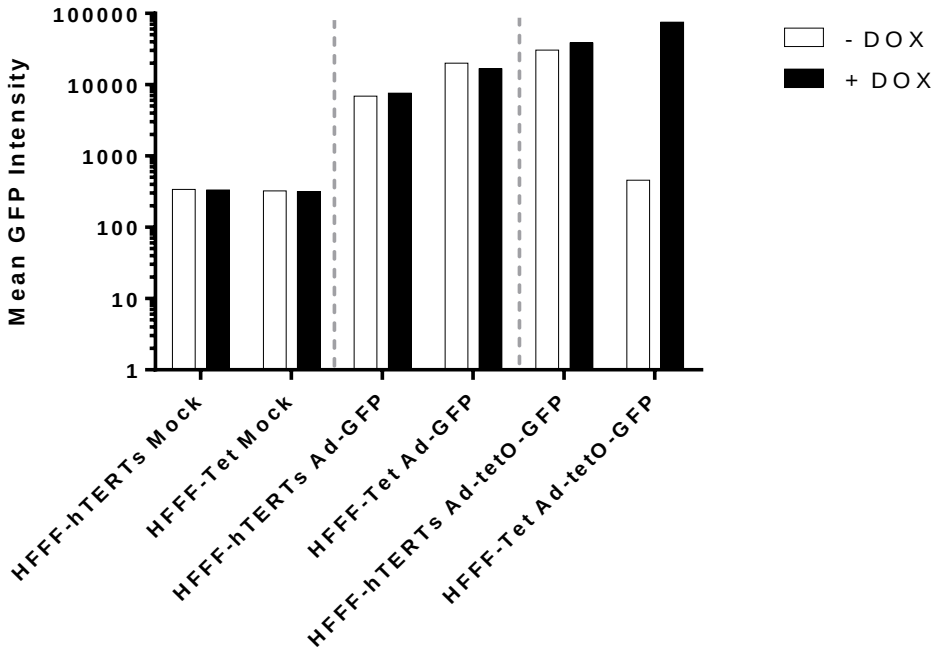

Figure 11: Expression of inducible GFP by adenovirus vector (Ad-tetO-GFP) was inhibited to background levels in fibroblasts constitutively expressing tetR (HFFF-Tet). The cells were infected (MOI=50) with control adenovirus encoding GFP (Ad-GFP) or Ad-tetO-GFP comprising of 2 tetO 10 bp upstream of eGFP. DOX was added at a concentration of 1 µg/ml to relieve repression of GFP expression. GFP expression levels were compared at 72 h pi BD Accuri C6 Cytometer.

3.1.2. Characterization of HCMV vector replication *in vitro*

3.1.2.1. The impact of doxycycline on growth kinetics of HCMV *in vitro*

The 28 tetR-regulated HCMV vectors (Table 15) generated in the study contained one or more tetO inserted upstream genes essential for efficient virus replication. In the absence of DOX, tetR should block expression of these genes thereby inhibiting virus propagation. To reconstitute all the viruses, I transfected the BACs into HFFF-hTERTs and supplemented the growth media every two days with 1 µg/ml of DOX. To facilitate dissemination of the virus, the transfected cells were trypsinized twice a week and re-seeded back into the same flask. To see whether virus growth could be controlled in a reversible manner, the cells showing CPE were split into two flasks, where one continually received DOX and the other one did not. Comparison of plaque numbers (indicative of the replicative capacity of the virus) over the course of infection revealed that only three viruses (H_{RSV}2UL54, H_{MCMVie}2UL75 and H_{RSV}1UL123) grew at a faster rate (Table 17) in the presence of DOX. For all of the remaining viruses, the plaques formed at a similar or sometimes somewhat faster rate in the cells where no DOX was present. This was contrary to what was predicted – if essential genes were tet-repressed, then plaque sizes/numbers should have been reduced in the absence of DOX.

3.1.2.2. Evaluation of HFFF-Tet cells

The inability of DOX to provide conditional control over virus replication could be due to DOX not being stable in tissue culture or the tetR not being expressed at high enough levels to repress gene transcription. I therefore used a cell line (HFFF-Tet) that constitutively expresses tetR, at a level previously shown to inhibit gene transcription (Stanton et al. 2010), as a positive control. To ensure that these cells were functional, I infected the parental HFFF-hTERTs (which lack tetR expression) and HFFF-Tets with Ad-GFP and Ad-tetO-GFP viruses for 72 hours and compared GFP expression to mock-infected cells (Figure 11). Both vectors expressed GFP, however, the Ad-tetO-GFP vector contains tetO upstream of GFP, making expression tetR-regulatable. Since HFFF-hTERTs do not express tetR, infecting with Ad-tetO-GFP conditional vector then adding or removing DOX did not affect expression of GFP. In HFFF-Tets, however, tetR binds to tetO and thus, inhibited GFP expression to background levels in the absence of DOX. Adding DOX blocked the binding between tetR and tetO

leading to 165-fold increase in GFP expression levels in HFFF-Tets infected with Ad-tetO-GFP. Ad-GFP does not contain any tetO sequences, consequently infection of HFFF-hTERTs and HFFF-Tets resulted in comparable GFP levels in the absence and presence of DOX.

To evaluate the stability of DOX *in vitro* (Figure 12), I infected HFFF-hTERTs and HFFF-Tets with Ad-tetO-GFP under four different DOX conditions and compared GFP levels to uninfected cells. I wanted to see whether DOX was stable in cell culture over 4 days. Therefore, to some infected cells I added DOX once, only on the first day of infection, to other cells I changed DOX daily. GFP expression levels in infected HFFF-hTERTs served as a positive control. Similar GFP expression levels were observed in infected HFFF-Tets receiving DOX, suggesting that DOX is stable in culture for at least 4 days.

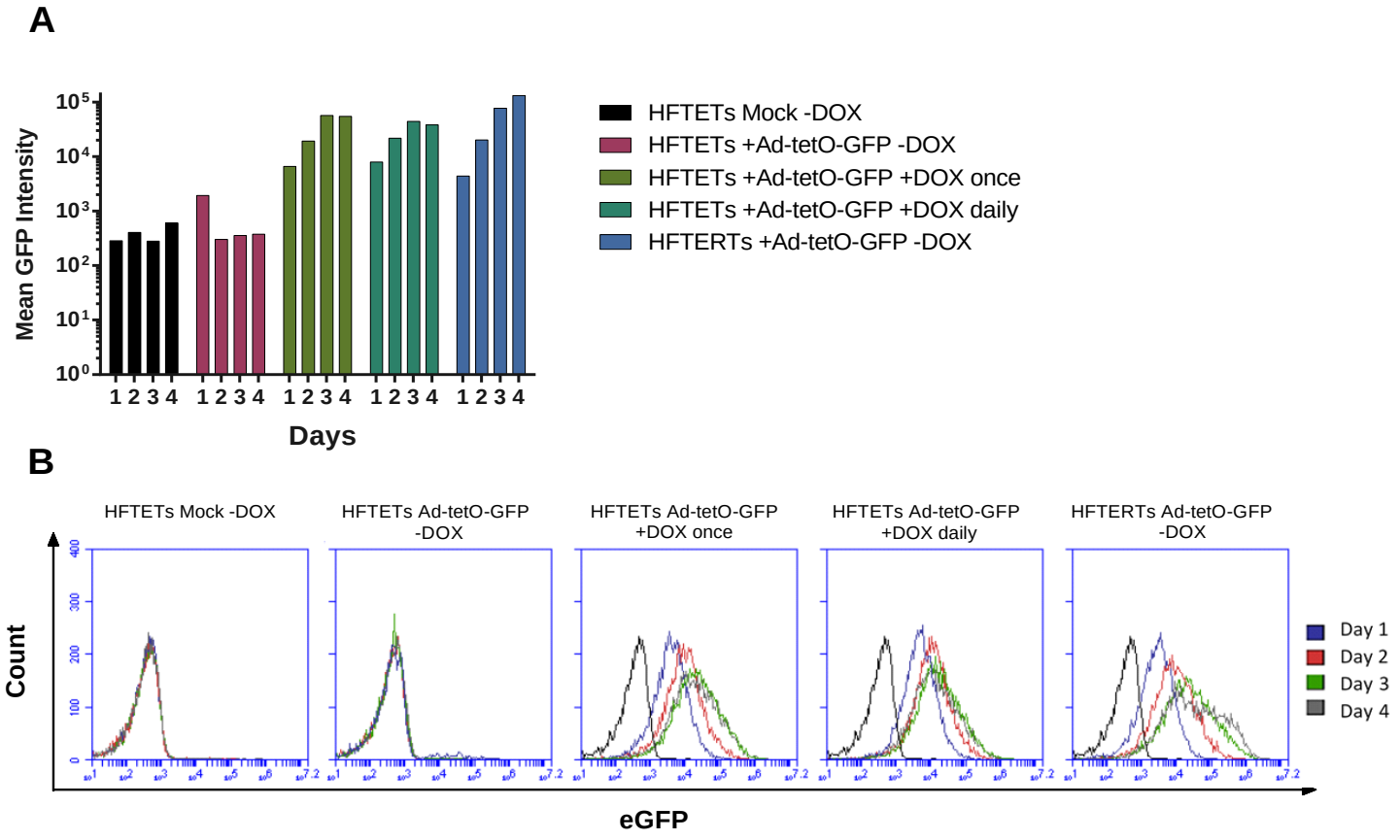

Figure 12: Doxycycline (DOX) is stable *in vitro* for at least 4 days. (A): DOX stability/functionality in HFFF-Tets and HFFF-hTERTs infected with Ad-tetO-GFP (MOI=50). The vector contains an *eGFP* gene downstream of tet-regulated HCMV MIE promoter. Infected cells were either supplemented with DOX once (day 0 of the experiment); daily or not supplemented at all. After 4 days, GFP expression in these cells was analysed using BD Accuri C6 Cytometer. (B) FACS plots showing the shift in eGFP expression levels in Ad-tetO-GFP infected fibroblasts over a course of 4 days. DOX was added to a 1 µg/ml concentration.

3.1.2.3. Comparative analysis of cell-cell HCMV spread

Cytomegaloviruses disseminate via cell-free release as well as cell-to-cell spread that makes the virus less susceptible to neutralising antibodies. Both means of transmission may be important in vaccination. Clinically, cell-free spread is thought to be more relevant for inter-host spread whereas cell-to-cell spread is thought to be responsible for dissemination through the host (intra-host spread).

To look in detail at the capacity of tet-regulated CMV vectors to spread via the cell-to-cell route, I infected HFFF-hTERTs and HFFF-Tets in parallel and compared plaque sizes grown under a semi-solid overlay that inhibits cell-free virus spread. The HFFF-Tets constitutively expressing tetR, served as a positive control for tetR expression. Since I had previously tested virus growth in HFFF-hTERTs in the presence and absence of DOX (Table 17) and did not observe major differences in the virus ability to replicate (all viruses grew in DOX), testing in HFFF-Tets showed whether the lack of differences was due to tetR expression. Each individual plaque was indicative of a single infection event/initially infected cell. Since WT Merlin does not contain *tetR* or tetO genes, it was used as a negative control in plaque size measurements (Figure 13). In addition to this, I used a previously described H2UL131A virus that contains tetracycline operators upstream of UL131A, a gene that inhibits growth in fibroblasts. In the presence of tetR, UL131A expression is repressed and, as a result, the virus is able to spread more rapidly. As expected, WT Merlin virus spread was comparable in HFFF-Tets and HFFF-hTERTs. Although the majority of tetR-regulated viruses infected the two cell lines to a similar degree, for H_{RSV}1UL54, H_{RSV}2UL54, H_{RSV}2UL75, H_{RSV}1UL85, H_{MCMVie}2UL85, H_{MCMVie}1UL85 and H_{MCMVie}2UL100 there was a slight, yet non-significant repression of virus replication in HFFF-Tet cells. The most striking difference, however, was observed for H_{RSV}1UL123 and H_{MCMVie}1UL123, where fewer and smaller plaques were detected in HFFF-Tets than in HFFF-hTERTs. In fact, H_{MCMVie}1UL123 was not detectable in HFFF-Tets at all thus demonstrating the significance of UL123/IE1 expression on virus replication also identifying it as a key target in vaccine development.

Next, I wanted to see whether repression of virus replication could be relieved by addition of DOX and whether tetR-regulated virus would grow to titres similar to WT virus. I selected H_{RSV}1UL123 as the most promising vector and infected HFFF-hTERTs in the presence and absence of DOX and compared plaque sizes to those observed

in HFFF-Tets. As expected, plaque sizes (Figure 14) of WT Merlin were similar in the presence and absence of DOX. Surprisingly, however, I observed a 2.2-fold reduction in plaque size in HFFF-Tets. I also observed a 3-fold difference in H2UL131A growth in HFFF-hTERTs when compared to HFFF-Tets. H2UL131A virus served as a positive control since expression of UL131A results in inhibition of HCMV replication. In HFFF-Tet cells expressing tetR, expression of UL131A gene is blocked thus, permitting virus replication. Larger H2UL131A plaques in HFFF-Tets were indicative that tetR was functional in the HFFF-Tet cells, although wide variation in plaque sizes meant that this was not statistically significant. As before, I could not detect infectious H_{RSV}1UL123 virus in HFFF-Tets, whereas cell-to-cell spread in the presence and absence of DOX was similar. This result suggests that stronger or earlier tetR expression as observed in HFFF-Tet cells that constitutively express tetR could suppress virus replication even more.

Propagation of virus can lead to the accumulation of mutations that enable the virus to grow better *in vitro* (Dargan et al. 2010; Murrell et al. 2016). I wanted to see whether the reason for not observing a significant effect in different DOX conditions was due to acquisition of mutations that affected gene regulation by DOX. To limit mutagenesis of the virus genomes, I used purified BAC DNA and transfected both HFFF-hTERTs and HFFF-Tets with H2UL131A (positive control) and H_{RSV}1UL123 and measured plaque sizes (Figure 15). I observed higher number of plaques in HFFF-TET cells as well as an 8.5-fold difference in infectivity for H2UL131A. H_{RSV}1UL123, on the other hand, was more prominently repressed in HFFF-TETs with a 74-fold difference, thus, suggesting that the virus had not mutated in *tetR* or tetO regions and other factors were affecting regulation of virus replication.

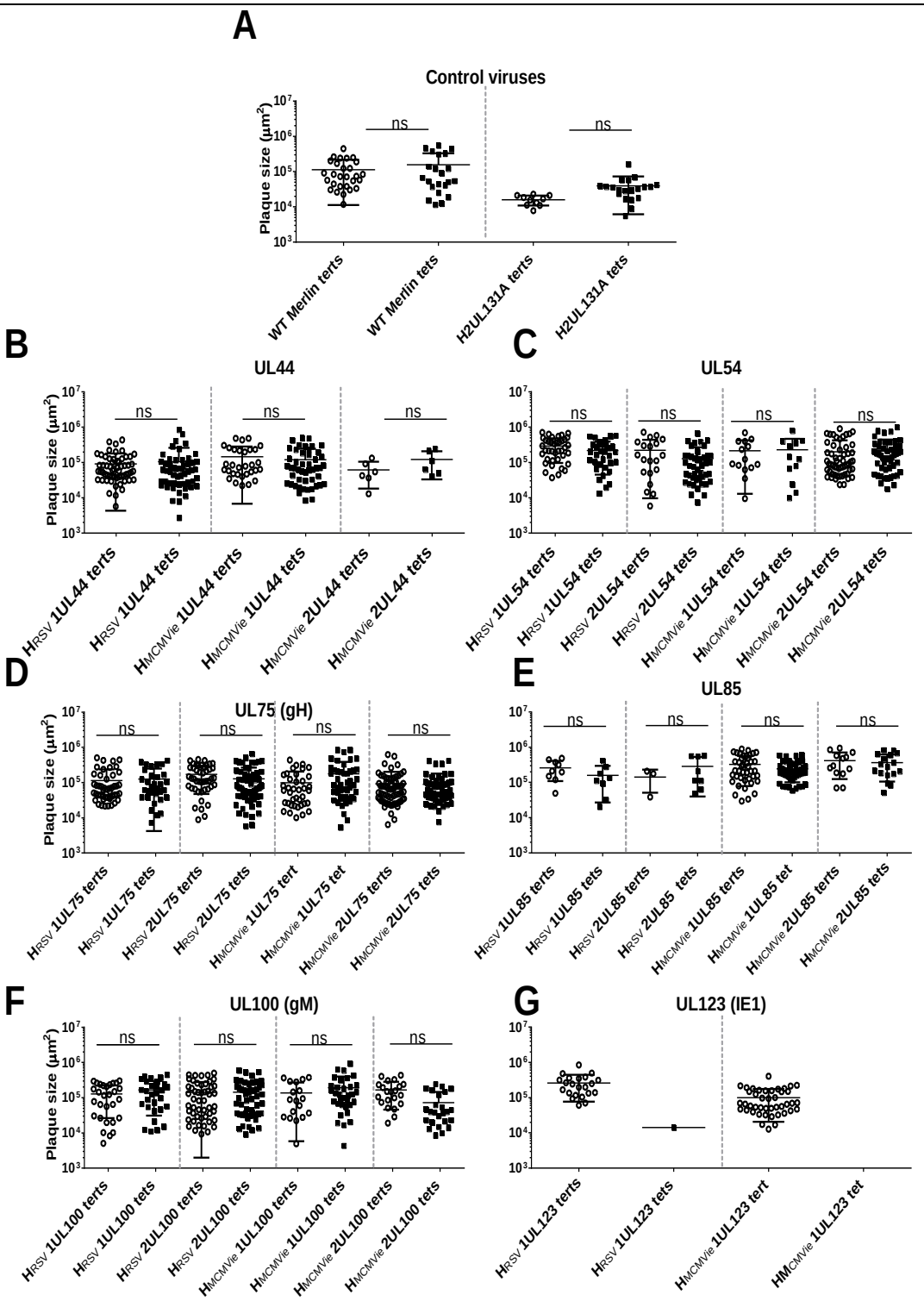

Figure 13: Repression of UL123 in HCMV inhibits cell-to-cell spread. Cell-to-cell spread of control HCMV viruses (A) and tetR-based BAC-derived HCMV containing tetO upstream of UL44 (B), UL54 (C), UL75 (D), UL85 (E), UL100 (F), and UL123 (G). Plaque sizes of viruses were measured (using Fiji) after infecting HFFFs (○) or HFFF-TETs (■) for 2 weeks under a semi-solid overlay medium to prevent cell-free virus spread. A single data point represents an individual plaque. Error bars show means ±SD. Panels B-F were analysed with one-way Analysis of Variance (ANOVA) with Tukey post-tests whilst panels A and G were assessed using unpaired 2-tailed t-test.

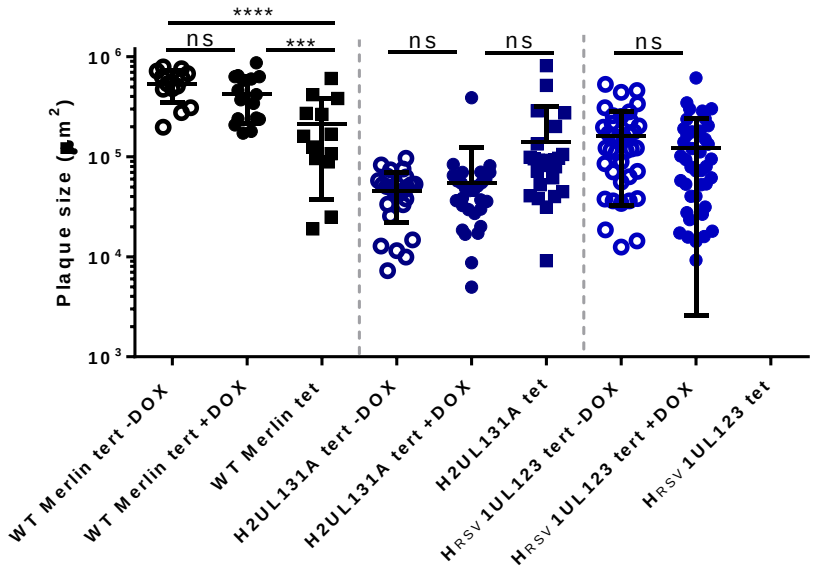

Figure 14: Addition of DOX relieves suppression of H_{RSV}1UL123 growth.. WT Merlin (negative control), H2UL131A (positive control) and H_{RSV}1UL123 were used to infect HFFF-TETs (■) and HFFF-hTERTs in the absence (○), presence (●) of DOX for 14 days. The cells were overlaid with semi-solid overlay media to impede cell-free virus spread. DOX in the media was replaced every three days. Data points denote individual plaque sizes. Error bars represent means ±SD. One-way ANOVA with Tukey post-test results are presented (***p< 0.001; ****p<0.0001).

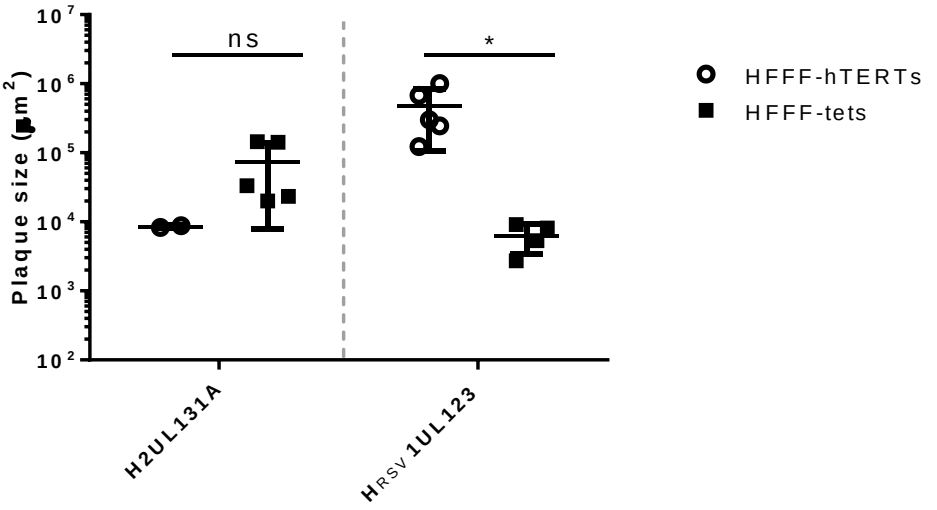

Figure 15: Growth of BAC-derived viruses in HFFF-hTERT (○) and HFFF-TET (■) cells. Sizes of plaques were measured at 2 weeks post-transfection (PT), with cells overlaid with semi-solid media to prevent cell-free spread of virus. 4 µg of DNA. Error bars represent means ±SD. One-way ANOVA with Tukey's multiple comparisons post-test are displayed (*p<0.05).

3.1.3. Construction of MCMV vectors using TREx system

3.1.3.1. Replacing m157 with *tetR* gene

Safety and efficacy evaluation of HCMV vectors needs to be carried out in animal models. Due to species specificity, it is not possible to grow HCMV in mice. I therefore modified the MCMV K181^{Perth} strain in parallel to HCMV vectors (described in section 3.1.1). To circumvent disruption of essential viral genes, I selected a region within m157 for inserting *tetR*. The m157 gene product binds to and stimulates the NK cell activation receptor Ly49H that is expressed by 50% of NK cells in the C57BL/6 mice strain (Smith et al. 2000). This in turn, leads to rapid clearance of the virus, making mice more resistant to MCMV. The majority of MCMV strains circulating in WT mice, however, encode m157 protein unable to activate NK cells via Ly49H (Voigt et al. 2003). In addition to this, majority of wild mice lack the Ly49H receptor (Abolins et al. 2017). Analogously to HCMV, *tetR* was inserted into MCMV via two recombineering steps (Figure 16). To establish early and high expression of tetR, a selection cassette was inserted upstream of the *tetR* gene and then replaced with either RSV, SV40 or HCMV IE promoter to give M_{RSV}, M_{SV40} or M_{HCMVie}, respectively. Next, I compared the levels of tetR expression driven by each of the promoters by performing a western blot analysis (Figure 17). Expression regulated by the SV40 promoter was not detected even at 72 hpi. RSV and HCMV IE promoter-driven tetR expression, on the other hand, was detected as early as 24 hpi and continued increasing until 72 hpi.

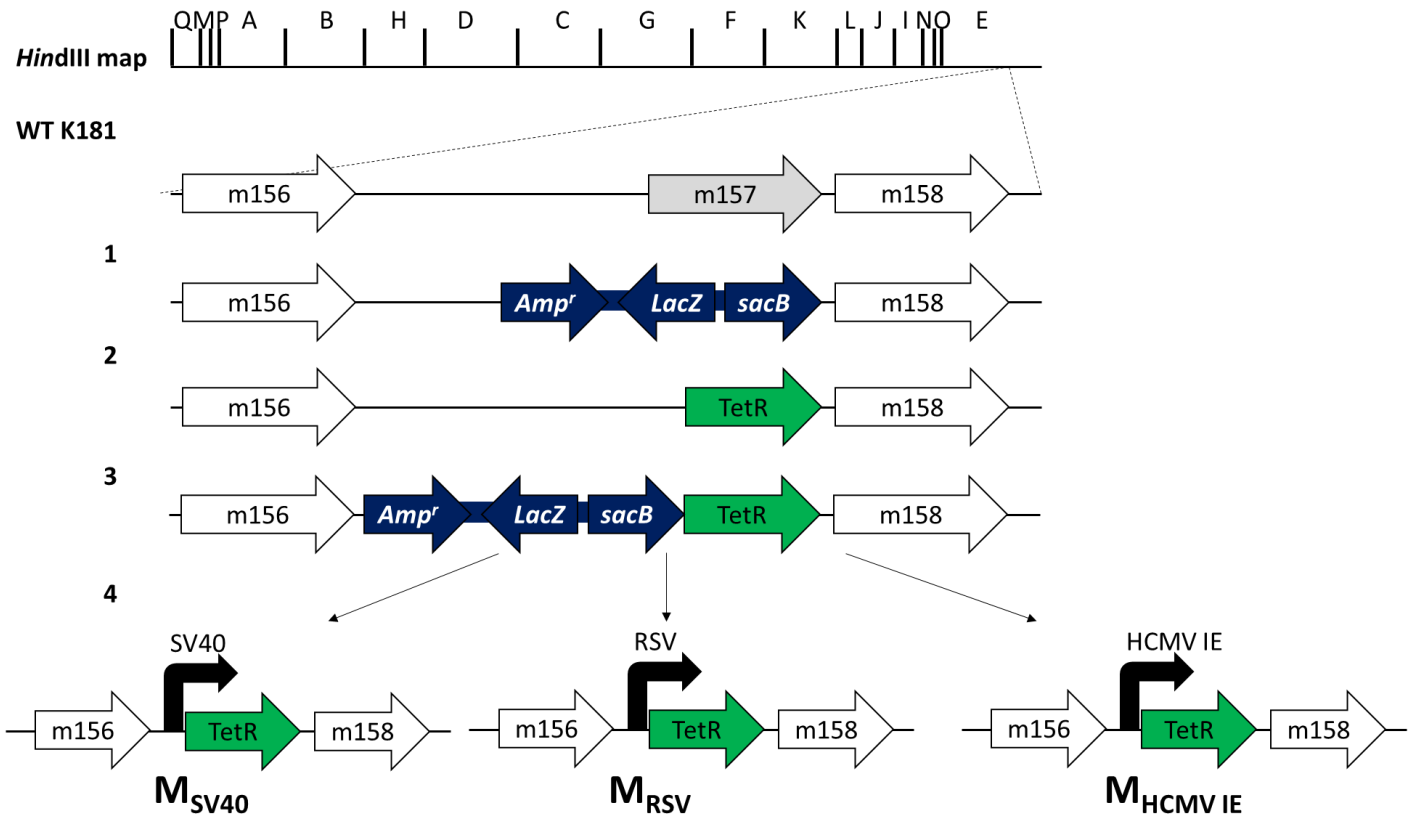

Figure 16: Cloning of conditionally replicating MCMV vectors using the TREx system. MCMV genome comprises of a single unique sequence containing short terminal direct and internal repeats. To indicate location of m157, *Hin*dIII restriction digest fragments of the genome are shown. Each schematic diagram shows the four steps in recombineering performed and modifications made to the WT K181 genome in order to generate M_{SV40}, M_{RSV} and M_{HCMVie}. The m157 gene was replaced with *Amp^r/LacZ/sacB* selection cassette (dark blue) which in the second round of recombineering was replaced with the tetR gene (green). Next, the selection cassette was cloned upstream of tetR and then replaced with either SV40, RSV or HCMV IE promoter. Arrows indicate the gene and its orientation. Black arrows upstream of *tetR* in the bottom panel are indicative of the promoter that was inserted upstream to drive tetR expression.

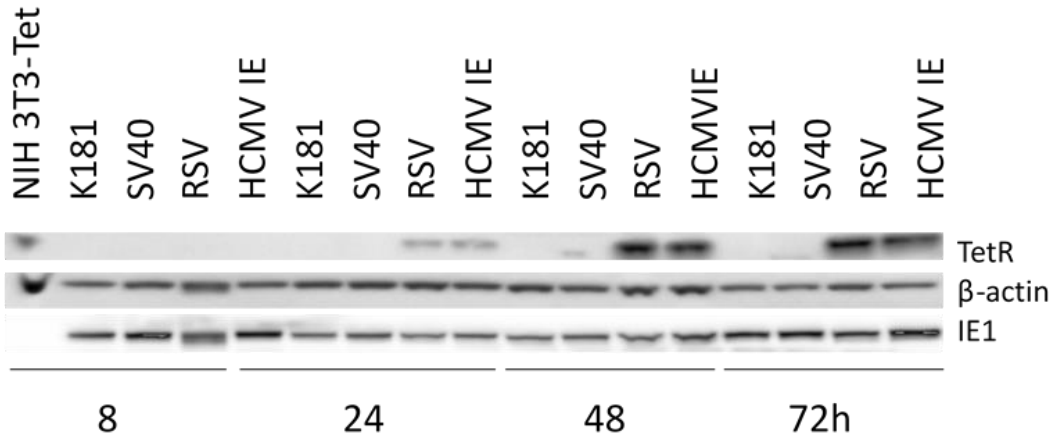

Figure 17: RSV and HCMV IE promoters drive expression of tetR in MCMV vector as early as 24 h pi. NIH-3T3 cells were infected at an MOI of 3 and cells were harvested at either 8, 24, 48 or 72h. TetR (inserted in m157) expression in M_{SV40}, M_{RSV} and M_{HCMVie} viruses was compared to WT K181 (negative control) and NIH-3T3-TET cell line (positive control) transduced with a lentivirus to constitutively express tetR. IE1 expression reports on MCMV infection whereas β-actin expression serves as a loading control.

3.1.3.2. Insertion of tetO before M44, M75, M85, gM/M100 and IE1/M123 genes

Either one or two tetO were inserted 20 bp upstream of MCMV genes, homologous to HCMV genes listed in section 3.1.1.2. Overall, 24 MCMV vectors were generated via two rounds of recombineering (Figure 18). Cloning of vectors with regulated M54 gene expression was omitted due to insufficient spacing (8 bp) between the genes M54 and M55. All purified BACs were transfected into NIH 3T3s and grown in media supplemented with DOX. Twenty of the transfected BACs except for M_{SV40}1M44, M_{SV40}2M44, M_{SV40}1M75 and M_{SV40}2M75 (Table 18) produced infectious virions.

3.1.4. Growth phenotype of MCMV vectors *in vitro*

3.1.4.1. The impact of doxycycline on growth kinetics of MCMV *in vitro*

Growth efficiency of all 20 tetR-regulated MCMV vectors was tested in the presence and absence of DOX (Table 18). First, BAC DNA was transfected into NIH 3T3 cells and the media was supplemented with DOX until plaques started to form. Next, the effect of removal of DOX in half of infected cells was monitored until late stages of infection. All the transfected BACs produced infectious virions that spread through the cell monolayer at similar rates in the presence as well as absence of DOX.

3.1.4.2. Functionality of NIH 3T3-Tet cells

As with the HCMV vectors, I constructed a tetR expressing cell line as a control (NIH 3T3-Tet). To ensure that NIH 3T3-Tets express functional tetR, NIH 3T3s and NIH 3T3-Tets were infected with two Ads: Ad-GFP that constitutively expresses GFP and Ad-tetO-GFP in which GFP expression is controlled from a tet-regulated HCMV promoter (Figure 19). In the absence of tetR (NIH 3T3), GFP expression was not affected by DOX. I observed a 22-fold higher expression in NIH 3T3-Tets infected with Ad-tetO-GFP in the presence of DOX compared to the absence of DOX, thus showing that NIH 3T3-Tets were expressing tetR, and expression levels were sufficient to inhibit gene expression.

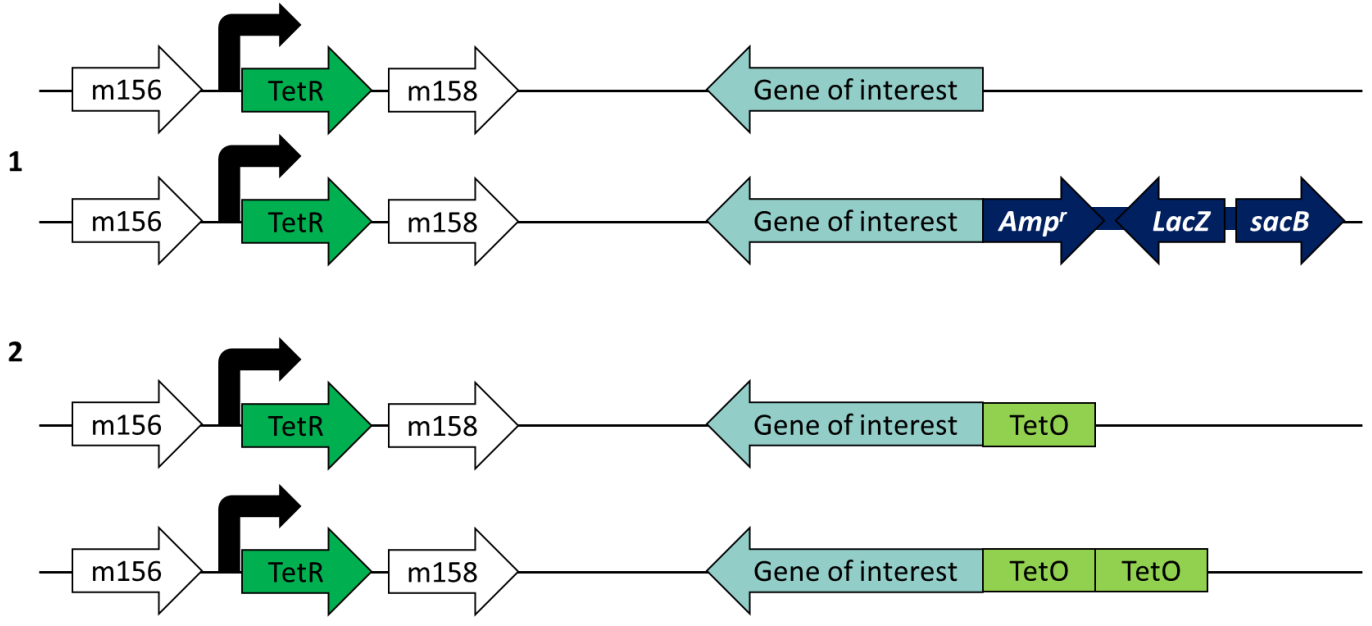

Figure 18: Recombineering steps to insert tetO upstream of genes essential for MCMV replication. In the first round of recombineering, an *Amp*^{r}*/LacZ/SacB* selection cassette (dark blue) was cloned upstream of the 'gene of interest' (either M44, M75, M85, M100 or M123). In the second round, either one or two copies of tetO were used to replace the selection cassette. Arrows show the orientation of genes. *TetR* is shown in dark green whilst tetO are represented by light green boxes.

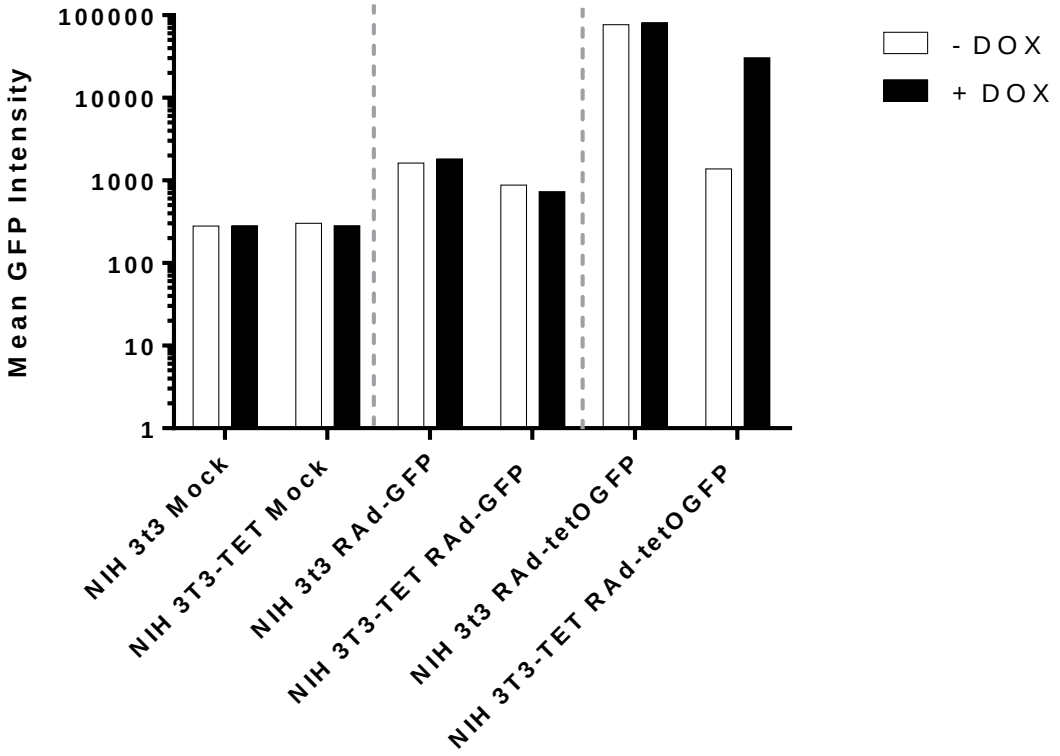

Figure 19: TREx system works efficiently in the context of adenovirus. NIH 3T3 and NIH 3T3-Tet cells were infected (MOI=500) with either a control adenovirus (Ad-GFP) or an Ad expressing eGFP (Ad-tetO-GFP). The *GFP* gene expression in Ad-tetO-GFP is under a tetR-regulated HCMV MIE promoter (2 tetO inserted 10 bp downstream of the TATA box). GFP expression was measured at 48 h pi . NIH 3T3-TET constitutively express tetR.

3.1.4.3. Cell-to-cell MCMV spread in mouse fibroblasts

Analysis of tet-regulated MCMV growth in the presence and absence of DOX (described in section 3.1.4.1) showed comparable virus growth kinetics in both conditions. To test whether the lack of transcriptional repression was due to insufficient tetR expression, plaque sizes of tet-regulated MCMVs were compared in NIH 3T3s and NIH 3T3-Tets in a 6-day plaque (Figure 20). All plaque measurements of recombinant viruses were compared to K181 MCMV (parental, non-tet regulated virus). Plaque sizes for the majority of the viruses, including the WT K181 MCMV strain, were slightly larger in NIH 3T3-Tets, suggesting that the production of the tetR cell line may have selected for cells that support slightly more efficient virus growth. Four of the viruses (M_{RSV}1M100, M_{RSV}2M100, M_{HCMVie}1M100 and M_{HCMVie}2M100), however, produced larger plaques in NIH 3T3s. It is noteworthy that all of these viruses contain tetO sequences upstream of M100.

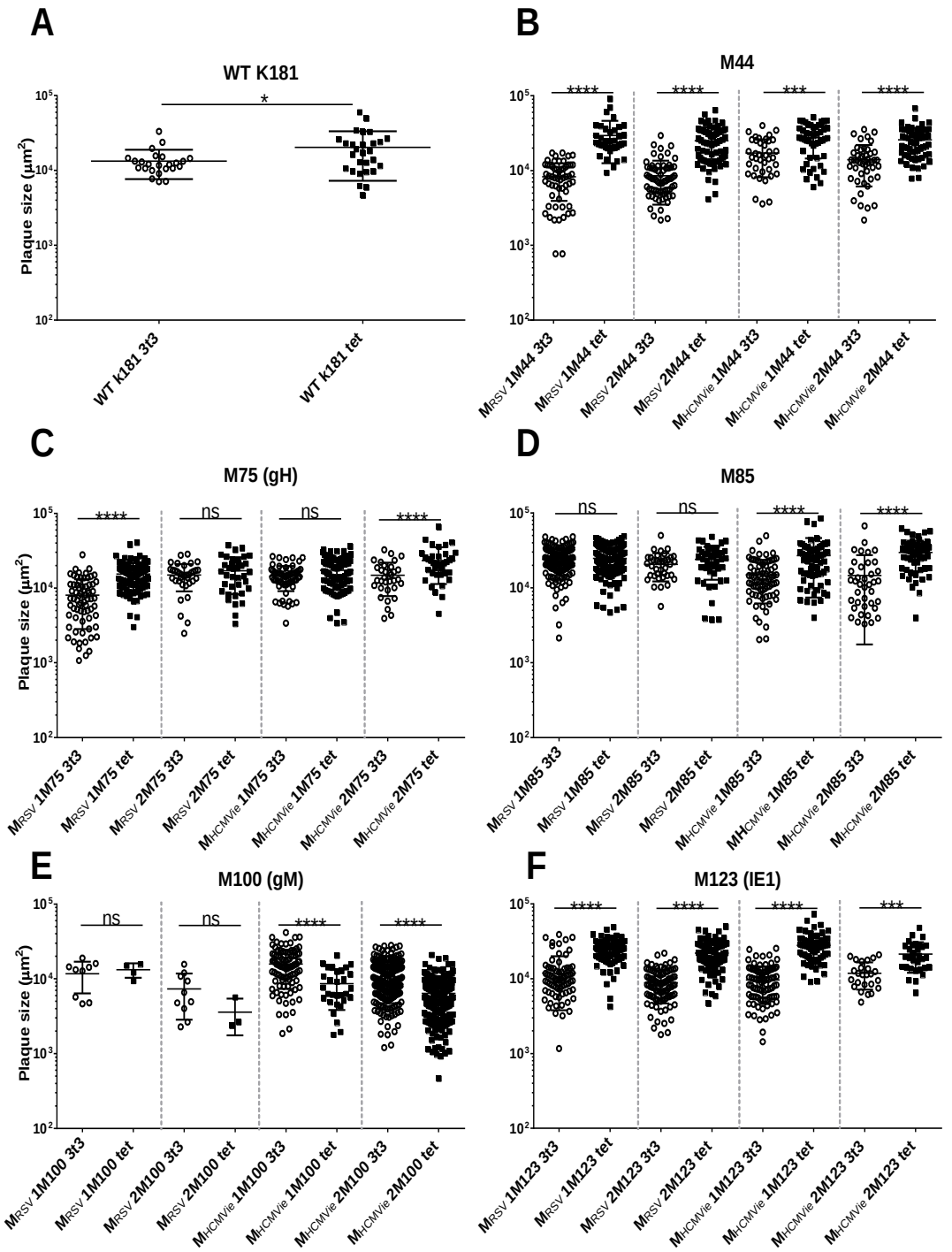

Figure 20: Repression of M100/gM expression inhibits cell-to-cell virus spread. NIH 3T3 (○) and NIH 3T3-Tets (■) were infected with WT K181 (A) and MCMV containing tet-regulated M44 (B), M75 (C), M85 (D), M100 (E) and M123 (F). Cells were overlaid to prevent cell-free virus spread and plaque sizes of viruses were measured at 6 days pi. Each data point represents a single plaque. Error bars show means ±SD. The control viruses in panel A were analysed with unpaired 2-tailed t-test (*p<0.05). For panels B-F one-way ANOVA with Tukey post-test results are presented (*p<0.05; ***p< 0.001; ****p<0.0001).

3.1.4.4. Comparative analysis of tetR-regulated gM (M100) vectors to vectors described in the literature

To compare my most encouraging tetR-regulated vectors to existing conditional MCMV vectors described in the literature, I obtained bacterial stabs of two MCMV vectors (M50-1 and SCP-GFP) from Zsolt Ruzsics, Ulrich Koszinowski's laboratory (Rupp et al. 2005), both of which are based on the Smith strain of MCMV. M50-1 virus contains an M50 gene (encodes the structural major capsid protein), inserted at a different site in the genome, and expressed from a HCMV ie promoter, in which expression is de-repressed by the addition of DOX. SCP-GFP, on the other hand, has a tet-regulated m58.2 gene (codes for small capsid protein, SCP) fused with eGFP. SCP is essential for virus replication, fusion of eGFP to SCP gene has a dominant-negative effect whereby expression of SCP-GFP fusion protein inhibits infectious virion production (Borst et al. 2001). Since tetO was inserted upstream of SCP-GFP fusion gene, addition of DOX would result in repression of growth even with the insertion of an additional SCP gene at an ectopic location which allows virus growth in the absence of DOX. Both of the vectors (Figure 21) were generated using a TREx-like system in the Smith strain of MCMV, and DOX administration regulated virus release by 3-fold and 1,000,000-fold *in vitro* for M50-1 and SCP-GFP, respectively (Rupp et al. 2005). *In vitro*, Smith produces larger plaques, replicates to higher titres than K181 and spreads faster in the cell monolayer. *In vivo*, on the other hand, K181 is considered to be more virulent than Smith and produces higher titres in salivary glands. This may in part be because Smith lacks intact MCK-2 gene, which limits virus tropism for peripheral blood leukocytes (PBLs) and reduces titres in salivary glands (Jordan et al. 2011).

BAC DNA was isolated and analysed by restriction digest analysis (Figure 22) to confirm that no major genome re-arrangement had occurred. BAC DNA was transfected into NIH 3T3s and grown in media with and without DOX for M50-1 and SCP-GFP, respectively. Following this, I compared the spread (Figure 23) of M50-1, SCP-GFP and my tet-regulated vectors in mouse fibroblasts under three conditions: with or without DOX and in cells constitutively expressing tetR to control for tetR expression levels. To prevent virus cell-free dissemination, infections were carried out under semi-solid overlay. The overlay was replaced three times a week to maintain DOX concentrations in the media. Interestingly, I observed a 3.6-fold decrease in M_{RSV}1M100 plaque sizes in NIH 3T3-Tet cells as compared to growth in NIH 3T3s.

Two tetO upstream of gM/M100 with the same virus backbone (M_{RSV}2M100) resulted in tighter repression of virus growth where only six plaques where found in the absence of DOX. This repression was relieved with addition of DOX, with plaque sizes increasing by about 3-fold. In addition to this, virus replication was completely inhibited in NIH 3T3-Tets. Less efficient control of virus replication was observed for M50-1 and SCP-GFP viruses. M50-1 displayed smaller plaques in the absence of DOX and produced larger plaques (by a 2-fold) where DOX was added. Seven smaller plaques, indicative of productive virus infection were detected in NIH 3T3-Tet cells thus demonstrating that even high levels of tetR failed to control this virus. Plaque sizes for SCP-GFP, on the other hand, were comparable in all three different conditions.

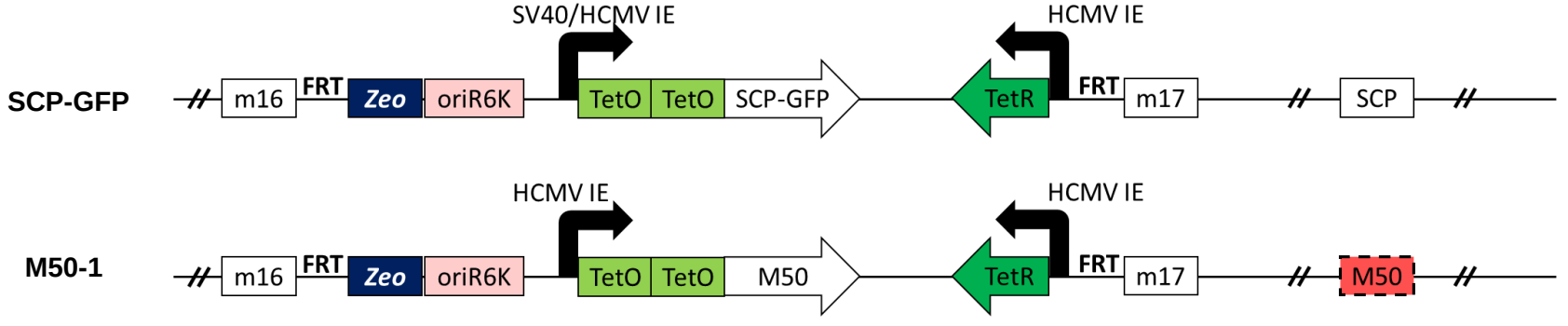

Figure 21: Structure of SCP-GFP and M50-1 viruses sent by Zsolt Ruzsics. Two tet operators (light green) driven by either SV40 or HCMV IE promoters were inserted upstream of SCP (m48.2) (top figure) and M50 (bottom figure), respectively. TetR in both of these vectors was regulated by the HCMV immediate-early promoter-enhancer. OriR6K represents the origin of replication whereas *Zeo* depicts zeocin resistance gene. Two FRT sites are flanking the zeocin gene, oriR6K and the regulation cassette between genes m16 and m17.The endogenous M50 gene in M50-1 vector is deleted.

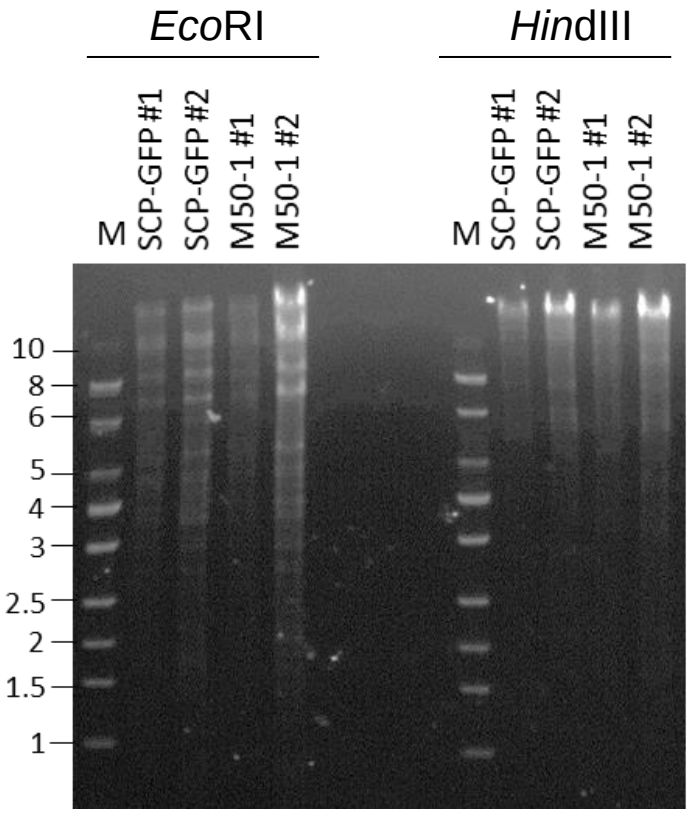

Figure 22: Genomic stability of SCP-GFP and M50-1 BAC DNA. BAC DNA was purified from bacterial stabs (kindly provided by Zsolt Ruzsics) and digested at 37 ˚C for 1 hour with either EcoRI or *Hin*dIII. Digested fragments were compared in size to digest profiles published in the literature (not shown) to test for recombination events/genome stability.

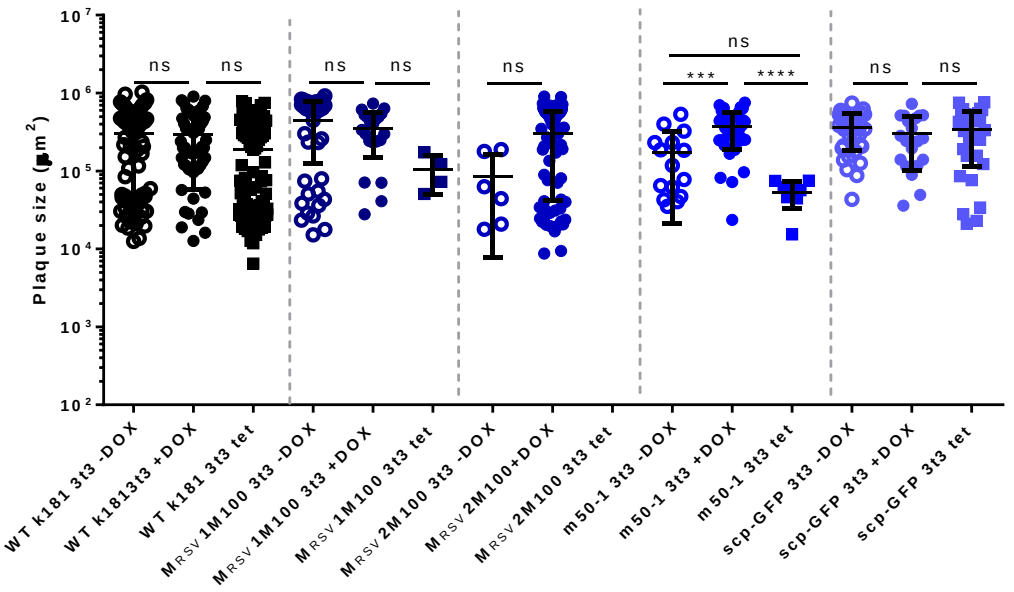

Figure 23: More stringent control of virus cell-to-cell spread in M100/gM tetR-regulated vectors than vectors described in the literature. Plaque sizes of tetR-regulated viruses in NIH 3T3-Tets (■), and NIH 3T3s in the absence (○) and presence (●) of DOX were compared to inducible M50-1 and SCP-GFP vectors described in the literature as well as a WT control (WT K181). Infected cells were incubated for 6 days under a semi-solid overlay to prevent cell-free virus spread. DOX in the overlay media was replaced every two days. Each symbol shows an individual plaque. Error bars represent means ±SD. One-way ANOVA results with Tukey post-tests are presented (***p<0.001; ****p<0.0001).

3.1.5. Fusing a second copy of *tetR* to M36 or IE2 (M122)

Plaque assay data, using viruses in which gM/M100 was tet-regulated, showed some repression of MCMV in the absence of DOX, but complete ablation of virus replication in tetR expressing cells. This suggested that higher and/or more rapid tetR expression from the virus backbone could inhibit virus replication completely. To test this theory, two regions in the MCMV genome for inserting a second copy of *tetR* were selected: IE2 (M122) and M36. IE2 is a commonly used region in MCMV vector design since it is non-essential for virus replication *in vivo* and does not have a counterpart in HCMV (Messerle et al. 1991; Manning & Mocarski 1988). M36, a homolog of UL36, was selected on the basis of proteomic data from HCMV (Weekes et al. 2014), which demonstrated that UL36 was expressed early in the HCMV replication cycle, and was one of the most abundant genes at this time, which circumvents the need to insert exogenous promoters. Although IE2 is expressed early in the virus replication cycle, members in our laboratory have shown that its expression is not abundant, therefore for this vector, I inserted either the RSV or HCMV IE promoters upstream of *tetR*.

To generate M_{RSV}2M100-tetR-P2A-M36 (Figure 24), a selection cassette was inserted downstream of M36 in M_{RSV}2M100 and then replaced with a codon optimised *tetR* gene fused to the M36 ORF by a P2A linker. This linker functions to separate the M36 and tetR proteins during translation, thus ensuring the function of one is not affected by the other. M_{HCMVie}2M100$_{RSV}$IE2 vector and M_{RSV}2M100$_{HCMVIE}$IE2 were both generated (Figure 25) via 4 rounds of recombineering. First, I inserted a selection cassette in IE2 and replaced it with *tetR* gene. Then, by inserting a selection cassette upstream of *tetR* I replaced it with the appropriate promoter. All BACs were transfected, grown in media supplemented with DOX and produced infectious virions.

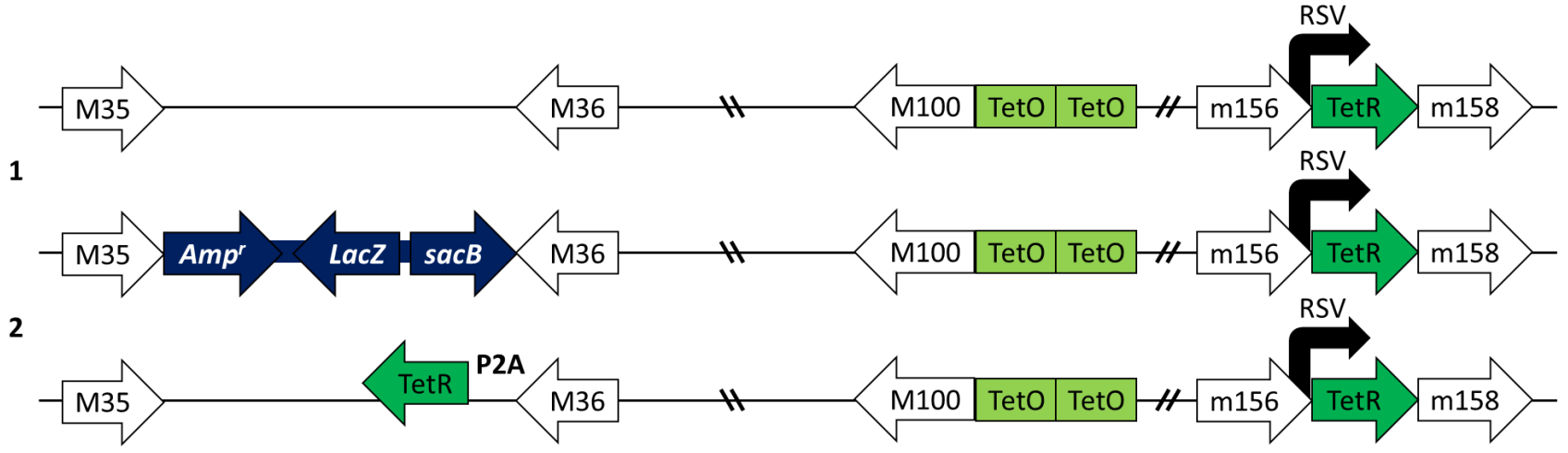

Figure 24: Steps undertaken to generate M_{RSV}2M100-tetR-P2A-M36. M_{RSV}2M100-tetR-P2A-M36 was generated via two rounds of homologous recombineering. First, an *Amp^r/LacZ/sacB* selection cassette was inserted at the end of M36. In the second step, the cassette was replaced with gene synthesized tetR-p2A. Arrows represent genes and their orientations. The selection cassette is displayed in blue whilst *tetR* and tetO genes are shown in green. Letters P2A represent the P2A linker used to fuse *tetR* to M36. Black arrows show the promoter driving tetR expression.

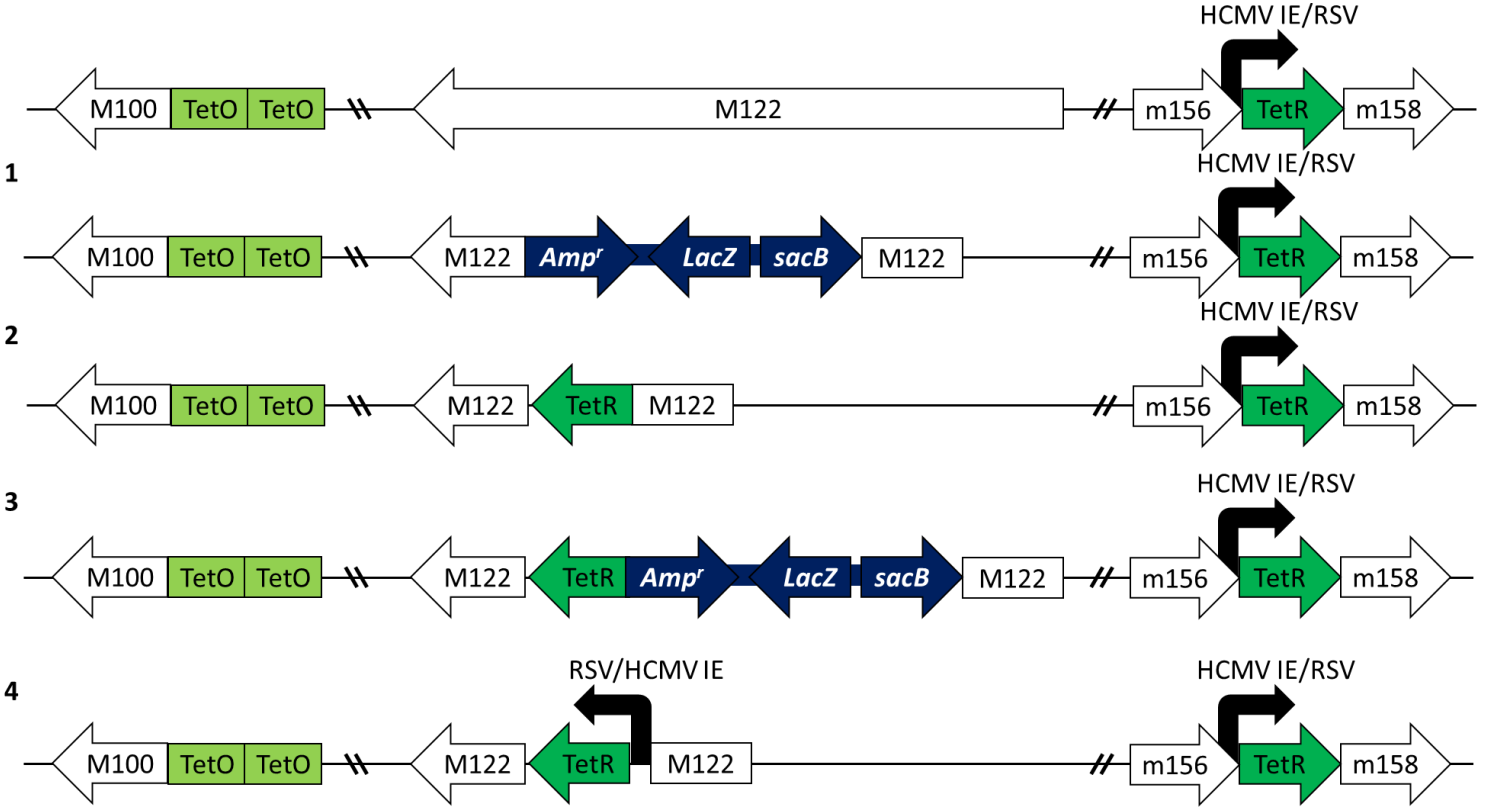

Figure 25: Cloning of $M_{HCMVie}2M100_{RSV}IE2$ and $M_{RSV}2M100_{HCMVIE}IE2$. Four recombineering steps showing insertion of a second copy of tetR and either an RSV or HCMV IE promoter upstream of *tetR*. In the first step, *Amp^r/LacZ/SacB* selection cassette was inserted in M122/IE2 gene in either $M_{HCMVie}2M100$ or $M_{RSV}2M100$. In the second round, the selection cassette was replaced with tetR gene. Then, to insert a promoter upstream of tetR, two more recombineering steps were carried out: the selection cassette was cloned upstream of tetR and then replaced with either RSV or HCMV IE promoter to generate $M_{HCMVie}2M100_{RSV}IE2$ or $M_{RSV}2M100_{HCMVIE}IE2$, respectively. Arrows represent coding regions in the virus and their orientations. *Amp^r/LacZ/SacB* selection cassette is displayed in blue whereas *tetR* and tetO is shown in dark and light green, respectively. Black arrows depict the promoters upstream of *tetR*.

3.1.6. Comparative analysis of cell-free release of M50-1, SCP-GFP and tet-regulated glycoprotein M (gM/M100) MCMV viruses in NIH 3T3

M50-1 and SCP-GFP viruses have been analysed *in vitro* and have shown significant growth defects in the absence and presence of DOX, respectively (Rupp et al. 2005). Since the effect I observed in cell-to-cell spread of these viruses was minor (Figure 23), I wanted to see whether I could recapitulate the previously published effects on cell-free release of these viruses. For this, I performed multistep growth assays whereby NIH 3T3s and NIH 3T3-Tets were infected at an MOI of 0.1. Supernatants were collected daily and then titrated on NIH 3T3 in the presence of DOX to relieve tetR repression and enable virus replication. In the absence of DOX, release of M50-1 was reduced by as much as 14 orders of magnitude (Figure 26A). SCP-GFP, on the other hand (Figure 26B), was released to similar levels as M50-1 in the absence of DOX whilst addition of DOX resulted in maximum 211-fold decrease in cell-free virus titres. As expected, addition of DOX did not alter release of control virus.

For comparison, I also infected NIH 3T3s and NIH 3T3-Tets with tet-regulated gM/M100 viruses M_{RSV}2M100, M_{RSV}2M100-tetR-P2A-M36, M_{RSV}2M100$_{HCMVIE}$IE2 and M_{HCMVie}2M100$_{RSV}$IE2 in the absence and presence of DOX (Figure 27). Since M_{RSV}2M100 contains only one copy of *tetR* it is unsurprising that this virus was inhibited by 11-fold at day 5 (Figure 27C), in the absence of DOX. Although M_{RSV}2M100$_{HCMVIE}$IE2 and M_{HCMVie}2M100$_{RSV}$IE2 only differ in the placing of their promoters, the cell release profiles of these viruses were surprisingly distinct. M_{RSV}2M100$_{HCMVIE}$IE2 growth (Figure 27A) could be inhibited by 193-fold (day 5) in the absence of DOX whereas for M_{HCMVie}2M100$_{RSV}$IE2 (Figure 27B) there was only an 8.5-fold difference. In addition to this, M_{HCMVie}2M100$_{RSV}$IE2 was the only virus that released infectious virions in 3T3 NIH-Tet cells. M_{RSV}2M100-tetR-P2A-M36 (Figure 27D) displayed the strongest reduction in virus spread, with peak titres delayed from day 3 until day 15 when grown in the absence of DOX. Furthermore, there was a 369-fold reduction (day 5) in virus release in NIH 3T3s where no DOX was added.

M50-1 and SCP-GFP viruses have been well characterized in the literature and although the viruses can be controlled to high degree by removal of DOX, the replication phenotype resembled that of M_{RSV}2M100 and M_{HCMVie}2M100$_{RSV}$IE2 viruses. Cell-free virus spread of M_{RSV}2M100$_{HCMVIE}$IE2 and M_{RSV}2M100-tetR-P2A-M36 was

most effectively controlled by addition/removal of DOX. It is evident that expression of two copies of *tetR* may improve regulation of virus replication and the place for insertion of *tetR* plays a critical role.

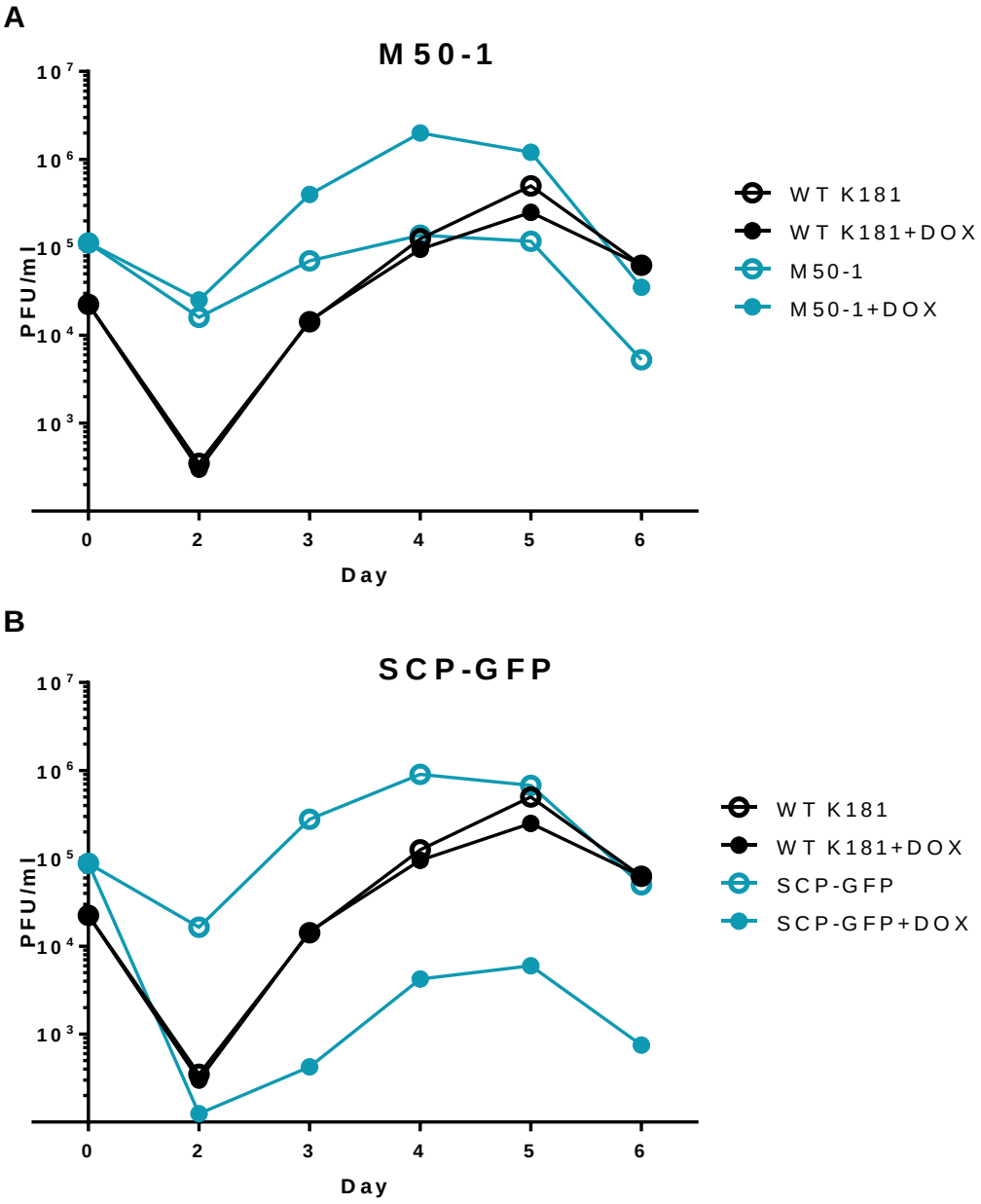

Figure 26: Greater inhibition of cell-free virus release of double-negative tetR-regulated SCP virus than M50. Supernatants of infected (MOI=0.1) NIH 3T3s and NIH 3T3-Tets in the presence **(●)** and absence **(○)** of DOX were collected daily and titrated on NIH 3T3s as a measure of cell-free released virus. For a more sensitive detection of infectious cell-released virus particles, DOX was added to the overlay media three times a week. Cell-free M50-1 (A) and SCP-GFP (B) were compared to WT K181 control (shown in black). TetR-regulated viruses are shown in light blue.

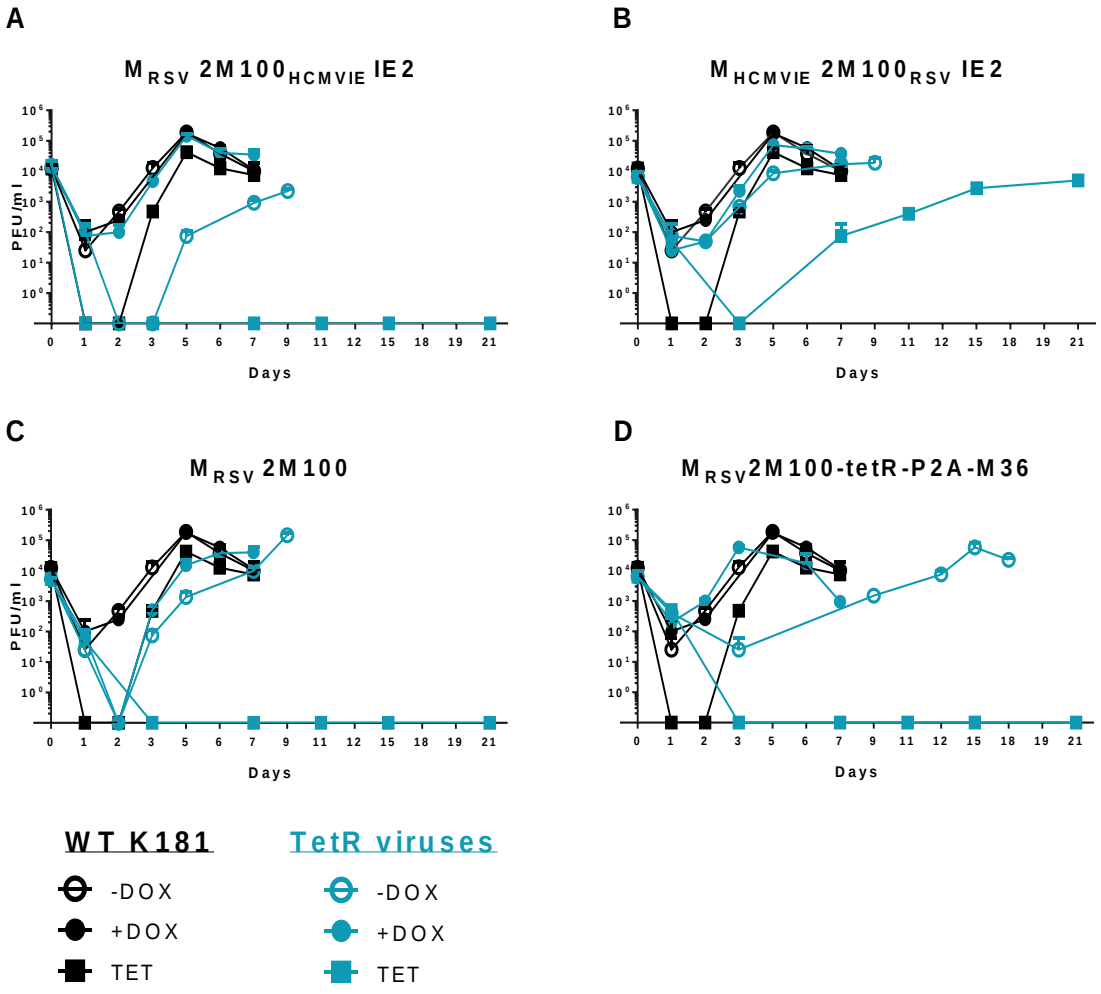

Figure 27: Insertion of second copy of tetR enhances control of virus replication. Virus titres released into the supernatant after infection of NIH 3T3 and NIH 3T3-Tets (■) (MOI of 0.1) in the absence (○) and presence (●) of DOX were titrated on NIH 3T3s for 6 days. A) $M_{RSV}2M100_{HCMVIE}IE2$; B) $M_{HCMVie}2M100_{RSV}IE2$; C) $M_{RSV}2M100$ and D) $M_{RSV}2M100$-tetR-P2A-M36 virus (shown in light blue) titres were compared to WT K181 (shown in black). Each dilution was performed in duplicates. Error bars represent mean ±SD.

3.1.7. Comparative sequence analysis of mutations acquired in MCMV during virus propagation

Multi-step growth assays (discussed in section 3.1.6) indicated that even in the absence of DOX, viruses were able to replicate to some extent. This raised the possibility that they could have acquired mutations, or would be able to do so following further passage. To test whether this occurred, eleven virus samples were deep-sequenced. To determine whether initial stocks had acquired mutations during amplification in the presence of DOX, I selected stocks of the following viruses: 1) WT K181; 2) M_{RSV}; 3) M_{RSV}2M100; 4) M_{HCMIie}2M100; 5) M_{RSV}2M100$_{HCMVie}$IE2; 6) M_{HCMVie}2M100$_{RSV}$IE2 7) M_{RSV}2M100-tetR-P2A-M36; 8) M50-1 and 9) WT FRT. In addition to this, I extracted M_{HCMVie}2M100$_{RSV}$IE2 virus from NIH 3T3-tet passaged for 17 days (further referred to as M_{HCMVie}2M100$_{RSV}$IE2 tet d17) as well as M_{RSV}2M100-tetR-P2A-M36 isolated from cells grown in the absence of DOX for 22 days (referred to as M_{RSV}2M100-tetR-P2A-M36 -dox d22). First, I compared (Table 19) all of the viruses with a WT K181 backbone to a previously published K181 sequence (GenBank: AM886412.1). Altogether there were 45 sequence insertions/deletions or mutations in non-coding regions, 2 silent mutations, 3 missense mutations and 4 nonsense mutations resulting in truncation of protein-coding sequence. Since the majority of the differences were shared by all the viruses, they either represent errors in the initial sequencing of the K181 BAC, or differences acquired by the BAC clone that we received, during propagation in *E. coli*. In addition to this, the reference sequence contained unknown nucleotides in two regions of the genome. My viruses were missing these nucleotides in the M58-M69 region, whereas in m142 gene, I identified the unknown sequence missing from the reference.

To determine whether any mutations had spontaneously arisen due to *in vitro* passage, all of the tetR-regulated viruses were aligned with Multiple Alignment using Fast Fourier Transform (MAFFT) program. Sequence analysis (Table 20) revealed that all viruses except for M_{RSV}2M100-tetR-P2A-M36 contained a silent base pair substitution in the *tetR* gene. This mutation appeared during the PCR amplification step whilst generating virus BACs. Although M_{RSV}2M100$_{HCMVie}$IE2 was lacking 197 bases in m58-m69 intron, the deletion had occurred in the non-coding region, and thus is unlikely to affect translation of any genes. The main focus was to investigate how viruses were able to replicate in the absence of DOX or in tetR expressing cells and comparison of

M_{RSV}2M100-tetR-P2A-M36 to M_{RSV}2M100-tetR-P2A-M36 -dox d22 provided some insights. Interestingly, the virus passaged in the absence of DOX mutated in the second copy of *tetR* gene (fused to M36) and had a 5 bp deletion that resulted in a frameshift and deletion of a stop codon. In addition to this, genes M70 and m139 mutated, however, the base substitutions did not affect m139 sequence whilst for M70 there was one amino acid change.

The viruses sent by Zsolt Ruzsics (WT FRT and M50-1) had not been sequenced before, therefore I wanted to see whether the sequence of WT FRT was identical to previously published WT Smith strain (GU305914.1) as well as compare M50-1 to WT FRT. A consensus sequence could not be generated for M50-1 as it clearly contained multiple virus variants. Some of the variants contained a 25 bp deletion in a non-coding region (data not shown) . In addition to this, there were deletions in M51 and m59 genes and a large deletion spanning m151-m158 genes. Comparison of WT FRT to WT Smith reference sequence (Table 21), revealed that the identity of the two sequences was 99.5%. The WT FRT sequence contained 642 single-nucleotide polymorphisms (SNPs) (532 SNPs in ORFs), 9 deletions (7 in genes) and 9 insertions. The differences were found in 40 different genes; however, the majority of the mutations were silent or missense and did not affect protein translation. The genes that were severely affected with frameshift mutations resulting in premature stop codon insertion included m01, m03, m59, m150 and m161.

3.1.8. Summary

I applied TREx system to generate 55 virus vectors in which I identified a gene in HCMV (UL123/IE1) and MCMV (gM/M100) that can be targeted to control virus replication using DOX *in vitro.* Data revealed that my vectors could be further inhibited in cells constitutively expressing tetR thus suggesting that earlier/higher expression of tetR may improve vector safety. In MCMV, addition of a second copy of *tetR* improved the control of cell-free virus spread, particularly when expressed from the endogenous M36 promoter. In addition to this, comparison of gM/M100-targeting vectors to other vectors revealed that cell-free and cell-cell spread of my vectors could be controlled to a higher degree than those previously published (M50-1 and SCP-GFP). Deep-sequencing of viruses suggested that escape mutants can occur by mutation of *tetR*, in the absence of DOX.

Table 19: Comparative analysis of tetR-regulated viruses and published WT K181 sequence (GenBank: AM886412.1)

Virus	Location	Mutation	ORFs/introns affected	Effect of mutation
All	0-41	41 bp deletion	Non-coding region	-
All	735-736	C insertion	m01	Frameshift no stop codon
All	28926	A deletion	M25-m25.1 intron	-
All except M_{RSV}2M100-tetR-P2A-M36	47566-47567	T insertion	M35-M36 intron	-
All	48938-48939	C insertion	M36 intron	-
All	59492	T deletion	M44-M45 intron	-
All	79556	T deletion	M53-M54 intron	-
All	85439-85440	Insertion of CG	M55-M56 intron	-
All	85440	G>A	M55-M56 intron	-
All	92645-92701	Deletion (ref sequence has n's)	M58-M69 intron	-
All	93275-93276	Insertion of G	M58-M69 intron	-
All	93340	C deletion	M58-M69 intron	-
All	103004-103005	AT deletion	M71-M72 intron	-
All	103006	A>T	M71-M72 intron	-
All	110069-110070	Insertion of ggggggtcccggctcg	M76-M78 intron	-
All	112651	T>G	M78-M79 intron	-
All	112654-112655	Insertion of TT	M78-M79 intron	-
All	115679	A deletion	M80-M82 intron	-
All	121943	A deletion	M84-m84.2 intron	-
All	140164	A deletion	M96-M97 intron	-
All	155092-155093	G insertion	m106-m108 intron	-
All	155757	A deletion	m106-m108 intron	-
All	155781	A deletion	m106-m108 intron	-
All	155927-155928	TC deletion	m106-m108 intron	-
All	155929	T>C	m106-m108 intron	-
All	157821	G>C	m106-m108 intron	-
All	157822	T>G	m106-m108 intron	-
All	160178	T deletion	m106-m108 intron	-
All	160329	T deletion	m106-m108 intron	-
All	160718	T deletion	m106-m108 intron	-
All	161497	A deletion	m106-m108 intron	-
All	161533	A deletion	m106-m108 intron	-
All	166840	C>T	m115	Missense
All	166842	T>G	m115	Silent
All	171404	T deletion	m118-m119 intron	-

All	171929	C deletion	m119	Missense; frameshift and premature stop codon
All	177098	G>T	m121	Missense
All	177100	T>G	m121	Silent
All	179680-179681	G insertion	m121-m124 intron	-
All	179786	A deletion	m121-m124 intron	-
All	183129-183130	C insertion	m124.1-m125 intron	-
All	183230	A deletion	m124.1-m125 intron	-
All	183250-183251	CA deletion	m124.1-m125 intron	-
All	183917	T deletion	m125-m126 intron	-
All	188729-188730	Insertion of AG	m132.1	Premature stop codon
All	190386	Deletion of T	m134	Frameshift, premature stop codon
All	197762-197763	G insertion	m140-m141 intron	-
All	199778-199779	39 bp insertion	m142	In-frame insertion
All	199779-199785	CGCAGCC (in reference sequence five n's)	m142	n/a
All	208756-208757	C insertion	m150-m151 intron	-
All	214337-214338	C insertion	m154.4-m155 intron	-
All	211539	T deletion	m152-m153 intron	-
All	211561	T deletion	m152-m153 intron	-
All	211576	A deletion	m152-m153 intron	-
All	228037	A deletion	m168	Frameshift; premature stop codon
All	230301	Insertion of ccccccccggccgtctgagtgcgcgc gggcccc (sequence 41-72 in ref sequence)	Non-coding region	-

TetR-regulated viruses sequenced and listed in the table: M_{RSV}; M_{RSV}2M100; M_{HCMIie}2M100; M_{RSV}2M100$_{HCMVie}$IE2; M_{HCMVie}2M100$_{RSV}$IE2; M_{RSV}2M100-tetR-P2A-M36; M_{HCMVie}2M100$_{RSV}$IE2 virus from NIH 3T3-tet passaged for 17 days (referred to as M_{HCMVie}2M100$_{RSV}$IE2 tet d17) and M_{RSV}2M100-tetR-P2A-M36 -dox d22 isolated from cells grown in the absence of DOX for 22 days. The viruses were sequenced by Andrew Davison and sequences were compared to WT K181 sequence (GenBank: AM886412.1) by MAFFT.

Table 20: Mutations associated with PCR/*in vitro* passage of my tetR-regulated MCMV viruses

Virus	Location	Mutation	ORFs/introns affected	Effect of mutation
M_{RSV}, M_{RSV}2M100$_{HCMVie}$IE2, M_{HCMVie}2M100$_{RSV}$IE2 and M_{HCMVie}2M100$_{RSV}$IE2 tet d17	378	C>T	tetR in IE2 and m157	Silent
M_{RSV}2M100-tetR-P2A-M36 -dox d22	636-640	5 bp deletion	tetR in M36	Missense; no stop codon Frameshift/nonsense mutation?
M_{RSV}2M100$_{HCMVie}$IE2	93677-93873	197 bp deletion	M58-M69 intron	-
M_{RSV}2M100-tetR-P2A-M36 -dox d22	100946	G>T	M70	Missense
M_{RSV}2M100-tetR-P2A-M36 -dox d22	195227	C>T	m139	Silent

bp – base pairs; ORF – open reading frame; tetR-regulated MCMV vectors: M_{RSV}; M_{RSV}2M100; M_{HCMIie}2M100; M_{RSV}2M100$_{HCMVie}$IE2; M_{HCMVie}2M100$_{RSV}$IE2; M_{RSV}2M100-tetR-P2A-M36; M_{HCMVie}2M100$_{RSV}$IE2 tet d17 (passaged in NIH 3T3-tets for 17 days) and M_{RSV}2M100-tetR-P2A-M36 -dox d22 (grown in NIH 3T3 in the absence of DOX for 22 days) were sequenced by Andrew Davison and sequences were aligned using MAFFT.

Table 21: Comparison of WT FRT virus to published MCMV Smith reference sequence (GenBank: GU305914.1)

Genes affected	Mutations/differences	Effect
m01	1 deletion	Premature stop codon
m03	16 SNPs 1 insertion	Missense; premature stop codon
m04	69 SNPs 1 insertion	Missense
m05	32 SNPs 1 insertion	Missense
m06	2 SNPs 1 deletion	In-frame deletion; silent substitutions
m12	1 SNP	Missense
m16-m17	insertion of FRT (at 15679)	-
M50	5 SNPs	Silent
M51	1 SNP	Silent
M52	2 SNPs	Silent
M53	2 SNPs 1 insertion	Insertion of alanine; silent
M55	59 SNPs 1 insertion 1 deletion	Missense;
M56	1 SNP	Silent
m59	1 SNP 2 deletions	Frameshift; premature stop codon
M69	1 SNP	Silent
M70	2 SNPs	Silent
M72	5 SNPs	Missense
M72/M73	1 SNP	Missense
M73	7 SNPs	Missense
m74	19 SNPs	Missense
M75	29 SNPs	Missense
M76	2 SNPs	Silent
M78	4 SNPs	Missense
M79	2 SNPs	Missense
M80	10 SNPs 1 deletion	In-frame; missense
M82	6 SNPs 1 deletion	In-frame; silent
M83	12 SNPs	Missense
M84	10 SNPs	Missense
M85	1 SNP	Silent
M88	2 SNP	Silent
M94	11 SNPs	Missense
M97	1 SNP	Missense
m150	62 SNPs 1 insertion	No start codon; frameshift; premature stop codon
m151	136 SNPs 1 insertion	Insertion of glutamic acid; In-frame; missense
m152	2 SNPs	Silent
m154	4 SNPs	Missense
m155	8 SNPs	Missense
m156	2 SNPs 1 insertion	Insertion of proline; missense
m158	1 SNP	Silent
m161	1 insertion	Frameshift; premature stop codon
m164	1 SNP	Silent
Introns	110 SNPs	-
Non-coding region	34 and 28bp deletions at ends of genome	-

bp- base pairs; FRT –flippase (Flp) recognition site; SNP- single nucleotide polymorphism. WT FRT virus was sequenced by Andrew Davison and compared to MCMV Smith reference sequence (GenBank: GU305914.1) using MAFFT.

3.2. *In vivo* characterization of tetracycline-controlled MCMV vectors

Having generated CMV vectors that can be controlled by DOX *in vitro*, I next wanted to test vector safety as well as see how the viruses replicated in an animal system. In addition to this, I wanted to investigate the immunogenicity of my vectors since it has been suggested that limited virus replication may induce stronger immune responses in comparison to responses induced by replication-deficient viruses (O'Hara et al. 2012).

3.2.1. Detection of M50-1, M_{RSV}2M100, M_{HCMVie}2M100 and M_{RSV}2M100-tetR-P2A-M36 *in vivo*

First, to test the safety of my vectors, BALB/c mice were infected with two of my most promising tet-regulated MCMV vectors (from *in vitro* analysis described in sections 3.1.4 and 3.1.6) and virus growth was compared to WT MCMV in the absence of DOX in an acute MCMV infection setting (4 days). M50-1 has been well characterized by our collaborators *in vitro,* however, replication and safety profile of this virus has not been analysed in an animal system. I wanted to compare growth properties of my most promising MCMV vectors (M_{RSV}2M100, M_{HCMVie}2M100 and M_{RSV}2M100-tetR-P2A-M36) to those of M50-1 in BALB/c mice in the absence of DOX to determine whether they would exhibit similar levels of control *in vivo,* as I had seen *in vitro* (3.1.4.4 and 3.1.6). Weight loss data (Figure 28 and Figure 29), indicative of virulence of the vectors, showed that infection with WT K181 resulted in loss of weight over the 4 days. In contrast, no weight loss was seen with the majority of tetR-regulated viruses. One tetR-regulated virus (M_{RSV}2M100-tetR-P2A-M36) resulted in some initial weight loss, however the weight recovered by day 4.

Following the 4-day infection, I measured virus titres in spleen, lung, liver and salivary glands. I homogenized the organs to release virus, and infected NIH 3T3s under a semi-solid overlay in the presence of DOX for 6 days. I detected high WT K181 titres (Figure 30) in spleen and liver of infected mice. Infectious virus was also found in lungs of three infected mice whereas in salivary glands, WT K181 was detected only in one mouse. Although I didn't detect any infectious M_{RSV}2M100 virions in the spleen or lung, I found low titres in the liver and salivary glands of one mouse. M_{HCMVie}2M100 was present in all tissues except for salivary glands at titres similar to the WT virus. Interestingly, I could not detect any replicating M_{RSV}2M100-tetR-P2A-M36 virions in

any of the organs. Although significantly lower than WT virus, M50-1 virus was detected in all of the tissues analysed (Figure 31).

For a more thorough evaluation of growth characteristics of tetR-regulated viruses I extracted DNA from aforementioned tissues and performed qPCR (Figure 32). Lower genome copies of all tetR-regulated viruses were found in all tissues analysed. In spleen and liver, the levels of M50-1, M_{RSV} and M_{RSV}2M100-tetR-P2A-M36 were significantly lower than WT virus control. In addition to this, M50-1 genome copies were significantly lower in the lung. Although the difference in genome copies of the WT virus and M50-1 were statistically more significant in three of the organs tested, the overall genome copy levels were comparable to those observed for other tetR-regulated viruses. In fact, M_{RSV}2M100-tetR-P2A-M36 DNA levels were the lowest observed in the spleen, liver and salivary glands. Since virus DNA levels in salivary glands were close to the limit of detection, it was difficult to draw conclusions on the levels of repression of virus replication in this organ.

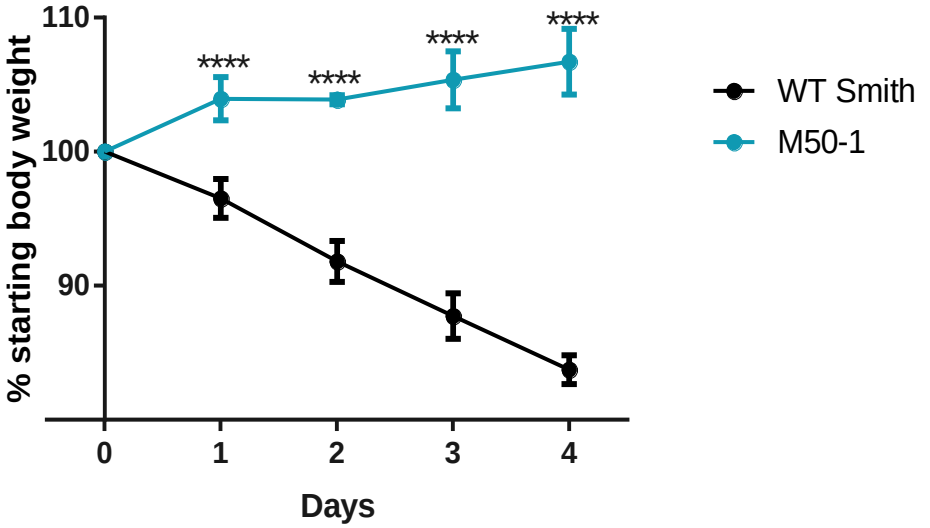

Figure 28: Conditional M50-1 virus does not induce weight loss in BALB/c mice. Weight loss (mean ±SD of 4 mice per group) in BALB/c mice infected with $2x10^5$ PFU of MCMV was monitored daily for 4 days post-injection and compared to weight loss in mice infected with WT Smith MCMV (positive control). Weight loss is expressed as percentage of original weight. 2-way ANOVA with Sidak's multiple comparisons test results are presented in this graph (****p<0.0001).

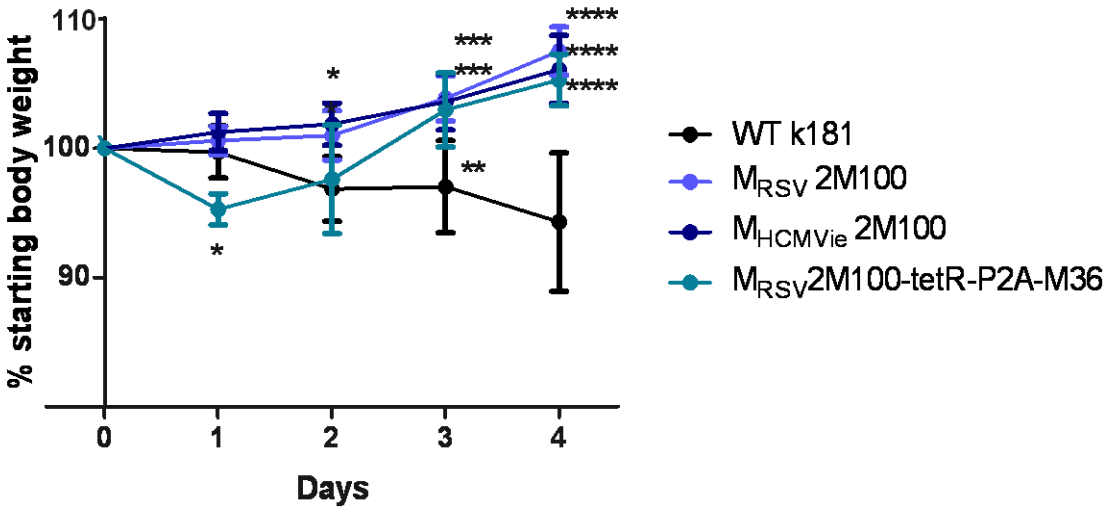

Figure 29: M100/gM-regulated MCMV vectors do not induce illness-associated weight loss in BALB/c mice. Weight loss in MCMV-infected BALB/c mice ($2x10^5$ PFU) was measured daily post-infection and compared to WT K181 (positive control). Weight loss is expressed as mean ±SD (4 mice/group) of percent of starting weight. Data was analysed using 2-way ANOVA with Dunnett's multiple comparisons test (*p<0.05; **p<0.01; ***p< 0.001; ****p<0.0001).

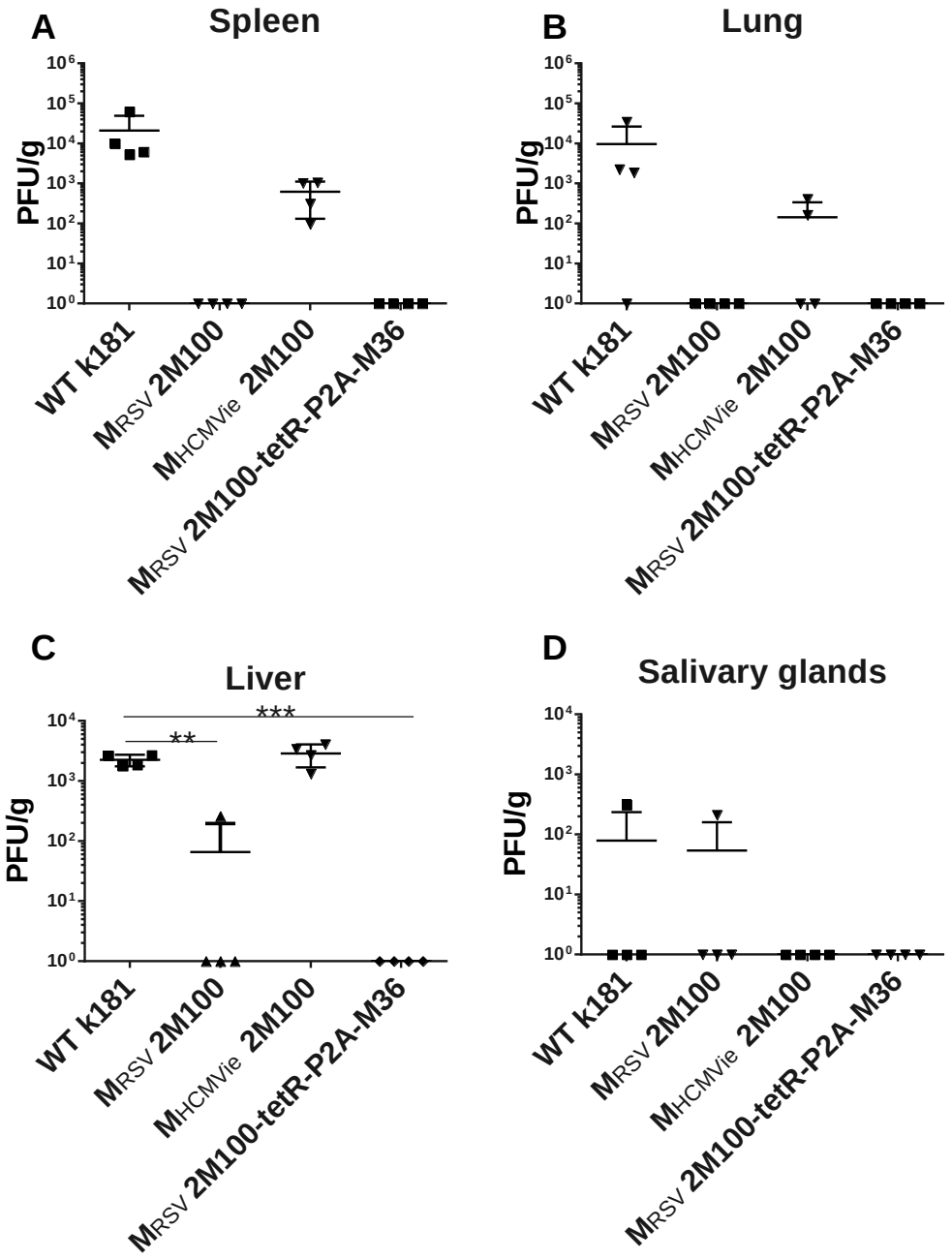

Figure 30: M_{RSV}2M100-tetR-P2A-M36 is undetectable in mouse tissues in acute MCMV infection model. MCMV replication in the (A) spleen, (B) lung, (C) liver and (D) salivary glands at 4 days post infection was quantified by plaque assay. Organ homogenates were used to infect NIH 3T3 cells and incubated for 6 days under carboxymethyl cellulose overlay media to inhibit cell-free virus release. Results are expressed as mean ±SD (4 mice/group) PFU/g of tissue. Each symbol represents a single mouse. Data was analysed using 1-way ANOVA with Dunnett's multiple comparisons post-tests ($p<0.05$. **$p<0.01$; ***$p< 0.001$).

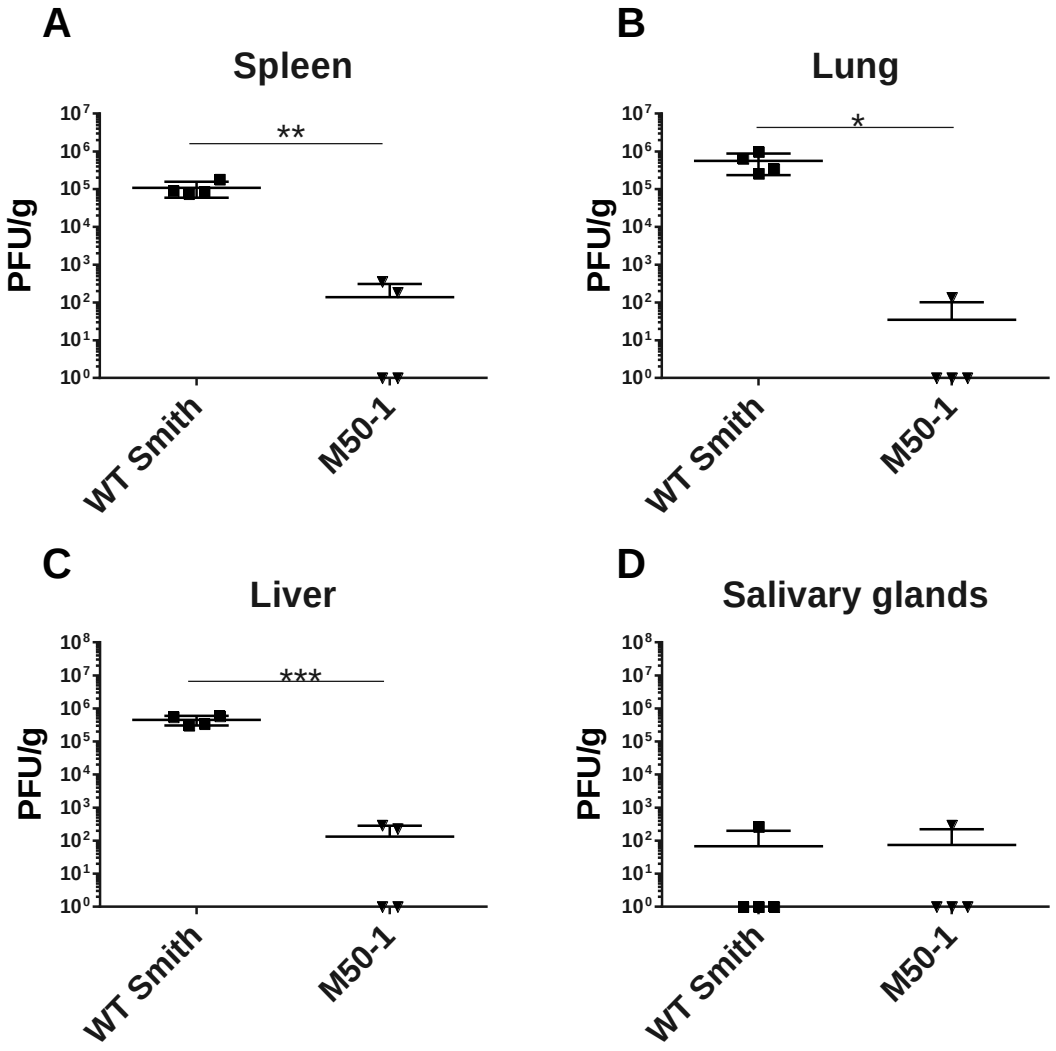

Figure 31: M50-1 is detected at low levels in spleen, lung and liver of infected BALB/c mice. MCMV titres in the spleen (A), lung (B), liver (C) and salivary glands (D) of acutely infected BALB/c mice was measured by plaque assay. The aforementioned organs of mice infected with $2x10^5$ PFU of MCMV at 4 days pi, were homogenised and used to infect NIH 3T3s under a semi-solid overlay media to prevent cell-to-cell spread. Virus titres are expressed as PFU/g (mean ±SD of 4 mice/group). Each symbol represents a single mouse. Data was compared using unpaired 2-tailed t-test (*p<0.05; **p<0.01; ***p<0.001).

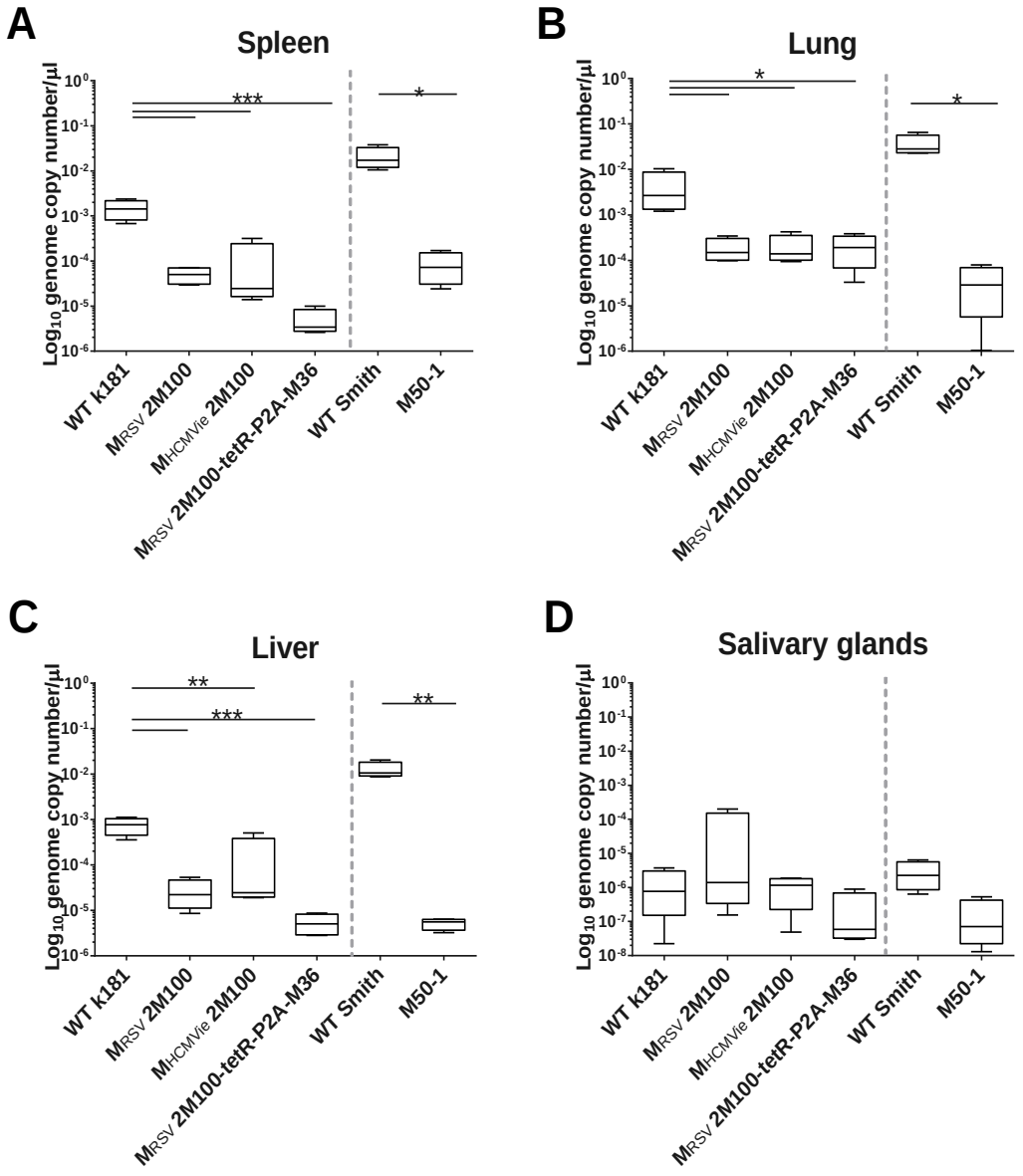

Figure 32: M_{RSV}2M100-tetR-P2A-M36 is the most stringently *in vivo* controlled virus tested. Genome copy numbers in the spleen (A), lung (B), liver (C) and salivary glands (D) of BALB/c infected with $2x10^5$ PFU MCMVs (at 4 d pi) were quantified by qPCR. Genome copies are displayed as mean (4 mice per group) ±SD. Virus genome copy numbers were compared by 1-way ANOVA followed by Dunnett's multiple comparisons post-test whereas M50-1 data was analysed using unpaired 2-tailed t-test (*p<0.05; **p<0.01; ***p<0.001).

3.2.2. Replicative capacity and immunogenicity of M_{RSV}2M100-tetR-P2A-M36 virus in BALB/c mice

Comparative analysis of all of the TREx vectors identified M_{RSV}2M100-tetR-P2A-M36 as the conditionally replicating vector with the greatest potential as it was unable to replicate in the absence of DOX *in vivo*, more tightly controlled than vectors previously described in the literature. I therefore sought to look at effects of DOX administration on virus replication *in vivo* to see whether I could induce virus replication by feeding mice DOX. In this experiment, BALB/c mice were intra-peritoneally injected with either M_{RSV} or M_{RSV}2M100-tetR-P2A-M36 (absence of DOX, or presence of DOX in feed for one or two weeks). Instead of using WT K181 for comparison with a replication-competent virus, I opted for M_{RSV}, since this virus has the same backbone as M_{RSV}2M100-tetR-P2A-M36 (i.e. it contains *tetR* in place of m157 gene and an RSV promoter upstream), however, it does not contain any tetO therefore its replication is not regulated.

To investigate the virulence of my vectors, I monitored mice weight loss (Figure 33). Interestingly, mice infected with M_{RSV}2M100-tetR-P2A-M36 did not lose any weight. On day 2, one of the groups receiving DOX displayed a statistically significant weight gain compared to M_{RSV} virus infected mice. The following day (day 3), the weights of both groups infected with M_{RSV}2M100-tetR-P2A-M36 and receiving DOX were significantly different to the M_{RSV} control. This distinction, however, waned on day 3 as the mice infected with M_{RSV} recovered and gradually gained weight.

Following systemic administration (intraperitoneal route of injection), MCMV establishes acute infection in the spleen and liver as early as 48 hours (Hsu et al. 2009). The virus then replicates in the lungs and eventually, at 6-8 days pi initiates productive replication in the salivary glands. Although the virus is cleared from the majority of susceptible tissues, it remains persistent in salivary glands and reaches peak titres at days 14-20. Salivary glands are also the site of virus transmission as it is secreted into saliva and spreads to other hosts. I wanted to see whether mice infected with either of my vectors were shedding infectious virions at 14 days post injection. To test this, I used 1 µl of saliva to perform qPCR (Figure 34). Surprisingly, none of the mice infected with the control virus (M_{RSV}) shed any infectious virus. M_{RSV}2M100-tetR-P2A-M36, on the other hand, was detected in some mice under all three different conditions (absence of DOX, addition of DOX for a week and two

weeks), however, this difference was not statistically significant when compared to control virus.

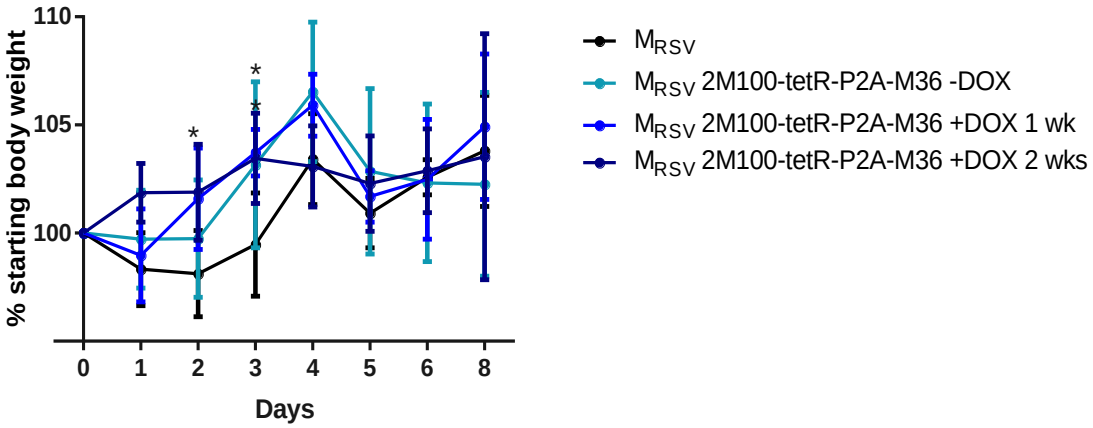

Figure 33: M_{RSV}2M100-tetR-P2A-M36 does not induce weight loss in the presence/absence of DOX. Weight loss in MCMV-infected BALB/c mice were monitored daily on the day of injection and 8 d pi. M_{RSV}2M100-tetR-P2A-M36 – DOX represent a group of mice injected with M_{RSV}2M100-tetR-P2A-M36 that did not receive DOX. M_{RSV}2M100-tetR-P2A-M36+DOX 1 wk and M_{RSV}2M100-tetR-P2A-M36 + DOX 2 wks a groups of mice fed DOX for 1 and 2 weeks, respectively. The weights were compared to weights in mice infected with non-inducible M_{RSV} vector (tetR in m157 and no tetO sequences). Mouse weight is expressed as percentage of original weight. Weight loss is shown as mean ±SD of five mice per group. Weight differences were compared by 2-way ANOVA followed by Dunnett's multiple comparisons post-test (*$p<0.05$).

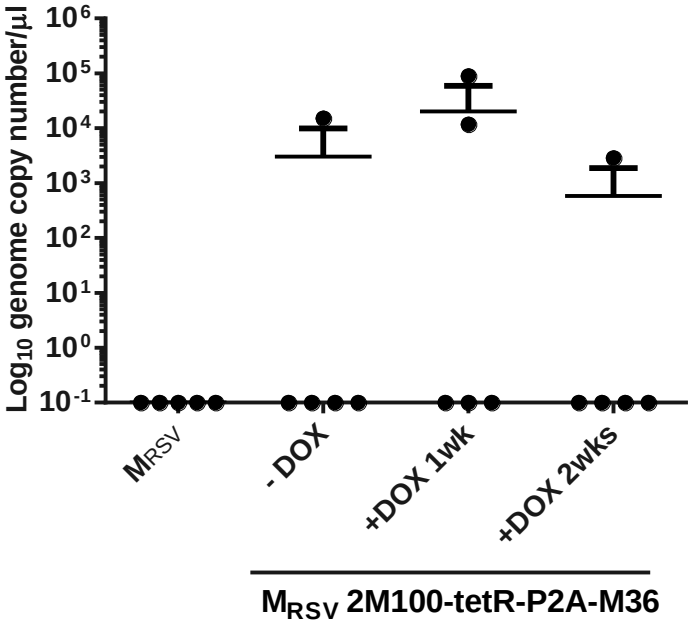

Figure 34: M_{RSV}2M100-tetR-P2A-M36 is shed into saliva in 20% of infected mice. Saliva shedding of MCMV at day 14 pi was measured by collecting saliva and performing qPCR using IE1/M123 primers. Each symbol represents MCMV genome copy numbers in a single mouse. Data is shown as individual mice means (5 mice/group) ±SD. M_{RSV} represents control virus (non-inducible)-infected mice. Mice infected with M_{RSV}2M100-tetR-P2A-M36 were either fed regular diet (no DOX) or DOX supplemented diet for either 1 or 2 weeks. Symbols represent average (of three) genome copy number/µl/mouse.

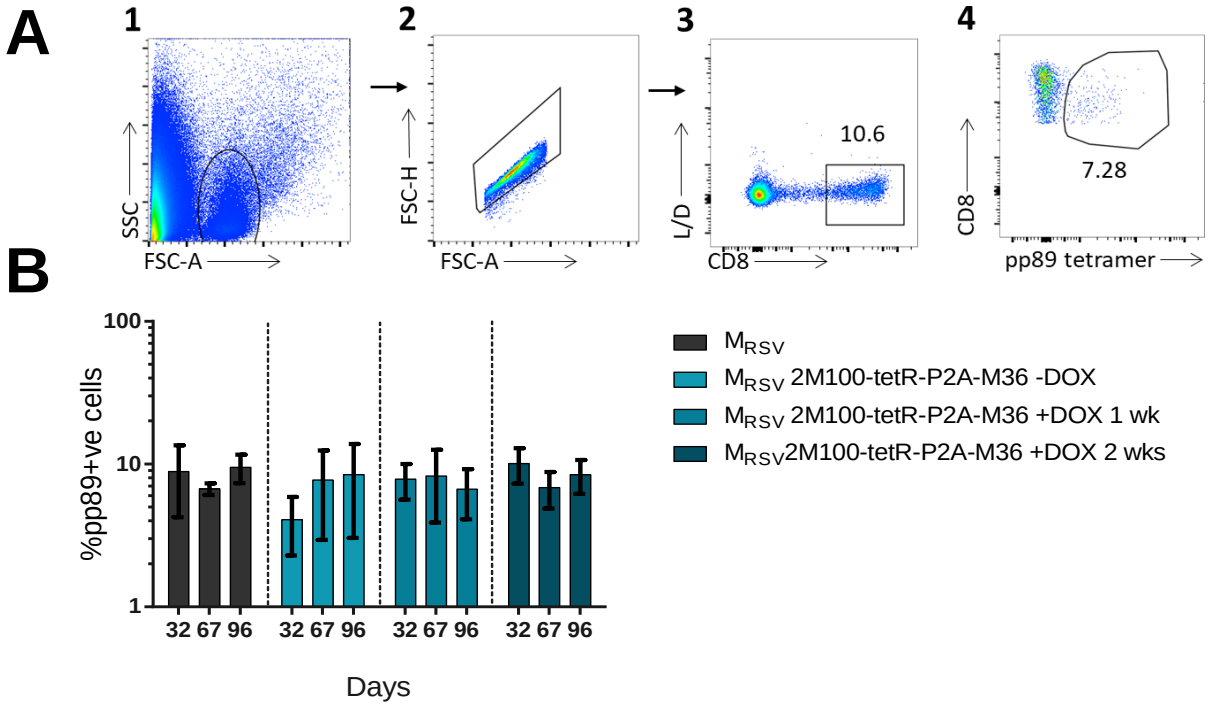

Figure 35: Early control of M_{RSV}2M100-tetR-P2A-M36 in the absence of DOX is overcome later in the infection. A: Gating strategy on lymphocytes in the peripheral blood at 32, 67 or 96 d pi. Lymphocytes were discriminated based on side scatter (SSC) and forward scatter height (FSC-H) profile (panel 1). Panel 2: Singlets were then selected based on forward scatter height (FSC-H) and FSC-A. Panel 3: Live CD8 lymphocytes were sorted into M123/pp89 tetramer-specific $CD8^+$ T cells (panel 4). B: Frequencies of MCMV-specific $CD8^+$ T cells in blood of infected BALB/c mice were measured on days 32, 67 and 96. The frequencies of circulating leukocyte populations in blood were quantified by FACs using a M123/pp89 (IE1) tetramer. Data represent the mean ±SD of 5 mice per group. Data obtained from mice infected with conditional M_{RSV}2M100-tetR-P2A-M36 in the absence of DOX or presence of DOX (1 or 2 weeks) was compared to data from mice infected with non-conditional M_{RSV} vector.

Next, I sought to analyse peripheral blood responses (by using a tetramer) to the viral protein M123/pp89 (IE1) at three timepoints: 32, 67 and 96 days pi (d pi) (for gating strategy see Figure 35A). Interestingly, similar frequencies of M123/pp89-specific lymphocytes were detected at 32 d pi (Figure 35B) in mice infected with the control virus (M_{RSV}) as well as DOX-regulatable M_{RSV}2M100-tetR-P2A-M36 that received DOX in the feed. Mice infected with M_{RSV}2M100-tetR-P2A-M36 that did not receive DOX had lower levels of pp89-specific $CD8^+$ T cells in comparison to the other two groups (not statistically significantly). However, during the course of infection, the levels increased and by day 96 were comparable to frequencies in mice infected with the control virus as well as mice infected with M_{RSV}2M100-tetR-P2A-M36 receiving DOX.

To determine in more detail whether CMV-specific lymphocyte populations varied in the spleen, lung, salivary glands and lamina propria at late stages (102 d pi) of MCMV infection, the organs were isolated from the mice and extracted lymphocytes were analysed by FACs. A M123/pp89 (IE1) tetramer was again used to distinguish MCMV-specific lymphocyte populations within different experimental groups. In the spleen, (for gating strategy see Figure 36) the frequencies of pp89-specific $CD8^+$ T cells were comparable within different groups (Figure 37). To further characterize CMV-specific lymphocyte populations, into tissue-resident memory T cells, cells expressing CD69 (T-cell activation and tissue resident memory cell marker) and CD103 αE integrin (known to bind to E-cadherin on epithelial cells) were selected (Cepek et al. 1994). In addition to this, effector memory T cells were quantified based on expression of CD44 (memory marker) and Killer cell lectin-like receptor subfamily G member 1, KLRG1 (differentiation marker). High expression of CD27 was used to distinguish effector memory and central memory T lymphocyte populations.

Analysis of lymphocytes in the spleen (Figure 38) revealed a trend whereby mice vaccinated with M_{RSV}2M100-tetR-P2A-M36 receiving regular feed had lower frequencies of T_{CM}, T_{EM} and T_{RM} cells. Although the percentage of T_{CM} lymphocytes from mice injected with M_{RSV}2M100-tetR-P2A-M36 was significantly lower than mice injected with M_{RSV} virus, the total cell counts were similar.

Interestingly, analysis of CMV-specific lymphocytes in the lung (for gating strategy see Figure 39) revealed that the percentage of tetramer-specific $CD8^+$ (Figure 40) T cells was significantly lower in mice infected with M_{RSV}. In addition to this, the percentage of

T_{CM} population in M_{RSV}2M100-tetR-P2A-M36 infected mice receiving DOX for 2 weeks was significantly lower than the control mice group. Total cell counts, on the other hand, showed that there were lower levels of $CD4^+$, T_{CM}, T_{EM}, and T_{RM} (Figure 41) in mice infected with the control virus (M_{RSV}) although this difference was not statistically significant.

In the salivary glands (for gating strategy see Figure 42) of mice injected with M_{RSV}2M100-tetR-P2A-M36 receiving regular feed and feed containing DOX, tetramer-specific $CD8^+$ and T_{EM} cell counts (Figure 43 and Figure 44) were significantly lower than in mice infected with M_{RSV}. T_{CM} levels were significantly lower in mice infected with M_{RSV}2M100-tetR-P2A-M36 receiving regular feed and mice receiving DOX feed for 1 week whereas T_{RM} levels were only lower in mice infected with M_{RSV}2M100-tetR-P2A-M36 receiving regular feed.

We discovered CMV-specific lymphocytes (for gating strategy see Figure 45) in lamina propria of infected mice (Figure 46). Frequencies of CMV-specific T lymphocyte populations of MCMV-infected mice were low and thus, highly variable (Figure 47) Interestingly, however, phenotypic analysis of MCMV-specific $CD8^+$ populations revealed that there were no central memory T cells detected in the lamina propria of any of the mice.

To characterize the functionality of T cell responses, I carried out intracellular cytokine staining whereby lymphocytes isolated from spleens of MCMV-infected mice were stimulated for 6 hours with either MHC class I (M123/pp89) or class II (M53 - IAHQRITLTARCLRL and M78 - SQQKMTSLPMSVFYS) peptides. Cytokines (TNF-α and IFN-γ) accumulating in the ER were quantified by FACS. I elected to look at TNF-α since this cytokine plays an antiviral role by blocking viral gene expression. IFN-γ, on the other hand, activates macrophages and NK cells and upregulates antigen presentation by increasing expression of class I and class I MHC molecules. Stimulation of $CD4^+$ lymphocytes (for gating strategy see Figure 48) with M53 peptide resulted in higher production of IFN-γ in mice infected with M_{RSV}2M100-tetR-P2A-M36 (Figure 49) compared to M_{RSV} infected mice. TNF-α levels were higher in M_{RSV}2M100-tetR-P2A-M36 groups receiving DOX for 1 and 2 weeks whereas production in M_{RSV}2M100-tetR-P2A-M36-infected mice receiving regular feed was comparable to control mice. Stimulation with M78 peptide induced higher production of IFN-γ in M_{RSV},

M_{RSV}2M100-tetR-P2A-M36 receiving regular feed and M_{RSV}2M100-tetR-P2A-M36 receiving DOX for 1 week whilst the levels of TNF-α^+ $CD4^+$ T cells were comparable among the different groups. Interestingly, stimulation with pp89 peptide (gating strategy shown in Figure 50) promoted accumulation of higher IFN-γ levels by $CD8^+$ T cells (Figure 51) isolated from mice immunized with M_{RSV}2M100-tetR-P2A-M36. TNF-α levels, on the other hand, were similar in M_{RSV} and M_{RSV}2M100-tetR-P2A-M36 injected mice receiving DOX but were higher in M_{RSV}2M100-tetR-P2A-M36 receiving regular feed.

3.2.3. Summary

From my *in vitro* analysis of tetR-regulated virus vectors (section 3.1) it was evident that early and abundant tetR expression could inhibit virus replication to a high degree. Interestingly, the level of virus repression *in vivo* was even more pronounced. When mice were injected with M_{RSV}2M100-tetR-P2A-M36 virus in the absence of DOX, virus was not detectable in any of the four tissues (spleen, lung, liver and salivary glands) analysed. M50-1 (a virus vector previously published in the literature), on the other hand, was present at low titre at all sites. Immunization of mice with M_{RSV}2M100-tetR-P2A-M36 (absence and presence of DOX) showed that 25-50% of the animals were shedding virus at 14 d pi as opposed to mice infected with the control vector (M_{RSV}). Although this observation is surprising, it was not statistically significant due to the sample size in the experiment. At early times, where animals were not fed DOX, the DOX-regulated virus (M_{RSV}2M100-tetR-P2A-M36) did not induce the same magnitude of immune response in the periphery as when animals were fed DOX suggesting that it was unable to replicate to the same extent. However, at later times, the immunogenicity of the vector was comparable to the control vector in the spleen, lung and gut implying that the virus either mutated or was able to overcome immune control mechanisms. In the salivary glands, M_{RSV} (control virus) induced higher levels of central memory, effector memory and tissue-resident memory T cells thus suggesting that in this organ tetR vectors were unable to induce an immune response of a similar magnitude.

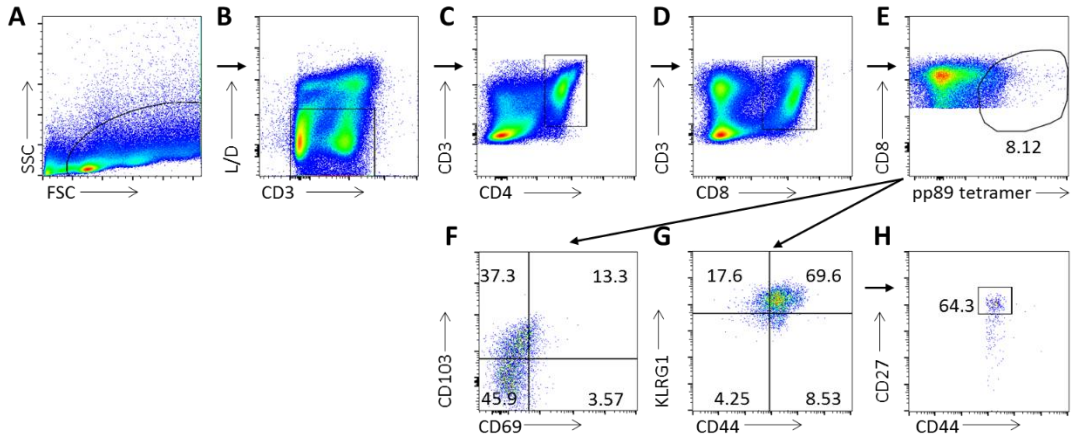

Figure 36: Gating strategy of lymphocyte populations in the spleen (102 d pi). A: The gate for lymphocytes was based on side scatter (SSC) and forward scatter (FSC) profile; live $CD3^+$ lymphocytes (B); $CD3^+CD4^+$ T cells (C); $CD3^+CD8^+$ T cells (D); M123/pp89 tetramer (MCMV) specific $CD8^+$ T cells (E). MCMV-specific $CD8^+$ T cells were further classed into resident memory T cells ($CD69^{high}CD103^{high}$) (F); effector memory ($CD44^{high}KLRG1^{high}$) (G) and central memory ($CD44^{high}KLRG1^{low}CD27^{high}$) (H) cells.

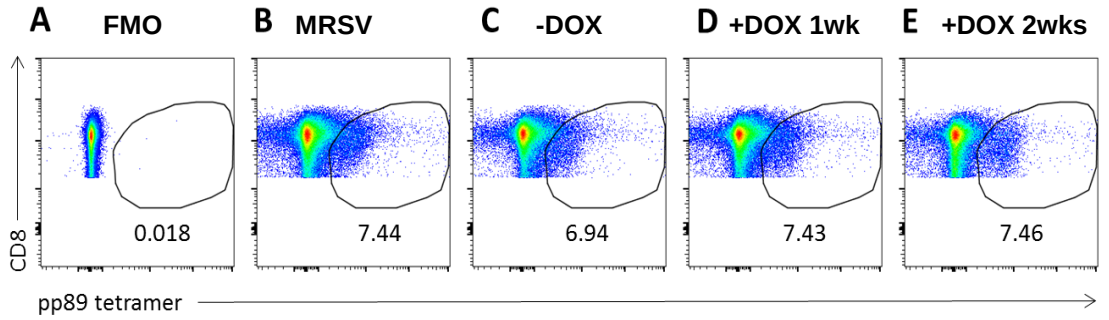

Figure 37: Representative FACs plots of CMV-specific $CD8^+$ T cells in the spleen at 102 d pi. Concatenated FACs plots of: fluorescence minus one (FMO) of all four groups (A), tetramer-specific lymphocytes from M_{RSV} infected mice (B), mice infected with M_{RSV}2M100-tetR-P2A-M36 (regular feed) (C), mice infected with M_{RSV}2M100-tetR-P2A-M36 that received DOX for 1 week (D) and 2 weeks pi (E).

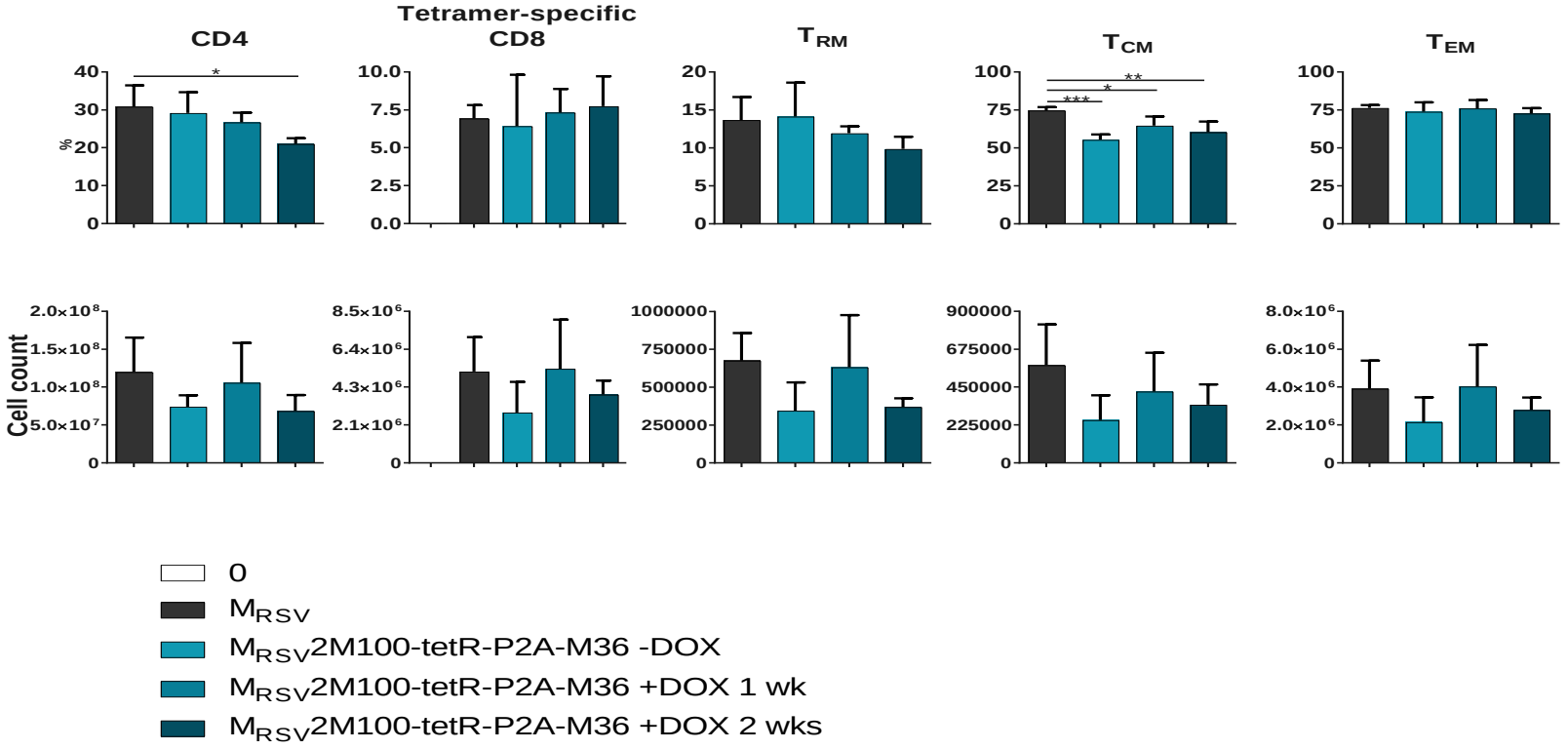

Figure 38: Comparable frequencies of CMV-specific T_{RM}, T_{CM} and T_{EM} populations in spleens of BALB/c mice infected (102 d pi) with conditional M100/gM-regulated MCMV and control virus. Top panel: Percentage of $CD4^+$, tetramer-specific $CD8^+$ T lymphocytes, tissue resident memory, central memory and effector memory $CD8^+$ T lymphocytes. Bottom panel: total count of $CD4^+$ T cells; tetramer-specific $CD8^+$ T cells; T_{RM}, tissue resident $pp89^+$ T cells; T_{CM}, central memory and T_{EM}, effector memory lymphocytes. Data was compared using one-way ANOVA with Dunnett's post-test (*p<0.05; **p<0.01; ***p<0.001).

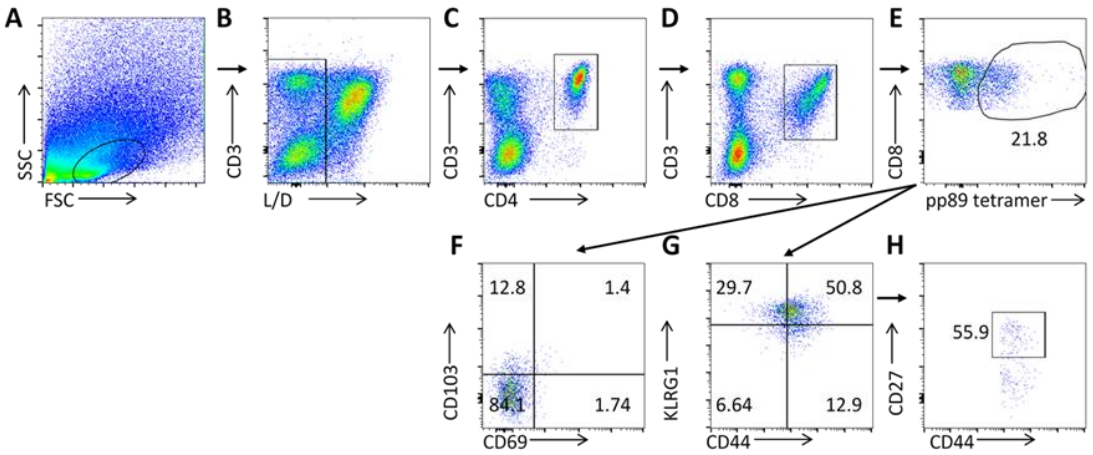

Figure 39: Gating strategy on lymphocyte populations in the lungs of MCMV-infected (102 d pi) BALB/c mice. Side scatter (SSC) and forward scatter (FSC) profile was used to distinguish lymphocyte population (A); live $CD3^+$ lymphocytes (B); $CD3^+$ $CD4^+$ T cells (C); $CD3^+$ $CD8^+$ T cells (D); M123/pp89 tetramer (MCMV) specific $CD3^+CD8^+$ T cells (E) identified as resident memory T cells ($CD69^{high}CD103^{high}$) (F); effector memory ($CD44^{high}KLRG1^{high}$) G) and central memory ($CD44^{high}KLRG1^{low}CD27^{high}$) (H) T cells.

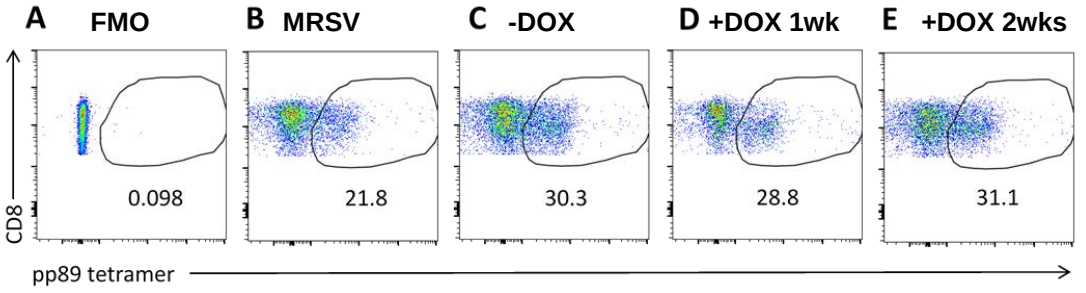

Figure 40*:* Representative FACs plots of $pp89^+$ tetramer specific $CD8^+$ T cells in lungs of MCMV infected mice at 102 d pi. Concatenated FACs plots of FMO of all four groups (A), tetramer-specific lymphocytes from M_{RSV} infected mice (B), mice infected with M_{RSV}2M100-tetR-P2A-M36 (regular feed) (C), mice infected with M_{RSV}2M100-tetR-P2A-M36 that received DOX for 1 week (D) and 2 weeks pi (E).

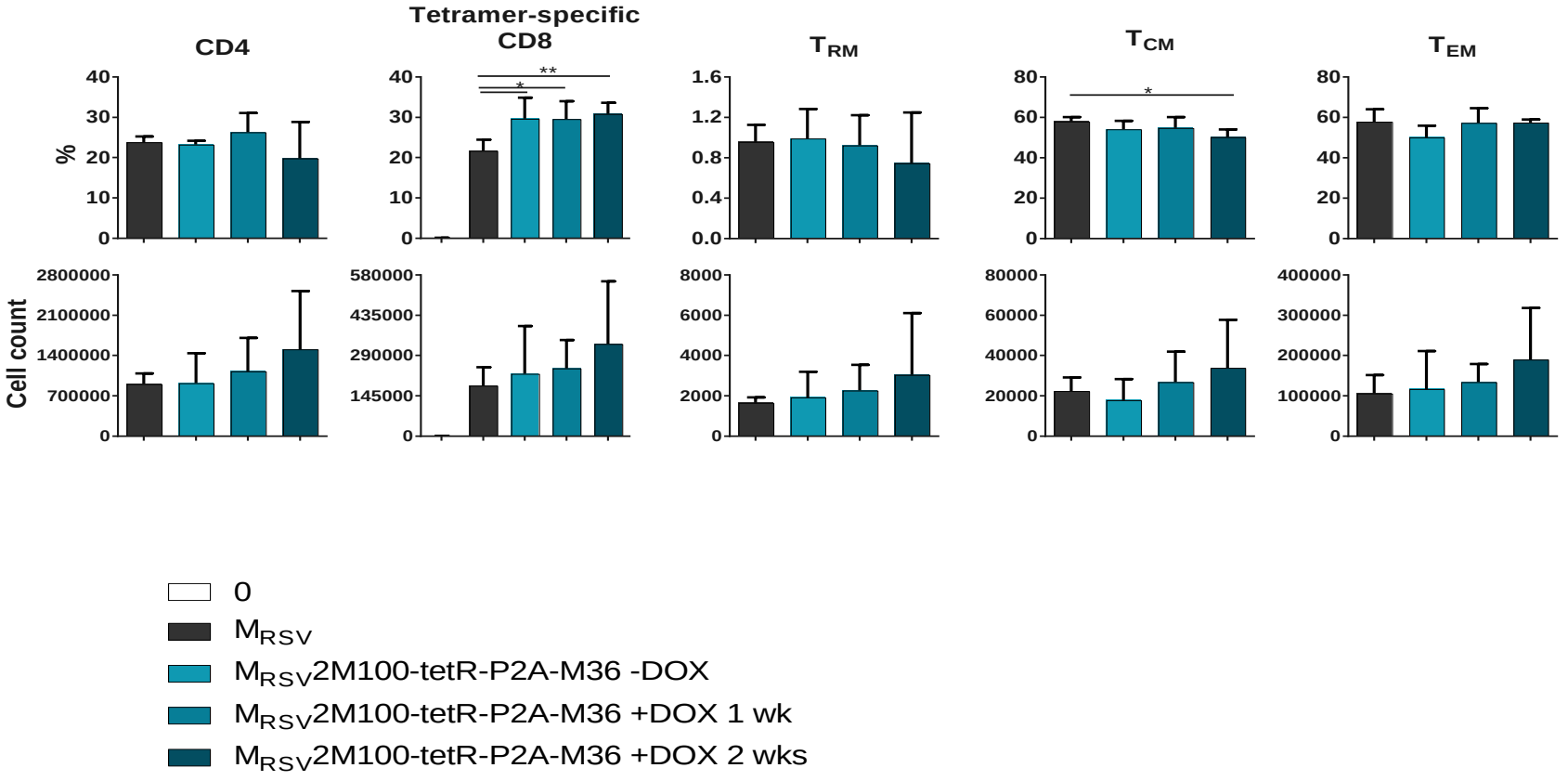

Figure 41: Higher frequencies of CMV-specific lymphocyte populations in lungs of mice infected (at 102 d pi) with conditional M_{RSV}2M100-tetR-P2A-M36 virus than control virus. Top panel: frequencies of $CD4^+$, tetramer-specific $CD8^+$ T cells and tissue-resident memory, central memory and effector memory CD8 T cell populations. Bottom panel: total cell counts of (left to right) $CD4^+$; tetramer-specific $CD8^+$ T cells; T_{RM}, tissue resident memory, T_{CM}, central memory and T_{EM}, effector memory $CD8^+$ T cells. Data was analysed by one-way ANOVA with Dunnett's post-test (*p<0.05; **p<0.01).

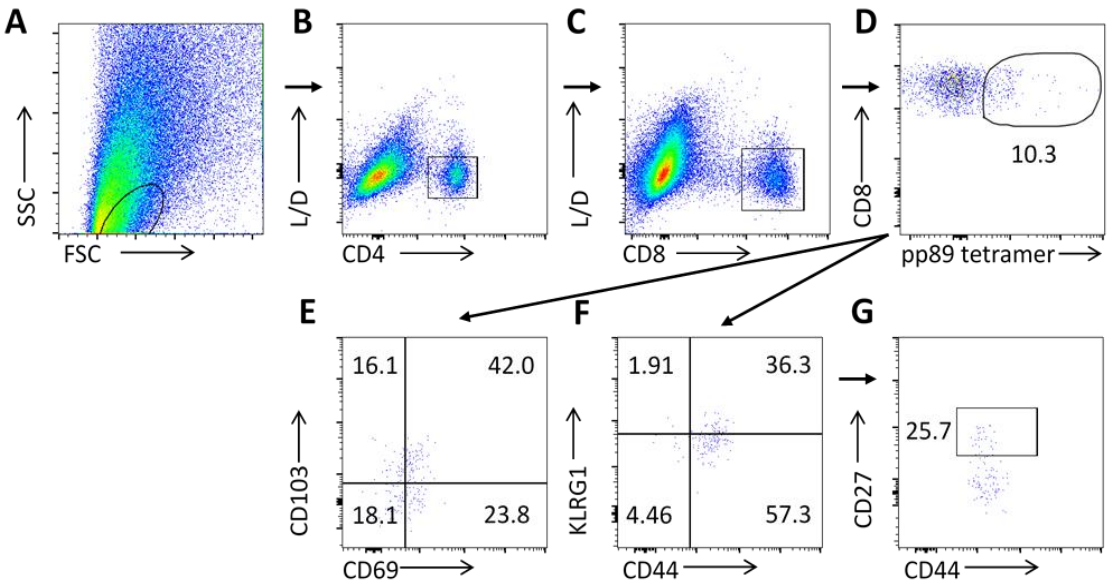

Figure 42: Gating strategy on lymphocyte populations in salivary glands (102 d pi). Lymphocytes were selected based on side scatter (SSC) and forward scatter (FSC) profile (A); live $CD4^+$ lymphocytes (B); live $CD8^+$ lymphocytes (C); M123/pp89-specific $CD8^+$ T cells (D) were classified into tissue resident memory cells (E), effector memory ($CD44^{high}KLRG1^{high}$) (F) and central memory ($CD44^{high}KLRG1^{low}CD27^{high}$) (G) populations.

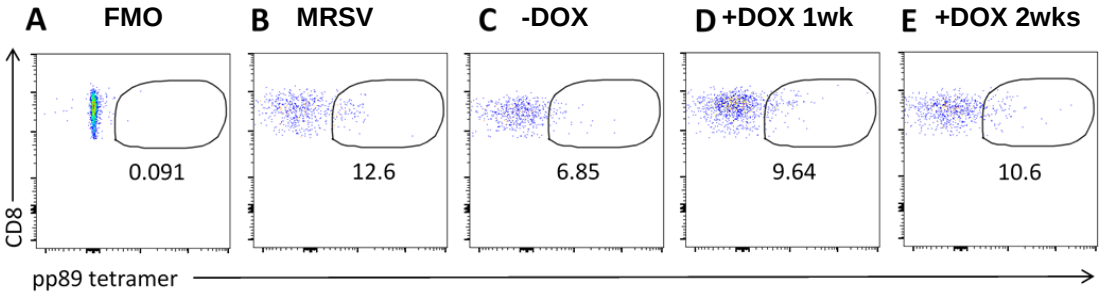

Figure 43: Representative FACs plots of CMV tetramer (pp89) specific lymphocyte populations in salivary glands of MCMV infected (at 102 d pi) BALB/c mice. Concatenated FACs plot of FMO of all four groups (A), tetramer-specific lymphocytes from M_{RSV} infected mice (B), mice infected with M_{RSV}2M100-tetR-P2A-M36 (regular feed) (C), mice infected with M_{RSV}2M100-tetR-P2A-M36 that received DOX for 1 week (D) and 2 weeks pi (E)

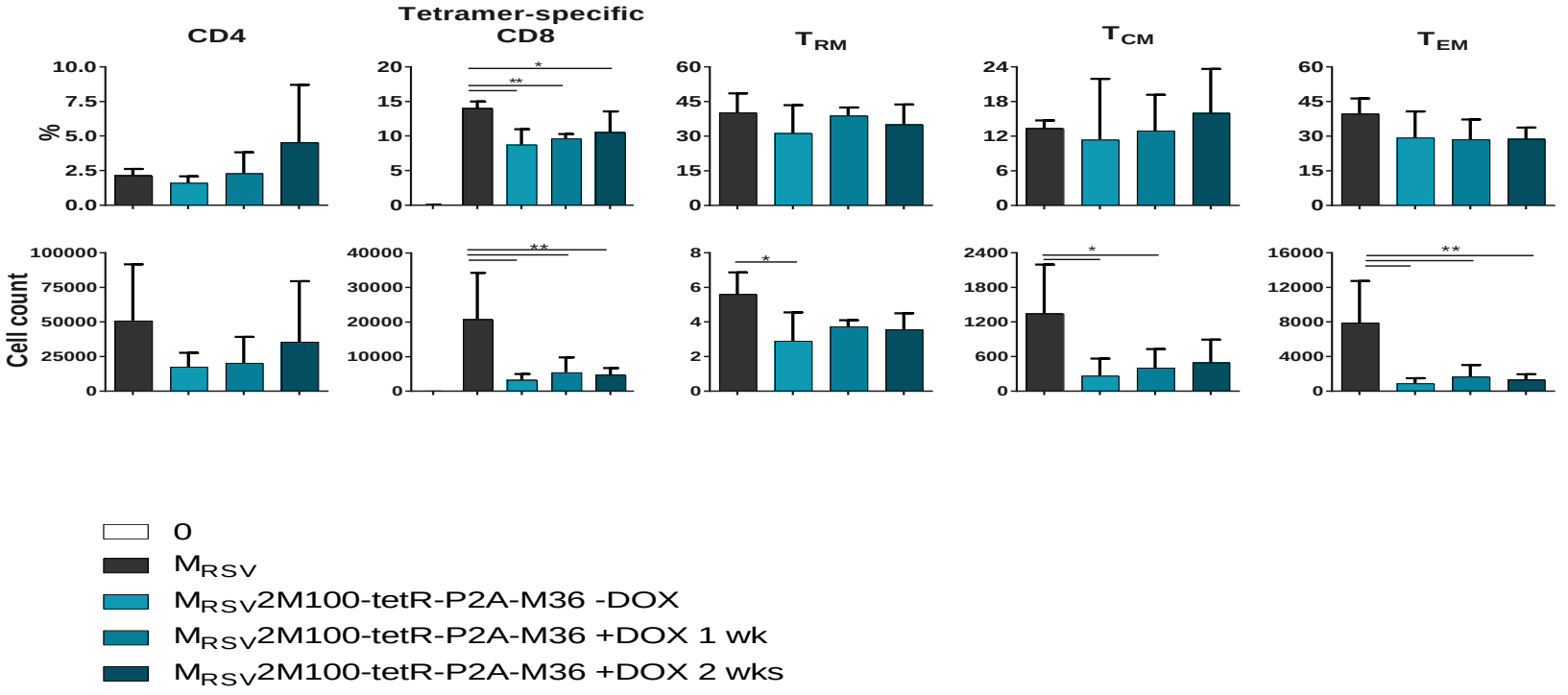

Figure 44: Lower frequencies of CMV-specific lymphocyte populations in salivary glands of mice infected with conditional MRSV2M100-tetR-P2A-M36 virus at 102 d pi. Top panel: frequency of $CD4^+$ T lymphocytes, tetramer (CMV, pp89) specific $CD8^+$ T cells, tissue resident memory, central memory and effector memory $CD8^+$ T cells. Bottom panel: total cell counts of $CD4^+$ T cells; tetramer-specific CD8 T cells; T_{RM}, tissue-resident memory cells; T_{CM}, central memory and T_{EM}, effector memory T cells. Data was compared using one-way ANOVA with Dunnett's post-test (*p<0.05; **p<0.01).

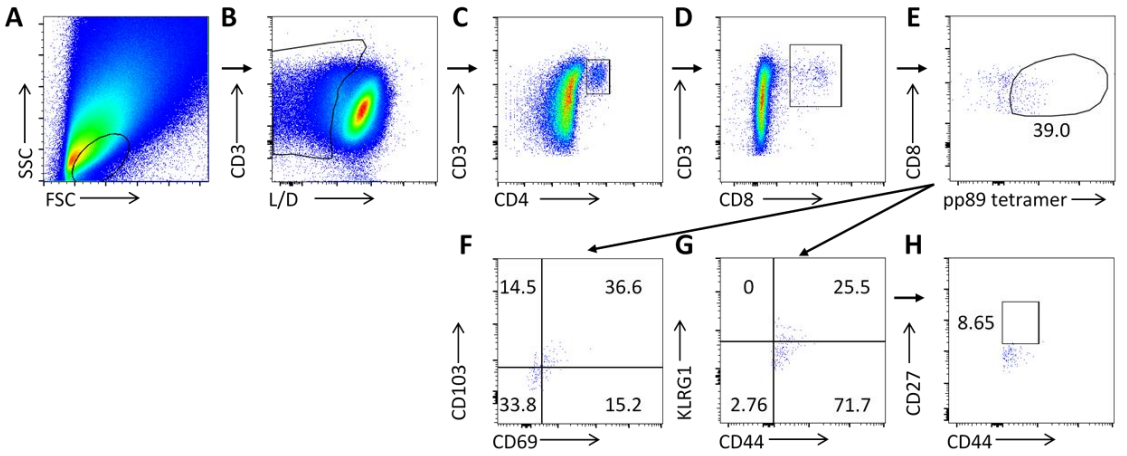

Figure 45: Gating strategy of lymphocytes from intestinal lamina propria of MCMV infected (102 d pi) BALB/c mice. A: lymphocytes were discriminated based on side scatter (SSC) and forward scatter (FSC) profile. B: Live $CD3^+$ lymphocytes; C: $CD3^+$ $CD4^+$ T cells; D: $CD3^+$ $CD8^+$ T cells; E: pp89 tetramer (MCMV) specific $CD3^+CD8^+$ T cells. MCMV-specific $CD8^+$ T cells were further sorted into resident memory T cells ($CD69^{high}CD103^{high}$) (panel F); effector memory ($CD44^{high}KLRG1^{high}$) (panel G) and central memory ($CD44^{high}KLRG1^{low}CD27^{high}$) (panel H).

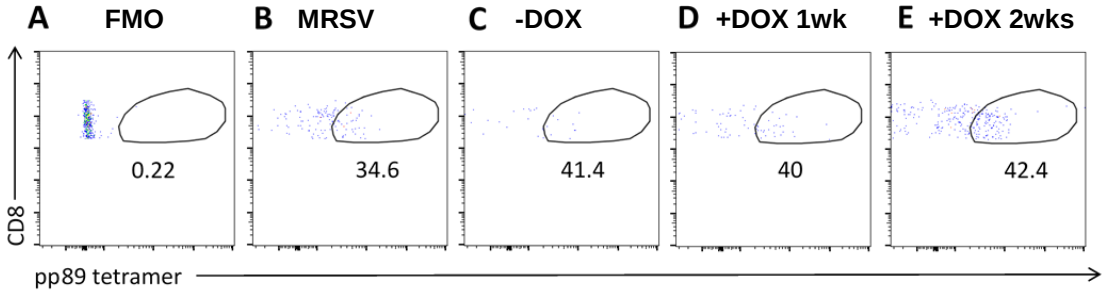

Figure 46: Concatenated FACs plots of MCMV-specific (IE1/pp89) $CD8^+$ T lymphocytes in intestinal lamina propria at 102 d pi. (A): FMO in all groups; (B): M_{RSV}-infected mice, (C): M_{RSV}2M100-tetR-P2A-M36 (regular feed); (D): mice infected with M_{RSV}2M100-tetR-P2A-M36 that received DOX for 1 week and (E): 2 weeks pi.

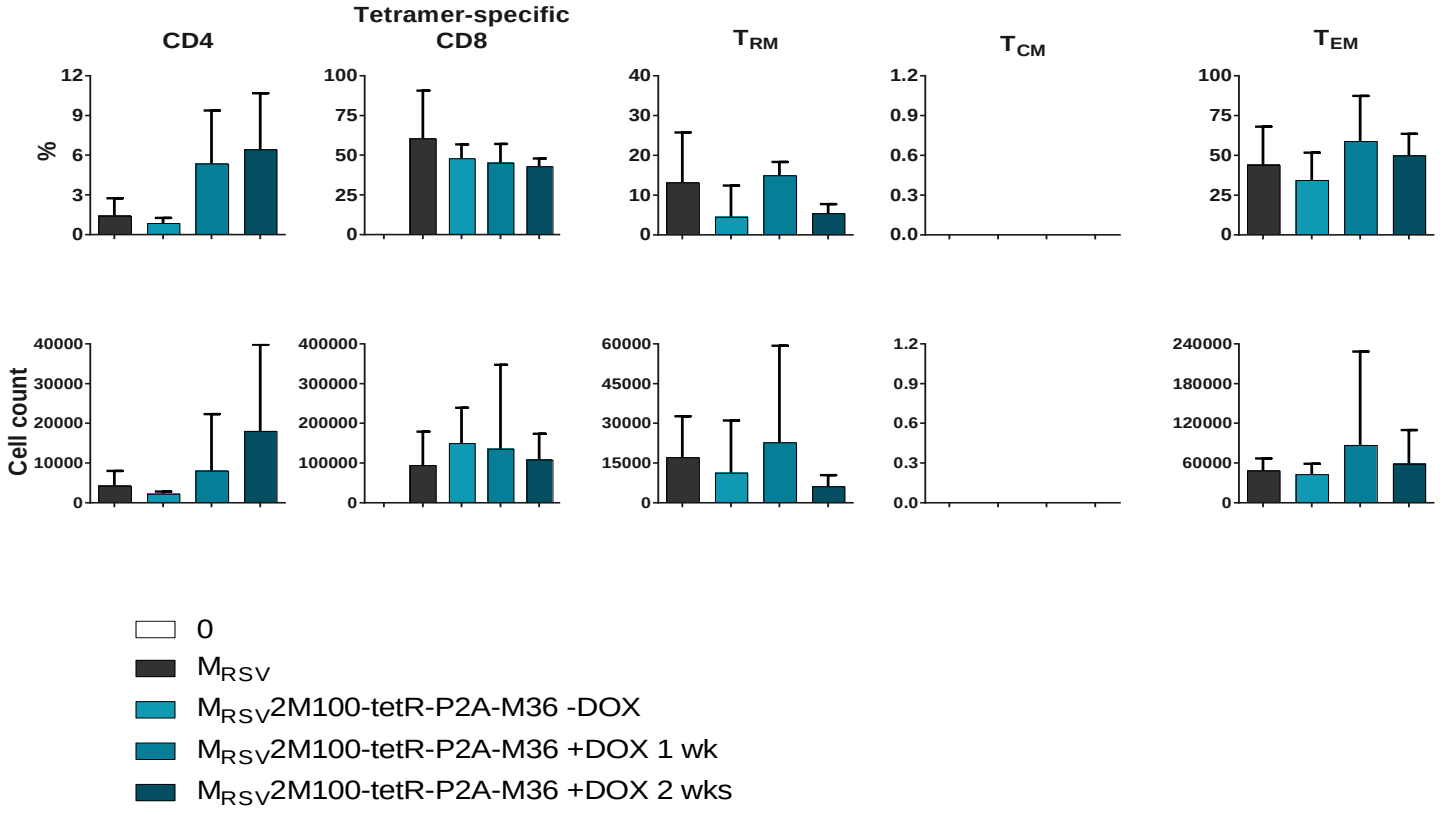

Figure 47: Conditional MCMV (M_{RSV}2M100-tetR-P2A-M36) induces comparable frequencies of lymphocyte populations in the intestinal lamina propria as control virus. Lymphocytes from intestinal lamina propria of MCMV infected BALB/c mice were isolated and analysed by FACs. Top panel: percentage of $CD4^+$ T cells, MCMV tetramer (pp89) specific $CD8^+$ T cells and tissue resident memory, central memory and effector memory CMV-specific CD8 T cells. Bottom panel (left to right): total cell counts of $CD4^+$ T cells; tetramer (CMV, pp89) specific $CD8^+$ T cells; T_{RM}, tissue resident memory, T_{CM}, central memory and T_{EM}, effector memory $CD8^+$ T cells.

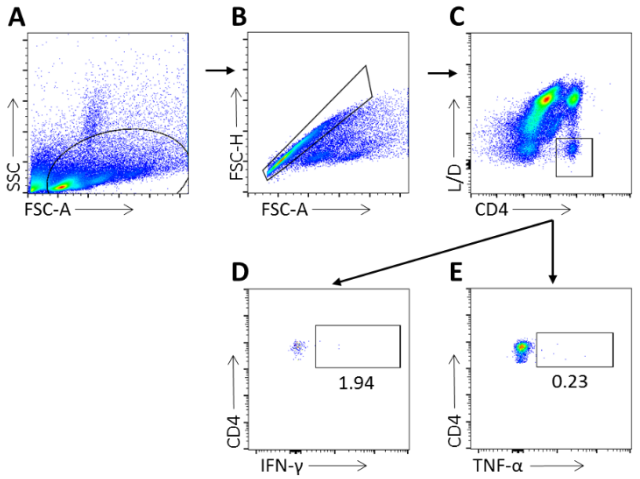

Figure 48: Gating strategy for IFN-γ and TNF-α producing CD4⁺ T cells. A: lymphocytes were discriminated based on side scatter (SSC) and forward scatter area (FSC-A) profile. B: Single lymphocytes were then selected based on forward scatter height (FSC-H) and FSC-A. C: Live CD4 lymphocytes were further sorted into IFN-γ⁺ (D), TNF-α⁺ (E) T lymphocytes.

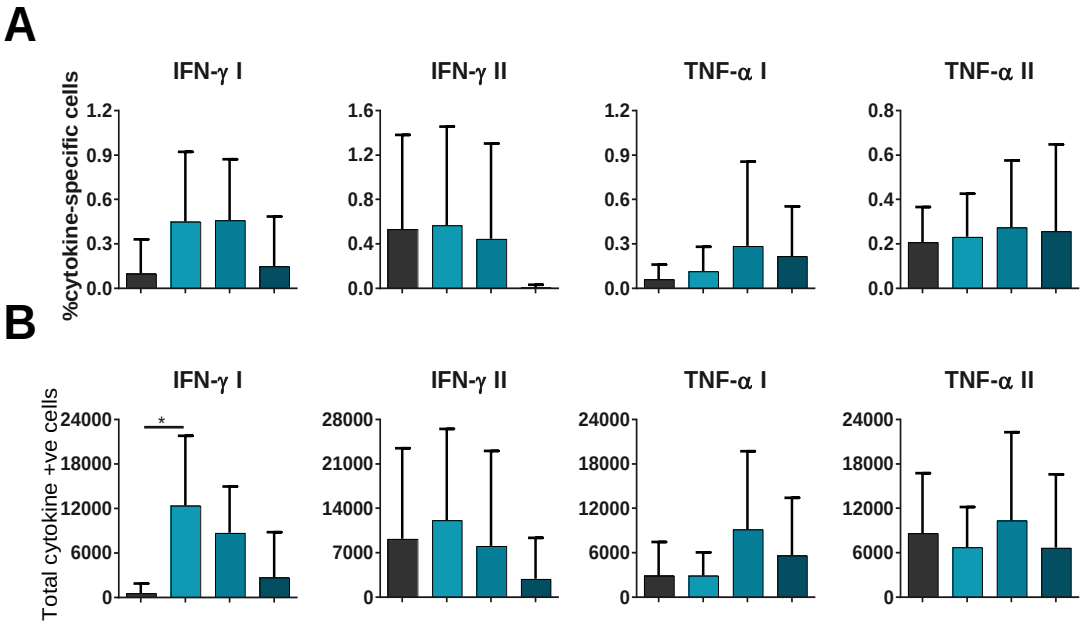

Figure 49: M_{RSV}2M100-tetR-P2A-M36-specific CD4⁺ lymphocytes are functional and secrete IFN-γ and TNF-α. A: Frequency of IFN-γ and TNF-α secreted upon 6 h stimulation with either IAHQRITLTARCLRL (peptide I, M53) or SQQKMTSLPMSVFYS (peptide II, M78). Total count of IFN-γ and TNF-α-specific cells upon 6 h stimulation with peptide I (IAHQRITLTARCLRL) or peptide II (SQQKMTSLPMSVFYS). Values represent mean ±SD. Data was analysed by one-way ANOVA with Dunnett's post-tests (*p<0.05).

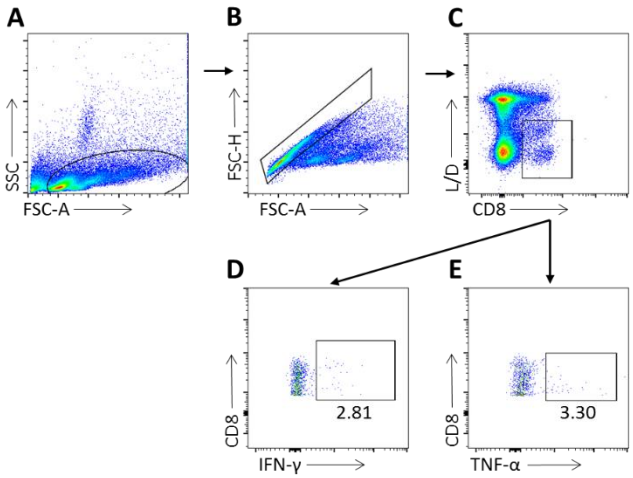

Figure 50: Gating strategy for IFN-γ and TNF-α producing CD8⁺ T cells. A: lymphocytes were discriminated based on side scatter (SSC) and forward scatter area (FSC-A) profile. B: Singlets were then selected based on forward scatter height (FSC-H) and FSC-A. C: Live CD8 lymphocytes were further sorted into IFN-γ⁺ (D) and TNF-α⁺ (E) T cells.

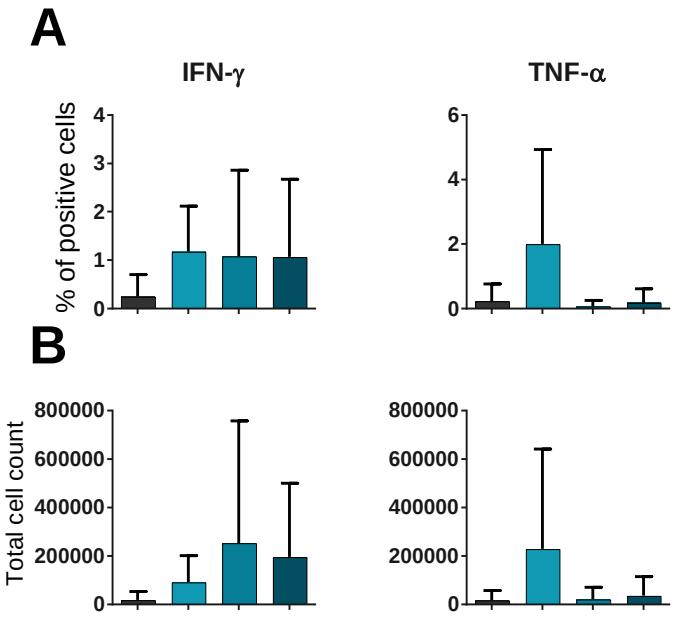

Figure 51: M_{RSV}2M100-tetR-P2A-M36-specific CD8⁺ lymphocytes are functional and secrete IFN-γ and TNF-α. A: Frequencies of IFN-γ (left) and TNF-α (right); B: total counts of IFN-γ⁺ (left) and TNF-α⁺ (right) cells. Intracellular IFN-γ and TNF-α were quantified following a 6 h stimulation with pp89 CMV peptide. Data is represented as mean ±SD.

3.3. Adenovirus and cancer models

As described in section 1.10.6, adenoviruses (Ads) have been widely used in humans as gene delivery agents, and have an excellent safety profile. I therefore wished to compare the immunogenicity and effectiveness of my CMV vectors with Ads expressing cancer antigens. We also took this opportunity to establish murine cancer models in which my vectors could be tested.

3.3.1. Generation of first- and second-generation Ad-h5T4 vectors

The adenoviruses used in this study are listed in Table 22. Two vector backbones (AdZ and AdZ2) were used, both based on adenovirus serotype 5 (Ad5). In the AdZ vector system, the E1 and E3 regions are deleted whereas in AdZ2, the E4 region is also deleted, except for E4-ORF6. ORF6 facilitates virus propagation in the helper cell line and stimulates expression from the HCMV major IE promoter in target cells upon vector delivery. Vectors expressed either GFP, human 5T4, or lacked a transgene (control, CTRL). Of the constructs used in this study, four (Ad-GFP, Ad-tetO-GFP, AdZ-CTRL and AdZ2-CTRL) had been previously cloned by members in the laboratory. Initially, vectors AdZ-h5T4 and AdZ2-h5T4 were used that had been generated by other colleagues in the laboratory, however, due to reasons described in section 3.3.3, vectors AdZ-h5T4 and AdZ2-h5T4 had to be re-engineered and re-made.

To generate AdZ-h5T4 and AdZ2-h5T4, BACs AdZ-CTRL and AdZ2-CTRL were used, respectively. A codon-optimised *h5T4* gene containing a HCMV IE promoter upstream (GeneArt) was inserted via 2 rounds of recombineering. First, a selection cassette (*Amp^r/LacZ/sacB*) was inserted into a cloning site between the HCMV MIE promoter, and the MIE polyA, within the E1A region, then the cassette was taken out and replaced with the *h5T4* gene (Appendix B). The clones were analysed by restriction digest analysis and then sequenced to ensure that no mutations had occurred as result of cloning. The BACs were transfected into T-REx-293cells and infectious virus was collected and purified. Next, expression of 5T4 by these two vectors was analysed by western blot (Figure 52) and compared to first and second-generation control vectors AdZ-CTRL and AdZ2-CTRL, respectively. Both AdZ-h5T4 and AdZ2-h5T4 expressed strong levels of 5T4, that were comparable between vectors.

Table 22: Adenovirus vectors used in this study

Name	pAL number	Serotype	Deleted genes	Modifications
Ad-GFP	1136	5	E1 and E3	HCMV promoter+ GFP inserted in E1.
Ad-tetO-GFP	1423	5	E1 and E3	HCMV promoter+2 tet operators-GFP-polyA inserted in E1.
AdZ-CTRL	1253	5	E1 and E3	HCMV promoter-GFP-polyA inserted in E1. No transgene inserted.
AdZ2-CTRL	1926	5	E1, E3 and E4 (except ORF6)	HCMV promoter -poly A region in E1. No transgene inserted.
AdZ-h5T4	2143	5	E1 and E3	HCMV promoter+2 tet operators-h5T4-polyA inserted in E1.
AdZ2-h5T4	2144	5	E1, E3 and E4 (except ORF6)	HCMV promoter+2 tet operators-h5T4-polyA inserted in E1.

*pAL number represents plasmid number in our laboratory database for internal reference. Ad – adenovirus; CTRL – control; GFP – green fluorescent protein; h5T4-human 5T4 antigen; HCMV – human cytomegalovirus; ORF – open reading frame.

Figure 52: Recombinant adenovirus vectors express strong levels of 5T4. HFFF-CARs were infected at MOI=10 and expression of h5T4 was detected at 48 h pi using mouse 5T4 antibody (AF5049, R&D Systems) (1:2000). AdZ-CTRL and AdZ2-CTRL were first- and second-generation empty vectors that served as a negative control, respectively. AdZ-h5T4 and AdZ2-h5T4 both contained codon-optimised *h5T4* gene with HCMV promoter inserted into E1 region. AdZ-h5T4 had deleted E1 and E3 genes whereas AdZ2-h5T4 was also lacking E4 gene (except for ORF6). β-actin was used as a housekeeping gene control.

3.3.2. Establishment of mouse models expressing 5T4 antigen

5T4 expression is normally restricted to foetal trophoblasts, yet it is also recognized as a tumour antigen found in a range of solid cancers (see section 1.9.3.1). I aimed to develop murine tumour challenge models in order to test the efficacy of an Ad vector encoding 5T4 as an immunization agent. The well characterized murine cell lines – CT26 and 4T1 (obtained from Awen Gallimore) have been used extensively *in vivo* in the development of anti-cancer immunotherapies and, more specifically, evaluation of the TroVAx vaccine efficacy (Abern et al. 2011). CT26 is a colon carcinoma cell line whereas 4T1 is a highly metastatic murine mammary carcinoma cell line (Mulryan et al. 2002). Tumour growth and metastatic spread of 4T1 cells in BALB/c mice very closely mimics stage IV of human breast cancer. Both CT26 and 4T1 cells are tumour cell lines syngeneic with the BALB/c mouse strain. Since I was also interested in looking at C57BL/6-derived cancer models, a Lewis lung carcinoma 1 (LLC1) cell line was sourced from ATCC. LLC1 cells have been described as highly tumorigenic and metastatic, forming tumour nodules in the lung (Bertram & Janik 1980). Intestinal epithelial cells from a murine colorectal cancer model were also kindly provided by Lee Parry (Cardiff University). *Apc*$^{fl/fl}$ mice express an intestinal stem cell marker (leucine-rich repeat-containing G-protein coupled receptor 5; LGR5) linked to a tamoxifen-inducible cre recombinase, and have an adenomatous polyposis coli (*APC*) gene flanked by loxP sites. Treatment of these mice with tamoxifen induces a deletion of the *APC* gene in intestinal stem cells. Since APC is a tumour suppressor and plays a role in WNT signalling pathway, deletion of the gene induces colorectal tumorigenesis.

5T4 expression in the different cell lines and cancer models was compared in a western blot analysis (Figure 53). Interestingly, the 4T1 cell line exhibited higher levels of 5T4 than either CT26 or LLC1 cell lines. Epithelial cells extracted from the large intestine of *Apc*$^{fl/fl}$ mice (treated with tamoxifen) expressed 5T4 to similar levels as LLC1 cells.

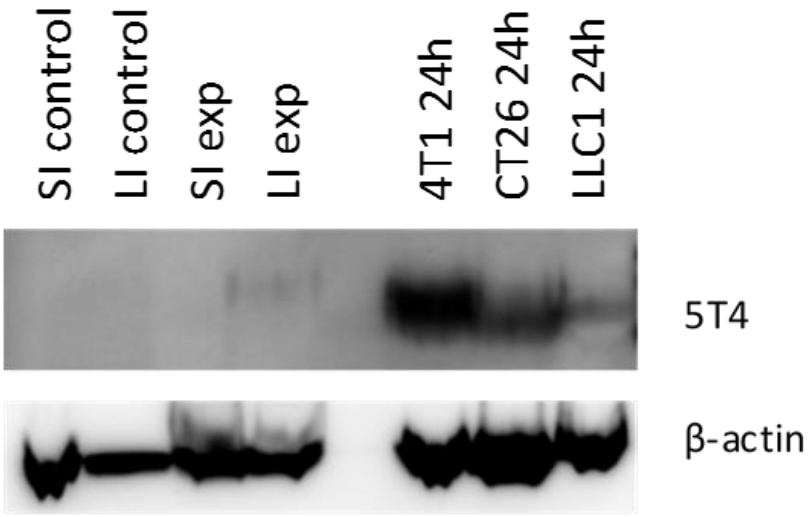

Figure 53: Mouse cancer models/cells expressing 5T4 . Small and large intestine samples from *Apc*$^{fl/fl}$ mice were obtained from Lee Parry. Small intestine (SI) and large intestine (LI) control samples were isolated from control mice whilst SI and LI exp represent experimental samples from mice treated with tamoxifen resulting in deletion of APC in the intestine, thus leading to cancer progression. Prior to lysis, the cells were sonicated for 30s. 4T1 (mammary carcinoma) and CT26 (colon carcinoma) cells were kindly provided by Awen Gallimore whereas Lewis lung carcinoma (LLC1) cells were purchased from ATCC. 250,000 cells were incubated in relevant media for 24h hours at 37˚C 5% CO_2. β-actin serves as a loading control.

3.3.3. Mapping 5T4 epitopes in C57BL/6 mice

In order to track $CD8^+$ T cell responses following immunisation, a strategy was devised to map 5T4 peptide antigens presented in the C57BL/6 mouse model. Mice were immunised with either the AdZ-h5T4 or the control vector, then boosted after 6 weeks to stimulate a memory response. A week later, splenocytes were isolated and stimulated with whole 5T4 protein (Figure 54 panel A) in an Enzyme-Linked ImmunoSpot (ELISpot) assay. Since responses to whole 5T4 protein were low, I also tried stimulating the cells with thirteen peptide pools spanning the entire 5T4 protein (Figure 54 panel B). As expected, shorter peptides that do not require processing were more immunogenic. Peptide pools 1, 2, 5, 6, 8, 9 and 11 were identified as positive hits. By using the matrix system (Table 13) and the peptide prediction program NetMHC 3.4, I was able to identify the following 9mer peptides as strong binding candidates: VSFRNLTHL; NSLVSLTYV; SAPSPLVEL and TSYVFLGIV. To verify 5T4 candidate epitopes predicted by NetMHC 3.4, splenocytes were stimulated overnight and IFN-γ release was quantified and compared for each peptide (Figure 54 panel C). All of the peptides induced responses higher than the positive control (PHA), thus confirming the previous prediction.

While mapping the 5T4 epitopes progressed, it was considered prudent to sequence the adenovirus constructs used in the studies. This analysis revealed an in-frame 81 bp deletion in the *5T4* gene. This deletion surrounded a short region of homology within the gene, suggesting that it could have been deleted by homologous recombination, during recombineering. AdZ-5T4 and AdZ2-5T4 viruses were therefore re-generated, this time using a codon-optimized *5T4* gene to minimize internal homology. In addition to re-mapping the epitopes, I also wanted to compare 5T4-induced immune responses to our first and second-generation vectors. By deleting E4 sequences, the second-generation replication-deficient Ad vectors were developed to reduce the level of breakthrough early and late gene expression from the vector *in vivo* and thus be less inflammatory. Previous data from our laboratory (unpublished) showed that AdZ2 does not induce stress ligands recognised by NK cells on the cell surface, to the same extent as AdZ. The lower induction of stress ligands by AdZ2 had the potential to alter immunogenicity, either by promoting vector persistence, or by reducing NK activation. I was interested in how the altered backbone of the AdZ2 impacted its utility as a vaccination agent.

Sixteen C57BL/6 mice were vaccinated with newly generated first- and second-generation control and 5T4 Ad vectors. A week after the boost, splenocytes were stimulated overnight with one of VSFRNLTHL, NSLVSLTYV, SAPSPLVEL, TSYVFLGIV peptides or a random peptide pool and then IFN-γ production was used as a readout of positive responses. Although 5T4-specific responses were variable, 3/4 peptides induced T cell activation and high IFN-γ production (Figure 55 B). The negative control AdZ-CTRL and AdZ2-CTRL injected mice did not induce 5T4-specific responses (Figure 55 A). There was also no obvious difference in the magnitude of the 5T4 responses induced by the two types (first- and second-generation) of vectors. On the basis of this finding, further investigations were restricted to the more extensively studied first-generation Ad vector (AdZ).

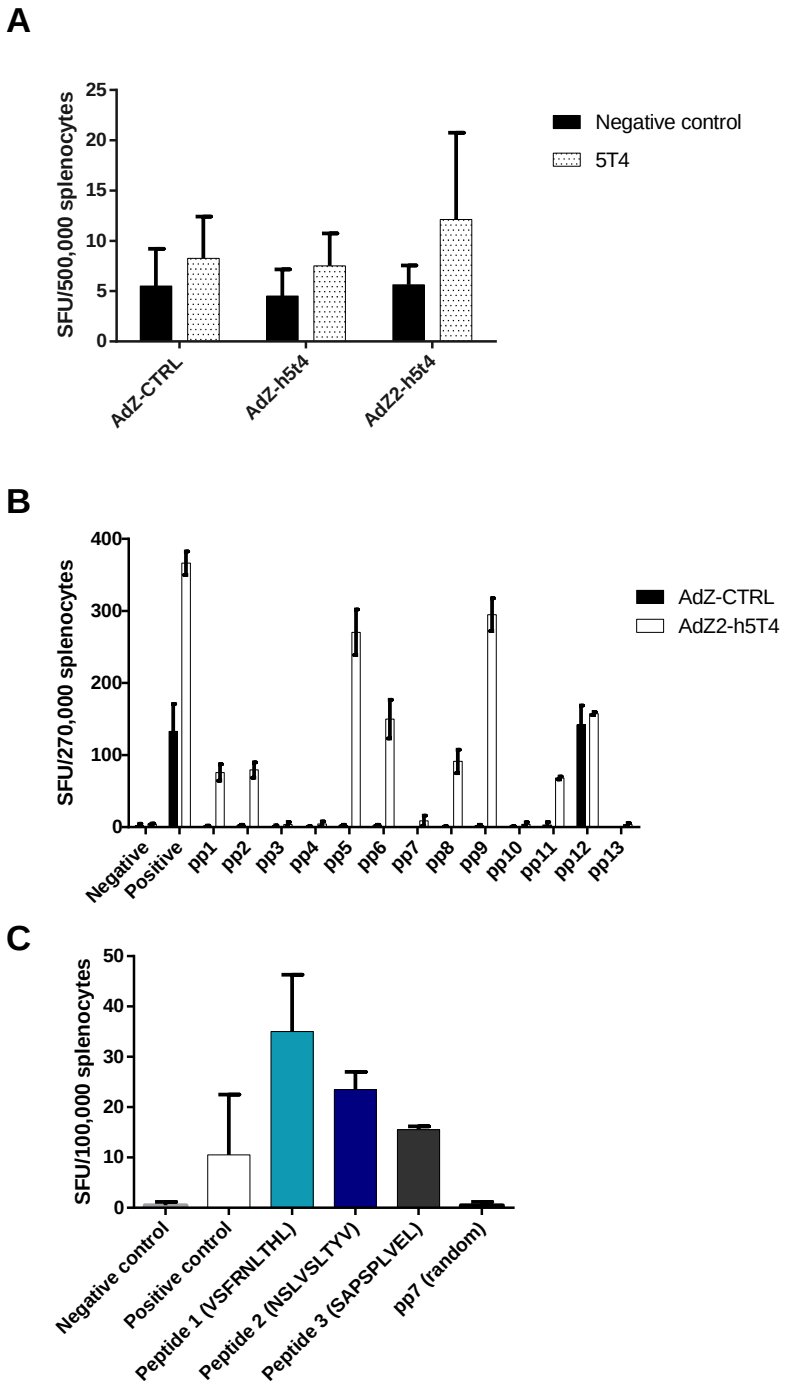

Figure 54: *Ex vivo* IFN-γ responses to 5T4 peptides. A: 500,000 mouse splenocytes were stimulated with whole 5T4 protein (10 µg/ml) overnight. B: 270,000 splenocytes from mice injected with either AdZ-CTRL or AdZ2-h5T4 were incubated overnight with 5T4 peptide pools spanning the entire protein. C: 100,000 splenocytes from a mouse injected with AdZ2-h5T4 were stimulated with 5T4 peptides at 5 µg/ml for 24 h. Peptide pool 7 and RPMI (supplemented with 10% FBS) were used as a negative and 1 µg of phytohemagglutinin (PHA) served as a positive control. Data represent the mean of duplicate samples ± SD. Responses are shown as the number of spot forming units (SFU) per well.

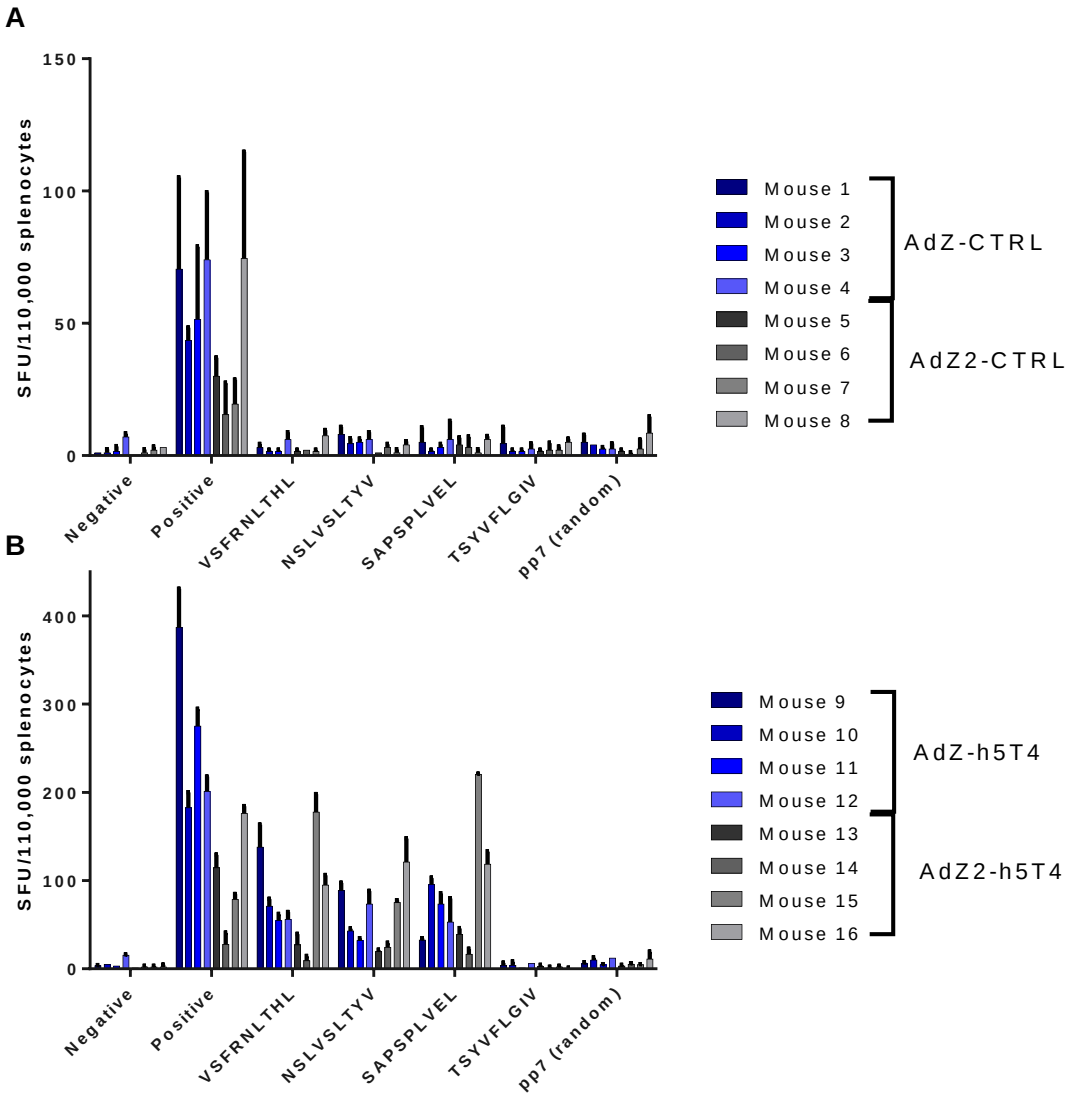

Figure 55: Recombinant first- and second-generation Ad-h5T4 vectors are immunogenic in C57BL/6 mice. 110,000 splenocytes isolated from mice vaccinated with AdZ-CTRL (mouse 1-4), AdZ2-CTRL (mouse 5-8), AdZ-h5T4 (mouse 9-12) and AdZ2-h5T4 (mouse 13-16) were stimulated overnight with 5 µg/ml of 5T4 peptides. For the negative control RPMI (supplemented with 5% FBS) was used whereas for the positive control it was 1 µg of PHA. Each response/mouse is represented as a mean of duplicate samples ± SD. IFN-γ release was quantified and is presented as spot forming unit (SFU) per well.

3.3.4. MHC restriction of 5T4 epitopes in C57BL/6

Using the ELISpot assay, I was able to identify 5T4 epitopes, however, the assay does not provide information as to which of the MHC alleles are involved in the T cell response induced. According to the NetMHC 3.4 epitope prediction program, two of the identified 5T4 epitopes (NSLVSLTYV and SAPSPLVEL) may be presented to T cells by H-2D^b molecule, TSYVFLGIV may be presented by H-2 K^b, whereas VSFRNLTHL may be presented by either/both. To test these predictions, a stability assay was carried out using T2 lymphocytes that had been transfected with either K^b or D^b molecules. T2 cells are a human lymphoblast line that is class II MHC antigen-deficient and lacks TAP that is involved in delivering peptides from the cytosol into ER or Golgi. T2 cells therefore express low amounts of MHC on the cell surface, until a peptide is added and binds to the MHC class I complex, thereby stabilizing it. Peptide dissociation rates greater than 3 hours indicate that a peptide is a promising T cell epitope (Burshtyn & Barber 1993; van der Burg et al. 1996; Peter et al. 2001).

T-2K^b and T-2D^b cells were pulsed with the four peptides at 37°C for 0, 2 and 4 hours and the ability of the peptides to stabilize H-2K^b and H-2D^b was compared to a characterized peptide (KAVYNFATC), known to bind both K^b and D^b complexes, by FACS. My results (Figure 56 A) confirmed the prediction generated by NetMHC; TSYVFLGIV stabilizes cell surface expression of H-2K^b as it quickly binds and remains relatively stable over the 4-hour period with half-life greater than 4 hours. The remaining three peptides (VSFRNLTHL, NSLVSLTYV and SAPSPLVEL) do bind Kb, and P1 binding was relatively stable. P2 and P3 complexes were less stable and dissociated quickly. D^b data (Figure 56 B), on the other hand, was in disagreement with the prediction program. However, since I could not detect any binding of my positive control peptide, even after an experimental repeat, I concluded that the cells may have lost the plasmid encoding the D^b complex. I was unfortunately unable to obtain fresh aliquots of the T-2D^b cells within the timeframe of this study.

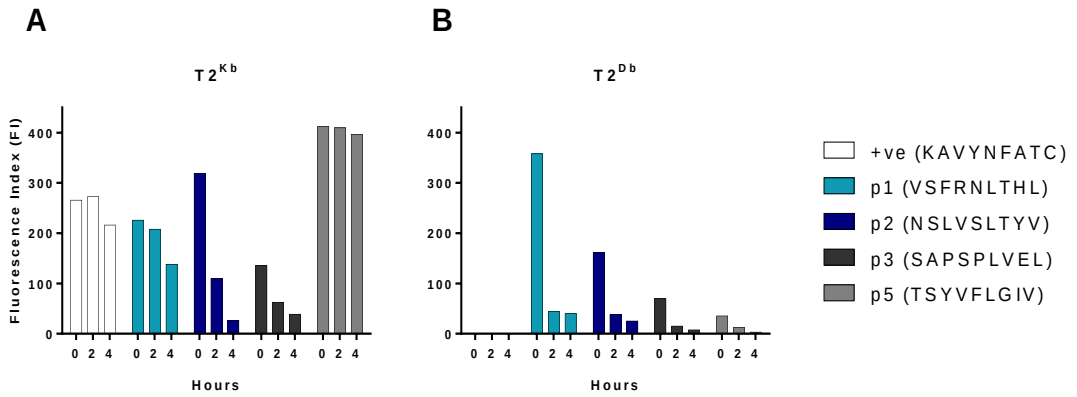

Figure 56: Binding and stability of K^b/peptide and D^b/peptide complexes. 400,000 T2-K^b and T2-D^b cells were incubated with 20 µM peptide for 0, 2 or 4 hours. At each time point, the cells were thoroughly washed with ice-cold PBS and stained for D^b or K^b molecules. Fluorescence index (FI) was calculated using the following formula: FI= (mean fluorescence sample – mean fluorescence background)/(mean fluorescence with no peptide – mean fluorescence background). KAVYNFATC peptide was used as a positive control as it is known to bind both K^b and D^b molecules.

3.3.5. Effect of vaccination with Ad-h5T4 on tumorigenesis in Lewis lung carcinoma (LLC) model

To establish the LLC1 tumour model, it was necessary first to determine the dosage of cells required to induce a gradual growth of subcutaneous tumours. In a survey of the literature, the route of tumour cell injection was highly variable and included intravenous injections, intratracheal instillations and subcutaneous intrascapular regions (Bertram & Janik 1980; Reppert et al. 2011; Savai et al. 2009). In addition to this, the dosage also varied between 5×10^4-10^6 cells per mouse (Bertram & Janik 1980; Reppert et al. 2011; Savai et al. 2009). In our model, we wanted to implant LLC1 cells subcutaneously into the left flank as we have done for all of our other cancer models. Based on other people's work, three different concentrations were selected: 10^5, 2×10^5 and 4×10^5 cells. Tumour growth in mice was monitored 3 times a week and once tumours were palpable, the growth rates were compared between different groups. Mice receiving 10^5 cells did not all develop tumours even at 20 days post challenge (Figure 57). Although mice receiving the highest dose all developed tumours, the rate of growth was too rapid, depriving the surrounding cells of oxygen and reaching the size constraints set by the Home Office, resulting in sacrifice of mice. Since 2×10^5 dose was sufficient to induce tumour growth in all the tested animals at a steady rate, it was used in future experiments.

Peptide mapping demonstrated that immunisation with Ad vectors encoding 5T4 induces an efficient T cell response specific for the expressed oncofoetal antigen in C57BL/6 mice (see previous section). To test the efficacy of the Ad recombinants in the LLC1 cancer model, the mice were immunized 6 weeks apart with 5×10^8 PFU of either AdZ-CTRL or AdZ-h5T4. In addition to this, a naïve control group was also included that did not receive anything. After the first Ad injection, the weight of the mice was monitored (Figure 58 A) as weight loss would indicate vaccine-induced illness. Since the weight of Ad-injected mice was comparable to naïve mice and exceeded the starting weight, monitoring was halted at 3 days post-injection and I concluded that these vectors were safe. At 7 weeks (1 week after the boost) all of the mice received 2×10^5 LLC1 cells. Tumour formation was monitored 3 times a week. The first tumour growth was observed at 7 days post challenge (Figure 58 B). Surprisingly, mice that received AdZ-h5T4 developed tumours more rapidly than ones immunized with AdZ-CTRL. In addition to this, naïve mice had delayed tumour growth. These results were not reflected in the survival data (Figure 58 C) as the majority of the mice needed to

be sacrificed due to Home Office regulations. The mice developed tumours that had a crater-like appearance and red discharge. Comparison of the spleen sizes showed that mice injected with AdZ-h5T4 had smaller spleens than the other two groups (Figure 58 D).

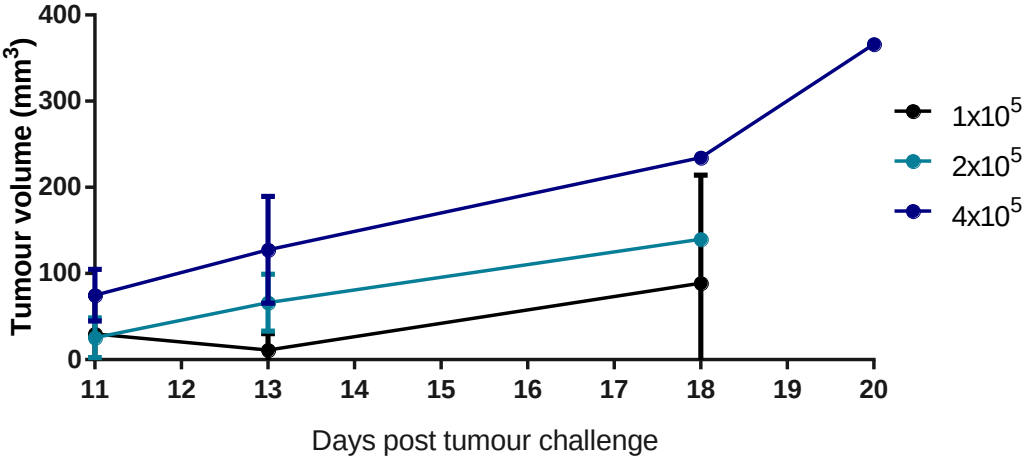

Figure 57: LLC1 tumour growth rate dependency on tumour cell dose. C57BL/6 mice were subcutaneously challenged with either 1×10^5, 2×10^5 or 4×10^5 of LLC1 cells and tumour development was monitored weekly. Values represent average of 4-5 mice ± SD. Tumour sizes were measured with a caliper and tumour volume was calculated using the following formula: (mm^2) = width × length × smaller value (width or length) × (3.14⁄6).

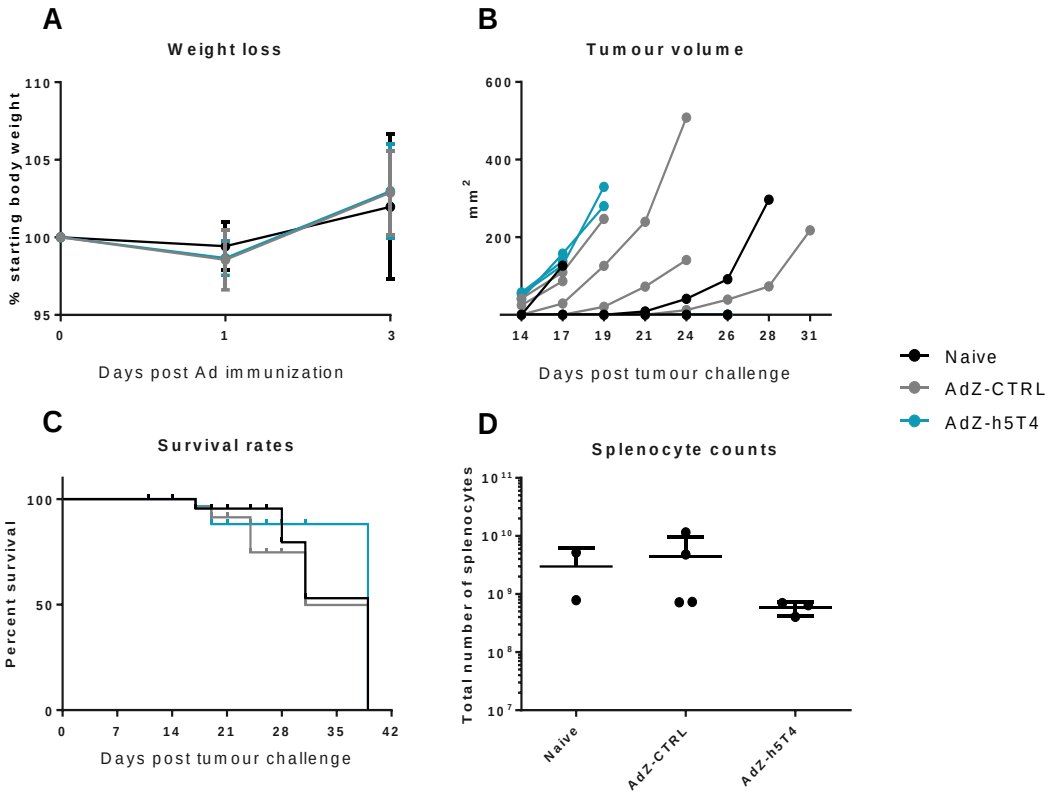

Figure 58: AdZ-h5T4 is safe but not protective in the LLC1 cancer model. A: Weight loss induced by immunization with Ad vectors. Weight loss is expressed as mean ±SD (4-6 mice/group) of percent of starting weight. B: Tumour volume was calculated using the following formula: (mm^2) = width × length × smaller value (width or length) × (3.14⁄6). C: Survival rates for naïve mice, mice immunized with AdZ-CTRL and AdZ-h5T4 challenged with LLC1 tumours. D: Myeloid cell numbers in the spleen quantified and are shown as mean ±SD of four-six mice per group.

3.3.6. Responses to first-generation Ad5 vs second-generation Ad5 in BALB/c mice

Two of the cancer models (4T1 and CT26) that I wanted to study were in BALB/c mice strain therefore the 5T4 epitopes identified in C57BL/6 would not be relevant. To see whether Ad vectors encoding 5T4 were also immunogenic in BALB/c mice, the same procedure was performed whereby mice were primed then boosted mice with 5×10^8 PFU six weeks apart. First- and second-generation Ad vectors were used for a comparison. A week later, splenocytes from these mice were isolated and I used them to perform an ELISpot assay. Interestingly, the results (Figure 59 and Figure 60) showed that first-generation Ad vectors induced relatively stronger responses as both peptide pool 2 and 3 had more spot forming units (SFU). As a result, we opted for first-generation vectors in preclinical tumour protection models. The peptide pools 1, 2, 3, 7, 9 and 10 were identified as positive hits and a prediction program NetMHC 3.4 identified four candidate peptide epitopes (data not shown) from these panels (LSHNPLADL, RGPAAGDGR, GGCSRGPAA and RSFEGMVVAALLAGR). The synthesized peptides were then tested using the remaining splenocytes from the same experiment, however, responses were weak and variable as compared to the positive control suggesting that 5T4 is less immunogenic in BALB/c mice.

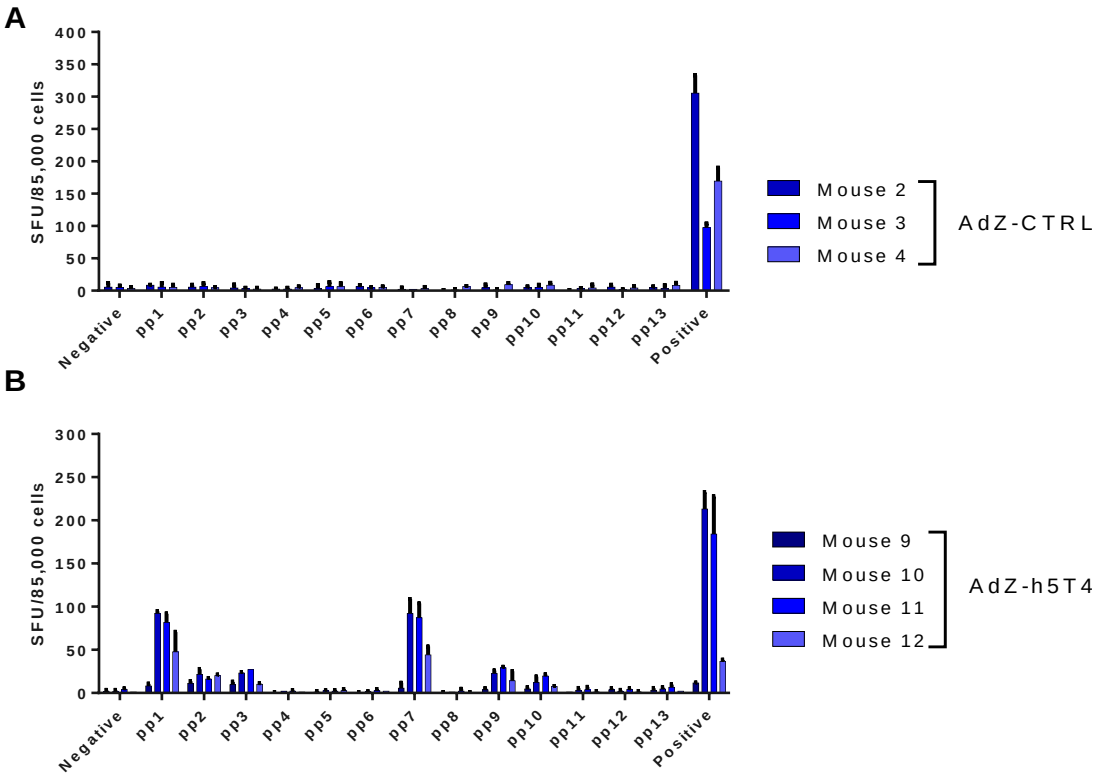

Figure 59: AdZ-h5T4 induces 5T4-specific responses in BALB/c mice . 85,000 splenocytes extracted from mice vaccinated with AdZ-CTRL (mouse 2-4) and AdZ-5T4 (mouse 9-12) were stimulated overnight with 5T4 peptide pools (at a concentration of 5 µg/ml/peptide) overlapping the entire 5T4 protein. RPMI (supplemented with 5% FBS) was used as a negative control whereas for the positive control 1 µg of PHA was added to the cells. Each bar represents a response/mouse that is a mean of duplicate samples ±SD. Spot forming unit (SFU) is indicative of a single lymphocyte releasing IFN-γ upon stimulation with 5T4.

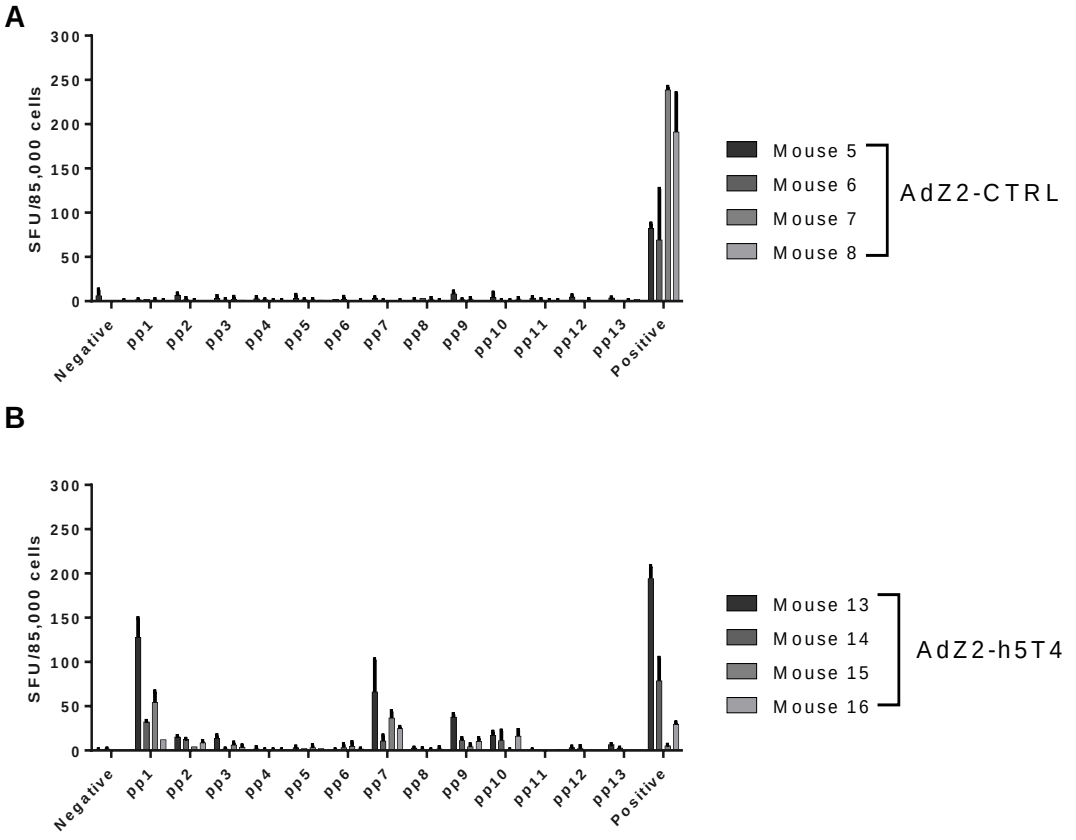

Figure 60: AdZ2-h5T4 is immunogenic in BALB/c mice. 85,000 splenocytes isolated from mice vaccinated with AdZ2-CTRL (mouse 5-8) and AdZ2-h5T4 (mouse 13-16) were stimulated overnight with 5T4 peptide pools (5 µg/ml/peptide) covering the entire 5T4 protein. For the negative control, the cells were incubated with RPMI (supplemented with 5% FBS) whilst for the positive control, 1 µg of PHA was added. Responses are represented as spot forming units (SFU)/well (mean of duplicate samples ±SD).

3.3.7. 4T1 cancer model: Tumour growth in BALB/c mice vaccinated with Ad-h5T4 vectors

Although 5T4 responses induced in BALB/c mice were weak in comparison to responses in C57BL/6, I wanted to see whether they were sufficient to protect mice from tumour challenge with 4T1 cells. The mice in my study received two injections (prime and boost) of either AdZ-CTRL or AdZ-h5T4 six weeks apart. One week later, 10^5 4T1 cancer cells were implanted subcutaneously into the left flank of the animal. Following immunisation with the Ad recombinants, the animals did not lose any weight (Figure 61 A). Palpable tumours started to develop at 7 days post challenge (Figure 61 B) and comparative analysis of the three groups showed that all the mice were developing tumours at a similar rate. I observed a small (statistically insignificant) delay by 4 days in death of naïve mice (Figure 61 C) and no differences were observed when the number of splenocytes was counted between the three groups (Figure 61 D).

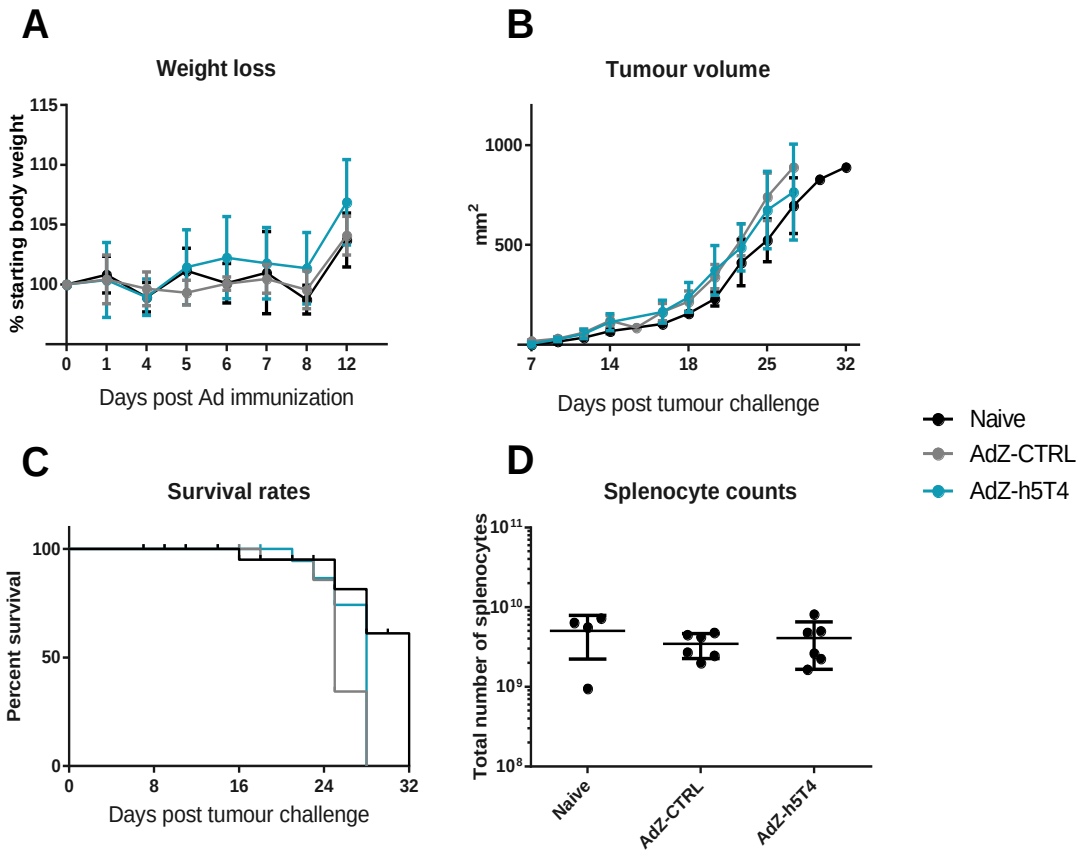

Figure 61: Homologous prime-boost with AdZ-h5T4 does not protect from 4T1 mammary carcinoma model. BALB/c mice were vaccinated twice (day 0 and week 6) with 5×10^8 PFU AdZ-CTRL or AdZ-h5T4.Following the boost,10^5 4T1 cells were subcutaneously implanted into the left flank. Weight loss of naïve mice or mice that received 5×10^8 PFU AdZ-CTRL or AdZ-h5T4 injection represented as mean ±SD (4-6 mice/group) of percent of starting weight (A). Tumour burden in naïve mice and mice prophylactically immunized with AdZ-CTRL or AdZ-h5T4 and challenged with 10^5 4T1 cells a week after the boost (B). Tumours were measured with a caliper and tumour volume was calculated by using the formula: (mm^2) = width × length × smaller value (width or length) × (3.14⁄6). Survival in mice with 4T1 cancer pre-treated with Ad vaccine (C). Splenocyte numbers (D) expressed as mean ±SD of four-six mice per group.

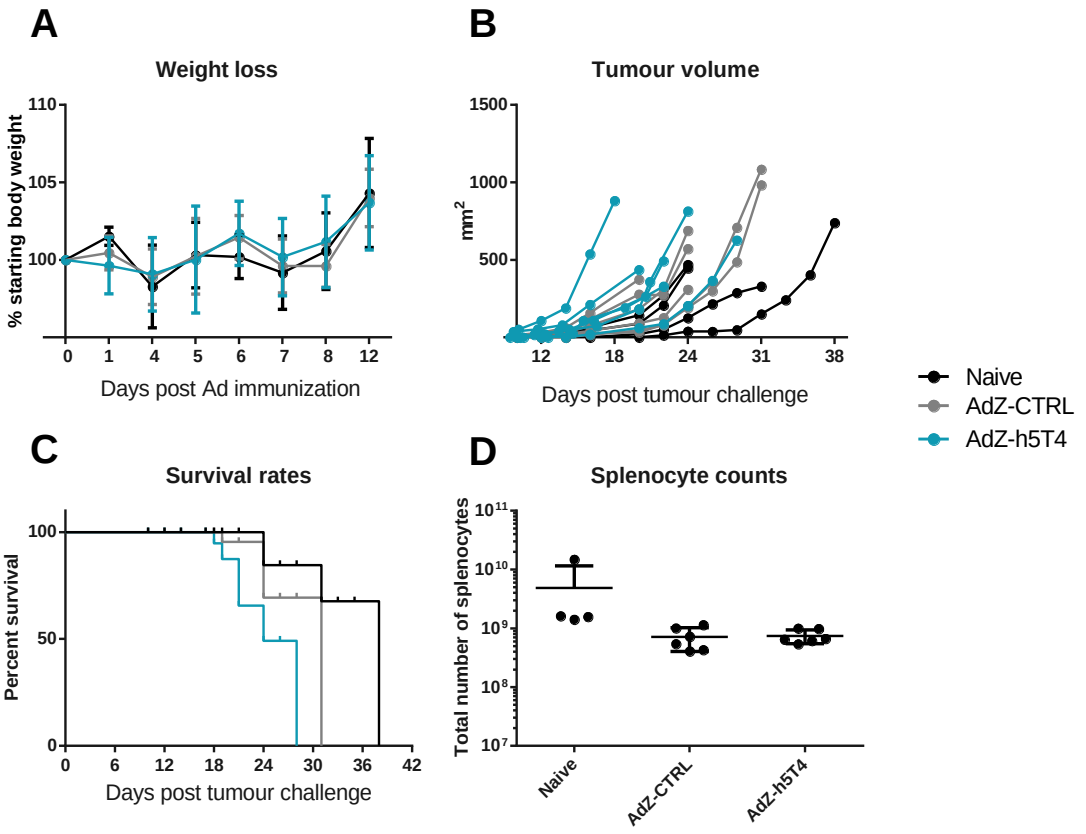

Figure 62: Naïve mice challenged with CT26 colon carcinoma survive longer than mice vaccinated with AdZ-h5T4. .BALB/c mice were vaccinated with 5×10^8 PFU of recombinant adenoviruses twice six weeks apart. A week after the boost, the mice were injected with 10^5 CT26 cells. A: weight loss associated with vector-induced illness expressed as mean ±SD (4-6 mice/group) of percent of starting weight. B: Tumour growth was measured at least 3 times a week using a caliper. Tumour sizes were calculated using the formula (mm^2) = width × length × smaller value (width or length) × (3.14⁄6). C: overall survival of mice challenged with CT26 cells. D: cell numbers in the spleen calculated and shown as mean ±SD of 4-6 mice per group.

3.3.8. CT26 cancer model: Tumour growth in BALB/c mice vaccinated with Ad-h5T4 vectors

In addition to the 4T1 model, I also wanted to test the prophylactic effect of my Ad-h5T4 vector in a colon cancer model setting. As with the other cancer models, BALB/c mice were immunized with the Ads six weeks apart. On week 7 they were challenged with 10^5 CT26 cells. Vaccination with Ad vectors resulted in slight weight loss (Figure 62A) on day 4, however by day 6 all of the mice had recovered. Tumour development was first observed at 10 days post tumour challenge. Interestingly, the naïve mice remained disease-free longer (Figure 62B) than mice injected with AdZ-CTRL or AdZ-h5T4. In addition to this, I observed prolonged survival (Figure 62C) in naïve mice which was statistically significant. In a repeat experiment, however, I did not see any differences in survival rates of mice injected with AdZ-CTRL or AdZ-h5T4. However, the repeat experiment did not include a naïve control, therefore the significance of the naïve group cannot be entirely dismissed. Comparison of the sizes of the spleens showed that they were highly variable, however spleens in naïve mice were larger than those in mice injected with AdZ-CTRL or AdZ-h5T4 (Figure 62D).

3.3.9. Summary

I identified 5T4 epitopes in C57BL/6 mice and compared 5T4 expression in four different cells and tissues (4T1, CT26, LLC1 and intestine from *Apc*$^{fl/fl}$ mice). 5T4 immune responses in BALB/c mice were weaker than C57BL/6, therefore, I could not confirm individual epitopes in this mouse strain. Although the adenovirus vectors I generated encoding 5T4 expressed high levels of this antigen, prophylactic immunization of BALB/c and C57BL/6 strains did not induce tumour rejection or improve overall survival.

Chapter 4 Discussion

4.1. Generation and analysis of conditionally replicating CMV *in vitro*

4.1.1. Conditional expression systems in the literature

In this work, I attempted to generate conditionally replicating viruses whereby gene expression induced by a chemical agent would enable replication to occur. Previous studies have shown that conditional replication can be induced in different ways. One of the most established systems called Cre-lox recombination system consists of Cre recombinase enzyme and loxP splice sites that Cre recombinase binds to (Nagy 2000). LoxP sites flanking a gene of interest are recognized by the enzyme and cleaved, thus resulting in deletion of the flanked gene. Analogous systems such as flippase- flippase recognition target (FLP-FRT) have been based on the Cre-lox recombination system and work in a similar way (Lacroix et al. 2011). To establish temporal control of the protein of interest, Cre recombinase may be placed under the control of tissue-specific promoters (e.g. endothelial cell-specific Flt-1 promoter) and inducible promoters (interferon-inducible Mx dynamin-like GTPase 1 promoter or steroid-regulated promoters fused to ecdysone and oestrogen receptors). Cre-recombinase system has been previously used in the context of CMV to study virus spread *in vivo* (Sacher et al. 2012). In that study, they inserted LoxP sites together with eGFP under the control of HCMV MIE promoter into an MCMV reporter virus. Infection of Cre mice allowed the investigators to study virus dissemination in cre-expressing tissues.

Another strategy to achieve temporal protein expression is by fusing a destabilising domain (dd) (e.g. FK506 binding protein (FKBP) derived) to an essential virus gene that results in stable gene expression only in the presence of a stabilising ligand such as shield-1 or guard-1 (Banaszynski et al. 2006). This degron-based technology is highly-specific, non-toxic and has been tested both *in vitro* and *in vivo.* Although the safety and biodistribution of shield-1 has not yet been tested in humans, it has been shown to be safe in mice (Banaszynski et al. 2008). A structurally similar FKBP ligand (AP1903) to Shield-1, however, has shown safety in a human phase I dose study (Iuliucci et al. 2001). In addition to this, a well-established ligand (trimethoprim; TMP), has been used by Iwamoto *et al* together with dd from *E.coli* dihydrofolate reductase and showed regulation of yellow fluorescent protein levels (Iwamoto et al. 2010). TMP

is an antibiotic with a well characterized safety profile in humans. Fusion of ddFKBP to immediate early genes IE1/IE2 and IE1/IE3 in both HCMV and MCMV, respectively, has been shown to result in tight regulation of virus replication that was shield-1-dependent (Glass et al. 2009). In addition to this, escape mutants were not selected during the course of the study.

The most interesting results, when generating conditionally replicating viruses, however, have been obtained using a tetracycline-based approach (Tet-On) in Benjamin Berkhout's lab. In an attempt to generate conditionally replicating HIV-1 virus vector, the accessory Nef gene of the virus was replaced with rtTA whereas eight tetO sequences were placed in the long terminal repeat (LTR) region (Das & Berkhout 2016). Due to the high mutation rate of HIV-1, the viruses did accumulate mutations that resulted in loss of six tetO sequences as well as an adaptation of more active rtTA variants. Interestingly, the loss of tetO did not lead to less efficient virus replication and the authors suggest that eight copies of tetO may have impeded a virus replication process. The group identified loss-of-function mutations in the rtTA and developed a safety lock where they introduced amino acid changes that would prevent virus mutations, as the mutations would need to be more complex (i.e. purine to pyrimidine and vice versa). Further development of the vector led to mutagenesis (mutations identified in a resistant virus variant) of the Env gene making replication-dependent on an additional chemical (entry inhibitor enfuvirtide; T20) (Das & Berkhout 2016). The HIV-1 vectors generated could thus be more strictly controlled as their replication was dependent on two drugs.

All of the aforementioned conditional systems have been used in virus vectors to provide inducible gene expression and ensure safety. Since the virus I am working on (CMV) is linked to disease, I wanted to develop it in a way that would make it safe in the population but also induce immune responses similar to WT virus.

4.1.2. *In vitro* analysis of M50-1 and SCP-GFP conditional Tet-On viruses

TetR-based technology has been previously used to generate conditional MCMV vectors (Rupp et al. 2005). Rupp *et al,* used the Smith MCMV strain and regulated expression of either the M50 gene (only replicates in the presence of DOX) or a small capsid protein (dominant-negative mutant, replication is inhibited in the presence of

DOX). *In vitro*, the M50-1 virus replication was regulated by 1000-fold whereas SCP-GFP-regulated virus by 100-1,000,000-fold. Interestingly, when I tested these two viruses *in vitro*, M50-1 was inhibited by 14-fold whereas for SCP-GFP it was 211-fold. It is noteworthy, however, that the purification protocol in the paper entailed additional steps to remove any traces of DOX (e.g. pelleting the viruses at 23,450 × g for 3 h, ultracentrifugation step over a 15% sucrose cushion and purification using an OptiPrep gradient). Our standard purification protocol, on the other hand, consisted only of pelleting the viruses at 21,612 × g for 1h 40 min followed by centrifugation over 20% sorbitol cushion. In addition to this, the differences in the control of virus replication observed by Koszinowski's group were highly variable between different cell types and in their work, they used mouse embryonic fibroblasts (MEFs) whereas all of my *in vitro* experiments were carried out in a different fibroblast cell line (NIH 3T3). Finally, numerous sources recommend using tetracycline-free FBS whilst culturing the cells to reduce the leakiness of the system. Members in the lab have tested our FBS batch with adenovirus vectors encoding tetR-regulated GFP and showed that in the absence of DOX, GFP expression was not relieved, thus suggesting that tetracycline in the FBS was not present/at low levels. Although it is not stated in Rupp *et al* whether tetracycline-free FBS was used, it could have enhanced the difference in DOX-free condition (Rupp et al. 2005). When I performed plaque assays using SCP-GFP and M50-1 viruses, I showed that the cell-cell spread of these viruses was barely affected by the addition/removal of DOX, whereas cell-free virus spread was better controlled. In comparison, my K181-based viruses showed good control of both cell-free and cell-cell spread. One possibility is that M50-1 and SCP-GFP have genetic differences that result in a lower efficiency of cell-cell spread to start with. However, since there are numerous differences between the virus strain used in M50/SCP, and my K181-based constructs, it is difficult to know whether this is the case. Importantly, however, more M50-1 virus genome copies were detected in mouse tissues than my most promising virus (M_{RSV}2M100-tetR-P2A-M36) thus suggesting that M50-1 vector is not as safe *in vivo* as my vaccine vectors.

4.1.3. Generation of TREx vectors

4.1.3.1. Promoter expression

By using the TREx system I generated 31 HCMV and 30 MCMV BACs. The *tetR* gene was placed under control of one of three different promoters. To minimize the chance

of homologous recombination with native promoters, the HCMV IE promoter was used in the MCMV vectors and vice versa. The promoters in this study were selected on the basis that they were strong and have been widely used in vector development. Both of the CMV promoters contain powerful enhancers. Interestingly, the MCMV enhancer is bidirectional whereas HCMV enhancer is unidirectional (Keil et al. 1987). In addition to the CMV MIE promoter I also tested expression by the SV40 and RSV promoters. Although I tested three different promoters in HCMV as well as MCMV vectors, only the RSV promoter showed efficient expression of tetR protein in both vectors. Interestingly, expression driven by RSV appeared earlier in human fibroblasts than in mouse fibroblasts. This difference in expression is likely due to the fact that the RSV promoter is more adapted to human cells. The lack of expression observed for the SV40 promoter in both HCMV and MCMV vector was surprising. Although the length and sequence of my SV40 promoter was identical to that used in other vectors, some SV40 promoters in the literature were longer and may have contained regions necessary for better expression in my CMV vectors. It is also possible that CMV modulates transcription factors required for SV40 promoter expression. I was surprised to see that the HCMV vector encoding the MCMV IE promoter did not express any detectable tetR levels. The MCMV ie promoter is a well-established promoter and widely used in gene cloning. To design my vectors I used a sequence previously published in (Chatellard et al. 2007). One possible explanation is that during virus stock preparation, homologous recombination occurred within the virus backbone that did not affect virus replication but affected the promoter itself.

The majority of promoters used in molecular biology show comparable levels of transgene expression in different cell types. The CMV promoter, however has been shown to be the most variable displaying varying strength in regulation in different cell types (Qin et al. 2010). The EF1-α promoter, on the other hand, induces strong expression without major fluctuations in different cell types (Qin et al. 2010). I tried inserting this promoter into my vectors, however, the second round of recombineering was problematic. Not only was the efficacy of the insertion of the promoter low, the promoter was not inserted in the colonies sequenced even after numerous attempts.

The most important conclusion from the use of different promoters however, was that the tightest control of viral expression was achieved by the M_{RSV}2M100-tetR-P2A-M36 vector. This suggests that the use of an endogenous viral promoter, that expresses at

IE times, is the best candidate for rapid and high expression of regulatory proteins that can control virus growth. It is noteworthy that although the exogenous promoters rarely produced detectable protein by 24h, pUL36 is detectable by 6h, reaches a maximum after just 18h, and is one of the most abundant proteins during infection (Weekes et al. 2014). By inserting a second copy at the end of M36 (a UL36 homologue in MCMV) I showed that vectors containing two copies of *tetR* were inhibited more in the absence of DOX than vectors containing a single *tetR*, thus suggesting that the level of tetR is crucial to reducing background expression of gene of interest in the absence of DOX, and M36 endogenous promoter is able to provide early and strong tetR expression.

4.1.4. TetR-based vector growth *in vitro*

It is interesting to note that although all of the HCMV viruses produced infectious virions, four MCMV BACs did not. These four BACs (M_{SV40}1M44, M_{SV40}2M44, M_{SV40}1M75 and M_{SV40}2M75) all contained SV40 promoters which is surprising, considering the fact that I could not observe any tetR expression from this promoter in the parental vector (M_{SV40}) which only contains tetR and no tetO. The four viruses contained tetO upstream of M44 and M75 (gH), however this placement of tetO still gave viable virus in combination with other promoters driving tetR expression. We have occasionally observed the insertion of transposons into BACs during recombineering (Murrell et al. 2016). It is possible that such an insertion occurred in an essential region of the genome of these viruses, or that other unintended recombination events had occurred that prevented virus replication.

When virus dissemination was tested in the absence and presence of DOX, HCMV viruses were more likely to be inhibited than MCMV viruses. In H_{RSV}2UL54, H_{MCMVie}2UL75 and H_{RSV}1UL123 (Table 17) plaques were all inhibited in the absence of DOX whereas nearly all MCMV virions grew similarly (Table 18) in both conditions. However, when the viruses were tested in plaque assay conditions whereby cells were overlaid with semi-solid media, MCMV viruses were inhibited more stringently than HCMV viruses. During replication in cells without an overlay, the viruses would thus use both cell-cell and cell-free spread methods. These results may indicate differential reliance of each virus on cell-cell as opposed to cell-free spread. Clinically, cell-cell spread of the virus plays a role in intra-host virus dissemination whilst cell-free release is more crucial for inter-host spread. Cell-free release may thus play a more significant role in ensuring safety of a vaccine in the population. Another possible explanation for

differences in HCMV and MCMV spread is the purification method used to purify HCMV, since it did not include a sorbitol cushion step, which could have left low traces of DOX.

I also observed more efficient spread of virus in fibroblasts expressing tetR, as opposed to the parental fibroblasts, for the majority of HCMV and MCMV viruses, irrespective of the presence or absence of DOX. During the production stages of tetR expressing fibroblasts, cell clones enabling more efficient virus replication may have been selected. Nevertheless, my *in vitro* analysis of the vectors showed that MCMV vectors containing tetO upstream of M100 (gM) and HCMV vectors with inducible UL123 (IE1) expression could be controlled in a conditional manner. The majority of MCMV and HCMV vectors, however, were not DOX-dependent and replicated irrespective of DOX in the media. It is possible that this variation in how controllable gene expression was, resulted from differences in promoter structures. In previous work by Stanton, not only was the positioning of tetO sequences essential to the level of control of gene expression, but it also depended on the copy number of tetO, and this can be gene-dependent (Stanton et al. 2010). Nevertheless, it appeared from Stanton *et al* that placing tetO approximately 20bp upstream of the ATG worked well. My work shows that this is not necessarily the case, and the positioning of tetO for each candidate gene needs to be tested individually, a single rule does not apply to every gene. It is possible that targeting of IE1 and gM in HCMV and MCMV, respectively, may be improved further by adjusting the location of tetO sequence inserted.

4.1.5. Stability of tetR-based vectors *in vitro*

To determine whether propagation of my tetR-regulated viruses in the absence of DOX selected for escape mutants, I sent samples to be sequenced. Previous work with the Smith MCMV strain showed that MCMV genome, unlike HCMV (Dargan et al. 2010; Murrell et al. 2016), is stable *in vitro* and only mutated in m09 gene and a non-coding region, thus the mutation rate of the virus is 1.4×10^{-7}/bp/day (Cheng et al. 2010). In addition to this, comparison of $K181^{Perth}$ and $K181^{Birmingham}$ variants have shown that although the two viruses had been passaged for thirty years, they only differed in 13 nucleotides (Timoshenko et al. 2009). However, by passaging M_{RSV}2M100-tetR-P2A-M36 *in vitro*, I was able to select out a mutant that grew well even in the absence of DOX. Sequencing revealed that one of the copies of *tetR* had a 5 bp deletion,

presumably making the protein non-functional. Whether this would also occur *in vivo* is currently unknown, however an activation system such as Tet-On could reduce this problem. Since Tet-On is an activation system, any mutations in the rtTA would mean that the virus would not be able to replicate in the presence of DOX thus making the virus vector safer. As shown by Berkhout *et al*, rtTA can mutate, however, they used HIV-1 as a vector which is an RNA virus with notably higher rate of mutation (4.1 ± 1.7) $\times 10^{-3}$/base/cell *in vivo*) across the whole genome than CMV (Cuevas et al. 2015). The Tet-On regulatory system is unlikely to mutate as rapidly in the CMV vector and insertion of multiple copies (as in this study) or the use of safety lock nucleotide changes would diminish the likelihood of spontaneous mutations and escape mutants (Das & Berkhout 2016).

The M_{RSV}2M100-tetR-P2A-M36 virus we sequenced had also mutated in M70 and m139 genes. M70 is the viral helicase/primase protein whereas m139 contains an inflationary epitope in C57BL/6 mice and plays a role in mediating viral replication in macrophages and spleen. It would not be surprising to see such mutations in viruses isolated from *in vivo* studies, as escape mutants may mutate in genes that would facilitate DNA synthesis or in immunogenic epitopes that may be presented to T cells. It is interesting to note that a group in Birmingham have identified mutations in a temperature sensitive K181 (Birmingham) variant generated by exposing the virus to *N*-methyl-*N*'-nitro-*N*-nitrosoguanidine (NTG) and two of the genes that had mutated were M70 and m139 (Timoshenko et al. 2009). The selective pressure under which these viruses mutated in these two genes was different, however, and more studies need to be carried out to understand the stability of different MCMV strains.

4.1.6. Comparison of WT FRT Smith strain to previously published sequences

We sequenced WT FRT MCMV to determine whether any mutations had arisen whilst generating virus stocks. Sequence alignment to the most recently published WT Smith strain (GU305914.1) showed that the two viruses shared 99.5% similarity, however, frameshift disruptions were found in m01, m03, m59, m150 and m161 genes (Cheng et al. 2010). In order to see whether the virus sequence matched better to that sequenced by a different group, I aligned the WT FRT sequence to a sequence (U68299) published by Rawlinson and others (Rawlinson et al. 1996). Surprisingly, the sequence was more similar (99.78%) but contained more frameshift-disrupting

mutations (m20, m29.1, m30, m31, m45.1, m58, m129, m143, m150 and m161), most of the disrupted genes being at the genomic termini. Interestingly, Smith *et al.,* have hypothesized that the Smith strain sequenced by Cheng and others may be a recombinant variant of the Smith and K181 virus strains (Smith et al. 2013). In addition to this, the Smith virus sequenced by Cheng *et al* had been propagated *in vitro* for longer and therefore may have selected for adaptive mutations. Two plaque purification steps prior to sequencing may have resulted in selection of a clone that was not representative of the virus. I thus, think Rawlinson's sequence is a more accurate representation of our WT FRT sequence.

Work by Alec Redwood's lab have shown that MCMV genomes isolated from wild mice in different parts of Australia had a conserved genome size without major genome rearrangements, insertions or deletions (Smith et al. 2008). Interestingly, 151 ORFs out of 190 displayed >98% amino acid similarity to the Smith strain and most differences were observed in genomic termini. These subtle differences, however, resulted in different replicative capacity in mouse tissues *in vivo*. It is possible that MCMV strains used in different labs around the world are Smith variants that contain mutations and cell culture adaptations, and thus it is important to identify and clone a WT-like ('clinical') MCMV strain into a BAC for use as a reference as has been done for HCMV (Stanton et al. 2010). BAC cloning is crucial for maintaining a stable genomic clone of the virus with minimal chance of recombination.

4.2. *In vivo* characterization of tetracycline-controlled MCMV vectors

4.2.1. Replication-deficient or replication-competent CMV vaccine?

CMV use in vector development has been hindered due to safety concerns, as replication-competent virus has disease associations in immuno-naïve and immunosuppressed individuals. Replication-defective virus, however, may not retain the immunogenicity of WT virus. Several studies have compared replication-competent and incompetent vectors and analysed the immune responses induced. Live-attenuated HCMV containing destabilising domains flanking two target genes replicated selectively in the presence of Shield-1 and proved to be safe in different animal systems (Wang et al. 2016). Analysis of immunogenicity of this CMV vector in multiple animals (mice, rabbits and rhesus macaques) showed induction of $CD4^+$,

$CD8^+$ T cells as well as neutralising antibodies (Wang et al. 2016). It is difficult to compare the breadth of immunogenicity of this vector, however, since the animals tested are not a natural host to the virus, so there is no 'replication competent' vector for comparison. In a different study, a spread-defective MCMV lacking glycoprotein L was compared to WT virus in two mouse strains (BALB/c and C57BL/6). Although ΔgL virus elicited memory inflation in both strains of mice and they followed a similar trend (contraction and maintenance of peptide-specific T cells), the responses were lower than those induced by WT virus, especially in C57BL/6. In BALB/c mice, no IE1/M123 (pp89)-specific responses were detected at 1 or 4 weeks post- injection but they accumulated later during the course of infection. Interestingly, the data showed that in BALB/c and C57BL/6 mice viral antigens were expressed for at least 20 weeks and 36-74 weeks, respectively (Snyder et al. 2011).

In an acute infection, a spread-defective MCMV vector (lacking M94 gene) also elicited strong $CD4^+$, $CD8^+$ responses that were similar to those induced by WT virus (Mohr et al. 2010). The levels of neutralising antibodies induced, on the other hand, were lower than in WT CMV immunized mice. In addition to this, UV-irradiated virus failed to induce any neutralising antibodies. When persistence of virus was analysed in different tissues, viral genomes were found in the lungs a year post infection, thus suggesting that persistent expression of virus antigens facilitated the immune response observed (Mohr et al. 2010). In unpublished data from our own laboratory it has been shown that a WT virus (replication-competent) induces stronger virus-specific immune responses to CMV antigens (m139; M38 and IE3) than a replication-deficient virus ΔgL MCMV in C57BL/6 mice at 7 and 60 days pi. It has been previously shown in the literature by Louis Picker's lab that the use of live-attenuated RhCMV vector encoding SIV antigen in rhesus macaques induced strong effector-memory responses capable of inducing protection against a highly pathogenic SIV strain (Hansen et al. 2011), however the basis for the unique immune responses described in the SIV model have not yet been elucidated. In addition to this, the use of live-attenuated CMV vectors would be unlikely to be permitted in humans due to safety concerns. Together this data argues that some level of replication is required to induce the same magnitude of immune response as a wildtype infection.

4.2.2. Immunogenicity of my conditionally-replicating MCMV vectors in BALB/c mice

I wanted to see whether conditionally replicating viruses would surpass the immune responses observed for spread-defective and live-attenuated CMV vectors previously described in the literature. Peripheral $CD8^+$ T cell responses to pp89/IE1 peptide showed that M_{RSV}2M100-tetR-P2A-M36 immunized mice receiving DOX had higher levels of CMV-specific lymphocytes (comparable to control virus immunized mice) than those receiving regular feed up until day 32. On day 64, however, the levels were comparable between all groups. This strongly suggests that permitting limited viral replication can significantly improve T-cell induction at early times post-infection. It is possible that at later times, the conditional virus may have overcome its sensitivity to DOX, and thus replicated, resulting in an equal induction of T-cells with or without DOX addition. Tissues were kept from this experiment, and will be tested for virus load, as well as the *tetR* sequenced, to test this hypothesis.

To determine whether T cell responses and/or T cell phenotype in tissues were affected by viral replication, BALB/c mice were immunized with my most promising M_{RSV}2M100-tetR-P2A-M36 in the presence and absence of DOX. Overall, I did not observe distinct trends in my data. In mice immunized with M_{RSV}2M100-tetR-P2A-M36 I observed induction of CMV-specific $CD8^+$ T lymphocytes in the spleen and lung at levels comparable to the control virus. In the salivary glands, however, the frequencies of CMV-specific lymphocytes were significantly higher than conditionally replicating virus. T_{CM}, T_{EM}, T_{RM} populations were also lower in salivary glands of mice immunized with conditional CMV. This suggests that the M_{RSV}2M100-tetR-P2A-M36 may be less efficient at replicating in salivary glands even in the presence of DOX. When I tested functionality of CMV-specific $CD4^+$ and $CD8^+$ T lymphocytes, I observed higher production of IFN-γ by IE1-specific $CD8^+$ T and M53-specific $CD4^+$ T cells in mice immunized with conditional virus. Even though statistically not significant, I observed a trend for higher levels of TNF-α produced in IE1-specific $CD8^+$ T cells in M_{RSV}2M100-tetR-P2A-M36 immunized mice receiving regular feed. Both IFN-γ and TNF-α play a role as proinflammatory cytokines that are released by activated $CD4^+$ and cytotoxic effector T cells. These cytokines are important for their antiviral effect aiding in viral clearance, as previously shown for MCMV (Pavic et al. 1993; Lučin et al. 1992). It has been previously shown that HCMV acts to disrupt TNF-α expression by downregulating its cell surface receptor (Baillie et al. 2003). It is possible that

M_{RSV}2M100-tetR-P2A-M36 virus in mice receiving regular feed is less efficient at downregulating TNF-α cellular receptor. In addition to this, the virus may have acquired mutations that have allowed it to escape transcriptional repression and would thus explain ongoing virus replication that would induce higher production of TNF-α (but not lower levels of IFN-γ by IE1-specific $CD8^+$ T cells).

A further complication is that in my studies, I used viruses propagated *in vitro*. Tissue culture-derived virus has been previously shown to be less pathogenic than salivary gland-derived virus, due to non-genetic differences. As a result, viral infection may not be detectable *in vivo* up to 2 weeks pi with tissue culture-derived virus, but is detectable with salivary gland passaged virus (Osborn & Walker 1971; Reddehase 2002). The spread-deficient ΔgL virus described by Snyder *et al* has also been generated *in vitro* (Snyder et al. 2011). Interestingly, they observed more attenuated peripheral immune responses to CMV-specific peptides in C57BL/6 than BALB/c mice. Others in my lab, however, have conducted a similar experiment and showed (data not published) that although ΔgL virus induces comparable %pp89/IE1 responses in the BALB/c mouse strain as WT virus, ΔgL virus induces lower $CD8^+$ T cell expansion, thus resulting in lower total $pp89^+$ cells in the blood as well as tissues. This suggests that C57BL/6 would thus be a better mouse strain to look for differences in immune responses induced by the different viruses.

4.2.3. Safety profile of my conditional MCMV vectors *in vivo*

Importantly, although my MCMV vectors were not completely inhibited *in vitro* in the absence of DOX, they were much more strictly controlled in the absence of DOX *in vivo*. A possible explanation for this observation is the interaction of the virus with immune cells *in vivo* which in turn aids in the control of virus replication such that even a modest inhibition of vector replication *in vivo* is sufficient to 'tip the balance' between the virus and the host, towards the host. The fact that virus control is more stringent in an animal model thus suggests that vectors safety evaluation *in vitro* should be interpreted with caution.

In an acute MCMV infection model, these conditional viruses were detected at low levels in the four organs tested. Rescue (with DOX administration) of any possibly replicating virus by plaque assay showed that no M_{RSV}2M100-tetR-P2A-M36 virus could be detected in any organ. In comparison to a previously described conditional

MCMV virus (M50-1), M_{RSV}2M100-tetR-P2A-M36 therefore displayed an improved safety profile. In a longitudinal experiment looking at chronic MCMV infection, saliva of infected mice was tested for presence of virus genomes. Interestingly, some mice did shed M_{RSV}2M100-tetR-P2A-M36 DNA, but not the control virus, however, due to high variability this difference was not statistically significant. In addition to this, the peripheral blood responses to CMV IE1 antigen increased in mice immunized with M_{RSV}2M100-tetR-P2A-M36 (receiving regular feed). This together with the sequencing data showing that propagation of M_{RSV}2M100-tetR-P2A-M36 can result in mutations leading to loss of functional tetR suggests that these vectors may need to be modified further prior to translation to HCMV vector design and use in humans.

Different strategies (described in section 4.1.1) have been developed to improve conditional vector safety. One approach would be to use the Tet-On system since it is an activation system and not a de-repression system such as the one I have used in my vector design. As mutations in the *rtTA* gene have been identified by Benjamin Berkhout's lab, the use of their safety-lock amino acid modifications would provide an additional safety mechanism. In addition to this, a destabilising domain or loxP sites could be inserted next to an essential virus gene thus making virus replication dependent on additional ligands and not just DOX. An additional way to make the virus safe would be by inserting a thymidine kinase gene that would render it sensitive to acyclovir treatment. Lastly, treatment with ganciclovir, Benzimidazole l-Riboside 1263W94 or 2-Bromo-5,6-dichloro-1-beta-D-ribofuranosyl benzimidazole (BDCRB) should reduce viral burden and improve safety of the vector as these are drugs that have been previously shown to inhibit CMV replication (Biron et al. 2002).

4.3. Adenovirus and cancer models

4.3.1. Efficacy of adenovirus vectors in tumour models in the literature

Extensive research has been carried out using replication-deficient adenovirus vectors encoding tumour-associated antigens in anti-cancer vaccine development. Colorectal cancer antigen GUCY2C encoding Ad5 vector has been tested in conjunction with radiotherapy and showed anti-tumour effect in CT26-GUCY2C cancer model (Witek et al. 2014). Both of these treatments individually, however, did not display efficacy. An adenovirus vector (containing deletions in E1 and E2b (DNA polymerase) gene regions) encoding CEA displayed significantly stronger immune responses than first-generation (E1 deleted) Ad-CEA vector (Gabitzsch et al. 2010). In addition to this, the immunogenicity of the vector provided an anti-tumour response in mice injected with MC38-cea2 (murine colon adenocarcinoma) cells and delayed tumour development. A recombinant adenovirus vector encoding PSA and prostate stem cell antigen demonstrated efficacy in murine prostate cancer model (RM11-PSA/PSCA) (Karan et al. 2011). Therapeutic immunization with the vaccine led to eradication of tumours in 80% of immunized mice. It is therefore evident that adenovirus vectors make effective anti-cancer vaccines in mouse models when used in conjunction with tumour expressing antigens and have the potential to delay or even eradicate tumour development.

Several studies have utilized the fact that a variety of different tumours express 5T4 antigen in an attempt to treat cancer. T cells expressing chimeric receptors targeting h5T4 have been tested *in vivo* alongside bone marrow-derived DC (BMDC) and Ad-h5T4 and showed that the use of h5T4-specific CR T cells alone, delayed progression of CT26-h5T4 tumours in 60% of mice for as long as 8 weeks post challenge (Jiang et al. 2006). In a therapeutic setting, the use of h5T4-specific CR T cells with Ad-h5T4 and BMDC (locally but not systemically) significantly improved mouse survival rates and delayed tumour growth. In a different study, retrovirally transduced DC lines DCh5T4 and Ad-h5T4 induced tumour growth delay in a B16 melanoma model (Ali et al. 2006). Prophylactically, DCh5T4/Adh5T4 was shown to be the most effective regimen inducing tumour protection in 5/7 mice for the entire length of the study. Immunization of C57BL/6 5T4 knock out (5T4 KO) mice with Ad-m5T4 resulted in induction of $CD4^+$ and $CD8^+$ immune responses sufficient to protect against B16

tumour challenge (F. V. Castro et al. 2012). WT mice immunized with the same vector, however, activated $CD4^+$ and $CD8^+$ T cells that displayed poor cytokine release profiles. As a result, WT mice were not protected from B16 melanoma. The anti-tumour responses were attributed to $CD4^+$ T cells since depletion of these cells resulted in significantly ablated anti-tumour activity. Altogether this data provided the basis for the use of adenovirus vectors in my studies to examine anti-cancer efficacy, and to compare them to the efficacy of my CMV vectors.

4.3.2. 5T4 epitope mapping

In order to generate tetramers that would allow us to look at immune responses *in vivo*, I mapped 5T4 epitopes in two mouse strains (BALB/c and C57BL/6). The responses in C57BL/6 were strong and the epitopes identified were in line with epitopes predicted by NetMHC online program. I was unable to determine restriction of the epitopes due to T2 D^b cells having lost the expression of Db encoding plasmid. H-2^{Db}-restricted peptides tend to be nonamers whilst H-2^{Kb} peptides are octamers. Since Db is known to bind peptides that have asparagine at position 5 and methionine or isoleucine at positions 8-10 (Miller & Collins 2006), it is likely that VSFRNLTHL is a Db-binder. The prediction program, however, suggested that it may bind both molecules. Kb, on the other hand, binds peptides that contain tyrosine or leucine at position 3 (minor anchor), either phenylalanine or tyrosine at position 5 and leucine at position 8 (Falk et al. 1991; Mutnts et al. 1991). Taking this criterion, peptide prediction output as well as peptide stability assay results into consideration, TSYVFLGIV is most certainly a H2-Kb-restricted peptide. Peptide stability assays showed that peptides VSFRNLTHL, NSLVSLTYV and SAPSPLVEL did bind to T2 K^b cells, but the complexes were not stable. This can be explained by lack of anchor residue at position 5. Although the peptide prediction program predicted that NSLVSLTYV and SAPSPLVEL to be H-2Db-restricted, I cannot confirm this entirely since T2 D^b cell data was not reliable due to possible loss of Db molecule expression.

4.3.3. LLC1 cancer model

To my knowledge, no one had previously shown that LLC1 cells express 5T4 tumour-associated antigen. Although in comparison to the other two cell lines (4T1 and CT26) I tested, LLC1 exhibited the lowest 5T4 expression, LLC1 cancer model is syngeneic for the C57BL/6 mouse strain. Since my epitope mapping studies showed that 5T4 was more immunogenic in this mouse strain than in BALB/c, I wanted to establish a

cancer model and test h5T4-expressing Ad vectors. We performed a pilot study to elucidate the dosage of cells required to implant subcutaneously to induce tumour growth. Interestingly, although the highest dose used was 4×10^5 whereas in the literature it was 10^6, the rate of tumour growth was more rapid than that previously observed (Bertram & Janik 1980). One possible explanation for this is that the cells we used were of very early passage whereas those used by other groups may have been more heavily passaged resulting in longer doubling time. The tumours in the majority of the animals formed ulcerations as a result of high growth rate whereby hypoxic and necrotic centres in the tumours could be observed due to incomplete vasculature. Another hypothesis is that the location of tumour implantation resulted in easier accessibility for the animal to irritate the tissues surrounding the tumour through scratching or grooming. This hypothesis was supported by the fact that the size of the tumour did not affect the degree of ulceration. There were mice that had small tumours with discharge whereas others with large tumours did not. We injected the cells into the left flank whereas previous studies had injected LLC1 cells intravenously, intratracheally and subcutaneously in the intrascapular region which would not be as easily accessible for the animals thereby prolonging the endpoint of the experiment. Our animals, on the other hand, had to be sacrificed with tumours smaller than those previously reported in the literature due to Home Office regulations.

Having identified a dose that induced tumours in all the animals at a steady rate, we tested Ad-h5T4 efficacy prophylactically. Surprisingly, naïve mice that had not received Ad vaccine displayed delayed tumour progression. Comparison of spleen sizes showed that AdZ-h5T4 vaccinated mice had smaller spleens than other mice. It is interesting to note that other investigators have suggested that splenomegaly may be related to the breadth of immune response induced in tumour-bearing mice (Cao et al. 2011). Spleen enlargement in tumour-bearing mice has been previously linked to extramedullary haematopoiesis and thus, the requirement for red blood cells (Casbon et al. 2015; Bronte & Pittet 2013). It would be interesting to analyse the phenotype of lymphocytes in these animals as it may explain why naïve animals were protected for longer. One of the hypothesis as to why the Ad-injected animals did not delay disease progression is T cell exhaustion and/or the induction of regulatory T cells.

The efficacy of T_{Reg} depletion has been previously demonstrated in a B16m5T4 melanoma (F. V. Castro et al. 2012). Phenotypic analysis of the splenic lymphocytes

would thus reveal the cause for the lack of tumour-specific response. It has been observed in the literature that LLC cancer model is not as immunogenic as 4T1 or CT26 and these cells also express less co-stimulatory markers on the cell surface (Lechner et al. 2013). This, together with the fact that 5T4 expression was lower than in 4T1 and CT26 could thus explain why a protective response was not observed in this cancer model.

4.3.4. Lack of Efficacy of Ad-h5T4 in CT26 and 4T1 cancer models

My work showed that 5T4 was not as immunogenic in BALB/c as it was in C57BL/6. Members from Adrian Hill's lab have also observed similar levels of immunogenicity in this mouse strain (correspondence). I showed that 5T4 expression in CT26 and 4T1 cells was very strong hence why I wanted to establish cancer models and test AdZ-h5T4 vectors. Similarly to the LLC1 cancer model, both CT26 and 4T1-injected mice were not protected by vaccination with 5T4 expressing Ads. In the 4T1 model, survival of naïve mice was prolonged by 4 days whereas in CT26 model it was 7 days. Comparison of splenocyte numbers showed that they were comparable between different groups, however, in the CT26 naïve mice the spleens were slightly larger (not statistically significantly).

Other groups have also used the CT26 cancer model and looked at prophylactic as well as therapeutic effect of MVA-h5T4 vaccination (Harrop et al. 2006; Mulryan et al. 2002). Interestingly, the cell line they used was transfected with h5T4, thus increasing the expression of this antigen and enhancing the possible effect observed. In a prophylactic setting, the mice were immunized with MVA-h5T4 twice (2 weeks apart) and mice were challenged with 5×10^5 CT26-h5T4 cells i.v. 2 weeks after the boost. The vaccine induced a long-term (at least 6 months) protection against CT26 and was antibody-dependent since depletion of both $CD4^+$ and $CD8^+$ T cells did not have an effect on tumour development. In a therapeutic setting, however, $CD4^+$ T cells played a significant role in anti-tumour protection. Although the dose of cells used was higher and the mode of administration was intravenous as opposed to subcutaneous, MVA-h5T4 did induce protection in the CT26 model. It may be possible that the effect observed was due to higher expression of h5T4. It has been previously shown that CT26 and 4T1 express high levels of immunosuppressive factors compared to other cancer models (Lechner et al. 2013). CT26 model also displays higher levels of T_{Reg} frequencies, thus enhancing the immunosuppressive effect that would explain the lack

of efficacy of my Ad vectors (Lechner et al. 2013). To determine whether this was the case, T_{Reg} depletion would need to be carried out. In previous studies, depletion of T_{Reg} cells resulted in more potent responses to 5T4 (F. V. Castro et al. 2012; Elkord et al. 2008). 4T1 cells, on the other hand, have been described as a highly heterogeneous cell line whereby different cell clones would display variable proliferation and metastasis potential. It cannot be ruled out that the cells implanted differed in the rate of proliferation, although this would explain high variability between mice and not experimental groups.

4.3.5. The route of administration

The route of administration of adenovirus vectors in cancer models described in the literature is primarily intratumoral. Some cancer cells, however, have low HF-CAR expression (the receptor to which Ad serotype 5 binds), thus resulting in limited antigen expression at the site of injection. In such cases, systemic delivery may be more favourable. Systemic injection (such as intravenous immunization) enables targeting of multiple different organs, and targeting of tumours where direct injection is not feasible, however high expression of HF-CAR in hepatocytes leads to liver uptake of adenoviruses. It has been shown that the half-life of adenovirus type 5 in the blood is less than 2 minutes (Alemany et al. 2000). Moreover, neutralising antibodies in the blood may inactivate the virus following subsequent injections. Interestingly, a study comparing intravenous and intratumoral routes of injection showed that only higher doses (5×10^8 PFU) of recombinant adenovirus vector (Ad-mIFN) injected intravenously displayed an anti-tumour effect in mice receiving intratumoral injections (Narumi et al. 2010). In addition to this, IFN-α, $CD4^+$ and $CD8^+$ levels within the tumour were higher following intratumoral administration than intravenous. Interestingly, intratumoral injection was shown to be effective not only at the site of injection but displayed a suppressive effect against a tumour implanted at a different location. There have also been studies comparing i.v. route of administration and subcutaneous immunization. It was shown that both routes of injection induced IFN-γ secreting $CD8^+$ T cells, however, T cells elicited by i.v. injection were localized in the liver (Holst et al. 2010). In addition to this, cytokine production/effector functions of these T cells became impaired at 2-4 months post-administration and accumulated in the spleen. Interestingly, it has also been demonstrated that more virus was required to be injected intravenously to induce a response of the same magnitude as the vector injected subcutaneously (Holst & Thomsen 2011). Induction of the response was more gradual

for intravenous injection, however, over time became stronger than s.c. (Holst & Thomsen 2011). Although s.c. injection is a type of local delivery, the use of higher virus doses (more than 10^9 virus particles) has been shown to result in viral entry into the bloodstream (Holst et al. 2010).

In my experiments, each mouse received 5×10^8 PFU of recombinant adenoviruses. The inoculum was injected subcutaneously into the abdominal cavity. The tumours, on the other hand, were implanted into the left flank. Since we tested my vaccine vectors prophylactically, intratumoral injection was not considered. The fact that the vectors used were replication-deficient and I did not observe any anti-tumour effects could suggest that the virus particles did not manage to disseminate systemically and it is likely that they were either neutralized or were sequestered by the liver. Moreover, the responses induced may have been local and did not reach the site of tumour challenge. In the future, it would be interesting to administer the vaccine closer to the site of tumour injection site to see whether there would be an improvement in the efficacy of the anti-cancer vaccine. In addition to this, alternative injection approaches such as the microneedle-mediated immunization should be experimented with to reduce anti-vector immunity and enhance responses to the antigen and increase the numbers of tumour-infiltrating lymphocytes (Carey et al. 2015).

The majority of vaccines in humans are injected intramuscularly (hepatitis A, hepatitis B, tetanus and rabies); subcutaneously (measles, mumps, rubella, varicella, zoster and meningococcal polysaccharide) or intradermally (rabies and influenza). In a cancer setting, however, anti-cancer agents are delivered subcutaneously (monoclonal antibodies; i.e. trastuzumab and chemotherapy drugs azacitidine), intravenously (Cytoxan – chemotherapy drug and DC Sipuleucel-T (Provenge)) or intramuscularly (human papillomavirus) (Leveque 2014). Although intratumoral route of injection has shown a lot of potential in an animal model, it would not be applicable to all types of cancers as some of them may not be easily accessible. Therefore, it is crucial to select the most appropriate route of immunization for the type of cancer at hand, however a vaccine that could be administered systemically would have wider utility than one requiring intratumoral delivery. In addition to this, a number of factors need to be taken into consideration when selecting the route of injection: type of immune responses required; whether there would be any cytotoxicity at the site of delivery and the volume of the inoculum.

4.3.6. Homologous prime/boost

In humans, the majority of the population have neutralising antibodies to adenoviruses, which limits the efficacy to Ad vectors, however this is not the case in laboratory mice. In addition to this, the selected dose (5×10^8 PFU) had been previously optimised by members in the lab to induce a strong response to the transgene, but not to the vector itself, even following a homologous prime/boost regimen. In addition to this, it has been shown by another group that the use of 2×10^8–2×10^9 PFU results in significant accumulation of antigen-specific $CD8^+$ T cells thus supporting the idea that not only is this dose safe but also immunogenic (Krebs et al. 2005).

It has been suggested in the literature that a heterologous prime/boost regimen may be more effective than homologous regimen. In the prime stage of the vaccination, a naïve T cell is presented with antigens derived from the recombinant antigen as well as the vector which results in T cell activation and development of memory T cells. Heterologous boost entails immunization with a different delivery vector encoding the same antigen. Consequently, the memory response only to the antigen is induced. When the same delivery vector is used (in the case of homologous regimen), memory T cells specific to the vector may also be expanded. Lemckert *et al* has showed that injection of naïve mice with 10^9 virus particles (4 weeks apart) with either Ad11-Gag or Ad35-Gag resulted in significantly weaker immune responses than in mice that received a heterologous Ad11-Gag/Ad35-Gag or Ad35-Gag/Ad11-Gag injection (Lemckert et al. 2005). In addition to this, studies in which homologous regime with MVA vector encoding h5T4 was used or canary pox virus vector ALVAC(2)-h5T4, no 5T4-specific responses were induced when analysed by an *ex vivo* ELISpot assay (Hanwell et al. 2013). In a murine cancer model immunized with MVA-h5T4 (homologous regime), depletion of $CD4^+$ and $CD8^+$ T cells did not affect protection against tumour formation thus supporting the hypothesis that homologous vaccination regimens may reduce T cell immune responses induced (Harrop et al. 2006). The use of simian adenovirus ChAdOx1.h5T4 and MVA-h5T4 in a heterologous vaccination regimen resulted in protective 5T4-specific immune response in a B16 melanoma model. Homologous vaccination (MVA-h5T4), on the other hand, failed to induce a 5T4-specific cellular response, thus suggesting that a heterologous prime/boost regimen may be more effective (Cappuccini et al. 2017). Interestingly, the order in which delivery vectors are injected may also play a crucial role in development of the immune response. It has been shown that vaccination with Adh5T4 followed by

DCh5T4 induced protection in B16 melanoma model when used prophylactically whereas injection with DCh5T4 followed by Adh5T4 did not (Ali et al. 2006). In a therapeutic setting, however, DCh5T4/Adh5T4 was more beneficial.

In addition to the vaccination regimen used, it is possible that the T cell activation mechanism was faulty and the cells may have been exhausted (Krebs et al. 2005). It has been previously shown that replication-deficient adenovirus vector encoding lacZ was able to induce as many as 5-15% β-gal-specific CTL, however, these T cells displayed reduced effector cytokine production and consequently, Ad-lacZ vectors did not have a therapeutic effect in mice with βgal-expressing tumours.

In this study, proof-of-concept experiments were performed to look at the capacity of Ad-h5T4 vectors in inducing protection against 5T4-expressing tumour challenge. The end-goal was to use CMV and Ad vectors in a prime boost regimen, however, due to time constraints these experiments were not conducted. Members in our lab have previously shown (data not published) that immunization with Ad serotype 4 encoding IE3 MCMV epitope followed by an MCMV boost resulted in induction of as many as 40% of IE3-specific $CD8^+$ T cells. Ad4-IE3 alone, induced 10% tetramer-specific $CD8^+$ T cells. Ad serotype 5, on the other hand was less immunogenic (30% tetramer-specific $CD8^+$ T cells) although the responses were less variable. It will be interesting to determine whether the use of this approach will protect mice against LLC1, 4T1 and CT26 challenge. In addition to this, the previously established intestinal cancer model by Lee Parry would be another opportunity to analyse the responses induced by these two vectors.

4.4. Overall conclusions and future perspectives

To summarize, I have shown that in the context of CMV, the TREx system can be safely used *in vivo*. In order to achieve stringent control of virus replication, it was necessary to achieve early and abundant expression of tetR. Endogenous virus promoters (M36) showed efficacy in driving gene expression and thus, controlling virus replication. In addition to this, I showed that the location of tetO was crucial and highly variable between different genes, thus it is necessary to experiment with positioning tetO at different locations upstream of each candidate gene. These positions may also differ between human and mouse CMV genomes as gM and IE1 gene regulation in

MCMV (M100 and M123) and HCMV (UL100 and UL123), respectively, played a role in controlling virus replication.

Immune responses to the vectors *in vivo* in the absence and presence of DOX did not follow strict trends. At 32 days pi, the conditional MCMV vector did, however, induce weaker immune responses in the absence of DOX in comparison to presence of DOX or control virus. This result suggests that the conditional virus is suppressed by the immune system in absence of DOX and is unable to replicate, however, at later timepoints in the infection the virus may have overcome this modulation. Although currently I do not know whether the virus escapes strict control of virus replication in the absence of DOX *in vivo,* by mutating in the *tetR* or tetO regions, sequencing of viruses isolated from mouse tissues would reveal this information.

The results obtained in the course of this study provide a better understanding of CMV conditional replication *in vitro* and *in vivo.* The fact that conditional MCMV vector mutated *in vitro* in the absence of DOX, thus enabling virus replication, suggests that in place of the TREx system described in this study, Tet-On system should be used instead, although this in turn could present issues with the controlled gene not being expressed with the correct kinetics (immediate early, early and late). The sequence of *rtTA* gene could be optimised to prevent the chances of any possible mutations. My work identified M36 gene as a good location for insertion of *tetR*, thus fusing of rtTA at the end of M36 should therefore also result in stringent control of virus replication. In addition to this, I determined the positions for inserting tetO sequences that successfully enabled conditional expression of gM and IE1 genes in MCMV and HCMV, respectively. Further development of the vector could also involve insertion of a destabilising domain to regulate an essential virus protein. Both of these mechanisms would ensure conditional control of virus at the transcriptional as well as post-translational level. Ligands such as TMP or AP1903 should be tested in a mouse model as they have previously been characterized in humans and in the future, could be used in conjunction with HCMV vectors. My colleagues have observed stronger differences in immune responses elicited by replication-deficient viruses compared to WT viruses in C57BL/6 and since I only looked at responses in BALB/c mouse strain it would be interesting to test my conditional MCMV vectors in C57BL/6.

In addition to CMV work, I mapped 5T4 epitopes in C57BL/6 and BALB/c mouse strains by using Ad-h5T4 replication-deficient vectors. I compared immunogenicity of first- and second-generation Ad vectors and showed that it was comparable in the BALB/c mouse strain. I showed that h5T4 is less immunogenic in BALB/c mice than C57BL/6. In preliminary experiments, the use of Ad-h5T4 vectors did not show prophylactic efficacy in 5T4-expressing cancer models (4T1, CT26 and LLC1). Adenovirus serotype 5 (used in this study), although highly immunogenic in mice, is rapidly neutralised in humans due to pre-existing antibodies. Other, less common serotypes (e.g. serotype 4) should be used instead. Since previous work by colleagues in the lab has shown that adenovirus prime immunization followed by a boost using CMV vector induced strong immune responses in mice, it would be interesting to repeat this experiment in a cancer model with vectors expressing 5T4 antigen/epitopes.

Paul Klenerman's group have previously shown that Ad-minigenes induce inflationary immune responses characteristic of CMV vectors (Colston et al. 2016). I therefore generated Ad minigenes that contain 5T4 individual epitopes identified in this study. In addition to this, I made Ad vectors expressing UL40 HCMV gene fused to individual 5T4 peptides. UL40 gene has a leader sequence containing an HLA-E ligand. Replacing HLA-E peptide sequence with 5T4 epitopes should result in efficient loading of epitopes onto HLA-E which consequently would induce strong inflationary T-cell responses. It would therefore be of interest to use Ad-5T4-minigene or Ad-UL40-5T4 peptide vectors together with CMV vectors encoding 5T4 epitopes in a mouse model to identify the most effective combination in a prophylactic immunization regimen.

As 5T4-specific immune responses are low in BALB/c mouse strain and we only established LLC1 cancer model in C57bl/5 mice, future work should focus on looking at anti-cancer efficacy in *Apc*$^{fl/f}$ mice (C57BL/6 background) kindly provided by Dr Lee Perry. This model represents a more natural progression of cancer since tumour cells do not need to be implanted into the mouse. Instead, treatment with tamoxifen leads to loss of *APC* and tumour formation in the intestine. Since we detected CMV-specific lymphocytes in intestines of infected mice, I believe that Ad/CMV prophylaxis should be effective in this cancer model.

References

Abern, M., Kaufman, H.L. & Latchamsetty, K., 2011. An update on TroVax for the treatment of progressive castration-resistant prostate cancer. *OncoTargets and therapy*, 4, pp.33–41. Available at: http://www.ncbi.nlm.nih.gov/pubmed/21691576 [Accessed May 26, 2017].

Abgueguen, P. et al., 2010. Venous thrombosis in immunocompetent patients with acute cytomegalovirus infection: a complication that may be underestimated. *Clinical Microbiology and Infection*, 16(7), pp.851–854. Available at: http://www.ncbi.nlm.nih.gov/pubmed/19686279 [Accessed February 2, 2017].

Abolins, S. et al., 2017. The comparative immunology of wild and laboratory mice, Mus musculus domesticus. *Nature Communications*, 8, p.14811. Available at: http://www.ncbi.nlm.nih.gov/pubmed/28466840 [Accessed July 12, 2017].

Ahlfors, K. & Ivarsson, S.A., 1985. Cytomegalovirus in breast milk of Swedish milk donors. *Scandinavian journal of infectious diseases*, 17(1), pp.11–3. Available at: http://www.ncbi.nlm.nih.gov/pubmed/2986279 [Accessed February 2, 2017].

Ahlqvist, J. & Mocarski, E., 2011. Cytomegalovirus UL103 Controls Virion and Dense Body Egress. *Journal of Virology*, 85(10), pp.5125–5135. Available at: http://www.ncbi.nlm.nih.gov/pubmed/21345947 [Accessed February 3, 2017].

Akulian, J.A. et al., 2013. High-quality CMV-specific CD4+ memory is enriched in the lung allograft and is associated with mucosal viral control. *American journal of transplantation : official journal of the American Society of Transplantation and the American Society of Transplant Surgeons*, 13(1), pp.146–56. Available at: http://www.ncbi.nlm.nih.gov/pubmed/23016698 [Accessed March 22, 2017].

Al-Taei, S. et al., 2012. Overexpression and potential targeting of the oncofoetal antigen 5T4 in malignant pleural mesothelioma. *Lung Cancer*, 77(2), pp.312–318. Available at: http://www.ncbi.nlm.nih.gov/pubmed/22498111 [Accessed April 10, 2017].

Alba, R., Baker, A.H. & Nicklin, S.A., 2012. Vector Systems for Prenatal Gene Therapy: Principles of Adenovirus Design and Production. In C. Coutelle & S. N. Waddington, eds. *Prenatal Gene Therapy: Concepts, Methods, and Protocols, Methods in Molecular Biology*. Humana Press, pp. 55–84. Available at: http://books.google.com/books?id=Ku2wPAAACAAJ%5Cnhttp://www.ncbi.nlm.nih.gov/pubmed/23296648%5Cnhttp://link.springer.com/10.1007/978-1-61779-873-3.

Alcami, A. & Koszinowski, U.H., 2000. Viral mechanisms of immune evasion. *Trends in Microbiology*, 8(9), pp.410–418. Available at: http://linkinghub.elsevier.com/retrieve/pii/S0966842X00018308 [Accessed February 24, 2017].

Alemany, R., Curiel, D.T. & Suzuki, K., 2000. Blood clearance rates of adenovirus type 5 in mice. *Journal of General Virology*, 81(11), pp.2605–2609. Available at: http://www.ncbi.nlm.nih.gov/pubmed/11038370 [Accessed August 6, 2017].

Ali, S. et al., 2006. Immunotherapy success in prophylaxis cannot predict therapy: prime-boost vaccination against the 5T4 oncofoetal antigen. *Cancer Immunology, Immunotherapy*, 56(2), pp.165–180. Available at: http://www.ncbi.nlm.nih.gov/pubmed/16758205 [Accessed April 10, 2017].

Amato, R.J. et al., 2010. Vaccination of metastatic renal cancer patients with MVA-5T4: A randomized, double-blind, placebo-controlled phase III study. *Clinical Cancer Research*, 16(22), pp.5539–5547. Available at: http://www.ncbi.nlm.nih.gov/pubmed/20881001 [Accessed April 10, 2017].

Amato, R.J. et al., 2009. Vaccination of Renal Cell Cancer Patients With Modified Vaccinia Ankara Delivering the Tumor Antigen 5T4 (TroVax) Alone or Administered in Combination With Interferon-α (IFN-α): a phase 2 trial. *Journal of Immunotherapy*, 32(7), pp.765–772. Available at: http://www.ncbi.nlm.nih.gov/pubmed/19561532 [Accessed April 10, 2017].

Andtbacka, R.H.I. et al., 2015. Talimogene Laherparepvec Improves Durable Response Rate in Patients With Advanced Melanoma. *Journal of Clinical Oncology*, 33(25), pp.2780–2788. Available at: http://www.ncbi.nlm.nih.gov/pubmed/26014293 [Accessed April 14, 2017].

Appledorn, D.M. et al., 2008. Adenovirus Vector-Induced Innate Inflammatory Mediators, MAPK Signaling, As Well As Adaptive Immune Responses Are Dependent upon Both TLR2 and TLR9 In Vivo. *The Journal of Immunology*, 181, pp.2134–2144. Available at: http://www.jimmunol.org/content/181/3/2134 [Accessed March 20, 2017].

Arnberg, N., 2012. Adenovirus receptors: implications for targeting of viral vectors. *Trends in Pharmacological Sciences*, 33(8), pp.442–448. Available at: http://linkinghub.elsevier.com/retrieve/pii/S0165614712000697 [Accessed March 17, 2017].

Arribas, J.R. et al., 1996. Cytomegalovirus encephalitis. *Annals of internal medicine*, 125(7), pp.577–87. Available at: http://www.ncbi.nlm.nih.gov/pubmed/8815757 [Accessed February 2, 2017].

Arvin, A.M. et al., 2004. Vaccine development to prevent cytomegalovirus disease: report from the National Vaccine Advisory Committee. *Clinical infectious diseases : an official publication of the Infectious Diseases Society of America*, 39(2), pp.233–239.

Asanuma, H. et al., 1996. Role of milk whey in the transmission of human cytomegalovirus infection by breast milk. *Microbiology and immunology*, 40(3), pp.201–4. Available at: http://www.ncbi.nlm.nih.gov/pubmed/8934674 [Accessed February 2, 2017].

Ashiru, O. et al., 2009. NKG2D ligand MICA is retained in the cis-Golgi apparatus by human cytomegalovirus protein UL142. *Journal of virology*, 83(23), pp.12345–12354.

Avdic, S. et al., 2011. Viral interleukin-10 expressed by human cytomegalovirus during the latent phase of infection modulates latently infected myeloid cell

differentiation. *Journal of virology*, 85(14), pp.7465–71. Available at: http://www.ncbi.nlm.nih.gov/pubmed/21593144 [Accessed March 2, 2017].

Bai, J., Li, J. & Mao, Q., 2013. Construction of a Single Lentiviral Vector Containing Tetracycline-Inducible Alb-uPA for Transduction of uPA Expression in Murine Hepatocytes Y. Wu, ed. *PLoS ONE*, 8(4), p.e61412. Available at: http://www.ncbi.nlm.nih.gov/pubmed/23626683 [Accessed March 2, 2017].

Baillie, J., Sahlender, D.A. & Sinclair, J.H., 2003. Human cytomegalovirus infection inhibits tumor necrosis factor alpha (TNF-alpha) signaling by targeting the 55-kilodalton TNF-alpha receptor. *Journal of virology*, 77(12), pp.7007–16. Available at: http://www.ncbi.nlm.nih.gov/pubmed/12768019 [Accessed August 5, 2017].

Baldick, C.J. & Shenk, T., 1996. Proteins associated with purified human cytomegalovirus particles. *Journal of virology*, 70(9), pp.6097–105. Available at: http://www.pubmedcentral.nih.gov/articlerender.fcgi?artid=190631&tool=pmcentrez&rendertype=abstract.

Banaszynski, L.A. et al., 2006. A Rapid, Reversible, and Tunable Method to Regulate Protein Function in Living Cells Using Synthetic Small Molecules. *Cell*, 126(5), p.995. Available at: https://www.ncbi.nlm.nih.gov/pmc/articles/PMC3290523/ [Accessed July 27, 2017].

Banaszynski, L.A. et al., 2008. Chemical control of protein stability and function in living mice. *Nature medicine*, 14(10), pp.1123–1127. Available at: http://wandless.stanford.edu/pdfs/TJW44.pdf [Accessed August 12, 2017].

Bartlett, D.L. et al., 2013. Oncolytic viruses as therapeutic cancer vaccines. *Molecular cancer*, 12(1), p.103. Available at: http://www.molecular-cancer.com/content/12/1/103.

Bassett, J.D., Swift, S.L. & Bramson, J.L., 2011. Optimizing vaccine-induced CD8+ T-cell immunity: focus on recombinant adenovirus vectors. *Expert Review of Vaccines*, 10(9), pp.1307–1319. Available at: http://www.tandfonline.com/doi/full/10.1586/erv.11.88 [Accessed March 16, 2017].

Bate, S.L., Dollard, S.C. & Cannon, M.J., 2010. Cytomegalovirus Seroprevalence in the United States: The National Health and Nutrition Examination Surveys, 1988–2004. *Clinical Infectious Diseases*, 50(11), pp.1439–1447. Available at: https://academic.oup.com/cid/article-lookup/doi/10.1086/652438 [Accessed February 28, 2017].

Becke, S. et al., 2010. Optimized recombinant dense bodies of human cytomegalovirus efficiently prime virus specific lymphocytes and neutralizing antibodies without the addition of adjuvant. *Vaccine*, 28(38), pp.6191–6198. Available at: http://www.ncbi.nlm.nih.gov/pubmed/20655401 [Accessed February 2, 2017].

Bego, M. et al., 2005. Characterization of an antisense transcript spanning the UL81-82 locus of human cytomegalovirus. *Journal of virology*, 79(17), pp.11022–34.

Available at: http://www.ncbi.nlm.nih.gov/pubmed/16103153 [Accessed March 2, 2017].

Beisser, P.S. et al., 2001. Human cytomegalovirus chemokine receptor gene US28 is transcribed in latently infected THP-1 monocytes. *Journal of virology*, 75(13), pp.5949–57. Available at: http://www.ncbi.nlm.nih.gov/pubmed/11390596 [Accessed March 2, 2017].

Berencsi, K. et al., 2001. A Canarypox Vector–Expressing Cytomegalovirus (CMV) Phosphoprotein 65 Induces Long- Lasting Cytotoxic T Cell Responses in Human CMV- Seronegative Subjects. *The Journal of Infectious Diseases*, 183(8), pp.1171–1179. Available at: http://www.ncbi.nlm.nih.gov/pubmed/11262198 [Accessed February 2, 2017].

Bernstein, D.I. et al., 2009. Randomized, double-blind, Phase 1 trial of an alphavirus replicon vaccine for cytomegalovirus in CMV seronegative adult volunteers. *Vaccine*, 28(2), pp.484–493. Available at: http://www.ncbi.nlm.nih.gov/pubmed/19857446 [Accessed February 3, 2017].

Bertram, J.S.J. & Janik, P.P., 1980. Establishment of a cloned line of Lewis lung carcinoma cells adapted to cell culture. *Cancer Letters*, 11(1), pp.63–73. Available at: http://linkinghub.elsevier.com/retrieve/pii/0304383580901305.

Beswick, M. et al., 2013. An attenuated temperature-sensitive strain of cytomegalovirus (*tsm5*) establishes immunity without development of CD8 $^{+}$ T cell memory inflation. *Journal of Medical Virology*, 85(11), pp.1968–1974. Available at: http://www.ncbi.nlm.nih.gov/pubmed/23852921 [Accessed March 22, 2017].

Beverley, P.C.L. et al., 2014. A Novel Murine Cytomegalovirus Vaccine Vector Protects against Mycobacterium tuberculosis. *The Journal of Immunology*, 193, pp.2306–2316.

Beverley, P.C.L., 2002. Immunology of vaccination. *British Medical Bulletin*, 62, pp.15–28. Available at: https://oup.silverchair-cdn.com/oup/backfile/Content_public/Journal/bmb/62/1/10.1093/bmb/62.1.15/2/15.pdf?Expires=1490811840&Signature=gsAjFQKt-zaBCKTNCquzi4PO8ilCRS9nAna3GaU2D8eL0buELeuE4koYKq1ZvcLEP92Ov7zhvqgwc~Sp2LP-AnOgErRHZcoZnxU8t5cM4UjlX~Mrn--mOpNKs15x3zn59WbBb4XkwzdRLM2GT76eg1Db2KuDs8add6wGodTbEkFb32qQQWv3RgpLjpA9xhycM1ygJO~hvkWXHjDLbRJLFtoWPuPL8n2~Xo-XSe2Axw6V4pPLvYXYPeUGp108zxz7uKcUFY9mh45jy1fzFRwrxocNCGV2-016I1MT9nHY8~89IzeJiFXHCvYOyNzq1qwfeUgqwLMGRt3zAoHPzovXBA__&Key-Pair-Id=APKAIUCZBIA4LVPAVW3Q [Accessed March 27, 2017].

Bilsland, A.E., Spiliopoulou, P. & Evans, T.R.J., 2016. Virotherapy: cancer gene therapy at last? *F1000Research*, 5, p.2105. Available at: http://f1000research.com/articles/5-2105/v1 [Accessed April 12, 2017].

Birnbaum, M.E. et al., 2014. Molecular architecture of the αβ T cell receptor-CD3 complex. *Proceedings of the National Academy of Sciences of the United States of America*, 111(49), pp.17576–81. Available at:

http://www.ncbi.nlm.nih.gov/pubmed/25422432 [Accessed September 5, 2017].

Biron, K.K. et al., 2002. Potent and selective inhibition of human cytomegalovirus replication by 1263W94, a benzimidazole L-riboside with a unique mode of action. *Antimicrobial agents and chemotherapy*, 46(8), pp.2365–72. Available at: http://www.ncbi.nlm.nih.gov/pubmed/12121906 [Accessed July 26, 2017].

Bissinger, A.L. et al., 2002. Human cytomegalovirus as a direct pathogen: Correlation of multiorgan involvement and cell distribution with clinical and pathological findings in a case of congenital inclusion disease. *Journal of Medical Virology*, 67(2), pp.200–206. Available at: http://www.ncbi.nlm.nih.gov/pubmed/11992580 [Accessed February 19, 2017].

Bitmansour, A.D. et al., 2001. Clonotypic structure of the human CD4+ memory T cell response to cytomegalovirus. *Journal of immunology (Baltimore, Md. : 1950)*, 167(3), pp.1151–1163.

Black, P.H. et al., 1963. A Specific Complement-Fixing Antigen Present in SV40 Tumor and Transformed Cells. *Proceedings of the National Academy of Sciences of the United States of America*, 50, pp.1148–1156. Available at: https://www.jstor.org/stable/71859 [Accessed August 26, 2017].

Bobek, V. et al., 2010. A clinically relevant, syngeneic model of spontaneous, highly metastatic B16 mouse melanoma. *Anticancer Research*, 30(12), pp.4799–4804.

Boehme, K.W., Guerrero, M. & Compton, T., 2006. Human Cytomegalovirus Envelope Glycoproteins B and H Are Necessary for TLR2 Activation in Permissive Cells. *The Journal of Immunology*, 177(10). Available at: http://www.jimmunol.org/content/177/10/7094.long [Accessed August 31, 2017].

Bogner, E., 2002. Human cytomegalovirus terminase as a target for antiviral chemotherapy. *Reviews in Medical Virology*, 12(2), pp.115–127. Available at: http://www.ncbi.nlm.nih.gov/pubmed/11921307 [Accessed February 21, 2017].

Boppana, S.B. et al., 2005. Congenital cytomegalovirus infection: association between virus burden in infancy and hearing loss. *The Journal of pediatrics*, 146(6), pp.817–823.

Boppana, S.B. et al., 1992. Symptomatic congenital cytomegalovirus infection: neonatal morbidity and mortality. *The Pediatric infectious disease journal*, 11(2), pp.93–99.

Borst, E.M. et al., 2001. Genetic evidence of an essential role for cytomegalovirus small capsid protein in viral growth. *Journal of virology*, 75(3), pp.1450–1458.

Bradford, R.D. et al., 2005. Detection of Cytomegalovirus (CMV) DNA by Polymerase Chain Reaction Is Associated with Hearing Loss in Newborns with Symptomatic Congenital CMV Infection Involving the Central Nervous System. *The Journal of Infectious Diseases*, 191(2), pp.227–233. Available at: https://academic.oup.com/jid/article-lookup/doi/10.1086/426456 [Accessed February 2, 2017].

Bradford, R.D. et al., 2015. Murine CMV-Induced Hearing Loss Is Associated with Inner Ear Inflammation and Loss of Spiral Ganglia Neurons C. A. Benedict, ed. *PLOS Pathogens*, 11(4), p.e1004774. Available at: http://dx.plos.org/10.1371/journal.ppat.1004774 [Accessed July 13, 2017].

Bradley, R.R. et al., 2012. Adenovirus serotype 5 neutralizing antibodies target both hexon and fiber following vaccination and natural infection. *Journal of virology*, 86(1), pp.625–9. Available at: http://www.ncbi.nlm.nih.gov/pubmed/22072776 [Accessed March 21, 2017].

Breitbach, C.J. et al., 2011. Intravenous delivery of a multi-mechanistic cancer-targeted oncolytic poxvirus in humans. *Nature*, 477(7362), p.99. Available at: http://www.nature.com/nature/journal/v477/n7362/full/nature10358.html [Accessed March 28, 2017].

Bright, R.K., Bright, J.D. & Byrne, J.A., 2014. Overexpressed oncogenic tumor-self antigens. *Human Vaccines and Immunotherapeutics*, 10(11), pp.3297–3305.

Britt, B., 2007. Maturation and egress. In A. Arvin et al., eds. Cambridge.

ten Broeke, T., Wubbolts, R. & Stoorvogel, W., 2013. MHC class II antigen presentation by dendritic cells regulated through endosomal sorting. *Cold Spring Harbor perspectives in biology*, 5(12), p.a016873. Available at: http://www.ncbi.nlm.nih.gov/pubmed/24296169 [Accessed September 5, 2017].

Bronte, V. & Pittet, M.J., 2013. The Spleen in Local and Systemic Regulation of Immunity. *Immunity*, 39(5), pp.806–818. Available at: http://linkinghub.elsevier.com/retrieve/pii/S1074761313004706 [Accessed July 29, 2017].

Brownlie, R.J. & Zamoyska, R., 2013. T cell receptor signalling networks: branched, diversified and bounded. *Nature Reviews Immunology*, 13(4), pp.257–269. Available at: http://www.nature.com/doifinder/10.1038/nri3403 [Accessed September 5, 2017].

Budt, M. et al., 2009. Specific inhibition of the PKR-mediated antiviral response by the murine cytomegalovirus proteins m142 and m143. *Journal of virology*, 83(3), pp.1260–1270.

Bukowski, J.F., Woda, B.A. & Welsh ', R.M., 1984. Pathogenesis of Murine Cytomegalovirus Infection in Natural Killer Cell-Depleted Mice. *JOURNAL OF VIROLOGY*, 52(1), pp.119–128. Available at: https://www.ncbi.nlm.nih.gov/pmc/articles/PMC254497/pdf/jvirol00127-0129.pdf [Accessed September 1, 2017].

van der Burg, S.H. et al., 1996. Immunogenicity of peptides bound to MHC class I molecules depends on the MHC-peptide complex stability. *Journal of immunology (Baltimore, Md. : 1950)*, 156(9), pp.3308–14. Available at: http://www.ncbi.nlm.nih.gov/pubmed/8617954 [Accessed July 3, 2017].

Burshtyn, D.N. & Barber, B.H., 1993. Dynamics of peptide binding to purified antibody-bound H-2Db and H-2Db beta 2m complexes. *Journal of immunology*

(Baltimore, Md. : 1950), 151(6), pp.3082–93. Available at: http://www.ncbi.nlm.nih.gov/pubmed/7690793 [Accessed July 3, 2017].

Cannon, M.J., 2009. Congenital cytomegalovirus (CMV) epidemiology and awareness. *Journal of Clinical Virology*, 46, pp.S6–S10. Available at: http://www.ncbi.nlm.nih.gov/pubmed/19800841 [Accessed February 2, 2017].

Cannon, M.J., Hyde, T.B. & Schmid, D.S., 2011. Review of cytomegalovirus shedding in bodily fluids and relevance to congenital cytomegalovirus infection. *Reviews in Medical Virology*, 21(4), pp.240–255. Available at: http://www.ncbi.nlm.nih.gov/pubmed/21674676 [Accessed February 2, 2017].

Cannon, M.J., Schmid, D.S. & Hyde, T.B., 2010. Review of cytomegalovirus seroprevalence and demographic characteristics associated with infection. *Reviews in Medical Virology*, 20(4), pp.202–213. Available at: http://www.ncbi.nlm.nih.gov/pubmed/20564615 [Accessed February 2, 2017].

Cao, M. et al., 2011. Kinase inhibitor Sorafenib modulates immunosuppressive cell populations in a murine liver cancer model. *Laboratory Investigation*, 91(4), pp.598–608. Available at: http://www.nature.com/doifinder/10.1038/labinvest.2010.205 [Accessed July 24, 2017].

Cappuccini, F. et al., 2017. 5T4 oncofoetal glycoprotein: an old target for a novel prostate cancer immunotherapy. *Oncotarget*, 8(29), pp.47474–47489. Available at: http://www.oncotarget.com/fulltext/17666 [Accessed July 20, 2017].

Carey, J.B. et al., 2015. Microneedle-mediated immunization of an adenovirus-based malaria vaccine enhances antigen-specific antibody immunity and reduces anti-vector responses compared to the intradermal route. *Scientific Reports*, 4(1), p.6154. Available at: http://www.ncbi.nlm.nih.gov/pubmed/25142082 [Accessed August 6, 2017].

Carsberg, C.J. et al., 1995. Metastasis-associated 5T4 oncofoetal antigen is concentrated at microvillus projections of the plasma membrane. *Journal of cell science*, 108, pp.2905–16. Available at: http://www.ncbi.nlm.nih.gov/pubmed/7593330.

Carsberg, C.J., Myers, K.A. & Stern, P.L., 1996. Metastasis-associated 5T4 antigen disrupts cell-cell contacts and induces cellular motility in epithelial cells. *International Journal of Cancer*, 68(1), pp.84–92. Available at: http://www.ncbi.nlm.nih.gov/pubmed/8895545 [Accessed April 11, 2017].

Casbon, A.-J. et al., 2015. Invasive breast cancer reprograms early myeloid differentiation in the bone marrow to generate immunosuppressive neutrophils. *Proceedings of the National Academy of Sciences of the United States of America*, 112(6), pp.E566-75. Available at: http://www.ncbi.nlm.nih.gov/pubmed/25624500 [Accessed July 24, 2017].

Castro, F. V et al., 2012. 5T4 oncofetal antigen is expressed in high risk of relapse childhood pre-B acute lymphoblastic leukemia and is associated with a more invasive and chemotactic phenotype. *Leukemia*, 26(7), pp.1487–98. Available

at: http://www.ncbi.nlm.nih.gov/pubmed/22266911 [Accessed April 12, 2017].

Castro, F. V. et al., 2012. Regulation of autologous immunity to the mouse 5T4 oncofoetal antigen: implications for immunotherapy. *Cancer Immunology, Immunotherapy*, 61(7), pp.1005–1018. Available at: http://www.ncbi.nlm.nih.gov/pubmed/22127365 [Accessed August 6, 2017].

Cawood, R. et al., 2012. Recombinant viral vaccines for cancer. *Trends in Molecular Medicine*, 18(9), pp.564–574. Available at: http://www.cell.com/trends/molecular-medicine/pdf/S1471-4914(12)00143-8.pdf [Accessed March 27, 2017].

CenterWatch, 2017. FDA Approved Drugs in Oncology. Available at: https://www.centerwatch.com/drug-information/fda-approved-drugs/therapeutic-area/12/oncology [Accessed September 5, 2017].

Cepek, K.L. et al., 1994. Adhesion between epithelial cells and T lymphocytes mediated by E-cadherin and the αEβ7 integrin. *Nature*, 372(6502), pp.190–193. Available at: http://www.ncbi.nlm.nih.gov/pubmed/7969453 [Accessed July 10, 2017].

Cha, T. a et al., 1996. Human cytomegalovirus clinical isolates carry at least 19 genes not found in laboratory strains. *Journal of virology*, 70(1), pp.78–83. Available at: http://www.pubmedcentral.nih.gov/articlerender.fcgi?artid=189790&tool=pmcentrez&rendertype=abstract.

Challberg, M., 1996. Herpesvirus DNA Replication. *DNA Replication in Eukaryotic cells*, pp.721–750.

Chamuleau, M.E.D., Ossenkoppele, G.J. & van de Loosdrecht, A.A., 2006. MHC class II molecules in tumour immunology: Prognostic marker and target for immune modulation. *Immunobiology*, 211(6), pp.619–625. Available at: http://www.sciencedirect.com/science/article/pii/S0171298506000611 [Accessed April 3, 2017].

Chandler, S.H. et al., 1985. The epidemiology of cytomegaloviral infection in women attending a sexually transmitted disease clinic. *The Journal of infectious diseases*, 152(3), pp.597–605. Available at: http://www.ncbi.nlm.nih.gov/pubmed/2993442 [Accessed February 2, 2017].

Chapuis, A.G. et al., 2013. Transferred WT1-reactive CD8+ T cells can mediate antileukemic activity and persist in post-transplant patients. *Science translational medicine*, 5(174), p.174ra27. Available at: http://www.ncbi.nlm.nih.gov/pubmed/23447018 [Accessed April 7, 2017].

Chatellard, P. et al., 2007. The IE2 promoter/enhancer region from mouse CMV provides high levels of therapeutic protein expression in mammalian cells. *Biotechnology and bioengineering*, 96(1), pp.106–17. Available at: http://doi.wiley.com/10.1002/bit.21172 [Accessed July 21, 2017].

Chee, M.S. et al., 1990. Analysis of the Protein-Coding Content of the Sequence of

Human Cytomegalovirus Strain AD169. In J. K. McDougall, ed. *Cytomegaloviruses*. Berlin, Heidelberg: Springer Berlin Heidelberg, pp. 125–169. Available at: http://dx.doi.org/10.1007/978-3-642-74980-3_6.

Cheng, T.P. et al., 2010. Stability of murine cytomegalovirus genome after in vitro and in vivo passage. *Journal of virology*, 84(5), pp.2623–8. Available at: http://www.pubmedcentral.nih.gov/articlerender.fcgi?artid=2820925&tool=pmcentrez&rendertype=abstract.

Cheon, J. et al., 2000. Adenovirus-mediated suicide-gene therapy using the herpes simplex virus thymidine kinase gene in cell and animal models of human prostate cancer: changes in tumour cell proliferative activity. *BJU international*, 85(6), pp.759–66. Available at: http://www.ncbi.nlm.nih.gov/pubmed/10759680 [Accessed March 17, 2017].

Child, S.J. et al., 2004. Evasion of cellular antiviral responses by human cytomegalovirus TRS1 and IRS1. *Journal of virology*, 78(1), pp.197–205.

Childs, R. et al., 2000. Regression of Metastatic Renal-Cell Carcinoma after Nonmyeloablative Allogeneic Peripheral-Blood Stem-Cell Transplantation. *New England Journal of Medicine*, 343(11), pp.750–758. Available at: http://www.ncbi.nlm.nih.gov/pubmed/10984562 [Accessed April 7, 2017].

Cicin-Sain, L. et al., 2005. Frequent coinfection of cells explains functional in vivo complementation between cytomegalovirus variants in the multiply infected host. *Journal of virology*, 79(15), pp.9492–502. Available at: http://www.pubmedcentral.nih.gov/articlerender.fcgi?artid=1181553&tool=pmcentrez&rendertype=abstract.

Cobbold, M. et al., 2005. Adoptive transfer of cytomegalovirus-specific CTL to stem cell transplant patients after selection by HLA–peptide tetramers. *The Journal of Experimental Medicine*, 202(3), pp.379–386. Available at: http://www.ncbi.nlm.nih.gov/pubmed/16061727 [Accessed February 2, 2017].

Cobbs, C.S., 2011. Evolving evidence implicates cytomegalovirus as a promoter of malignant glioma pathogenesis. *Herpesviridae*, 2(1), p.10. Available at: http://www.ncbi.nlm.nih.gov/pubmed/22030012 [Accessed February 2, 2017].

Colston, J.M. et al., 2016. Modification of Antigen Impacts on Memory Quality after Adenovirus Vaccination. *Journal of immunology (Baltimore, Md. : 1950)*, 196(8), pp.3354–63. Available at: http://www.ncbi.nlm.nih.gov/pubmed/26944930.

Compton, T., Nepomuceno, R.R. & Nowlin, D.M., 1992. Human cytomegalovirus penetrates host cells by pH-independent fusion at the cell surface. *Virology*, 191(1), pp.387–95. Available at: http://www.ncbi.nlm.nih.gov/pubmed/1329327 [Accessed July 14, 2017].

Coonrod, D. et al., 1998. Association between cytomegalovirus seroconversion and upper genital tract infection among women attending a sexually transmitted disease clinic: a prospective study. *The Journal of infectious diseases*, 177(5), pp.1188–93. Available at: http://www.ncbi.nlm.nih.gov/pubmed/9593002 [Accessed February 2, 2017].

Correa, C. et al., 2011. Role of herpesvirus as a cause of mononucleosis-like and febrile syndromes in Cuba, 2006-2009. *MEDICC review*, 13(4), pp.45–9. Available at: http://www.ncbi.nlm.nih.gov/pubmed/22143607 [Accessed February 2, 2017].

Crespo, J. et al., 2013. T cell anergy, exhaustion, senescence, and stemness in the tumor microenvironment. *Current opinion in immunology*, 25(2), pp.214–21. Available at: http://www.ncbi.nlm.nih.gov/pubmed/23298609 [Accessed August 29, 2017].

Cuevas, J.M. et al., 2015. Extremely High Mutation Rate of HIV-1 In Vivo S. L. Rowland-Jones, ed. *PLOS Biology*, 13(9), p.e1002251. Available at: http://dx.plos.org/10.1371/journal.pbio.1002251 [Accessed August 15, 2017].

Cui, X. et al., 2012. Bacterial artificial chromosome clones of viruses comprising the Towne cytomegalovirus vaccine. *Journal of Biomedicine and Biotechnology*.

Cunningham, C. et al., 2010. Sequences of complete human cytomegalovirus genomes from infected cell cultures and clinical specimens. *Journal of General Virology*, 91(3), pp.605–615. Available at: http://www.ncbi.nlm.nih.gov/pubmed/19906940 [Accessed February 3, 2017].

Danthinne, X. & Imperiale, M., 2000. Production of first generation adenovirus vectors: a review. *Gene Therapy*, 7, pp.1707–1714. Available at: www.nature.com/gt [Accessed March 16, 2017].

Dargan, D.J. et al., 2010. Sequential mutations associated with adaptation of human cytomegalovirus to growth in cell culture. *Journal of General Virology*, 91(6), pp.1535–1546.

Das, A.T. & Berkhout, B., 2016. Conditionally replicating HIV and SIV variants. *Virus Research*, 216, pp.66–75. Available at: http://linkinghub.elsevier.com/retrieve/pii/S0168170215001756 [Accessed July 26, 2017].

Dasgupta, A. et al., 2014. Chapter 24 – Autoimmunity, Complement, and Immunodeficiency. In *Clinical Chemistry, Immunology and Laboratory Quality Control*. pp. 427–447. Available at: http://www.sciencedirect.com/science/article/pii/B9780124078215000243 [Accessed September 5, 2017].

Davila, M.L. et al., 2014. Efficacy and toxicity management of 19-28z CAR T cell therapy in B cell acute lymphoblastic leukemia. *Science translational medicine*, 6(224), p.224ra25. Available at: http://www.ncbi.nlm.nih.gov/pubmed/24553386 [Accessed March 25, 2017].

Davison, A.J., 2007. *Comparative analysis of the genomes*, Cambridge University Press. Available at: http://www.ncbi.nlm.nih.gov/pubmed/21348122 [Accessed February 15, 2017].

Davison, A.J. et al., 2003. The human cytomegalovirus genome revisited: comparison with the chimpanzee cytomegalovirus genome. *Journal of General*

Virology, 84(1), pp.17–28. Available at: http://www.ncbi.nlm.nih.gov/pubmed/12533697 [Accessed February 3, 2017].

Debowski, A.W. et al., 2013. Development of a Tetracycline-Inducible Gene Expression System for the Study of Helicobacter pylori Pathogenesis. *Applied and Environmental Microbiology*, 79(23), pp.7351–7359. Available at: http://www.ncbi.nlm.nih.gov/pubmed/24056453 [Accessed March 2, 2017].

Debowski, A.W. et al., 2015. Expansion of the Tetracycline-Dependent Regulation Toolbox for Helicobacter pylori J. L. Schottel, ed. *Applied and Environmental Microbiology*, 81(23), pp.7969–7980. Available at: http://www.ncbi.nlm.nih.gov/pubmed/26362986 [Accessed March 2, 2017].

Derhovanessian, E. et al., 2011. Infection with cytomegalovirus but not herpes simplex virus induces the accumulation of late-differentiated CD4+ and CD8+ T-cells in humans. *Journal of General Virology*, 92(12), pp.2746–2756. Available at: http://www.ncbi.nlm.nih.gov/pubmed/21813708 [Accessed February 2, 2017].

Dollard, S.C., Grosse, S.D. & Ross, D.S., 2007. New estimates of the prevalence of neurological and sensory sequelae and mortality associated with congenital cytomegalovirus infection. *Reviews in Medical Virology*, 17(5), pp.355–363. Available at: http://www.ncbi.nlm.nih.gov/pubmed/17542052 [Accessed February 2, 2017].

Doronin, K. et al., 2012. Coagulation factor X activates innate immunity to human species C adenovirus. *Science (New York, N.Y.)*, 338(6108), pp.795–8. Available at: http://www.ncbi.nlm.nih.gov/pubmed/23019612 [Accessed March 21, 2017].

Drew, W.L., 2007. Laboratory diagnosis of cytomegalovirus infection and disease in immunocompromised patients. *Current Opinion in Infectious Diseases*, 20(4), pp.408–411. Available at: http://www.ncbi.nlm.nih.gov/pubmed/17609601 [Accessed February 2, 2017].

Dunn, W. et al., 2003. Functional profiling of a human cytomegalovirus genome. *Proceedings of the National Academy of Sciences of the United States of America*, 100(24), pp.14223–8. Available at: http://www.pubmedcentral.nih.gov/articlerender.fcgi?artid=283573&tool=pmcentrez&rendertype=abstract.

Dunn, W. et al., 2005. Human cytomegalovirus expresses novel microRNAs during productive viral infection. *Cellular microbiology*, 7(11), pp.1684–1695.

Durrant, L.G., Spendlove, I. & Robins, R.A., 2000. Anti-idiotypic vaccination. In P. L. Stern, P. C. L. Beverley, & M. Carroll, eds. *Cancer Vaccines and Immunotherapy*. Cambridge: Cambridge University Press, pp. 162–173. Available at: https://books.google.co.uk/books?id=CCGg9C5b6ekC&pg=PA162&lpg=PA162&dq=t+helper+cells+recruit+nk+cells+tumour+site&source=bl&ots=TMksX6lRPa&sig=c9wem3wlAK9oj4B7Lja9jta_nLU&hl=en&sa=X&ved=0ahUKEwiaIIfU_o_TAhWGVhoKHQWxAQcQ6AEIVTAJ#v=onepage&q=t helper c [Accessed April 6, 2017].

Egli, A. et al., 2008. Cytomegalovirus-specific T-cell responses and viral replication in kidney transplant recipients. *Journal of Translational Medicine*, 6(1), p.29. Available at: http://translational-medicine.biomedcentral.com/articles/10.1186/1479-5876-6-29 [Accessed September 1, 2017].

Ehlinger, E.P. et al., 2011. Maternal Cytomegalovirus-Specific Immune Responses and Symptomatic Postnatal Cytomegalovirus Transmission in Very Low-Birth-Weight Preterm Infants. *Journal of Infectious Diseases*, 204(11), pp.1672–1682. Available at: http://www.ncbi.nlm.nih.gov/pubmed/21984738 [Accessed February 2, 2017].

Einsele, H. & Hamprecht, K., 2003. Immunotherapy of cytomegalovirus infection after stem-cell transplantation: a new option? *The Lancet*, 362(9393), pp.1343–1344. Available at: http://www.ncbi.nlm.nih.gov/pubmed/14585632 [Accessed February 2, 2017].

Eisen, T. et al., 2014. Naptumomab Estafenatox: Targeted Immunotherapy with a Novel Immunotoxin. *Current Oncology Reports*, 16(2), p.370. Available at: http://www.ncbi.nlm.nih.gov/pubmed/24445502 [Accessed April 11, 2017].

Elkord, E. et al., 2008. CD4+ T-cell recognition of human 5T4 oncofoetal antigen: implications for initial depletion of CD25+ T cells. *Cancer Immunology, Immunotherapy*, 57(6), pp.833–847. Available at: http://www.ncbi.nlm.nih.gov/pubmed/18004564 [Accessed April 10, 2017].

Elkord, E. et al., 2015. Immunological response and overall survival in a subset of advanced renal cell carcinoma patients from a randomized phase 2/3 study of naptumomab estafenatox plus IFN-alpha versus IFN-alpha. *Oncotarget*, 6(6), pp.4428–4439. Available at: http://www.ncbi.nlm.nih.gov/pubmed/25669986 [Accessed April 11, 2017].

Falagas, M.E. et al., 1997. Cytomegalovirus disease is associated with increased cost and hospital length of stay among orthotopic liver transplant recipients. *Transplantation*, 63(11), pp.1595–601. Available at: http://www.ncbi.nlm.nih.gov/pubmed/9197352 [Accessed February 2, 2017].

Falk, K. et al., 1991. Identification of naturally processed viral nonapeptides allows their quantification in infected cells and suggests an allele-specific T cell epitope forecast. *The Journal of experimental medicine*, 174(2), pp.425–34. Available at: http://www.ncbi.nlm.nih.gov/pubmed/1713253 [Accessed July 3, 2017].

Fan, X. et al., 2012. Transient, Inducible, Placenta-Specific Gene Expression in Mice. *Endocrinology*, 153(11), pp.5637–5644. Available at: http://www.ncbi.nlm.nih.gov/pubmed/23011919 [Accessed March 2, 2017].

Fielding, C.A. et al., 2017. Control of immune ligands by members of a cytomegalovirus gene expansion suppresses natural killer cell activation. *eLife*, 6. Available at: http://www.ncbi.nlm.nih.gov/pubmed/28186488 [Accessed August 27, 2017].

Fishman, J.A., 2007. Infection in Solid-Organ Transplant Recipients. *New England*

Journal of Medicine, 357(25), pp.2601–2614. Available at: http://www.ncbi.nlm.nih.gov/pubmed/18094380 [Accessed February 2, 2017].

Fishman, J.A., 2011. Infections in immunocompromised hosts and organ transplant recipients: Essentials. *Liver Transplantation*, 17(S3), pp.S34–S37. Available at: http://doi.wiley.com/10.1002/lt.22378 [Accessed February 2, 2017].

Fooks, A.R. et al., 1995. High-Level Expression of the Measles Virus Nucleocapsid Protein by Using a Replication-Deficient Adenovirus Vector: Induction of an MHC-1-Restricted CTL Response and Protection in a Murine Model. *Virology*, 210(2), pp.456–465. Available at: http://www.ncbi.nlm.nih.gov/pubmed/7618280 [Accessed September 4, 2017].

Freeman, R.B. et al., 2004. Risk factors for cytomegalovirus viremia and disease developing after prophylaxis in high-risk solid-organ transplant recipients. *Transplantation*, 78(12), pp.1765–1773.

Fux, C.A. et al., 2003. Cytomegalovirus-associated acute transverse myelitis in immunocompetent adults. *Clinical microbiology and infection : the official publication of the European Society of Clinical Microbiology and Infectious Diseases*, 9(12), pp.1187–90. Available at: http://www.ncbi.nlm.nih.gov/pubmed/14686983 [Accessed February 2, 2017].

Gabitzsch, E.S. et al., 2010. Anti-tumor immunotherapy despite immunity to adenovirus using a novel adenoviral vector Ad5 [E1-, E2b-]-CEA. *Cancer Immunology, Immunotherapy*, 59(7), pp.1131–1135. Available at: http://www.ncbi.nlm.nih.gov/pubmed/20361185 [Accessed August 6, 2017].

Gabrilovich, D.I., 2006. INGN 201 (Advexin®): adenoviral p53 gene therapy for cancer. *Expert Opinion on Biological Therapy*, 6(8), pp.823–832. Available at: http://www.tandfonline.com/doi/full/10.1517/14712598.6.8.823 [Accessed March 17, 2017].

Gallimore, A. et al., 1998. A protective cytotoxic T cell response to a subdominant epitope is influenced by the stability of the MHC class I/peptide complex and the overall spectrum of viral peptides generated within infected cells. *European Journal of Immunology*, 28(10), pp.3301–3311.

Galon, J. et al., 2006. Type, Density, and Location of Immune Cells Within Human Colorectal Tumors Predict Clinical Outcome. *Science*, 313(5795).

Gamadia, L.E. et al., 2004. Properties of CD4+ T cells in human cytomegalovirus infection. *Human Immunology*, 65(5), pp.486–492. Available at: http://www.ncbi.nlm.nih.gov/pubmed/15172448 [Accessed September 1, 2017].

Gatherer, D. et al., 2011. High-resolution human cytomegalovirus transcriptome. *Proceedings of the National Academy of Sciences of the United States of America*, 108(49), pp.19755–60. Available at: http://www.pubmedcentral.nih.gov/articlerender.fcgi?artid=3241806&tool=pmcentrez&rendertype=abstract.

Genini, E. et al., 2011. Serum antibody response to the gH/gL/pUL128–131 five-

protein complex of human cytomegalovirus (HCMV) in primary and reactivated HCMV infections. *Journal of Clinical Virology*, 52(2), pp.113–118. Available at: http://www.ncbi.nlm.nih.gov/pubmed/21820353 [Accessed March 22, 2017].

Geppert, T.D. & Lipsky, P.E., 1985. Antigen presentation by interferon-gamma-treated endothelial cells and fibroblasts: differential ability to function as antigen-presenting cells despite comparable Ia expression. *Journal of immunology (Baltimore, Md. : 1950)*, 135(6), pp.3750–62. Available at: http://www.ncbi.nlm.nih.gov/pubmed/3934267 [Accessed September 5, 2017].

Germain, R.N., 2002. T-cell development and the CD4–CD8 lineage decision. *Nature Reviews Immunology*, 2(5), pp.309–322. Available at: http://www.nature.com/doifinder/10.1038/nri798 [Accessed August 29, 2017].

Ghosh, S.K. et al., 2013. Expression of underglycosylated MUC1 antigen in cancerous and adjacent normal breast tissues. *Clinical breast cancer*, 13(2), pp.109–18. Available at: http://www.ncbi.nlm.nih.gov/pubmed/23122537 [Accessed April 4, 2017].

Glass, M. et al., 2009. Conditional and reversible disruption of essential herpesvirus proteins. *Nature methods*, 6(8), pp.577–9. Available at: http://dx.doi.org/10.1038/nmeth.1346%5Cnhttp://www.ncbi.nlm.nih.gov/pubmed/19578384.

Goldner, T. et al., 2011. The Novel Anticytomegalovirus Compound AIC246 (Letermovir) Inhibits Human Cytomegalovirus Replication through a Specific Antiviral Mechanism That Involves the Viral Terminase. *Journal of Virology*, 85(20), pp.10884–10893. Available at: http://www.ncbi.nlm.nih.gov/pubmed/21752907 [Accessed February 27, 2017].

Gooden, M.J.M. et al., 2011. The prognostic influence of tumour-infiltrating lymphocytes in cancer: a systematic review with meta-analysis. *British journal of cancer*, 105(1), pp.93–103. Available at: http://www.ncbi.nlm.nih.gov/pubmed/21629244 [Accessed April 7, 2017].

Goodrum, F. et al., 2007. Human cytomegalovirus sequences expressed in latently infected individuals promote a latent infection in vitro. *Blood*, 110(3), pp.937–945. Available at: http://www.ncbi.nlm.nih.gov/pubmed/17440050 [Accessed March 2, 2017].

Goral, S., 2011. The three-signal hypothesis of lymphocyte activation/targets for immunosuppression. *Dialysis & Transplantation*, 40(1), pp.14–16. Available at: http://doi.wiley.com/10.1002/dat.20527 [Accessed September 5, 2017].

Görzer, I. et al., 2010. Deep sequencing reveals highly complex dynamics of human cytomegalovirus genotypes in transplant patients over time. *Journal of virology*, 84(14), pp.7195–7203.

Görzer, I. et al., 2008. Virus load dynamics of individual CMV-genotypes in lung transplant recipients with mixed-genotype infections. *Journal of Medical Virology*, 80(8), pp.1405–1414. Available at: http://www.ncbi.nlm.nih.gov/pubmed/18551598 [Accessed February 3, 2017].

Graham, F.. & Smiley, J., 1977. Characteristics of a Human Cell Line Transformed by D N A from Human Adenovirus Type 5. *J.gen.Virol*, 36(2977), pp.59–72.

Gratacap-Cavallier, B. et al., 1998. Cytomegalovirus seroprevalence in French pregnant women: parity and place of birth as major predictive factors. *European journal of epidemiology*, 14(2), pp.147–152.

Greenberg, P.D., Kern, D.E. & Cheever, M.A., 1985. Therapy of disseminated murine leukemia with cyclophosphamide and immune Lyt-1+,2- T cells. Tumor eradication does not require participation of cytotoxic T cells. *The Journal of experimental medicine*, 161(5), pp.1122–34. Available at: http://www.ncbi.nlm.nih.gov/pubmed/3921652 [Accessed April 2, 2017].

Greijer, A.E., Dekkers, C.A. & Middeldorp, J.M., 2000. Human cytomegalovirus virions differentially incorporate viral and host cell RNA during the assembly process. *Journal of virology*, 74(19), pp.9078–82. Available at: http://www.ncbi.nlm.nih.gov/pubmed/10982353 [Accessed February 21, 2017].

Grey, F. et al., 2005. Identification and Characterization of Human Cytomegalovirus-Encoded MicroRNAs. *Society*, 79(18), pp.12095–12099.

Griffiths, P., Baboonian, C. & Ashby, D., 1985. The demographic characteristics of pregnant women infected with cytomegalovirus. *International journal of epidemiology*, 14(3), pp.447–452.

Griffiths, P.D. et al., 2011. Cytomegalovirus glycoprotein-B vaccine with MF59 adjuvant in transplant recipients: a phase 2 randomised placebo-controlled trial. *Lancet (London, England)*, 377(9773), pp.1256–63. Available at: http://linkinghub.elsevier.com/retrieve/pii/S0140673611601360 [Accessed February 6, 2017].

Griffiths, P.D. & Baboonian, C., 1984. A prospective study of primary cytomegalovirus infection during pregnancy: final report. *British journal of obstetrics and gynaecology*, 91(4), pp.307–15. Available at: http://www.ncbi.nlm.nih.gov/pubmed/6324849 [Accessed February 2, 2017].

Gulley, J.L. et al., 2014. Immune impact induced by PROSTVAC (PSA-TRICOM), a therapeutic vaccine for prostate cancer. *Cancer immunology research*, 2(2), pp.133–41. Available at: http://www.ncbi.nlm.nih.gov/pubmed/24778277 [Accessed April 12, 2017].

Haabeth, O.A.W. et al., 2014. How Do CD4(+) T Cells Detect and Eliminate Tumor Cells That Either Lack or Express MHC Class II Molecules? *Frontiers in immunology*, 5, p.174. Available at: http://www.ncbi.nlm.nih.gov/pubmed/24782871 [Accessed April 6, 2017].

Hahn, G. et al., 1998. Cytomegalovirus remains latent in a common precursor of dendritic and myeloid cells. *Microbiology*, 95, pp.3937–3942. Available at: http://www.pnas.org/content/95/7/3937.full.pdf [Accessed March 2, 2017].

Hall, D.B. & Struhl, K., 2002. The VP16 activation domain interacts with multiple transcriptional components as determined by protein-protein cross-linking in

vivo. *The Journal of biological chemistry*, 277(48), pp.46043–50. Available at: http://www.ncbi.nlm.nih.gov/pubmed/12297514 [Accessed July 12, 2017].

Hamprecht, K. et al., 2008. Cytomegalovirus transmission to preterm infants during lactation. *Journal of Clinical Virology*, 41(3), pp.198–205. Available at: http://www.ncbi.nlm.nih.gov/pubmed/18243784 [Accessed February 2, 2017].

Hamprecht, K. et al., 2001. Epidemiology of transmission of cytomegalovirus from mother to preterm infant by breastfeeding. *The Lancet*, 357(9255), pp.513–518. Available at: http://www.ncbi.nlm.nih.gov/pubmed/11229670 [Accessed February 2, 2017].

Hansen, S.G. et al., 2003. Complete Sequence and Genomic Analysis of Rhesus Cytomegalovirus Complete Sequence and Genomic Analysis of Rhesus Cytomegalovirus. *Journal of Virology*, 77(12), pp.6620–6636.

Hansen, S.G., Sacha, J.B., et al., 2013. Cytomegalovirus vectors violate CD8+ T cell epitope recognition paradigms. *Science*, 340(6135), p.doi:10.1126/science.1237874.

Hansen, S.G. et al., 2009. Effector memory T cell responses are associated with protection of rhesus monkeys from mucosal simian immunodeficiency virus challenge. *Nat.Med.*, 15(3), pp.293–299. Available at: http://www.ncbi.nlm.nih.gov/pubmed/19219024.

Hansen, S.G. et al., 2010. Evasion of CD8+ T Cells Is Critical for Superinfection by Cytomegalovirus. *Science*, 328(5974), pp.102–106. Available at: http://www.ncbi.nlm.nih.gov/pubmed/20360110 [Accessed March 5, 2017].

Hansen, S.G., Piatak, M., et al., 2013. Immune clearance of highly pathogenic SIV infection. *Nature*, 502(7469), pp.100–4. Available at: http://www.pubmedcentral.nih.gov/articlerender.fcgi?artid=3849456&tool=pmcentrez&rendertype=abstract.

Hansen, S.G. et al., 2011. Profound early control of highly pathogenic SIV by an effector memory T-cell vaccine. *Nature*, 473(7348), pp.523–7. Available at: http://www.pubmedcentral.nih.gov/articlerender.fcgi?artid=3102768&tool=pmcentrez&rendertype=abstract.

Hanwell, D.G. et al., 2013. Murine Responses to Recombinant MVA Versus ALVAC Vaccines Against Tumor-associated Antigens, gp100 and 5T4. *Journal of Immunotherapy*, 36(4), pp.238–247. Available at: http://content.wkhealth.com/linkback/openurl?sid=WKPTLP:landingpage&an=00002371-201305000-00002 [Accessed July 31, 2017].

Harding, F.A. et al., 1992. CD28-mediated signalling co-stimulates murine T cells and prevents induction of anergy in T-cell clones. *Nature*, 356(6370), pp.607–609. Available at: http://www.ncbi.nlm.nih.gov/pubmed/1313950 [Accessed September 5, 2017].

Harrington, K.J. et al., 2010. Phase I/II Study of Oncolytic HSVGM-CSF in Combination with Radiotherapy and Cisplatin in Untreated Stage III/IV

Squamous Cell Cancer of the Head and Neck. *Clinical Cancer Research*, 16(15), pp.4005–4015. Available at: http://www.ncbi.nlm.nih.gov/pubmed/20670951 [Accessed March 28, 2017].

Harrop, R. et al., 2006. Active treatment of murine tumors with a highly attenuated vaccinia virus expressing the tumor associated antigen 5T4 (TroVax) is CD4+ T cell dependent and antibody mediated. *Cancer Immunology, Immunotherapy*, 55(9), pp.1081–1090. Available at: http://www.ncbi.nlm.nih.gov/pubmed/16311730 [Accessed July 24, 2017].

Harrop, R. et al., 2010. Cross-trial Analysis of Immunologic and Clinical Data Resulting From Phase I and II Trials of MVA-5T4 (TroVax) in Colorectal, Renal, and Prostate Cancer Patients. *Journal of Immunotherapy*, 33(9), pp.999–1005. Available at: http://www.ncbi.nlm.nih.gov/pubmed/20948436 [Accessed April 14, 2017].

Harrop, R. et al., 2013. Vaccination of castration-resistant prostate cancer patients with TroVax (MVA–5T4) in combination with docetaxel: a randomized phase II trial. *Cancer Immunology, Immunotherapy*, 62(9), pp.1511–1520. Available at: http://www.ncbi.nlm.nih.gov/pubmed/23877659 [Accessed April 10, 2017].

Harrop, R. et al., 2007. Vaccination of Colorectal Cancer Patients with Modified Vaccinia Ankara Encoding the Tumor Antigen 5T4 (TroVax) Given Alongside Chemotherapy Induces Potent Immune Responses. *Clinical Cancer Research*, 13(15), pp.4487–4494. Available at: http://www.ncbi.nlm.nih.gov/pubmed/17671134 [Accessed April 10, 2017].

Harty, J.T. & Badovinac, V.P., 2008. Shaping and reshaping CD8+ T-cell memory. *Nature reviews. Immunology*, 8(2), pp.107–19. Available at: http://www.nature.com/doifinder/10.1038/nri2251%5Cnhttp://www.ncbi.nlm.nih.gov/pubmed/18219309.

Harvey, B.G. et al., 1999. Variability of human systemic humoral immune responses to adenovirus gene transfer vectors administered to different organs. *Journal of virology*, 73(8), pp.6729–42. Available at: http://www.ncbi.nlm.nih.gov/pubmed/10400771 [Accessed March 21, 2017].

Haspot, F. et al., 2012. Human Cytomegalovirus Entry into Dendritic Cells Occurs via a Macropinocytosis-Like Pathway in a pH-Independent and Cholesterol-Dependent Manner E. J. Kremer, ed. *PLoS ONE*, 7(4), p.e34795. Available at: http://dx.plos.org/10.1371/journal.pone.0034795 [Accessed February 20, 2017].

Hawkins, R.E. et al., 2016. A Randomized Phase II/III Study of Naptumomab Estafenatox + IFN versus IFN in Renal Cell Carcinoma: Final Analysis with Baseline Biomarker Subgroup and Trend Analysis. *Clinical Cancer Research*, 22(13), pp.3172–3181. Available at: http://www.ncbi.nlm.nih.gov/pubmed/26851187 [Accessed April 11, 2017].

Hawkins, R.E. et al., 2009. Vaccination of Patients With Metastatic Renal Cancer With Modified Vaccinia Ankara Encoding the Tumor Antigen 5T4 (TroVax) Given Alongside Interferon-α. *Journal of Immunotherapy*, 32(4), pp.424–429. Available at: http://www.ncbi.nlm.nih.gov/pubmed/19342962 [Accessed April 10,

2017].

Hecker, M. et al., 2004. Continuous cytomegalovirus seroconversion in a large group of healthy blood donors. *Vox sanguinis*, 86(1), pp.41–4. Available at: http://www.ncbi.nlm.nih.gov/pubmed/14984558 [Accessed February 2, 2017].

Heindorf, M. & Hasan, M.T., 2015. Fluorescent Calcium Indicator Protein Expression in the Brain Using Tetracycline-Responsive Transgenic Mice. *Cold Spring Harbor Protocols*, 2015(7), p.pdb.prot087627. Available at: http://www.ncbi.nlm.nih.gov/pubmed/26134909 [Accessed March 2, 2017].

Heineman, T.C. et al., 2006. A Phase 1 Study of 4 Live, Recombinant Human Cytomegalovirus Towne/Toledo Chimeric Vaccines. *The Journal of Infectious Diseases*, 193(10), pp.1350–1360. Available at: http://www.ncbi.nlm.nih.gov/pubmed/16619181 [Accessed February 2, 2017].

Heinz, N. et al., 2011. Retroviral and Transposon-Based Tet-Regulated All-In-One Vectors with Reduced Background Expression and Improved Dynamic Range. *Human Gene Therapy*, 22(2), pp.166–176. Available at: http://www.ncbi.nlm.nih.gov/pubmed/20825282 [Accessed March 2, 2017].

Henderson, R. et al., 2001. Multicenter US study of hospital resource utilization associated with cytomegalovirus-related readmission of renal and heart transplant patients. *Transplant infectious disease : an official journal of the Transplantation Society*, 3 Suppl 2, pp.57–9. Available at: http://www.ncbi.nlm.nih.gov/pubmed/11926752 [Accessed February 2, 2017].

Heslop, H.E. et al., 1996. Long-term restoration of immunity against Epstein-Barr virus infection by adoptive transfer of gene-modified virus-specific T lymphocytes. *Nature medicine*, 2(5), pp.551–5. Available at: http://www.ncbi.nlm.nih.gov/pubmed/8616714 [Accessed April 7, 2017].

Hewitt, E.W., 2003. The MHC class I antigen presentation pathway: strategies for viral immune evasion. *Immunology*, 110(2), pp.163–9. Available at: http://www.ncbi.nlm.nih.gov/pubmed/14511229 [Accessed September 5, 2017].

Hillen, W. & Berens, C., 1994. Mechanisms Underlying Expression of TN10 Encoded Tetracycline Resistance. *Annual Review of Microbiology*, 48(1), pp.345–369. Available at: http://www.annualreviews.org/doi/10.1146/annurev.mi.48.100194.002021 [Accessed March 10, 2017].

Ho, M., 1990. Epidemiology of Cytomegalovirus Infections. *Clinical Infectious Diseases*, 12(Supplement 7), pp.S701–S710. Available at: https://academic.oup.com/cid/article-lookup/doi/10.1093/clinids/12.Supplement_7.S701 [Accessed February 28, 2017].

Hole, N. & Stern, P.L., 1990. Isolation and characterization of 5T4, a tumour-associated antigen. *International journal of cancer*, 45(1), pp.179–84. Available at: http://www.ncbi.nlm.nih.gov/pubmed/2298503 [Accessed April 11, 2017].

Holst, P.J. et al., 2010. Quality of the Transgene-Specific CD8+ T Cell Response Induced by Adenoviral Vector Immunization Is Critically Influenced by Virus Dose and Route of Vaccination. *The Journal of Immunology*, 184(8), pp.4431–4439. Available at: http://www.ncbi.nlm.nih.gov/pubmed/20212099 [Accessed August 2, 2017].

Holst, P.J. & Thomsen, A.R., 2011. Harnessing the Potential of Adenovirus Vectored Vaccines. In K. Xu, ed. *Viral Gene Therapy*. Rijeka: InTech, pp. 169–192. Available at: http://dx.doi.org/10.5772/22821.

Hörig, H. et al., 2000. Phase I clinical trial of a recombinant canarypoxvirus (ALVAC) vaccine expressing human carcinoembryonic antigen and the B7.1 co-stimulatory molecule. *Cancer immunology, immunotherapy : CII*, 49(9), pp.504–14. Available at: http://www.ncbi.nlm.nih.gov/pubmed/11092617 [Accessed March 28, 2017].

Hotsubo, T. et al., 1994. Detection of human cytomegalovirus DNA in breast milk by means of polymerase chain reaction. *Microbiology and immunology*, 38(10), pp.809–11. Available at: http://www.ncbi.nlm.nih.gov/pubmed/7869960 [Accessed February 2, 2017].

Hsu, K.M. et al., 2009. Murine cytomegalovirus displays selective infection of cells within hours after systemic administration. *The Journal of general virology*, 90(Pt 1), pp.33–43. Available at: http://www.ncbi.nlm.nih.gov/pubmed/19088270 [Accessed July 10, 2017].

Hu, J.C.C. et al., 2006. A Phase I Study of OncoVEXGM-CSF, a Second-Generation Oncolytic Herpes Simplex Virus Expressing Granulocyte Macrophage Colony-Stimulating Factor. *Clinical Cancer Research*, 12(22), pp.6737–6747. Available at: http://www.ncbi.nlm.nih.gov/pubmed/17121894 [Accessed March 28, 2017].

Huang, Y. et al., 2015. Development of all-in-one multicistronic Tet-On lentiviral vectors for inducible co-expression of two transgenes. *Biotechnology and Applied Biochemistry*, 62(1), pp.48–54. Available at: http://www.ncbi.nlm.nih.gov/pubmed/24825511 [Accessed March 2, 2017].

Hwang, T.-H. et al., 2011. A Mechanistic Proof-of-concept Clinical Trial With JX-594, a Targeted Multi-mechanistic Oncolytic Poxvirus, in Patients With Metastatic Melanoma. *Molecular Therapy*, 19(10), pp.1913–1922. Available at: http://www.ncbi.nlm.nih.gov/pubmed/21772252 [Accessed March 28, 2017].

Hyde, T.B., Schmid, D.S. & Cannon, M.J., 2010. Cytomegalovirus seroconversion rates and risk factors: implications for congenital CMV. *Reviews in Medical Virology*, 20(5), pp.311–326. Available at: http://www.ncbi.nlm.nih.gov/pubmed/20645278 [Accessed February 2, 2017].

International Committee on Taxonomy of Viruses (ICTV), 2016. International Committee on Taxonomy of Viruses (ICTV). *Virus Taxonomy: 2016 Release*. Available at: https://talk.ictvonline.org/ [Accessed March 16, 2017].

Ioudinkova, E. et al., 2006. Control of human cytomegalovirus gene expression by differential histone modifications during lytic and latent infection of a monocytic

cell line. *Gene*, 384, pp.120–128. Available at: http://www.sciencedirect.com/science/article/pii/S0378111906004719 [Accessed July 12, 2017].

Ison, M.G., 2006. Adenovirus Infections in Transplant Recipients. *Clinical Infectious Diseases*, 43(3), pp.331–339. Available at: http://www.ncbi.nlm.nih.gov/pubmed/16804849 [Accessed September 13, 2017].

Istas, A.S. et al., 1995. Surveillance for congenital cytomegalovirus disease: a report from the National Congenital Cytomegalovirus Disease Registry. *Clinical infectious diseases : an official publication of the Infectious Diseases Society of America*, 20(3), pp.665–70. Available at: http://www.ncbi.nlm.nih.gov/pubmed/7756493 [Accessed February 2, 2017].

Iuliucci, J.D. et al., 2001. Intravenous safety and pharmacokinetics of a novel dimerizer drug, AP1903, in healthy volunteers. *Journal of clinical pharmacology*, 41(8), pp.870–9. Available at: http://www.ncbi.nlm.nih.gov/pubmed/11504275 [Accessed August 12, 2017].

Iwamoto, M. et al., 2010. A general chemical method to regulate protein stability in the mammalian central nervous system. *Chemistry & biology*, 17(9), pp.981–8. Available at: http://www.ncbi.nlm.nih.gov/pubmed/20851347 [Accessed August 15, 2017].

Iwasenko, J.M. et al., 2011. Human Cytomegalovirus Infection Is Detected Frequently in Stillbirths and Is Associated With Fetal Thrombotic Vasculopathy. *Journal of Infectious Diseases*, 203(11), pp.1526–1533. Available at: http://www.ncbi.nlm.nih.gov/pubmed/21592980 [Accessed February 2, 2017].

Jackson, S.E., Mason, G.M. & Wills, M.R., 2011. Human cytomegalovirus immunity and immune evasion. *Virus research*, 157(2), pp.151–160.

Jacobs, S.C., Stephenson, J.R. & Wilkinson, G.W.G., 1994. Protection elicited by a replication-defective adenovirus vector expressing the tick-borne encephalitis virus non-structural glycoprotein NS1. *Journal of General Virology*, 75(9), pp.2399–2402. Available at: http://www.ncbi.nlm.nih.gov/pubmed/8077939 [Accessed September 4, 2017].

Jacobson, M.A. et al., 2006. Antigen-specific T cell responses induced by Towne cytomegalovirus (CMV) vaccine in CMV-seronegative vaccine recipients. *Journal of Clinical Virology*, 35(3), pp.332–337. Available at: http://www.ncbi.nlm.nih.gov/pubmed/16387547 [Accessed February 2, 2017].

Jiang, B.C. et al., 2012. Doxycycline-regulated growth hormone gene expression system for swine. *Genetics and Molecular Research*, 11(3), pp.2946–2957. Available at: http://www.ncbi.nlm.nih.gov/pubmed/22869070 [Accessed March 2, 2017].

Jiang, H.-R. et al., 2006. Combination of vaccination and chimeric receptor expressing T cells provides improved active therapy of tumors. *Journal of immunology (Baltimore, Md. : 1950)*, 177(7), pp.4288–98. Available at:

http://www.ncbi.nlm.nih.gov/pubmed/16982863.

Jim, W.-T. et al., 2004. Transmission of cytomegalovirus from mothers to preterm infants by breast milk. *The Pediatric infectious disease journal*, 23(9), pp.848–51. Available at: http://www.ncbi.nlm.nih.gov/pubmed/15361725 [Accessed February 2, 2017].

Johnson, L.A. et al., 2009. Gene therapy with human and mouse T-cell receptors mediates cancer regression and targets normal tissues expressing cognate antigen. *Blood*, 114(3), pp.535–546.

Jones, E.Y. et al., 2006. MHC class II proteins and disease: a structural perspective. *Nature Reviews Immunology*, 6(4), pp.271–282. Available at: http://www.nature.com/doifinder/10.1038/nri1805 [Accessed September 5, 2017].

Jonjić, S. et al., 1994. Antibodies are not essential for the resolution of primary cytomegalovirus infection but limit dissemination of recurrent virus. *The Journal of experimental medicine*, 179(5), pp.1713–7. Available at: http://www.ncbi.nlm.nih.gov/pubmed/8163949 [Accessed February 3, 2017].

Jonjić, S. et al., 1990. Efficacious control of cytomegalovirus infection after long-term depletion of CD8+ T lymphocytes. *Journal of virology*, 64(11), pp.5457–64. Available at: http://www.ncbi.nlm.nih.gov/pubmed/1976821 [Accessed September 1, 2017].

Jordan, S. et al., 2011. Virus progeny of murine cytomegalovirus bacterial artificial chromosome pSM3fr show reduced growth in salivary Glands due to a fixed mutation of MCK-2. *Journal of virology*, 85(19), pp.10346–53. Available at: http://www.ncbi.nlm.nih.gov/pubmed/21813614 [Accessed July 6, 2017].

Kagermeier-Schenk, B. et al., 2011. Waif1/5T4 Inhibits Wnt/β-Catenin Signaling and Activates Noncanonical Wnt Pathways by Modifying LRP6 Subcellular Localization. *Developmental Cell*, 21(6), pp.1129–1143. Available at: http://www.ncbi.nlm.nih.gov/pubmed/22100263 [Accessed April 10, 2017].

Kaiser, W.J., Upton, J.W. & Mocarski, E.S., 2008. Receptor-interacting protein homotypic interaction motif-dependent control of NF-kappa B activation via the DNA-dependent activator of IFN regulatory factors. *Journal of immunology (Baltimore, Md. : 1950)*, 181(9), pp.6427–6434.

Karan, D. et al., 2011. Dual antigen target-based immunotherapy for prostate cancer eliminates the growth of established tumors in mice. *Immunotherapy*, 3(6), pp.735–746. Available at: http://www.ncbi.nlm.nih.gov/pubmed/21668311 [Accessed August 6, 2017].

Karrer, U. et al., 2004. Expansion of Protective CD8 ♀ T-Cell Responses Driven by Recombinant Cytomegaloviruses. *JOURNAL OF VIROLOGY*, 78(5), pp.2255–2264.

Karrer, U. et al., 2003. Memory inflation: continuous accumulation of antiviral CD8+ T cells over time. *Journal of immunology (Baltimore, Md. : 1950)*, 170(4),

pp.2022–9. Available at: http://www.ncbi.nlm.nih.gov/pubmed/12574372 [Accessed March 3, 2017].

Kattenhorn, L.M. et al., 2004. Identification of Proteins Associated with Murine Cytomegalovirus Virions. *Society*, 78(20), pp.11187–11197. Available at: http://jvi.asm.org/cgi/content/abstract/78/20/11187.

Kaufman, H.L. et al., 2010. Local and Distant Immunity Induced by Intralesional Vaccination with an Oncolytic Herpes Virus Encoding GM-CSF in Patients with Stage IIIc and IV Melanoma. *Annals of Surgical Oncology*, 17(3), pp.718–730. Available at: http://www.ncbi.nlm.nih.gov/pubmed/19915919 [Accessed March 28, 2017].

Kaye, S. et al., 2008. Virological and Immunological Correlates of Mother- to- Child Transmission of Cytomegalovirus in The Gambia. *The Journal of Infectious Diseases*, 197(9), pp.1307–1314. Available at: http://www.ncbi.nlm.nih.gov/pubmed/18422443 [Accessed February 2, 2017].

Keck, S. et al., 2014. Antigen affinity and antigen dose exert distinct influences on CD4 T-cell differentiation. *Proceedings of the National Academy of Sciences of the United States of America*, 111(41), pp.14852–7. Available at: http://www.ncbi.nlm.nih.gov/pubmed/25267612 [Accessed September 5, 2017].

Keil, G.M., Ebeling-Keil, A. & Koszinowski, U.H., 1987. Immediate-early genes of murine cytomegalovirus: location, transcripts, and translation products. *Journal of virology*, 61(2), pp.526–33. Available at: http://www.pubmedcentral.nih.gov/articlerender.fcgi?artid=253977&tool=pmcentrez&rendertype=abstract.

Kelly, C., Van Driel, R. & Wilkinson, G.W.G., 1995. Disruption of PML-associated nuclear bodies during human cytomegalovirus infection. *Journal of General Virology*, 76(11), pp.2887–2893. Available at: http://www.ncbi.nlm.nih.gov/pubmed/7595400 [Accessed August 30, 2017].

Kenneson, A. & Cannon, M.J., 2007. Review and meta-analysis of the epidemiology of congenital cytomegalovirus (CMV) infection. *Reviews in Medical Virology*, 17(4), pp.253–276. Available at: http://www.ncbi.nlm.nih.gov/pubmed/17579921 [Accessed February 2, 2017].

Kerk, S.A. et al., 2016. 5T4-Targeted Therapy Ablates Cancer Stem Cells and Prevents Recurrence of Head and Neck Squamous Cell Carcinoma. *Clinical Cancer Research*. Available at: http://www.ncbi.nlm.nih.gov/pubmed/27780858 [Accessed April 10, 2017].

Khan, N. et al., 2002. Cytomegalovirus seropositivity drives the CD8 T cell repertoire toward greater clonality in healthy elderly individuals. *Journal of immunology (Baltimore, Md. : 1950)*, 169(4), pp.1984–92. Available at: http://www.ncbi.nlm.nih.gov/pubmed/12165524 [Accessed March 3, 2017].

Khan, S. et al., 2017. Development of a replication-deficient adenoviral vector-based vaccine candidate for the interception of HPV16- and HPV18-induced infections and disease. *International Journal of Cancer*. Available at:

http://www.ncbi.nlm.nih.gov/pubmed/28263390 [Accessed March 16, 2017].

Kharfan-Dabaja, M.A. et al., 2012. A novel therapeutic cytomegalovirus DNA vaccine in allogeneic haemopoietic stem-cell transplantation: A randomised, double-blind, placebo-controlled, phase 2 trial. *The Lancet Infectious Diseases*, 12(4), pp.290–299. Available at: http://dx.doi.org/10.1016/S1473-3099(11)70344-9.

Kidney Disease: Improving Global Outcomes (KDIGO) Transplant Work Group, 2009. Special Issue: KDIGO Clinical Practice Guideline for the Care of Kidney Transplant Recipients. *American Journal of Transplantation*, 9, pp.S1–S155. Available at: http://www.ncbi.nlm.nih.gov/pubmed/19845597 [Accessed February 2, 2017].

Kim, D.W. et al., 2010. TroVax, a recombinant modified vaccinia Ankara virus encoding 5T4: lessons learned and future development. *Human vaccines*, 6(10), pp.784–91. Available at: http://www.ncbi.nlm.nih.gov/pubmed/20975327 [Accessed March 28, 2017].

Kim, J., Kim, A.-R. & Shin, E.-C., 2015. Cytomegalovirus Infection and Memory T Cell Inflation. *Immune network*, 15(4), pp.186–90. Available at: http://www.ncbi.nlm.nih.gov/pubmed/26330804 [Accessed March 23, 2017].

Klenerman, P. & Oxenius, A., 2016. T cell responses to cytomegalovirus. *Nature reviews. Immunology*, 16(6), pp.367–77. Available at: http://www.ncbi.nlm.nih.gov/pubmed/27108521.

Klyushnenkova, E.N. et al., 2012. A cytomegalovirus-based vaccine expressing a single tumor- specific CD8 + T cell epitope delays tumor growth in a murine model of prostate cancer. *J Immunother*, 35(5), pp.390–399.

Kondo, K. et al., 1996. Human cytomegalovirus latent gene expression in granulocyte- macrophage progenitors in culture and in seropositive individuals. *Microbiology*, 93, pp.11137–11142. Available at: https://www.ncbi.nlm.nih.gov/pmc/articles/PMC38297/pdf/pnas01524-0610.pdf [Accessed August 7, 2017].

Kondo, K., Kaneshima, H. & Mocarski, E.S., 1994. Human cytomegalovirus latent infection of granulocyte-macrophage progenitors. *Proceedings of the National Academy of Sciences of the United States of America*, 91(25), pp.11879–83. Available at: http://www.ncbi.nlm.nih.gov/pubmed/7991550 [Accessed March 2, 2017].

Kotton, C.N. et al., 2010. International Consensus Guidelines on the Management of Cytomegalovirus in Solid Organ Transplantation. *Transplantation*, 89(7), pp.779–795. Available at: http://www.ncbi.nlm.nih.gov/pubmed/20224515 [Accessed February 2, 2017].

Krebs, P. et al., 2005. Rapid Functional Exhaustion and Deletion of CTL following Immunization with Recombinant Adenovirus. *The Journal of Immunology*, 174(8). Available at: http://www.jimmunol.org/content/174/8/4559.long [Accessed July 31, 2017].

Krishnapuram, R. et al., 2013. Doxycycline-Regulated 3T3-L1 Preadipocyte Cell Line with Inducible, Stable Expression of Adenoviral E4orf1 Gene: A Cell Model to Study Insulin-Independent Glucose Disposal M. Kanzaki, ed. *PLoS ONE*, 8(3), p.e60651. Available at: http://www.ncbi.nlm.nih.gov/pubmed/23544159 [Accessed March 2, 2017].

Krmpotic, A. et al., 1999. The Immunoevasive Function Encoded by the Mouse Cytomegalovirus Gene m152 Protects the Virus against T Cell Control in Vivo. *Journal of Experimental Medicine*, 190(9).

Kuhns, M.S., Davis, M.M. & Garcia, K.C., 2006. Deconstructing the Form and Function of the TCR/CD3 Complex. *Immunity*, 24(2), pp.133–139. Available at: http://linkinghub.elsevier.com/retrieve/pii/S1074761306001051 [Accessed September 5, 2017].

Kumar, A. & Herbein, G., 2014. Epigenetic regulation of human cytomegalovirus latency: an update. *Epigenomics*, 6(5), pp.533–546. Available at: http://www.futuremedicine.com/doi/10.2217/epi.14.41 [Accessed February 28, 2017].

Kumar, M.L. et al., 1984. Congenital and postnatally acquired cytomegalovirus infections: long-term follow-up. *The Journal of pediatrics*, 104(5), pp.674–9. Available at: http://www.ncbi.nlm.nih.gov/pubmed/6325654 [Accessed February 2, 2017].

Kwon, Y. et al., 2012. Inhibition of p53 transcriptional activity by human cytomegalovirus UL44. *Microbiology and Immunology*, 56(5), pp.324–331.

Lacroix, C. et al., 2011. FLP/FRT-mediated conditional mutagenesis in pre-erythrocytic stages of Plasmodium berghei. *Nature Protocols*, 6(9), pp.1412–1428. Available at: http://www.nature.com/doifinder/10.1038/nprot.2011.363 [Accessed July 27, 2017].

Lamers, C.H.J. et al., 2006. Treatment of Metastatic Renal Cell Carcinoma With Autologous T-Lymphocytes Genetically Retargeted Against Carbonic Anhydrase IX: First Clinical Experience. *Journal of Clinical Oncology*, 24(13), pp.e20–e22. Available at: http://www.ncbi.nlm.nih.gov/pubmed/16648493 [Accessed April 7, 2017].

Lanari, M. et al., 2006. Neonatal Cytomegalovirus Blood Load and Risk of Sequelae in Symptomatic and Asymptomatic Congenitally Infected Newborns. *PEDIATRICS*, 117(1), pp.e76–e83. Available at: http://www.ncbi.nlm.nih.gov/pubmed/16326692 [Accessed February 2, 2017].

Lechner, M.G. et al., 2013. Immunogenicity of murine solid tumor models as a defining feature of in vivo behavior and response to immunotherapy. *Journal of immunotherapy (Hagerstown, Md. : 1997)*, 36(9), pp.477–89. Available at: http://www.ncbi.nlm.nih.gov/pubmed/24145359 [Accessed July 31, 2017].

Legendre, C.M. et al., 2000. Valaciclovir prophylaxis of cytomegalovirus infection and disease in renal transplantation: an economic evaluation. *Transplantation*, 70(10), pp.1463–8. Available at: http://www.ncbi.nlm.nih.gov/pubmed/11118091

[Accessed February 2, 2017].

Lemckert, A.A.C. et al., 2005. Immunogenicity of heterologous prime-boost regimens involving recombinant adenovirus serotype 11 (Ad11) and Ad35 vaccine vectors in the presence of anti-ad5 immunity. *Journal of virology*, 79(15), pp.9694–701. Available at: http://www.ncbi.nlm.nih.gov/pubmed/16014931 [Accessed July 21, 2017].

Leveque, D., 2014. Subcutaneous administration of anticancer agents. *Anticancer research*, 34(4), pp.1579–86. Available at: http://www.ncbi.nlm.nih.gov/pubmed/24692685 [Accessed August 14, 2017].

Li, X. et al., 2010. Efficient Treg depletion induces T-cell infiltration and rejection of large tumors. *European Journal of Immunology*, 40(12), pp.3325–3335. Available at: http://doi.wiley.com/10.1002/eji.201041093 [Accessed April 7, 2017].

Littler, E., Stuart, A.D. & Chee, M.S., 1992. Human cytomegalovirus UL97 open reading frame encodes a protein that phosphorylates the antiviral nucleoside analogue ganciclovir. *Nature*, 358(6382), pp.160–162. Available at: http://www.ncbi.nlm.nih.gov/pubmed/1319559 [Accessed February 2, 2017].

Liu, Q. & Muruve, D.A., 2003. Molecular basis of the inflammatory response to adenovirus vectors. *Gene Therapy*, 10(11), pp.935–940. Available at: http://www.nature.com/gt/journal/v10/n11/pdf/3302036a.pdf [Accessed March 20, 2017].

Liu, S.T.H. et al., 2011. Synaptic vesicle-like lipidome of human cytomegalovirus virions reveals a role for SNARE machinery in virion egress. *Proceedings of the National Academy of Sciences of the United States of America*, 108(31), pp.12869–12874.

Lučin, P. et al., 1992. Gamma interferon-dependent clearance of cytomegalovirus infection in salivary glands. *Journal of Virology*, 66(4), pp.1977–1984. Available at: https://www.scopus.com/inward/record.uri?eid=2-s2.0-0026525006&partnerID=40&md5=86d0a877b53868fd9e9e3fc5173aa09f.

Luoma, A.M., Castro, C.D. & Adams, E.J., 2014. Gamma delta T cell surveillance via CD1 molecules. Available at: http://www.cell.com/trends/immunology/pdf/S1471-4906(14)00154-9.pdf [Accessed April 6, 2017].

Ma, G. et al., 2009. Gene medicine for cancer treatment: commercially available medicine and accumulated clinical data in China. *Drug design, development and therapy*, 2, pp.115–22. Available at: http://www.ncbi.nlm.nih.gov/pubmed/19920899 [Accessed March 17, 2017].

Magri, G. et al., 2011. NKp46 and DNAM-1 NK cell receptors drive the response to human cytomegalovirus infected myeloid dendritic cells overcoming viral immune evasion strategies. *Blood*, 117(3), pp.848–856. Available at: http://www.ncbi.nlm.nih.gov/pubmed/21030563.

Manning, W.C. & Mocarski, E.S., 1988. Insertional mutagenesis of the murine cytomegalovirus genome: one prominent alpha gene (ie2) is dispensable for growth. *Virology*, 167(2), pp.477–84. Available at: http://www.ncbi.nlm.nih.gov/pubmed/2849236 [Accessed May 15, 2017].

Markomichelakis, N.N. et al., 2002. Cytomegalovirus as a cause of anterior uveitis with sectoral iris atrophy. *Ophthalmology*, 109(5), pp.879–82. Available at: http://www.ncbi.nlm.nih.gov/pubmed/11986091 [Accessed February 2, 2017].

Marshall, E.E. et al., 2009. Essential role for either TRS1 or IRS1 in human cytomegalovirus replication. *Journal of virology*, 83(9), pp.4112–4120.

Marshall, E.E. & Geballe, A.P., 2009. Multifaceted evasion of the interferon response by cytomegalovirus. *Journal of interferon & cytokine research : the official journal of the International Society for Interferon and Cytokine Research*, 29(9), pp.609–619.

Mason, G.M. et al., 2013. Human Cytomegalovirus Latency-Associated Proteins Elicit Immune-Suppressive IL-10 Producing CD4+ T Cells C. M. Rooney, ed. *PLoS Pathogens*, 9(10), p.e1003635. Available at: http://dx.plos.org/10.1371/journal.ppat.1003635 [Accessed February 28, 2017].

Matsuzaki, J. et al., 2015. Direct tumor recognition by a human CD4+ T-cell subset potently mediates tumor growth inhibition and orchestrates anti-tumor immune responses. *Scientific Reports*, 5, p.14896. Available at: http://www.nature.com/articles/srep14896 [Accessed March 27, 2017].

Maude, S.L. et al., 2014. Chimeric antigen receptor T cells for sustained remissions in leukemia. *The New England journal of medicine*, 371(16), pp.1507–17. Available at: http://www.ncbi.nlm.nih.gov/pubmed/25317870 [Accessed March 25, 2017].

Maul, G.G. & Negorev, D., 2008. Differences between mouse and human cytomegalovirus interactions with their respective hosts at immediate early times of the replication cycle. *Medical Microbiology and Immunology*, 197(2), pp.241–249. Available at: http://link.springer.com/10.1007/s00430-008-0078-1 [Accessed February 28, 2017].

Mauskopf, J.A. et al., 2000. Cost-effectiveness model of cytomegalovirus management strategies in renal transplantation. Comparing valaciclovir prophylaxis with current practice. *PharmacoEconomics*, 18(3), pp.239–51. Available at: http://www.ncbi.nlm.nih.gov/pubmed/11147391 [Accessed February 2, 2017].

McGinn, O.J. et al., 2017. Targeting the 5T4 oncofoetal glycoprotein with an antibody drug conjugate (A1mcmmaf) improves survival in patient derived xenograft models of acute lymphoblastic leukemia. *Haematologica*. Available at: http://www.haematologica.org/content/early/2017/03/17/haematol.2016.158485 [Accessed April 11, 2017].

McSharry, B., Avdic, S. & Slobedman, B., 2012. Human Cytomegalovirus Encoded Homologs of Cytokines, Chemokines and their Receptors: Roles in

Immunomodulation. *Viruses*, 4(12), pp.2448–2470. Available at: http://www.ncbi.nlm.nih.gov/pubmed/23202490 [Accessed February 24, 2017].

McSharry, B.P. et al., 2008. Adenovirus E3/19K promotes evasion of NK cell recognition by intracellular sequestration of the NKG2D ligands major histocompatibility complex class I chain-related proteins A and B. *Journal of virology*, 82(9), pp.4585–4594.

McSharry, B.P. et al., 2001. Human telomerase reverse transcriptase-immortalized MRC-5 and HCA2 human fibroblasts are fully permisive for human cytomegalovirus. *Journal of General Virology*, 82(Pt 4), pp.855–863.

Melnick, M. et al., 2012. Human cytomegalovirus and mucoepidermoid carcinoma of salivary glands: Cell-specific localization of active viral and oncogenic signaling proteins is confirmatory of a causal relationship. *Experimental and Molecular Pathology*, 92(1), pp.118–125. Available at: http://dx.doi.org/10.1016/j.yexmp.2011.10.011.

Mendelson, M. et al., 1996. Detection of endogenous human cytomegalovirus in CD34+ bone marrow progenitors. *Journal of General Virology*, 77(12), pp.3099–3102. Available at: http://www.microbiologyresearch.org/docserver/fulltext/jgv/77/12/JV0770123099.pdf?expires=1503591937&id=id&accname=sgid026269&checksum=E5E8184275D037772DF40BEAE188409A [Accessed August 24, 2017].

Mendez, R. et al., 2009. HLA and melanoma: multiple alterations in HLA class I and II expression in human melanoma cell lines from ESTDAB cell bank. *Cancer Immunology, Immunotherapy*, 58(9), pp.1507–1515. Available at: http://www.ncbi.nlm.nih.gov/pubmed/19340423 [Accessed April 6, 2017].

Messerle, M. et al., 1992. Structural organization, expression, and functional characterization of the murine cytomegalovirus immediate-early gene 3. *Journal of virology*, 66(1), pp.27–36. Available at: http://www.ncbi.nlm.nih.gov/pubmed/1309246 [Accessed March 3, 2017].

Messerle, M., Keil, G.M. & Koszinowski, U.H., 1991. Structure and expression of murine cytomegalovirus immediate-early gene 2. *Journal of virology*, 65(3), pp.1638–43. Available at: http://www.ncbi.nlm.nih.gov/pubmed/1847480 [Accessed May 15, 2017].

Meyers, J.D. et al., 1988. Acyclovir for Prevention of Cytomegalovirus Infection and Disease after Allogeneic Marrow Transplantation. *New England Journal of Medicine*, 318(2), pp.70–75. Available at: http://www.ncbi.nlm.nih.gov/pubmed/2827025 [Accessed February 27, 2017].

Miller, P.J. & Collins, E.J., 2006. Immunodominance: The Choice of the Immune System. In J. A. Frelinger, ed. *Immunodominance: The Choice of the Immune System*. Weinheim, FRG: Wiley-VCH Verlag GmbH & Co. KGaA, pp. 1–30. Available at: http://doi.wiley.com/10.1002/3527608028 [Accessed July 3, 2017].

Mocarski, E. et al., 2013. Cytomegalovirus. In D. M. Kipe & P. M. Howley, eds. *Fields Virology Vol II*. Philadelphia: Lippincott, Williams & Wilkins, pp. 1960–2014.

Mocarski Jr., E.S., 2007. *Betaherpes viral genes and their functions*, Cambridge University Press. Available at: http://www.ncbi.nlm.nih.gov/pubmed/21348118 [Accessed February 15, 2017].

Mofenson, L.M. et al., 2009. Guidelines for the Prevention and Treatment of Opportunistic Infections among HIV-exposed and HIV-infected children: recommendations from CDC, the National Institutes of Health, the HIV Medicine Association of the Infectious Diseases Society of America, t. *MMWR. Recommendations and reports : Morbidity and mortality weekly report. Recommendations and reports*, 58(RR-11), pp.1–166.

Mohr, C.A. et al., 2010. A spread-deficient cytomegalovirus for assessment of first-target cells in vaccination. *Journal of virology*, 84(15), pp.7730–42. Available at: http://jvi.asm.org/content/84/15/7730.full.pdf [Accessed August 3, 2017].

Morelli, A.E. et al., 2000. Recombinant adenovirus induces maturation of dendritic cells via an NF-kappaB-dependent pathway. *Journal of virology*, 74(20), pp.9617–28. Available at: http://www.ncbi.nlm.nih.gov/pubmed/11000234 [Accessed March 24, 2017].

Morgan, R.A. et al., 2006. Cancer Regression in Patients After Transfer of Genetically Engineered Lymphocytes. *Science*, 314(5796), pp.126–129. Available at: http://www.ncbi.nlm.nih.gov/pubmed/16946036 [Accessed April 7, 2017].

Mulder, D.J. et al., 2011. Antigen Presentation and MHC Class II Expression by Human Esophageal Epithelial Cells. *The American Journal of Pathology*, 178(2), pp.744–753. Available at: http://www.ncbi.nlm.nih.gov/pubmed/21281807 [Accessed September 5, 2017].

Mulryan, K. et al., 2002. Attenuated recombinant vaccinia virus expressing oncofetal antigen (tumor-associated antigen) 5T4 induces active therapy of established tumors. *Molecular cancer therapeutics*, 1(12), pp.1129–37. Available at: http://www.ncbi.nlm.nih.gov/pubmed/12481437 [Accessed May 26, 2017].

Murphy, E. et al., 2003. Coding potential of laboratory and clinical strains of human cytomegalovirus. *Proceedings of the National Academy of Sciences of the United States of America*, 100(25), pp.14976–81. Available at: http://www.pubmedcentral.nih.gov/articlerender.fcgi?artid=299866&tool=pmcentrez&rendertype=abstract.

Murphy, E. et al., 2003. Reevaluation of human cytomegalovirus coding potential. *Proceedings of the National Academy of Sciences*, 100(23), pp.13585–13590. Available at: http://www.ncbi.nlm.nih.gov/pubmed/14593199 [Accessed February 3, 2017].

Murrell, I. et al., 2016. Genetic stability of bacterial artificial chromosome-derived human cytomegalovirus during culture in vitro. *Journal of Virology*, 90(8).

Murrell, I. et al., 2013. Impact of sequence variation in the UL128 locus on production of human cytomegalovirus in fibroblast and epithelial cells. *Journal of virology*, 87(19), pp.10489–500. Available at:

http://www.pubmedcentral.nih.gov/articlerender.fcgi?artid=3807394&tool=pmcentrez&rendertype=abstract.

Muruve, D.A. et al., 1999. Adenoviral Gene Therapy Leads to Rapid Induction of Multiple Chemokines and Acute Neutrophil-Dependent Hepatic Injury in Vivo. *Human Gene Therapy*, 10(6), pp.965–976. Available at: http://www.liebertonline.com/doi/abs/10.1089/10430349950018364 [Accessed August 7, 2017].

Mussi- Pinhata, M.M. et al., 2009. Birth Prevalence and Natural History of Congenital Cytomegalovirus Infection in a Highly Seroimmune Population. *Clinical Infectious Diseases*, 49(4), pp.522–528. Available at: http://www.ncbi.nlm.nih.gov/pubmed/19583520 [Accessed February 2, 2017].

Mutnts, K. et al., 1991. The structure of the antigen-binding groove of major histocompatibility complex class I molecules determines specific selection of self-peptides. *Immunology*, 88, pp.11032–11036. Available at: http://www.pnas.org/content/88/24/11032.full.pdf [Accessed July 3, 2017].

Nagarajan, P. & Sinha, S., 2008. Development of an inducible gene expression system for primary murine keratinocytes. *Journal of Dermatological Science*, 49(1), pp.73–84. Available at: http://www.ncbi.nlm.nih.gov/pubmed/17964120 [Accessed March 2, 2017].

Nagy, A., 2000. Cre recombinase: The universal reagent for genome tailoring. *genesis*, 26(2), pp.99–109. Available at: http://doi.wiley.com/10.1002/%28SICI%291526-968X%28200002%2926%3A2%3C99%3A%3AAID-GENE1%3E3.0.CO%3B2-B [Accessed July 27, 2017].

Narumi, K. et al., 2010. Administration route-dependent induction of antitumor immunity by interferon-alpha gene transfer. *Cancer Science*, 101(7), pp.1686–1694. Available at: http://doi.wiley.com/10.1111/j.1349-7006.2010.01578.x [Accessed August 2, 2017].

Nemunaitis, J. & Nemunaitis, J., 2011. Head and neck cancer: Response to p53-based therapeutics D. W. Eisele, ed. *Head & Neck*, 33(1), pp.131–134. Available at: http://www.ncbi.nlm.nih.gov/pubmed/20222046 [Accessed March 17, 2017].

Nichols, W.G. et al., 2002. High Risk of Death Due to Bacterial and Fungal Infection among Cytomegalovirus (CMV)–Seronegative Recipients of Stem Cell Transplants from Seropositive Donors: Evidence for Indirect Effects of Primary CMV Infection. *The Journal of Infectious Diseases*, 185(3), pp.273–282. Available at: https://academic.oup.com/jid/article-lookup/doi/10.1086/338624 [Accessed February 2, 2017].

Nigro, G. et al., 2012. Immunoglobulin Therapy of Fetal Cytomegalovirus Infection Occurring in the First Half of Pregnancy--A Case-Control Study of the Outcome in Children. *Journal of Infectious Diseases*, 205(2), pp.215–227. Available at: http://www.ncbi.nlm.nih.gov/pubmed/22140265 [Accessed February 2, 2017].

Nigro, G. et al., 2005. Passive Immunization during Pregnancy for Congenital Cytomegalovirus Infection. *New England Journal of Medicine*, 353(13), pp.1350–1362. Available at: http://www.ncbi.nlm.nih.gov/pubmed/16192480 [Accessed February 2, 2017].

Novotny, J. et al., 2001. In silico structural and functional analysis of the human cytomegalovirus (HHV5) genome. *Journal of Molecular Biology*, 310(5), pp.1151–1166.

Nwanegbo, E. et al., 2004. Prevalence of neutralizing antibodies to adenoviral serotypes 5 and 35 in the adult populations of The Gambia, South Africa, and the United States. *Clinical and diagnostic laboratory immunology*, 11(2), pp.351–7. Available at: http://www.ncbi.nlm.nih.gov/pubmed/15013987 [Accessed March 20, 2017].

O'Hara, G.A. et al., 2012. Memory T cell inflation: understanding cause and effect. *Trends in Immunology*, 33(2), pp.84–90. Available at: http://linkinghub.elsevier.com/retrieve/pii/S1471490611002018 [Accessed March 5, 2017].

Osborn, J.E. & Walker, D.L., 1971. Virulence and attenuation of murine cytomegalovirus. *Infection and immunity*, 3(2), pp.228–36. Available at: http://www.ncbi.nlm.nih.gov/pubmed/16557958 [Accessed February 4, 2017].

Pachnio, A. et al., 2016. Cytomegalovirus Infection Leads to Development of High Frequencies of Cytotoxic Virus-Specific CD4+ T Cells Targeted to Vascular Endothelium R. F. Kalejta, ed. *PLOS Pathogens*, 12(9), p.e1005832. Available at: http://www.ncbi.nlm.nih.gov/pubmed/27606804 [Accessed March 10, 2017].

Palmer, D.H. et al., 2004. Virus-Directed Enzyme Prodrug Therapy: Intratumoral Administration of a Replication-Deficient Adenovirus Encoding Nitroreductase to Patients With Resectable Liver Cancer. *Journal of Clinical Oncology*, 22(9), pp.1546–1552. Available at: http://www.ncbi.nlm.nih.gov/pubmed/15051757 [Accessed March 17, 2017].

Pannuti, C.S. et al., 1985. Cytomegalovirus mononucleosis in children and adults: differences in clinical presentation. *Scandinavian journal of infectious diseases*, 17(2), pp.153–6. Available at: http://www.ncbi.nlm.nih.gov/pubmed/2992073 [Accessed February 2, 2017].

Pari, G.S., 2008. Nuts and Bolts of Human Cytomegalovirus Lytic DNA Replication. In T. E. Shenk & M. F. Stinski, eds. *Human Cytomegalovirus*. Berlin, Heidelberg: Springer Berlin Heidelberg, pp. 153–166. Available at: http://dx.doi.org/10.1007/978-3-540-77349-8_9.

Park, B.-H. et al., 2008. Use of a targeted oncolytic poxvirus, JX-594, in patients with refractory primary or metastatic liver cancer: a phase I trial. *The Lancet Oncology*, 9(6), pp.533–542. Available at: http://www.ncbi.nlm.nih.gov/pubmed/18495536 [Accessed March 28, 2017].

Park, J.R. et al., 2007. Adoptive Transfer of Chimeric Antigen Receptor Re-directed Cytolytic T Lymphocyte Clones in Patients with Neuroblastoma. *Molecular*

Therapy, 15(4), pp.825–833. Available at: http://www.ncbi.nlm.nih.gov/pubmed/17299405 [Accessed April 7, 2017].

Parks, R.J. et al., 1996. A helper-dependent adenovirus vector system: removal of helper virus by Cre-mediated excision of the viral packaging signal. *Proceedings of the National Academy of Sciences of the United States of America*, 93(24), pp.13565–70. Available at: http://www.ncbi.nlm.nih.gov/pubmed/8942974 [Accessed March 17, 2017].

Pass, R.F. et al., 2009. Vaccine Prevention of Maternal Cytomegalovirus Infection. *New England Journal of Medicine*, 360(12), pp.1191–1199. Available at: http://www.ncbi.nlm.nih.gov/pubmed/19297572 [Accessed February 2, 2017].

Paulson, K.G. et al., 2011. Transcriptome-wide studies of merkel cell carcinoma and validation of intratumoral CD8+ lymphocyte invasion as an independent predictor of survival. *Journal of clinical oncology : official journal of the American Society of Clinical Oncology*, 29(12), pp.1539–46.

Pavic, I. et al., 1993. Participation of endogenous tumour necrosis factor in host resistance to cytomegalovirus infection. *Journal of General Virology*, 74(10), pp.2215–2223. Available at: http://www.ncbi.nlm.nih.gov/pubmed/8105025 [Accessed August 5, 2017].

Pawelec, G. et al., 2009. Cytomegalovirus and human immunosenescence. *Reviews in Medical Virology*, 19(1), pp.47–56. Available at: http://www.ncbi.nlm.nih.gov/pubmed/19035529 [Accessed February 2, 2017].

Peacock, R.W.S., Sullivan, K.A. & Wang, C.L., 2012. Tetracycline-Regulated Expression Implemented through Transcriptional Activation Combined with Proximal and Distal Repression. *ACS Synthetic Biology*, 1(5), pp.156–162. Available at: http://www.ncbi.nlm.nih.gov/pubmed/23651153 [Accessed March 2, 2017].

Pearson, S., Jia, H. & Kandachi, K., 2004. China approves first gene therapy. *Nature Biotechnology*, 22(1), pp.3–4. Available at: http://www.nature.com/doifinder/10.1038/nbt0104-3 [Accessed April 12, 2017].

Peggs, K.S. et al., 2009. Cytomegalovirus- Specific T Cell Immunotherapy Promotes Restoration of Durable Functional Antiviral Immunity following Allogeneic Stem Cell Transplantation. *Clinical Infectious Diseases*, 49(12), pp.1851–1860. Available at: http://www.ncbi.nlm.nih.gov/pubmed/19911966 [Accessed February 2, 2017].

Peggs, K.S. et al., 2011. Directly Selected Cytomegalovirus-Reactive Donor T Cells Confer Rapid and Safe Systemic Reconstitution of Virus-Specific Immunity Following Stem Cell Transplantation. *Clinical Infectious Diseases*, 52(1), pp.49–57. Available at: http://www.ncbi.nlm.nih.gov/pubmed/21148519 [Accessed February 2, 2017].

Pembrey, L. et al., 2013. Seroprevalence of Cytomegalovirus, Epstein Barr Virus and Varicella Zoster Virus among Pregnant Women in Bradford: A Cohort Study M. Nevels, ed. *PLoS ONE*, 8(11), p.e81881. Available at:

http://dx.plos.org/10.1371/journal.pone.0081881 [Accessed February 28, 2017].

Peng, Y., Falck-Pedersen, E. & Elkon, K.B., 2001. Variation in Adenovirus Transgene Expression between BALB/c and C57BL/6 Mice Is Associated with Differences in Interleukin-12 and Gamma Interferon Production and NK Cell Activation. *Journal of Virology*, 75(10), pp.4540–4550. Available at: http://www.ncbi.nlm.nih.gov/pubmed/11312324 [Accessed July 14, 2017].

Peng, Z., 2005. Current Status of Gendicine in China: Recombinant Human Ad-p53 Agent for Treatment of Cancers. *Human Gene Therapy*, 16, pp.1016–1027. Available at: http://online.liebertpub.com/doi/pdf/10.1089/hum.2005.16.1016 [Accessed March 17, 2017].

Pereira, L. & Maidji, E., 2008. Cytomegalovirus infection in the human placenta: maternal immunity and developmentally regulated receptors on trophoblasts converge. *Current topics in microbiology and immunology*, 325, pp.383–95. Available at: http://www.ncbi.nlm.nih.gov/pubmed/18637517 [Accessed February 2, 2017].

Perica, K. et al., 2015. Adoptive T cell immunotherapy for cancer. *Rambam Maimonides medical journal*, 6(1), p.e0004. Available at: http://www.ncbi.nlm.nih.gov/pubmed/25717386 [Accessed March 24, 2017].

Peter, K. et al., 2001. Induction of a cytotoxic T-cell response to HIV-1 proteins with short synthetic peptides and human compatible adjuvants. *Vaccine*, 19(30), pp.4121–9. Available at: http://www.ncbi.nlm.nih.gov/pubmed/11457536 [Accessed July 3, 2017].

Pfeffer, S. et al., 2005. Identification of microRNAs of the herpesvirus family. *Nature methods*, 2(4), pp.269–276.

Piedra, P.A. et al., 1998. Incidence and Prevalence of Neutralizing Antibodies to the Common Adenoviruses in Children With Cystic Fibrosis: Implication for Gene Therapy With Adenovirus Vectors. *Pediatrics*, 101(6), pp.1013–9. Available at: http://www.ncbi.nlm.nih.gov/pubmed/8852455 [Accessed March 20, 2017].

Plotkin, S.A. et al., 1989. Protective effects of Towne cytomegalovirus vaccine against low-passage cytomegalovirus administered as a challenge. *The Journal of infectious diseases*, 159(5), pp.860–5. Available at: http://www.ncbi.nlm.nih.gov/pubmed/2540247 [Accessed February 2, 2017].

van Den Pol, A.N. et al., 1999. Cytomegalovirus cell tropism, replication, and gene transfer in brain. *The Journal of neuroscience : the official journal of the Society for Neuroscience*, 19(24), pp.10948–65. Available at: http://www.ncbi.nlm.nih.gov/pubmed/10594076 [Accessed February 17, 2017].

Poncet, D. et al., 2004. An Anti-apoptotic Viral Protein That Recruits Bax to Mitochondria. *Journal of Biological Chemistry*, 279(21), pp.22605–22614. Available at: http://www.ncbi.nlm.nih.gov/pubmed/15004026 [Accessed February 24, 2017].

Poole, E., Avdic, S., et al., 2014. Latency-associated viral interleukin-10 (IL-10)

encoded by human cytomegalovirus modulates cellular IL-10 and CCL8 Secretion during latent infection through changes in the cellular microRNA hsa-miR-92a. *Journal of virology*, 88(24), pp.13947–55. Available at: http://www.ncbi.nlm.nih.gov/pubmed/25253336 [Accessed February 28, 2017].

Poole, E. et al., 2013. The Myeloid Transcription Factor GATA-2 Regulates the Viral UL144 Gene during Human Cytomegalovirus Latency in an Isolate-Specific Manner. *Journal of Virology*, 87(8), pp.4261–4271. Available at: http://www.ncbi.nlm.nih.gov/pubmed/23365437 [Accessed March 2, 2017].

Poole, E., Wills, M. & Sinclair, J., 2014. Human Cytomegalovirus Latency: Targeting Differences in the Latently Infected Cell with a View to Clearing Latent Infection. *New Journal of Science*, 2014, p.e313761. Available at: http://www.hindawi.com/journals/njos/2014/313761/abs/%5Cnhttp://downloads.hindawi.com/journals/njos/2014/313761.pdf%5Cnhttp://www.hindawi.com/journals/njos/2014/313761/ref/.

Potena, L. & Valantine, H.A., 2007. Cytomegalovirus-associated allograft rejection in heart transplant patients. *Current Opinion in Infectious Diseases*, 20(4), pp.425–431. Available at: http://www.ncbi.nlm.nih.gov/pubmed/17609604 [Accessed February 2, 2017].

Pourgheysari, B. et al., 2007. The Cytomegalovirus-Specific CD4+ T-Cell Response Expands with Age and Markedly Alters the CD4+ T-Cell Repertoire. *Journal of Virology*, 81(14), pp.7759–7765. Available at: http://www.ncbi.nlm.nih.gov/pubmed/17409149 [Accessed March 3, 2017].

Prentice, H.G. et al., 1994. Impact of long-term acyclovir on cytomegalovirus infection and survival after allogeneic bone marrow transplantation. European Acyclovir for CMV Prophylaxis Study Group. *Lancet (London, England)*, 343(8900), pp.749–53. Available at: http://www.ncbi.nlm.nih.gov/pubmed/7907729 [Accessed February 27, 2017].

Prod'homme, V. et al., 2010. Human cytomegalovirus UL141 promotes efficient downregulation of the natural killer cell activating ligand CD112. *The Journal of general virology*, 91(Pt 8), pp.2034–2039.

Prod'homme, V. et al., 2012. Human cytomegalovirus UL40 signal peptide regulates cell surface expression of the NK cell ligands HLA-E and gpUL18. *Journal of immunology (Baltimore, Md. : 1950)*, 188(6), pp.2794–2804.

van Putten, E.H. et al., 2010. Sitimagene ceradenovec: a gene-based drug for the treatment of operable high-grade glioma. *Future Oncology*, 6(11), pp.1691–1710. Available at: http://www.futuremedicine.com/doi/10.2217/fon.10.134 [Accessed March 17, 2017].

Qin, J.Y. et al., 2010. Systematic comparison of constitutive promoters and the doxycycline-inducible promoter. *PLoS ONE*, 5(5), pp.3–6.

Qiu, Z. et al., 2015. Cytomegalovirus-Based Vaccine Expressing a Modified Tumor Antigen Induces Potent Tumor-Specific CD8+ T-cell Response and Protects Mice from Melanoma. *Cancer Immunology Research*, 3(5), pp.536–546.

Available at: http://www.ncbi.nlm.nih.gov/pubmed/25633711 [Accessed February 6, 2017].

Quezada, S.A. et al., 2010. Tumor-reactive CD4 $^{+}$ T cells develop cytotoxic activity and eradicate large established melanoma after transfer into lymphopenic hosts. *The Journal of Experimental Medicine*, 207(3), pp.637–650. Available at: http://www.ncbi.nlm.nih.gov/pubmed/20156971 [Accessed April 2, 2017].

Raghavan, M. et al., 2008. MHC class I assembly: out and about. *Trends in immunology*, 29(9), pp.436–43. Available at: http://www.ncbi.nlm.nih.gov/pubmed/18675588 [Accessed September 5, 2017].

Rawlinson, W.D., Farrell, H.E. & Barrell, B.G., 1996. Analysis of the complete DNA sequence of murine cytomegalovirus. *Journal of virology*, 70(12), pp.8833–49. Available at: http://www.ncbi.nlm.nih.gov/pubmed/8971012 [Accessed February 16, 2017].

Razonable, R.R., 2011. Management of viral infections in solid organ transplant recipients. *Expert Review of Anti-infective Therapy*, 9(6), pp.685–700. Available at: http://www.ncbi.nlm.nih.gov/pubmed/21692673 [Accessed February 2, 2017].

Reddehase, M.J., 2002. Antigens and immunoevasins: opponents in cytomegalovirus immune surveillance. *Nature Reviews Immunology*, 2(11), pp.831–844. Available at: http://www.nature.com/doifinder/10.1038/nri932 [Accessed February 4, 2017].

Redeker, A., Welten, S.P.M. & Arens, R., 2014. Viral inoculum dose impacts memory T-cell inflation. *European Journal of Immunology*, 44(4), pp.1046–1057. Available at: http://www.ncbi.nlm.nih.gov/pubmed/24356925 [Accessed March 22, 2017].

Redwood, A. et al., 2005. Use of a Murine Cytomegalovirus K181-Derived Bacterial Artificial Chromosome as a Vaccine Vector for Immunocontraception. *Journal of Virology*, 79(5), pp.2998–3008.

Reeves, M. & Sinclair, J., 2008. Aspects of human cytomegalovirus latency and reactivation. *Current topics in microbiology and immunology*, 325, pp.297–313.

Reeves, M.B. et al., 2005. An in vitro model for the regulation of human cytomegalovirus latency and reactivation in dendritic cells by chromatin remodelling. *Journal of General Virology*, 86(11), pp.2949–2954. Available at: http://jgv.microbiologyresearch.org/content/journal/jgv/10.1099/vir.0.81161-0 [Accessed March 2, 2017].

Reeves, M.B., 2011. Chromatin-mediated regulation of cytomegalovirus gene expression. *Virus research*, 157(2), pp.134–143.

Reeves, M.B. et al., 2005. Latency, chromatin remodeling, and reactivation of human cytomegalovirus in the dendritic cells of healthy carriers. *Proceedings of the National Academy of Sciences of the United States of America*, 102(11), pp.4140–4145.

Reeves, M.B. & Sinclair, J.H., 2010. Analysis of latent viral gene expression in natural and experimental latency models of human cytomegalovirus and its correlation with histone modifications at a latent promoter. *The Journal of general virology*, 91(Pt 3), pp.599–604.

Renzette, N. et al., 2011. Extensive Genome-Wide Variability of Human Cytomegalovirus in Congenitally Infected Infants. *PLoS Pathogens*, 7(5).

Reppert, S. et al., 2011. A role for T-bet-mediated tumour immune surveillance in anti-IL-17A treatment of lung cancer. *Nature Communications*, 2. Available at: https://www.nature.com/articles/ncomms1609.pdf [Accessed July 5, 2017].

Revello, M.G. & Gerna, G., 2010. Human cytomegalovirus tropism for endothelial/epithelial cells: scientific background and clinical implications. *Reviews in medical virology*, 20(3), pp.136–155.

Reynolds, D.W. et al., 1973. Maternal Cytomegalovirus Excretion and Perinatal Infection. *New England Journal of Medicine*, 289(1), pp.1–5. Available at: http://www.ncbi.nlm.nih.gov/pubmed/4350775 [Accessed February 2, 2017].

Rigoutsos, I. et al., 2003. In silico pattern-based analysis of the human cytomegalovirus genome. *Journal of virology*, 77(7), pp.4326–44. Available at: http://www.ncbi.nlm.nih.gov/pubmed/12634390 [Accessed February 23, 2017].

Rivailler, P. et al., 2006. Genomic sequence of rhesus cytomegalovirus 180.92: insights into the coding potential of rhesus cytomegalovirus. *Journal of virology*, 80(8), pp.4179–4182.

Rocha, N. & Neefjes, J., 2008. MHC class II molecules on the move for successful antigen presentation. *The EMBO journal*, 27(1), pp.1–5. Available at: http://www.ncbi.nlm.nih.gov/pubmed/18046453 [Accessed September 5, 2017].

Roth, J.A., 2006. Adenovirus p53 gene therapy. *Expert Opinion on Biological Therapy*, 6(1), pp.55–61. Available at: http://www.ncbi.nlm.nih.gov/pubmed/16370914 [Accessed March 17, 2017].

Rupp, B. et al., 2005. Conditional Cytomegalovirus Replication In Vitro and In Vivo. *Virology*, 79(1), pp.486–494.

Ruzek, M.C. et al., 2002. Adenoviral Vectors Stimulate Murine Natural Killer Cell Responses and Demonstrate Antitumor Activities in the Absence of Transgene Expression. *Molecular Therapy*, 5(2), pp.115–124. Available at: http://www.ncbi.nlm.nih.gov/pubmed/11829518 [Accessed July 14, 2017].

Ryckman, B.J. et al., 2006. Human cytomegalovirus entry into epithelial and endothelial cells depends on genes UL128 to UL150 and occurs by endocytosis and low-pH fusion. *Journal of virology*, 80(2), pp.710–22. Available at: http://jvi.asm.org/cgi/doi/10.1128/JVI.80.2.710-722.2006 [Accessed February 20, 2017].

Sacher, T. et al., 2012. The role of cell types in cytomegalovirus infection in vivo. *European Journal of Cell Biology*, 91(1), pp.70–77. Available at:

http://linkinghub.elsevier.com/retrieve/pii/S0171933511000331 [Accessed July 26, 2017].

Saffert, R.T. & Kalejta, R.F., 2006. Inactivating a Cellular Intrinsic Immune Defense Mediated by Daxx Is the Mechanism through Which the Human Cytomegalovirus pp71 Protein Stimulates Viral Immediate-Early Gene Expression. *Journal of Virology*, 80(8), pp.3863–3871. Available at: http://www.ncbi.nlm.nih.gov/pubmed/16571803 [Accessed February 24, 2017].

Sakaguchi, S. et al., 2009. Regulatory T cells: how do they suppress immune responses? *International Immunology*, 21(10), pp.1105–1111. Available at: https://academic.oup.com/intimm/article-lookup/doi/10.1093/intimm/dxp095 [Accessed April 6, 2017].

Sangro, B. et al., 2010. A phase I clinical trial of thymidine kinase-based gene therapy in advanced hepatocellular carcinoma. *Cancer Gene Therapy*, 17(12), pp.837–843. Available at: http://www.ncbi.nlm.nih.gov/pubmed/20689572 [Accessed March 17, 2017].

Sato, H. et al., 2004. Syndrome of inappropriate secretion of antidiuretic hormone and thrombocytopenia caused by cytomegalovirus infection in a young immunocompetent woman. *Internal medicine (Tokyo, Japan)*, 43(12), pp.1177–82. Available at: http://www.ncbi.nlm.nih.gov/pubmed/15645654 [Accessed February 2, 2017].

Sato, T., Muroyama, Y. & Saito, T., 2013. Inducible gene expression in postmitotic neurons by an in vivo electroporation-based tetracycline system. *Journal of Neuroscience Methods*, 214(2), pp.170–176. Available at: http://www.ncbi.nlm.nih.gov/pubmed/23357027 [Accessed March 2, 2017].

Savai, R. et al., 2009. Evaluation of Angiogenesis Using Micro-Computed Tomography in a Xenograft Mouse Model of Lung Cancer. *Neoplasia*, 11(1), pp.48–56. Available at: http://linkinghub.elsevier.com/retrieve/pii/S1476558609800882 [Accessed July 5, 2017].

Schagen, F.H.E. et al., 2004. Immune responses against adenoviral vectors and their transgene products: a review of strategies for evasion. *Critical Reviews in Oncology/Hematology*, 50, pp.51–70. Available at: http://ac.els-cdn.com/S1040842803001720/1-s2.0-S1040842803001720-main.pdf?_tid=24cd7cec-0d54-11e7-ac84-00000aab0f6c&acdnat=1490004250_2b870e0e221625f9084d89df2b00a400 [Accessed March 20, 2017].

Schleiss, M.R., 2009. VCL-CB01, an injectable bivalent plasmid DNA vaccine for potential protection against CMV disease and infection. *Current opinion in molecular therapeutics*, 11(5), pp.572–8. Available at: http://www.ncbi.nlm.nih.gov/pubmed/19806506 [Accessed February 27, 2017].

Schnell, M.A. et al., 2001. Activation of Innate Immunity in Nonhuman Primates Following Intraportal Administration of Adenoviral Vectors. *Molecular Therapy*, 3(5), pp.708–722. Available at: http://www.ncbi.nlm.nih.gov/pubmed/11356076

[Accessed August 7, 2017].

Schoenfisch, A.L. et al., 2011. Cytomegalovirus (CMV) shedding is highly correlated with markers of immunosuppression in CMV-seropositive women. *Journal of Medical Microbiology*, 60(6), pp.768–774. Available at: http://www.ncbi.nlm.nih.gov/pubmed/21393456 [Accessed February 2, 2017].

Schopfer, K., Lauber, E. & Krech, U., 1978. Congenital cytomegalovirus infection in newborn infants of mothers infected before pregnancy. *Archives of disease in childhood*, 53(7), pp.536–9. Available at: http://www.ncbi.nlm.nih.gov/pubmed/210722 [Accessed February 2, 2017].

Scurr, M. et al., 2013. Escalating Regulation of 5T4-Specific IFN- + CD4+ T Cells Distinguishes Colorectal Cancer Patients from Healthy Controls and Provides a Target for In Vivo Therapy. *Cancer Immunology Research*, 1(6), pp.416–425. Available at: http://www.ncbi.nlm.nih.gov/pubmed/24409450 [Accessed April 10, 2017].

Seckert, C.K. et al., 2012. Viral latency drives “memory inflation”: A unifying hypothesis linking two hallmarks of cytomegalovirus infection. *Medical Microbiology and Immunology*, 201(4), pp.551–566.

Senzer, N. & Nemunaitis, J., 2009. A review of contusugene ladenovec (Advexin) p53 therapy. *Current opinion in molecular therapeutics*, 11(1), pp.54–61. Available at: http://www.ncbi.nlm.nih.gov/pubmed/19169960 [Accessed March 17, 2017].

Senzer, N.N. et al., 2009. Phase II Clinical Trial of a Granulocyte-Macrophage Colony-Stimulating Factor–Encoding, Second-Generation Oncolytic Herpesvirus in Patients With Unresectable Metastatic Melanoma. *Journal of Clinical Oncology*, 27(34), pp.5763–5771. Available at: http://www.ncbi.nlm.nih.gov/pubmed/19884534 [Accessed March 28, 2017].

Sester, U. et al., 2005. Differences in CMV-Specific T-Cell Levels and Long-Term Susceptibility to CMV Infection after Kidney, Heart and Lung Transplantation. *American Journal of Transplantation*, 5(6), pp.1483–1489. Available at: http://www.ncbi.nlm.nih.gov/pubmed/15888058 [Accessed August 24, 2017].

Sharpe, M. & Mount, N., 2015. Genetically modified T cells in cancer therapy: opportunities and challenges. *Disease models & mechanisms*, 8(4), pp.337–50. Available at: http://www.ncbi.nlm.nih.gov/pubmed/26035842 [Accessed March 25, 2017].

Shaw, D.M. et al., 2002. Glycosylation and epitope mapping of the 5T4 glycoprotein oncofoetal antigen. *The Biochemical journal*, 363(Pt 1), pp.137–145.

Shedlock, D.J. & Shen, H., 2003. Requirement for CD4 T Cell Help in Generating Functional CD8 T Cell Memory. *Science*, 300(5617), pp.337–339. Available at: http://www.ncbi.nlm.nih.gov/pubmed/12690201 [Accessed April 3, 2017].

Shellam, G.R. et al., 2006. Murine Cytomegalovirus and Other Herpesviruses. In J. G. Fox et al., eds. *The Mouse in Biomedical Research: Diseases*. Academic

Press, pp. 1–49.

Shimizu, J., Yamazaki, S. & Sakaguchi, S., 1999. Induction of tumor immunity by removing CD25+CD4+ T cells: a common basis between tumor immunity and autoimmunity. *Journal of immunology (Baltimore, Md. : 1950)*, 163(10), pp.5211–8. Available at: http://www.ncbi.nlm.nih.gov/pubmed/10553041 [Accessed April 7, 2017].

Shklovskaya, E. et al., 2016. Tumour-specific CD4 T cells eradicate melanoma via indirect recognition of tumour-derived antigen. *Immunology and Cell Biology*, 94(6), pp.593–603. Available at: http://www.nature.com/doifinder/10.1038/icb.2016.14 [Accessed March 27, 2017].

Shuster, J., Freedman, S.O. & Gold, P., 1977. Oncofetal antigens. Increasing the specificity of the CEA radioimmunoassay. *American journal of clinical pathology*, 68(5 Suppl), pp.679–87. Available at: http://www.ncbi.nlm.nih.gov/pubmed/72501 [Accessed April 4, 2017].

Sijmons, S. et al., 2015. High-Throughput Analysis of Human Cytomegalovirus Genome Diversity Highlights the Widespread Occurrence of Gene-Disrupting Mutations and Pervasive Recombination. *Journal of Virology*, 89(15), pp.7673–7695. Available at: http://jvi.asm.org/content/89/15/7673.long.

Sinclair, J., 2010. Chromatin structure regulates human cytomegalovirus gene expression during latency, reactivation and lytic infection. *Biochimica et biophysica acta*, 1799(3–4), pp.286–295.

Sinzger, C., 2008. Entry route of HCMV into endothelial cells. *Journal of Clinical Virology*, 41(3), pp.174–179. Available at: http://linkinghub.elsevier.com/retrieve/pii/S1386653207004519 [Accessed July 14, 2017].

Sinzger, C. & Jahn, G., 1996. Human cytomegalovirus cell tropism and pathogenesis. *Intervirology*, 39(5–6), pp.302–19. Available at: http://www.ncbi.nlm.nih.gov/pubmed/9130041 [Accessed February 17, 2017].

Skaletskaya, A. et al., 2001. A cytomegalovirus-encoded inhibitor of apoptosis that suppresses caspase-8 activation. *Proceedings of the National Academy of Sciences of the United States of America*, 98(14), pp.7829–34. Available at: http://www.ncbi.nlm.nih.gov/pubmed/11427719%5Cnhttp://www.pubmedcentral.nih.gov/articlerender.fcgi?artid=PMC35427.

Slavuljica, I. et al., 2010. Recombinant mouse cytomegalovirus expressing a ligand for the NKG2D receptor is attenuated and has improved vaccine properties. *Journal of Clinical Investigation*, 120(12), pp.4532–4545.

Slobedman, B. & Mocarski, E.S., 1999. Quantitative analysis of latent human cytomegalovirus. *Journal of virology*, 73(6), pp.4806–4812.

Smith, C.B., Wei, L.S. & Griffiths, M., 1986. Mouse cytomegalovirus is infectious for rats and alters lymphocyte subsets and spleen cell proliferation. *Archives of*

virology, 90(3–4), pp.313–23. Available at: http://www.ncbi.nlm.nih.gov/pubmed/3015085 [Accessed August 23, 2017].

Smith, H.R. et al., 2000. Nonstochastic coexpression of activation receptors on murine natural killer cells. *The Journal of experimental medicine*, 191(8), pp.1341–1354.

Smith, L.M. et al., 2008. Laboratory strains of murine cytomegalovirus are genetically similar to but phenotypically distinct from wild strains of virus. *Journal of virology*, 82(13), pp.6689–96. Available at: http://www.ncbi.nlm.nih.gov/pubmed/18417589%5Cnhttp://www.pubmedcentral.nih.gov/articlerender.fcgi?artid=PMC2447069.

Smith, L.M. et al., 2013. The genome of murine cytomegalovirus is shaped by purifying selection and extensive recombination. *Virology*, 435(2), pp.258–268. Available at: http://dx.doi.org/10.1016/j.virol.2012.08.041.

Snook, A.E. et al., 2016. Preclinical Evaluation of a Replication-Deficient Recombinant Adenovirus Serotype 5 Vaccine Expressing Guanylate Cyclase C and the PADRE T-helper Epitope. *Human Gene Therapy Methods*, 27(6), pp.238–250. Available at: http://www.ncbi.nlm.nih.gov/pubmed/27903079 [Accessed March 16, 2017].

Snyder, C.M. et al., 2008. Memory inflation during chronic viral infection is maintained by continuous production of short-lived, functional T cells. *Immunity*, 29(4), pp.650–9. Available at: http://www.ncbi.nlm.nih.gov/pubmed/18957267 [Accessed March 23, 2017].

Snyder, C.M. et al., 2011. Sustained CD8+ T cell memory inflation after infection with a single-cycle Cytomegalovirus. *PLoS Pathogens*, 7(10).

Snydman, D.R. et al., 1993. Cytomegalovirus immune globulin prophylaxis in liver transplantation. A randomized, double-blind, placebo-controlled trial. *Annals of internal medicine*, 119(10), pp.984–91. Available at: http://www.ncbi.nlm.nih.gov/pubmed/8214995 [Accessed February 2, 2017].

Snydman, D.R. et al., 2011. Update and Review: State-of-the-Art Management of Cytomegalovirus Infection and Disease Following Thoracic Organ Transplantation. *Transplantation Proceedings*, 43(3), pp.S1–S17. Available at: http://www.ncbi.nlm.nih.gov/pubmed/21482317 [Accessed February 2, 2017].

Sohn, Y.M. et al., 1991. Cytomegalovirus infection in sexually active adolescents. *The Journal of infectious diseases*, 163(3), pp.460–463.

Soroceanu, L. et al., 2011. Human cytomegalovirus US28 found in glioblastoma promotes an invasive and angiogenic phenotype. *Cancer research*, 71(21), pp.6643–6653.

Southall, P.J. et al., 1990. Immunohistological distribution of 5T4 antigen in normal and malignant tissues. *British journal of cancer*, 61(1), pp.89–95. Available at: http://www.ncbi.nlm.nih.gov/pubmed/2404511 [Accessed April 11, 2017].

Southgate, T.D. et al., 2010. CXCR4 Mediated Chemotaxis Is Regulated by 5T4 Oncofetal Glycoprotein in Mouse Embryonic Cells S. A. Aziz, ed. *PLoS ONE*, 5(4), p.e9982. Available at: http://www.ncbi.nlm.nih.gov/pubmed/20376365 [Accessed April 10, 2017].

Spector, D.J. & Tevethia, M.J., 1994. Protein-protein interactions between human cytomegalovirus IE2-580aa and pUL84 in lytically infected cells. *Journal of virology*, 68(11), pp.7549–53. Available at: http://www.ncbi.nlm.nih.gov/pubmed/7933141 [Accessed February 21, 2017].

Sprague, E.R. et al., 2008. The human cytomegalovirus Fc receptor gp68 binds the Fc CH2-CH3 interface of immunoglobulin G. *Journal of virology*, 82(7), pp.3490–3499.

Stagno, S. et al., 1981. Infant pneumonitis associated with cytomegalovirus, Chlamydia, Pneumocystis, and Ureaplasma: a prospective study. *Pediatrics*, 68(3), pp.322–329.

Stagno, S. et al., 1982. Maternal cytomegalovirus infection and perinatal transmission. *Clinical obstetrics and gynecology*, 25(3), pp.563–76. Available at: http://www.ncbi.nlm.nih.gov/pubmed/6290121 [Accessed February 2, 2017].

Stagno, S. et al., 1986. Primary cytomegalovirus infection in pregnancy. Incidence, transmission to fetus, and clinical outcome. *JAMA*, 256(14), pp.1904–1908.

Stanton, R.J. et al., 2008. Re-engineering adenovirus vector systems to enable high-throughput analyses of gene function. *BioTechniques*, 45(6), pp.659–668.

Stanton, R.J. et al., 2010. Reconstruction of the complete human cytomegalovirus genome in a BAC reveals RL13 to be a potent inhibitor of replication. *Journal of Clinical Investigation*, 120(9), pp.3191–3208. Available at: http://www.ncbi.nlm.nih.gov/pubmed/20679731 [Accessed February 3, 2017].

Staras, S.A.S. et al., 2008. Cytomegalovirus seroprevalence and childhood sources of infection: A population-based study among pre-adolescents in the United States. *Journal of Clinical Virology*, 43(3), pp.266–271. Available at: http://linkinghub.elsevier.com/retrieve/pii/S138665320800259X [Accessed February 2, 2017].

Staras, S.A.S. et al., 2006. Seroprevalence of Cytomegalovirus Infection in the United States, 1988-1994. *Clinical Infectious Diseases*, 43(9), pp.1143–1151. Available at: http://www.ncbi.nlm.nih.gov/pubmed/17029132 [Accessed February 2, 2017].

Stark, T.J. et al., 2012. High-resolution profiling and analysis of viral and host small RNAs during human cytomegalovirus infection. *Journal of virology*, 86(1), pp.226–235.

Starzynska, T. et al., 1998. 5T4 oncofetal antigen in gastric carcinoma and its clinical significance. *European journal of gastroenterology & hepatology*, 10(6), pp.479–84. Available at: http://www.ncbi.nlm.nih.gov/pubmed/9855063 [Accessed April 11, 2017].

Starzynska, T., Rahi, V. & Stern, P.L., 1992. The expression of 5T4 antigen in colorectal and gastric carcinoma. *British journal of cancer*, 66(5), pp.867–9. Available at: http://www.ncbi.nlm.nih.gov/pubmed/1419629 [Accessed April 11, 2017].

Staveley-O'Carroll, K. et al., 1998. Induction of antigen-specific T cell anergy: An early event in the course of tumor progression. *Proceedings of the National Academy of Sciences of the United States of America*, 95(3), pp.1178–83. Available at: http://www.ncbi.nlm.nih.gov/pubmed/9448305 [Accessed August 29, 2017].

Steininger, C., Puchhammer-Stockl, E. & Popow-Kraupp, T., 2006. Cytomegalovirus disease in the era of highly active antiretroviral therapy (HAART). *Journal of clinical virology : the official publication of the Pan American Society for Clinical Virology*, 37(1), pp.1–9.

Stern-Ginossar, N. et al., 2012. Decoding human cytomegalovirus. TL - 338. *Science*, 338(6110), pp.1088–1093. Available at: /Users/yurikoharigaya/Documents/ReadCube Media/stern_ginossar2012suppl.pdf%5Cnhttp://dx.doi.org/10.1126/science.1227919.

Stern, P.L. et al., 2014. Understanding and exploiting 5T4 oncofoetal glycoprotein expression. *Seminars in Cancer Biology*, 29(C), pp.13–20. Available at: http://dx.doi.org/10.1016/j.semcancer.2014.07.004.

Stern, P.L. & Harrop, R., 2017. 5T4 oncofoetal antigen: an attractive target for immune intervention in cancer. *Cancer Immunology, Immunotherapy*, 66(4), pp.415–426. Available at: http://link.springer.com/10.1007/s00262-016-1917-3 [Accessed April 10, 2017].

Stinski, M.F. & Isomura, H., 2008. Role of the cytomegalovirus major immediate early enhancer in acute infection and reactivation from latency. *Medical microbiology and immunology*, 197(2), pp.223–231.

Stone, J.D., Harris, D.T. & Kranz, D.M., 2015. TCR affinity for p/MHC formed by tumor antigens that are self-proteins: impact on efficacy and toxicity. *Current Opinion in Immunology*, 33, pp.16–22. Available at: http://www.ncbi.nlm.nih.gov/pubmed/25618219 [Accessed April 7, 2017].

Stowell, J.D. et al., 2012. Cytomegalovirus survival on common environmental surfaces: opportunities for viral transmission. *The Journal of infectious diseases*, 205(2), pp.211–214.

Streblow, D.N. et al., 2006. A Proteomics Analysis of Human Cytomegalovirus Particles. In M. J. Reddehase, ed. *Cytomegaloviruses: Molecular Biology and Immunology*. Caister Academic Press, pp. 91–110.

Studahl, M. et al., 1994. Cytomegalovirus infection of the CNS in non-compromised patients. *Acta neurologica Scandinavica*, 89(6), pp.451–457.

Sung, H. & Schleiss, M.R., 2010. Update on the current status of cytomegalovirus

vaccines. *Expert review of vaccines*, 9(11), pp.1303–1314.

Sweet, C., 1999. The pathogenicity of cytomegalovirus. *FEMS Microbiology Reviews*, 23(4), pp.457–482. Available at: https://academic.oup.com/femsre/article-lookup/doi/10.1111/j.1574-6976.1999.tb00408.x [Accessed February 28, 2017].

Sylwester, A.W. et al., 2005. Broadly targeted human cytomegalovirus-specific CD4+ and CD8+ T cells dominate the memory compartments of exposed subjects. *The Journal of experimental medicine*, 202(5), pp.673–85. Available at: http://www.jem.org/lookup/doi/10.1084/jem.20050882 [Accessed February 6, 2017].

Tabeta, K. et al., 2004. Toll-like receptors 9 and 3 as essential components of innate immune defense against mouse cytomegalovirus infection. *Proceedings of the National Academy of Sciences of the United States of America*, 101(10), pp.3516–3521.

Tamanini, A. et al., 2006. Interaction of Adenovirus Type 5 Fiber with the Coxsackievirus and Adenovirus Receptor Activates Inflammatory Response in Human Respiratory Cells. *Journal of Virology*, 80(22), pp.11241–11254. Available at: http://www.ncbi.nlm.nih.gov/pubmed/16956941 [Accessed March 20, 2017].

Tandon, R. & Mocarski, E.S., 2012. Viral and host control of cytomegalovirus maturation. *Trends in microbiology*, 20(8), pp.392–401.

Tang, Q. & Maul, G.G., 2006. Mouse cytomegalovirus crosses the species barrier with help from a few human cytomegalovirus proteins. *Journal of virology*, 80(15), pp.7510–21. Available at: http://www.pubmedcentral.nih.gov/articlerender.fcgi?artid=1563706&tool=pmcentrez&rendertype=abstract.

Tashiro, H. & Brenner, M.K., 2017. Immunotherapy against cancer-related viruses. *Cell Research*, 27(1), pp.59–73. Available at: http://www.nature.com/doifinder/10.1038/cr.2016.153 [Accessed April 4, 2017].

Terhune, S.S., Schroer, J. & Shenk, T., 2004. RNAs Are Packaged into Human Cytomegalovirus Virions in Proportion to Their Intracellular Concentration. *Journal of Virology*, 78(19), pp.10390–10398. Available at: http://www.ncbi.nlm.nih.gov/pubmed/15367605 [Accessed February 21, 2017].

Tey, S.-K., 2014. Adoptive T-cell therapy: adverse events and safety switches. *Clinical & Translational Immunology*, 3(6), p.e17. Available at: http://www.nature.com/doifinder/10.1038/cti.2014.11 [Accessed March 24, 2017].

Tian, X. et al., 2009. An Improved Tet-On System for Gene Expression in Neurons Delivered by a Single Lentiviral Vector. *Human Gene Therapy*, 20(2), pp.113–123. Available at: http://www.ncbi.nlm.nih.gov/pubmed/20377365 [Accessed March 2, 2017].

Tierney, R. et al., 2012. A single-dose cytomegalovirus-based vaccine encoding tetanus toxin fragment C induces sustained levels of protective tetanus toxin antibodies in mice. *Vaccine*.

Tillack, K., Aboutalebi, H. & Kramer, E.R., 2015. An Efficient and Versatile System for Visualization and Genetic Modification of Dopaminergic Neurons in Transgenic Mice X. Zhuang, ed. *PLOS ONE*, 10(8), p.e0136203. Available at: http://www.ncbi.nlm.nih.gov/pubmed/26291828 [Accessed March 2, 2017].

Timoshenko, O. et al., 2009. Identification of mutations in a temperature-sensitive mutant (*tsm* 5) of murine cytomegalovirus using complementary genome sequencing. *Journal of Medical Virology*, 81(3), pp.511–518. Available at: http://doi.wiley.com/10.1002/jmv.21419 [Accessed July 25, 2017].

Ting, J.P.-Y. et al., 2002. Genetic control of MHC class II expression. *Cell*, 109 Suppl(2), pp.S21-33. Available at: http://www.ncbi.nlm.nih.gov/pubmed/11983150 [Accessed April 2, 2017].

Tollefson, A.E. et al., 2007. Identification of a New Human Adenovirus Protein Encoded by a Novel Late l-Strand Transcription Unit. *Journal of Virology*, 81(23), pp.12918–12926. Available at: http://www.ncbi.nlm.nih.gov/pubmed/17881437 [Accessed March 24, 2017].

Tooze, J. et al., 1993. Progeny vaccinia and human cytomegalovirus particles utilize early endosomal cisternae for their envelopes. *European journal of cell biology*, 60(1), pp.163–178.

Towler, J.C. et al., 2012. Human cytomegalovirus transcriptome activity differs during replication in human fibroblast, epithelial and astrocyte cell lines. *The Journal of general virology*, 93(Pt 5), pp.1046–1058.

Tran, E. et al., 2014. Cancer Immunotherapy Based on Mutation-Specific CD4+ T Cells in a Patient with Epithelial Cancer. *Science*, 344(6184), pp.641–645. Available at: http://www.ncbi.nlm.nih.gov/pubmed/24812403 [Accessed April 2, 2017].

Trgovcich, J. et al., 2016. Cytomegalovirus reinfections stimulate CD8 T-Memory inflation. *PLoS ONE*, 11(11), p.e0167097. Available at: https://www.ncbi.nlm.nih.gov/pmc/articles/PMC5117776/pdf/pone.0167097.pdf [Accessed March 10, 2017].

Trsan, T. et al., 2013. Superior induction and maintenance of protective CD8 T cells in mice infected with mouse cytomegalovirus vector expressing RAE-1γ. *Proceedings of the National Academy of Sciences of the United States of America*, 110(41), pp.16550–5. Available at: http://www.pubmedcentral.nih.gov/articlerender.fcgi?artid=3799388&tool=pmcentrez&rendertype=abstract.

Tsuda, Y. et al., 2015. A cytomegalovirus-based vaccine provides long-lasting protection against lethal Ebola virus challenge after a single dose. *Vaccine*, 33(19), pp.2261–2266.

Tsuda, Y. et al., 2011. A replicating cytomegalovirus-based vaccine encoding a single Ebola virus nucleoprotein CTL epitope confers protection against Ebola virus. *PLoS Neglected Tropical Diseases*.

Tykodi, S.S. et al., 2012. CD8+ T-cell Clones Specific for the 5T4 Antigen Target Renal Cell Carcinoma Tumor-initiating Cells in a Murine Xenograft Model. *Journal of Immunotherapy*, 35(7), pp.523–533. Available at: http://www.ncbi.nlm.nih.gov/pubmed/22892449 [Accessed April 10, 2017].

Upton, J.W., Kaiser, W.J. & Mocarski, E.S., 2012. DAI/ZBP1/DLM-1 complexes with RIP3 to mediate virus-induced programmed necrosis that is targeted by murine cytomegalovirus vIRA. *Cell host & microbe*, 11(3), pp.290–297.

Upton, J.W., Kaiser, W.J. & Mocarski, E.S., 2010. Virus inhibition of RIP3-dependent necrosis. *Cell host & microbe*, 7(4), pp.302–313.

Varnum, S.M. et al., 2004. Identification of proteins in human cytomegalovirus (HCMV) particles: the HCMV proteome. *Journal of virology*, 78(20), pp.10960–10966.

Veldhuis, W. et al., 2004. Coombs-negative severe haemolytic anaemia in an immunocompetent adult following cytomegalovirus infection. *European journal of clinical microbiology & infectious diseases : official publication of the European Society of Clinical Microbiology*, 23(11), pp.844–847.

Vetrini, F. & Ng, P., 2010. Gene therapy with helper-dependent adenoviral vectors: current advances and future perspectives. *Viruses*, 2(9), pp.1886–917. Available at: http://www.ncbi.nlm.nih.gov/pubmed/21994713 [Accessed March 24, 2017].

Vigneron, N., 2015. Human Tumor Antigens and Cancer Immunotherapy. *BioMed Research International*, 2015, pp.1–17. Available at: http://www.hindawi.com/journals/bmri/2015/948501/ [Accessed April 4, 2017].

Villard, J., 2011. The role of natural killer cells in human solid organ and tissue transplantation. *Journal of innate immunity*, 3(4), pp.395–402.

Vochem, M. et al., 1998. Transmission of cytomegalovirus to preterm infants through breast milk. *The Pediatric infectious disease journal*, 17(1), pp.53–58.

Voigt, V. et al., 2003. Murine cytomegalovirus m157 mutation and variation leads to immune evasion of natural killer cells. *Proceedings of the National Academy of Sciences of the United States of America*, 100(23), pp.13483–8. Available at: http://www.ncbi.nlm.nih.gov/pubmed/14597723%5Cnhttp://www.pubmedcentral.nih.gov/articlerender.fcgi?artid=PMC263840.

Walter, E.A. et al., 1995. Reconstitution of cellular immunity against cytomegalovirus in recipients of allogeneic bone marrow by transfer of T-cell clones from the donor. *The New England journal of medicine*, 333(16), pp.1038–1044.

Walton, S.M. et al., 2008. The dynamics of mouse cytomegalovirus-specific CD4 T cell responses during acute and latent infection. *Journal of immunology*

(Baltimore, Md. : 1950), 181(2), pp.1128–34. Available at: http://www.ncbi.nlm.nih.gov/pubmed/18606665.

Wang, D. et al., 2016. A replication-defective human cytomegalovirus vaccine for prevention of congenital infection. *Science Translational Medicine*, 8(362), p.362ra145-362ra145. Available at: http://stm.sciencemag.org/cgi/doi/10.1126/scitranslmed.aaf9387 [Accessed August 3, 2017].

Wang, J. Ben & McVoy, M.A., 2011. A 128-base-pair sequence containing the pac1 and a presumed cryptic pac2 sequence includes cis elements sufficient to mediate efficient genome maturation of human cytomegalovirus. *Journal of virology*, 85(9), pp.4432–4439.

Ward, S.M. et al., 2004. Virus-specific CD8+ T lymphocytes within the normal human liver. *European Journal of Immunology*, 34(6), pp.1526–1531.

Weekes, M.P. et al., 2014. Quantitative temporal viromics: An approach to investigate host-pathogen interaction. *Cell*, 157(6), pp.1460–1472. Available at: http://dx.doi.org/10.1016/j.cell.2014.04.028.

Wiley, 2017. Journal of Gene Medicine Clinical Trial Database. Available at: http://www.wiley.com/legacy/wileychi/genmed/clinical/ [Accessed August 7, 2017].

Wilkie, G.S. et al., 2015. First Fatality Associated with Elephant Endotheliotropic Herpesvirus 5 in an Asian Elephant: Pathological Findings and Complete Viral Genome Sequence. *Scientific Reports*, 4(1), p.6299. Available at: http://www.ncbi.nlm.nih.gov/pubmed/25199796 [Accessed August 25, 2017].

Wilkinson, G.W.G. et al., 1998. Disruption of PML-associated nuclear bodies mediated by the human cytomegalovirus major immediate early gene product. *Journal of General Virology*, 79, pp.1233–1245. Available at: http://www.microbiologyresearch.org/docserver/fulltext/jgv/79/5/0791233a.pdf?expires=1503869251&id=id&accname=guest&checksum=74B40D33E119AC45E64926CDBCAD0392 [Accessed August 27, 2017].

Wilkinson, G.W.G. et al., 2015. Human cytomegalovirus: taking the strain. *Medical Microbiology and Immunology*, 204(3), pp.273–284. Available at: http://dx.doi.org/10.1007/s00430-015-0411-4.

Witek, M. et al., 2014. Tumor radiation therapy creates therapeutic vaccine responses to the colorectal cancer antigen GUCY2C. *International journal of radiation oncology, biology, physics*, 88(5), pp.1188–95. Available at: http://www.ncbi.nlm.nih.gov/pubmed/24661671 [Accessed August 6, 2017].

Wloch, M.K. et al., 2008. Safety and Immunogenicity of a Bivalent Cytomegalovirus DNA Vaccine in Healthy Adult Subjects. *The Journal of Infectious Diseases*, 197(12), pp.1634–1642. Available at: http://www.ncbi.nlm.nih.gov/pubmed/18444883 [Accessed February 27, 2017].

Wold, W.S.M. & Ison, M.G., 2013. Adenovirus. In D. M. Kipe & P. M. Howley, eds.

Fields Virology Vol II. Philadelphia: Lippincott, Williams & Wilkins, pp. 1732–1767.

Woods, A.M. et al., 2002. Characterization of the murine 5T4 oncofoetal antigen: a target for immunotherapy in cancer. *The Biochemical journal*, 366(Pt 1), pp.353–365.

Wrigley, E. et al., 1995. 5T4 oncofetal antigen expression in ovarian carcinoma. *International journal of gynecological cancer : official journal of the International Gynecological Cancer Society*, 5(4), pp.269–274. Available at: http://www.ncbi.nlm.nih.gov/pubmed/11578488 [Accessed April 11, 2017].

Wurz, G., Kao, C.-J. & DeGregorio, M., 2016. Novel cancer antigens for personalized immunotherapies: latest evidence and clinical potential. *Therapeutic Advances in Medical Oncology* , 8(1), pp.4–31.

Xia, Z.-J. et al., 2004. Phase III randomized clinical trial of intratumoral injection of E1B gene-deleted adenovirus (H101) combined with cisplatin-based chemotherapy in treating squamous cell cancer of head and neck or esophagus. *Ai zheng = Aizheng = Chinese journal of cancer*, 23(12), pp.1666–70. Available at: http://www.ncbi.nlm.nih.gov/pubmed/15601557 [Accessed April 14, 2017].

Xu, G. et al., 2013. Cytomegalovirus-based cancer vaccines expressing TRP2 induce rejection of melanoma in mice. *Biochemical and Biophysical Research Communications*, 437(2), pp.287–291. Available at: http://dx.doi.org/10.1016/j.bbrc.2013.06.068.

Xu, Z. et al., 2013. Coagulation factor X shields adenovirus type 5 from attack by natural antibodies and complement. *Nature Medicine*, 19(4), pp.452–457. Available at: http://www.ncbi.nlm.nih.gov/pubmed/23524342 [Accessed March 21, 2017].

Yang, Y. et al., 1996. Immune responses to viral antigens versus transgene product in the elimination of recombinant adenovirus-infected hepatocytes in vivo. *Gene therapy*, 3(2), pp.137–44. Available at: http://www.ncbi.nlm.nih.gov/pubmed/8867861 [Accessed March 20, 2017].

Yang, Y., Ertl, H.C.J. & Wilson, J.M., 1994. MHC class I-restricted cytotoxic T lymphocytes to viral antigens destroy hepatocytes in mice infected with E1-deleted recombinant adenoviruses. *Immunity*, 1(5), pp.433–442. Available at: http://linkinghub.elsevier.com/retrieve/pii/1074761394900744 [Accessed March 20, 2017].

Yang, Z. & Bjorkman, P.J., 2008. Structure of UL18, a peptide-binding viral MHC mimic, bound to a host inhibitory receptor. *Proceedings of the National Academy of Sciences of the United States of America*, 105(29), pp.10095–10100.

Yao, F. et al., 1998. Tetracycline Repressor, tetR, rather than the tetR–Mammalian Cell Transcription Factor Fusion Derivatives, Regulates Inducible Gene Expression in Mammalian Cells. *Human Gene Therapy*, 9(13), pp.1939–1950. Available at: http://www.ncbi.nlm.nih.gov/pubmed/9741432 [Accessed March

10, 2017].

Yeager, A.S. et al., 1983. Sequelae of maternally derived cytomegalovirus infections in premature infants. *The Journal of Pediatrics*, 102(6), pp.918–922. Available at: https://www.ncbi.nlm.nih.gov/pubmed/6304275 [Accessed February 2, 2017].

Yee, C., 2005. Adoptive T cell therapy: Addressing challenges in cancer immunotherapy. *Journal of Translational Medicine*, 3(17), pp.6783–6790.

Yu, B. et al., 2013. Characteristics of neutralizing antibodies to adenovirus capsid proteins in human and animal sera. *Virology*, 437(2), pp.118–123. Available at: http://linkinghub.elsevier.com/retrieve/pii/S0042682212006423 [Accessed March 21, 2017].

Yu, D., Silva, M.C. & Shenk, T., 2003. Functional map of human cytomegalovirus AD169 defined by global mutational analysis. *Proceedings of the National Academy of Sciences of the United States of America*, 100(21), pp.12396–401. Available at: http://www.pnas.org/content/100/21/12396.short.

Zahn, K.E. et al., 2011. Phosphonoformic Acid Inhibits Viral Replication by Trapping the Closed Form of the DNA Polymerase. *Journal of Biological Chemistry*, 286(28), pp.25246–25255. Available at: http://www.ncbi.nlm.nih.gov/pubmed/21566148 [Accessed February 2, 2017].

Zarour, H.M. et al., 2003. Categories of Tumor Antigens. In D. W. Kufe et al., eds. *Holland-Frei Cancer Medicine*. BC Decker. Available at: https://www.ncbi.nlm.nih.gov/books/NBK12354/ [Accessed April 4, 2017].

Zendman, A.J.W., Ruiter, D.J. & Van Muijen, G.N.P., 2003. Cancer/testis-associated genes: Identification, expression profile, and putative function. *Journal of Cellular Physiology*, 194(3), pp.272–288. Available at: http://doi.wiley.com/10.1002/jcp.10215 [Accessed April 4, 2017].

Zhang, S. et al., 2013. Seroprevalence of neutralizing antibodies to human adenoviruses type-5 and type-26 and chimpanzee adenovirus type-68 in healthy Chinese adults. *Journal of Medical Virology*, 85(6), pp.1077–1084. Available at: http://www.ncbi.nlm.nih.gov/pubmed/23588735 [Accessed March 20, 2017].

Zhong, J. et al., 2008. Induction of Pluripotent Protective Immunity Following Immunisation with a Chimeric Vaccine against Human Cytomegalovirus D. F. Nixon, ed. *PLoS ONE*, 3(9), p.e3256. Available at: http://www.ncbi.nlm.nih.gov/pubmed/18806877 [Accessed February 2, 2017].

Zhou, X. et al., 2006. Optimization of the Tet-On system for regulated gene expression through viral evolution. *Gene Therapy*, 13(19), pp.1382–1390. Available at: http://www.nature.com/doifinder/10.1038/sj.gt.3302780 [Accessed March 2, 2017].

Zhu, J., Huang, X. & Yang, Y., 2007. Innate Immune Response to Adenoviral Vectors Is Mediated by both Toll-Like Receptor-Dependent and -Independent Pathways. *JOURNAL OF VIROLOGY*, 81(7), pp.3170–3180. Available at: http://jvi.asm.org/content/81/7/3170.full.pdf [Accessed March 20, 2017].

Zhu, J., Huang, X. & Yang, Y., 2010. NKG2D is required for NK cell activation and function in response to E1-deleted adenovirus. *Journal of immunology (Baltimore, Md. : 1950)*, 185(12), pp.7480–6. Available at: http://www.ncbi.nlm.nih.gov/pubmed/21076062 [Accessed August 7, 2017].

Appendices

Appendix A - Primers used in this study

No.	Primer	Sequence (5'>3')
Inserting tetR (in HCMV):		
1	TetR RL13 hom F	TTAAGTACATATCTACCATGAAATACAGCAAAGATATACTAATGTC TATCCATCCAATAGCGGTACCATGTCTAGATTAGATAAAAGTAAA GTGATTAA
2	TetR RL13 hom R	AAGTGATTAACTCAGAATAAACACACCCAAACATTAATGACTAAA GATAAAAAATTTTATTGATGTGCATATTATACCTTTCTCTTCTTTTT TGGATCAG
Inserting tetR (in MCMV):		
3	SacB/Amp/ lacZ into m157 MCMV K181 F	GGACTGTTGACCGCCATCTGTTCTTGATTTCCCGAACGTTGCTTT TTATCATATAGGTACCAATTTCTTTTGCGTCGGACCTGTGACGGA AGATCACTTC
4	SacB/Amp/ lacZ into m157 MCMV K181 R	ACTACCGATACGGTCAGGGTAGCGTATACAGGACAGACTGGTAA GATTAATATTCAAGGATCAGGAAAATTTTCAACTCTGAGGTTCTTA TGGCTCTTGT
5	tetR into m157 MCMV K181 F	GTGAACGGCACGTTCGACCTCGATGTGACCACACACGTGGTCAA GCCGGTCGTGTTGTACCAGAACTCGATTATACCTTTCTCTTCTTTT TTGGATCAGA
6	tetR into m157 MCMV K181 R	AAACGCAGGAGAATCTGAACCCCGATATTTGAGAAAGTGTACCC CGATATTCAGTACCTCTTGACATGTCTAGATTAGATAAAAGTAAAG TGATTAACAG
7	IE2 tetR F	CTTTATTTATTGATTAAAAACCATGACATACCTCGTGTCCTCTCAC TGAATCTTCTTCCTGACGGTCACCAGGTCTCTGGTTATACCTTTC TCTTCTTTT
8	IE2 tetR R	GGGTAGCAGCTGTAGTGAGAGTCTCTCGGGTCCGGGGGCGTGA GGGACGCGACTGCTCACGGTTCTGTTTGTCTGTAGATATGTCTA GATTAGATAAAAG
9	RpsL after M36 F	TCGCTTTTTATTAACCTCCGTTTTGTTTATTTTTTTTCTCCCCTCAC CCTCTCCGTCCCTTTCTTATCCGTTTTCCCTCCTGTGACGGAAGA TCACTTCG
10	RpsL after M36 R	CGGGATCAACGATCCACCGTGTCGGCGATGTATCGAGAGGAGG AGGGTCAAGCTCTTTAAGATGACACGGGGATATCGACTGAGGTT CTTATGGCTCTTG
11	P2A-tetR M36 F	TTTTTATTAACCTCCGTTTTGTTTATTTTTTTTCTCCCCTCACCCTC TCCGTCCCTTTCTTATCCGTTTTCCCTTTATACCTTTCTCTTCTTTT TTGGAT
12	P2A-tetR M36 R	ACCATCGGGATCAACGATCCACCGTGTCGGCGATGTATCGAGAG GAGGAGGGTCAAGCTCTTTAAGATGACACGGGGATATCGAAGCG GCTCCGGTGCCA
13	bef tetR IE2 F	TGTTAAACCTTCGATTCCGACCTCATTAAGCAGCTCTAATGCGCT GTTAATCACTTTACTTTTATCTAATCTAGACATCCTGTGACGGAAG ATCACTTCG
14	bef tetR IE2 R	GGTAGCAGCTGTAGTGAGAGTCTCTCGGGTCCGGGGGCGTGAG GGACGCGACTGCTCACGGTTCTGTTTGTCTGTAGATCTGAGGTT CTTATGGCTCTTG
Promoters upstream tetR (in HCMV):		

15	sacB before tetR HCMV F	ACACATGAAATTAAGTAACATATCTACCATGAAATACAGCAAAGATA TACTAATGTCTATCCATCCAATAGCGGTACCCCTGTGACGGAAGAT CACTTCG
16	sacB before tetR HCMV R	TTGTTAAACCTTCGATTCCGACCTCATTAAGCAGCTCTAATGCGCT GTTAATCACTTTACTTTTATCTAATCTAGACATCTGAGGTTCTTATG GCTCTTG
17	MCMV ie1 prom HCMV F	CACATGAAATTAAGTAACATATCTACCATGAAATACAGCAAAGATAT ACTAATGTCTATCCATCCAATAGCGGTACCCAAGTACACTGACTCA ATAGGGA
18	MCMV ie1 prom HCMV R	GGGTTGTTAAACCTTCGATTCCGACCTCATTAAGCAGCTCTAATGC GCTGTTAATCACTTTACTTTTATCTAATCTAGACATGAAGACTGCGA CGGTACC
19	RSV prom HCMV F	CACATGAAATTAAGTAACATATCTACCATGAAATACAGCAAAGATAT ACTAATGTCTATCCATCCAATAGCGGTACCACTCTCAGTACAATCT GCTCTGA
20	RSV prom HCMV R	GTTGTTAAACCTTCGATTCCGACCTCATTAAGCAGCTCTAATGCGC TGTTAATCACTTTACTTTTATCTAATCTAGACATTTGGAGGTGCACA CCAATGT
21	SV40 prom HCMV F	CACATGAAATTAAGTAACATATCTACCATGAAATACAGCAAAGATAT ACTAATGTCTATCCATCCAATAGCGGTACCTGCATCTCAATTAGTCA GCAACC
22	SV40 prom HCMV R	TGTTAAACCTTCGATTCCGACCTCATTAAGCAGCTCTAATGCGCTG TTAATCACTTTACTTTTATCTAATCTAGACATAAGCTTTTTGCAAAAG CCTAGG
Promoters upstream tetR (in MCMV):		
23	sacB before tetR k181 F	TTGTTAAACCTTCGATTCCGACCTCATTAAGCAGCTCTAATGCGCT GTTAATCACTTTACTTTTATCTAATCTAGACATCTGAGGTTCTTATGG CTCTTG
24	sacB before tetR k181 R	GAGGTGGCGTGTGAAACGCAGGAGAATCTGAACCCCGATATTTGA GAAAGTGTACCCCGATATTCAGTACCTCTTGACCCTGTGACGGAAG ATCACTTCG
25	RSV before tetR k181 F	GGTTGTTAAACCTTCGATTCCGACCTCATTAAGCAGCTCTAATGCG CTGTTAATCACTTTACTTTTATCTAATCTAGACATTTGGAGGTGCAC ACCAATG
26	RSV before tetR k181 R	AGGTGGCGTGTGAAACGCAGGAGAATCTGAACCCCGATATTTGAG AAAGTGTACCCCGATATTCAGTACCTCTTGACACTCTCAGTACAAT CTGCTCTGA
27	SV40 before tetR k181 F	TGTTAAACCTTCGATTCCGACCTCATTAAGCAGCTCTAATGCGCTG TTAATCACTTTACTTTTATCTAATCTAGACATAAGCTTTTTGCAAAAG CCTAGG
28	SV40 before tetR k181 R	AGGTGGCGTGTGAAACGCAGGAGAATCTGAACCCCGATATTTGAG AAAGTGTACCCCGATATTCAGTACCTCTTGACTGCATCTCAATTAGT CAGCAACC
29	HCMV MIE before tetR k181 F	ACGGGTTGTTAAACCTTCGATTCCGACCTCATTAAGCAGCTCTAAT GCGCTGTTAATCACTTTACTTTTATCTAATCTAGACATCAGGCTGGA TCGGTCC

30	HCMV MIE before tetR k181 R	TTGGAGGTGGCGTGTGAAACGCAGGAGAATCTGAACCCCGATATT TGAGAAAGTGTACCCCGATATTCAGTACCTCTTGACCTGGCATTAT GCCCAGTAC
31	RSV tetR IE2 F	GGTTGTTAAACCTTCGATTCCGACCTCATTAAGCAGCTCTAATGCG CTGTTAATCACTTTACTTTTATCTAATCTAGACATTTGGAGGTGCAC ACCAATG
32	RSV tetR IE2 R	GGGTAGCAGCTGTAGTGAGAGTCTCTCGGGTCCGGGGGCGTGAG GGACGCGACTGCTCACGGTTCTGTTTGTCTGTAGATACTCTCAGTA CAATCTGCTC
33	HCMV tetR IE2 F	TTGTTAAACCTTCGATTCCGACCTCATTAAGCAGCTCTAATGCGCT GTTAATCACTTTACTTTTATCTAATCTAGACATggtggCAGGCTGGAT CGGTCC
34	HCMV tetR IE2 R	GGGTAGCAGCTGTAGTGAGAGTCTCTCGGGTCCGGGGGCGTGAG GGACGCGACTGCTCACGGTTCTGTTTGTCTGTAGATCTGGCATTAT GCCCAGTACA
TetO-RpsL-TetO cassette before genes (in HCMV):		
35	before UL44 F	CCAGCGTCGGCGGCTCCGAGAGGCGCGTCTTGCGATCCATCCC GGACAGCGTGCAAGTCTTCTCTATCACTGATAGGGACTGAGGTT CTTATGGCTCTTG
36	before UL44 R	CCGGTCGTCGTGTGTGCTCTCTATAAAACTTTCGCTCGCTCGCGC CCGCTCCTTAGTCGTCCCTATCAGTGATAGAGACCTGTGACGGA AGATCACTTCG
37	before UL54 F	CGCCGGTCACGCCGCCGCTCAGATACGGGTTGAAAAACATAGCG GACCGTGAGAGGCTGATCTCTATCACTGATAGGGACTGAGGTTC TTATGGCTCTTG
38	before UL54 R	TAAACTGGATATCTAGGTGCTGCATGTGTATTTTCTTTGTGATTTT GCTTCGTAAGCTGTCCCTATCAGTGATAGAGACCTGTGACGGAA GATCACTTCG
39	before UL75 F	CGGCGAGGATGATGAGGTAGGAGGGGAGGCCTGGCCGCATAGC GCGGCCGCGCCGCTGGGTCTCTATCACTGATAGGGACTGAGGTT CTTATGGCTCTTG
40	before UL75 R	ATCCTTTCTCTCCTTCTCTCGGGTGTAACGCCAACCACCACCTGG ATCACGCCGCTGAATCCCTATCAGTGATAGAGACCTGTGACGGA AGATCACTTCG
41	before UL85 F	GGTCGAAAGTGCAGAAGATGTTGGCCTCCATGGCCGCCATAGCG GCGGTGAAATCCTGGCTCTCTATCACTGATAGGGACTGAGGTTCT TATGGCTCTTG
42	before UL85 R	CTCGCTCTGACGCCGCGCCCGGTGCAGACGTTGTTCGTCTCCGC TTCTCCTCCGTCGCGTCCCTATCAGTGATAGAGACCTGTGACGG AAGATCACTTCG
43	before UL100 F	ATGTCCGTGTATTCACCTTATCCACGTGCGAGGGGGCCATGGCG ATAGCGGCGGCCCGCTTCTCTATCACTGATAGGGACTGAGGTTC TTATGGCTCTTG
44	before UL100 R	TAGTATTTAACGACCCGCGAGCCTGTCGTCATCGGCGCGCCCCC ATCGCCTCCCGAGCGTCCCTATCAGTGATAGAGACCTGTGACGG AAGATCACTTCG
45	before UL123 F	TCTATGGAGGTCAAAACAGCGTGGATGGCGTCTCCAGGCGATCT GACGGTTCACTAAACGTCTCTATCACTGATAGGGACTGAGGTTCT TATGGCTCTTG
46	before UL123 R	CCCCATTGACGCAAATGGGCGGTAGGCGTTTACTATGGGAGGTC TATATAAGCAGAGCTTCCCTATCAGTGATAGAGACCTGTGACGGA AGATCACTTCG
TetO-RpsL-TetO cassette before genes (in MCMV):		

47	before M44 F	TCGGCGGTTCGTGCTCGCGAACTTTCCTACCACCCTCCATTCCC GCGGAGATGTATGTGATCTCTATCACTGATAGGGACTGAGGTTCT TATGGCTCTTG
48	before M44 R	CTCGCTCGGTCGGTCGGTCTGTCTCGTGTCCTTCTTTCGCCGGC GCGCCGCGATCTCGCTCCCTATCAGTGATAGAGACCTGTGACGG AAGATCACTTCG
49	before M75 F	TCGAACATAGCGCGATGGAGAGTATTAATGACAACTTCATGTCGC GGGTCGGGGTGCGGATCTCTATCACTGATAGGGACTGAGGTTCT TATGGCTCTTG
50	before M75 R	GCGCCGACGAGCGTAATTAAGATATTTAAACAGGATCGACGAGA TAGGGCCCTGCGACGTCCCTATCAGTGATAGAGACCTGTGACGG AAGATCACTTCG
51	before M85 F	TGAGGCGCTGCTCGAACGTGACCAAAACCGTCGTTTCCATGGTC GTGGGTGTCGGTCTCCTCTCTATCACTGATAGGGACTGAGGTTCT TATGGCTCTTG
52	before M85 R	CGTGATCGAGCGGGTCCTCCCGAGCGGAAGGCGCAGCGCCGTC GGACGTCACGCTCGCCTCCCTATCAGTGATAGAGACCTGTGACG GAAGATCACTTCG
53	before M100 F	GGTCCACGTGGGAGAGCGTCATGACGCCCGCTTTCGCCATCGTG CAGGTGTCTCGTGTCCTCTCTATCACTGATAGGGACTGAGGTTCT TATGGCTCTTG
54	before M100 R	CGAGGCTCGGACGGTCTCTCTAAGGATGCTCTCACTATTTGACC CGCCCCGTCGACCGCTCCCTATCAGTGATAGAGACCTGTGACGG AAGATCACTTCG
55	before M122/M123 F	CGATCATGATCATGTTGCAACTGGGTGCGGCGGGCTCCATCTCT CTAAAAAAATATAATTTCTCTATCACTGATAGGGACTGAGGTTCTT ATGGCTCTTG
56	before M122/M123 R	ATTAGCACTGTATACTTTAGATATCTTCTGGTCTCTGTGGACATCT GTTGATGATAAAATCCCTATCAGTGATAGAGACCTGTGACGGAAG ATCACTTCG
TetO before genes (in HCMV):		
57	UL44 TetO F	AGGCGCGTCTTGCGATCCATCCCGGACAGCGTGCAAGTCTTCTC TATCACTGATAGGGACGACTAAGGAGCGGGCGCGAGCGAGCGA AAGTTTTATAGAG
58	UL54 TetO F	CAGATACGGGTTGAAAAACATAGCGGACCGTGAGAGGCTGATCT CTATCACTGATAGGGACAGCTTACGAAGCAAAATCACAAAGAAAA TACACATGCAG
59	UL75 TetO F	GAGGGGAGGCCTGGCCGCATAGCGCGGCCGCGCCGCTGGGTC TCTATCACTGATAGGGATTCAGCGGCGTGATCCAGGTGGTGGTT GGCGTTACACCCGA
60	UL85 TetO F	TTGGCCTCCATGGCCGCCATAGCGGCGGTGAAATCCTGGCTCTC TATCACTGATAGGGACGCGACGGAGGAGAAGCGGAGACGAACA ACGTCTGCACCGG
61	UL100 TetO F	TCCACGTGCGAGGGGGCCATGGCGATAGCGGCGGCCCGCTTCT CTATCACTGATAGGGACGCTCGGGAGGCGATGGGGGCGCGCCG ATGACGACAGGCTC
62	UL123 TetO F	GTGGATGGCGTCTCCAGGCGATCTGACGGTTCACTAAACGTCTC TATCACTGATAGGGAAGCTCTGCTTATATAGACCTCCCATAGTAA ACGCCTACCGC
TetO TetO before genes (in HCMV):		
63	UL44 TetO-TetO F	TGCGATCCATCCCGGACAGCGTGCAAGTCTTCTCTATCACTGATA GGGAGATCTCTATCACTGATAGGGACGACTAAGGAGCGGGCGC GAGCGAGCGAAA
64	UL54 TetO-TetO F	TGAAAAACATAGCGGACCGTGAGAGGCTGATCTCTATCACTGATA GGGAGATCTCTATCACTGATAGGGACAGCTTACGAAGCAAAATCA CAAAGAAAAT

65	UL75 TetO-TetO F	CTGGCCGCATAGCGCGGCCGCGCCGCTGGGTCTCTATCACTGAT AGGGAGATCTCTATCACTGATAGGGATTCAGCGGCGTGATCCAG GTGGTGGTTGGC
66	UL85 TetO-TetO F	TGGCCGCCATAGCGGCGGTGAAATCCTGGCTCTCTATCACTGAT AGGGAGATCTCTATCACTGATAGGGACGCGACGGAGGAGAAGC GGAGACGAACAAC
67	UL100 TetO-TetO F	AGGGGGCCATGGCGATAGCGGCGGCCCGCTTCTCTATCACTGAT AGGGAGATCTCTATCACTGATAGGGACGCTCGGGAGGCGATGG GGGCGCGCCGATG
68	UL123 TetO-TetO F	TCTCCAGGCGATCTGACGGTTCACTAAACGTCTCTATCACTGATA GGGAGATCTCTATCACTGATAGGGAAGCTCTGCTTATATAGACCT CCCATAGTAA
TetO before genes (in MCMV):		
69	M44 TetO F	AACTTTCCTACCACCCTCCATTCCCGCGGAGATGTATGTGATCTC TATCACTGATAGGGAGCGAGATCGCGGCGCGCCGGCGAAAGAA GGACACGAGACA
70	M75 TetO F	GAGTATTAATGACAACTTCATGTCGCGGGTCGGGGTGCGGATCT CTATCACTGATAGGGACGTCGCAGGGCCCTATCTCGTCGATCCT GTTTAAATATCT
71	M85 TetO F	ACCAAAACCGTCGTTTCCATGGTCGTGGGTGTCGGTCTCCTCTCT ATCACTGATAGGGAGGCGAGCGTGACGTCCGACGGCGCTGCGC CTTCCGCTCGGG
72	M100 TetO F	CATGACGCCCGCTTTCGCCATCGTGCAGGTGTCTCGTGTCCTCT CTATCACTGATAGGGAGCGGTCGACGGGGCGGGTCAAATAGTGA GAGCATCCTTAG
73	M123 TetO F	GATATCTTCTGGTCTCTGTGGACATCTGTTGATGATAAAATCCCTA TCAGTGATAGAGAAATTATATTTTTTTAGAGAGATGGAGCCCGCC GCACCCAGT
TetO TetO before genes (in MCMV):		
74	M44 TetO-TetO F	CACCCTCCATTCCCGCGGAGATGTATGTGATCTCTATCACTGATA GGGAGATCTCTATCACTGATAGGGAGCGAGATCGCGGCGCGCC GGCGAAAGAAGG
75	M75 TetO-TetO F	ACAACTTCATGTCGCGGGTCGGGGTGCGGATCTCTATCACTGAT AGGGAGATCTCTATCACTGATAGGGACGTCGCAGGGCCCTATCT CGTCGATCCTGT
76	M85 TetO-TetO F	TCGTTTCCATGGTCGTGGGTGTCGGTCTCCTCTCTATCACTGATA GGGAGATCTCTATCACTGATAGGGAGGCGAGCGTGACGTCCGAC GGCGCTGCGCC
77	M100 TetO-TetO F	CTTTCGCCATCGTGCAGGTGTCTCGTGTCCTCTCTATCACTGATA GGGAGATCTCTATCACTGATAGGGAGCGGTCGACGGGGCGGGT CAAATAGTGAGA
78	M123 TetO-TetO F	GGTCTCTGTGGACATCTGTTGATGATAAAATCCCTATCAGTGATA GAGATCTCCCTATCAGTGATAGAGAAATTATATTTTTTTAGAGAGA TGGAGCCCG
Sequencing primers (in HCMV):		
79	In tetR for HCMV RL13 R	GAGCAAAGCCCGCTTATTTTTTAC
80	TetO-UL44 F	AATGGTCTTGGGCTGAAACG
81	TetO-UL44 R	AGGATGCTCAAGTGGTACC
82	TetO-UL54 F	ATAGAACATGAGAGGCAGCC

83	TetO-UL54 R	GATTCTTTGGACGGACGGAC
84	TetO-UL75 F	TGCTGTTGTAGGTACACTGG
85	TetO-UL75 R	GACGGTAGATGTCCAGGTG
86	TetO-UL85 F	GAGGATCTGGTTGCCTTCTA
87	TetO-UL85 R	CTACGTCCGAAACGCACTTTG
88	TetO-UL100 F	CCTTTCAAAGTCCACGACGTG
89	TetO-UL100 R	ACATTGTACGATAGGCACCG
90	TetO-UL123 F	TGCATAAGAAGCCAAGGGG
91	TetO-UL123 R	CAGTACATGACCTTACGGGA
Sequencing primers (in MCMV):		
92	tetR F	GTCAGTAACGATCGCAGAGC
93	tetR R	CACTCTTGTTAGTGCCGGT
94	In tetR for m158 F	GTAAAAAATCTTGCCAGCTTTCCC
95	In tetR R	GGGAAAGCTGGCAAGATTTTTTAC
96	In HCMV prom F	GAGTCAAACCGCTATCCACG
97	IE2 F	ATACTACTGCATGCCCCT
98	IE2 R	CGCTCGATCCATTCTTCT
99	TetO-M44 F	TTCTTGACGGTCTGGACGAT
100	TetO-M44 R	CGGCCAGACGATTGGTTTTC
101	TetO-M75 F	GTGCGTGTTGAAGAGACAGC
102	TetO-M75 R	GGATGCGCTTCTTGAAGTCG
103	TetO-M85 F	ATCATCTGGTTACCCTCGAC
104	TetO-M85 R	TGCAGTACATCTGCGTGGA
105	TetO-M100 F	TCGCGTTGTACATCGTCAGG
106	TetO-M100 R	GCAGGAAAGCATAGATGGAC
107	TetO-M123 F	AAGGGAGAGTTAGGAGAGG
108	TetO-M123 R	TGGCACCCTGAGAGAACAA
109	M36 F	CAACATGAGAGGTGCCAGAC
110	M36 R	ACCACCATCGGGATCAACG

Appendix B - Human 5T4 sequence

MPGGCSRGPAAGDGRLRLARLALVLLGWVSSSSPTSSASSFSSSAPFLASAVSAQ
PPLPDQCPALCECSEAARTVKCVNRNLTEVPTDLPAYVRNLFLTGNQLAVLPAGAF
ARRPPLAELAALNLSGSRLDEVRAGAFEHLPSLRQLDLSHNPLADLSPFAFSGSNA
SVSAPSPLVELILNHIVPPEDERQNRSFEGMVVAALLAGRALQGLRRLELASNHFLY
LPRDVLAQLPSLRHLDLSNNSLVSLTYVSFRNLTHLESLHLEDNALKVLHNGTLAEL
QGLPHIRVFLDNNPWVCDCHMADMVTWLKETEVVQGKDRLTCAYPEKMRNRVLL
ELNSADLDCDPILPPSLQTSYVFLGIVLALIGAIFLLVLYLNRKGIKKWMHNIRDACRD
HMEGYHYRYEINADPRLTNLSSNSDV